TECHNICAL REPORT STANDARD TITLE PAGE

1. Report No.	2. Government Accession No.	3. Recipient's Catalog No.
TX-01 1784-1		

4. Title and Subtitle	5. Report Date
Reproducibility of Texas Department of Transportation Falling Weight Deflectometer Fleet	September 2001
	6. Performing Organization Code

7. Author(s)	8. Performing Organization Report No.
S. Rocha, V. Tandon, and S. Nazarian	Research Report 1784-1

9. Performing Organization Name and Address	10. Work Unit No.
Center for Highway Materials Research The University of Texas at El Paso El Paso, Texas 79968-0516	11. Contract or Grant No. Study No. 0-1784

12. Sponsoring Agency Name and Address	13. Type of Report and Period Covered
Texas Department of Transportation P.O. Box 5051 Austin, Texas 78763	Interim Report Sept, 1999 –June, 2001
	14. Sponsoring Agency Code

15. Supplementary Notes

Research Performed in Cooperation with TxDOT and FHWA

16. Abstract

The degree of accuracy with which the Falling Weight Deflectometer (FWD) data are collected and analyzed has a direct impact on the conclusions drawn in many aspects of TxDOT operation. TxDOT owns 15 units, the largest FWD fleet of any single transportation agency in the world. TxDOT purchased its first unit in 1983 and has added additional FWDs on three- or four-year cycles over a span of 15 years. Therefore, the current fleet includes FWD units of different vintages and units with different components. Both good repeatability and reproducibility are considered to be of major importance for an adequate interchangeability of the FWD fleet. The first two tasks of the project consisted of evaluating the reproducibility and repeatability of the fleet and study the impact of the components on the reproducibility and repeatability of a given FWD. This report contains a summary of the results from these two tasks.

17. Key Words	18. Distribution Statement
Falling Weight Deflectometer, Remaining Life, Repeatability and Reproducibility, Calibration Process, Geophone, Load Cell	No restrictions. This document is available to the public through the National Technical Information Service, 5285 Port Royal Road, Springfield, Virginia 22161

19. Security Classif. (of this report)	20. Security Classif. (of this page)	21. No. of Pages	22. Price
Unclassified	Unclassified	122	

Reproducibility of Texas Department of Transportation Falling Weight Deflectometer Fleet

by

Sergio Rocha, BSEE
Vivek Tandon, PhD, PE
and
Soheil Nazarian, PhD, PE

Research Project 0-1784

Evaluate Reproducibility of TxDOT FWD Fleet and Recommend Improvements to FWD Calibration Procedure

Conducted for

Texas Department of Transportation

The Center for Highway Materials Research
The University of Texas at El Paso
El Paso, TX 79968-0516
Research Report 1784-1
September 2001

The contents of this report reflect the view of the authors, who are responsible for the facts and the accuracy of the data presented herein. The contents do not necessarily reflect the official views or policies of the Texas Department of Transportation or the Federal Highway Administration. This report does not constitute a standard, specification, or regulation.

NOT INTENDED FOR CONSTRUCTION, BIDDING, OR PERMIT PURPOSES

Sergio Rocha, BSEE
Vivek Tandon, PhD, P.E. (88219)
Soheil Nazarian, PhD, P.E. (69263)

Acknowledgements

The satisfactory progress of this project could not have happened without the help and input of many personnel of TxDOT. Andrew Wimsatt is the Project Director and Elias Rmeili is the Project Coordinator. Dar Hao Chen and Mike Murphy are the advisors to the project. The authors acknowledge Randy Beck and Carl Bertrand for their active participation in the progress of this project. Rob Light, Doug Chalman and Cy Helms are acknowledged for their assistance in field-testing. The authors are also grateful to John Ragsdale of TTI for coordinating our field work at Texas A&M Riverside Campus as well as assisting us in the fieldwork.

Abstract

The degree of accuracy with which the Falling Weight Deflectometer (FWD) data are collected and analyzed has a direct impact on the conclusions drawn in many aspects of TxDOT operation. TxDOT owns 15 units, the largest FWD fleet of any single transportation agency in the world. TxDOT purchased its first unit in 1983 and has added additional FWDs on three- or four-year cycles over a span of 15 years. Therefore, the current fleet includes FWD units of different vintages and units with different components. Both good repeatability and reproducibility are considered to be of major importance for an adequate interchangeability of the FWD fleet. The first two tasks of the project consisted of evaluating the reproducibility and repeatability of the fleet and study the impact of the components on the reproducibility and repeatability of a given FWD. This report contains a summary of the results from these two tasks.

Executive Summary

The Falling Weight Deflectometer (FWD) device has been extensively used by the Texas Department of Transportation (TxDOT) to support routine pavement design, to select rehabilitation strategies, to route super-heavy loads, to load zone, and to support other pavement management activities. A FWD primarily measures the pavement deflection at seven to nine points for a given load. The measured load and deflections, along with pavement parameters, are entered in a backcalculation program to obtain the stiffness profile of an existing pavement. These backcalculated moduli are then used to compute the strains at the interfaces of the pavement layers. The remaining life of the pavement is finally determined by using a semi-empirical relationship between the number of loads applied to the pavement and the critical strains at the interfaces of the different pavement layers. The degree of accuracy with which the FWD data are collected and analyzed has a direct impact on the conclusions drawn in many aspects of TxDOT operation.

The current fifteen-unit FWD fleet is of different vintages, and as such is manufactured of different components. Both good repeatability and reproducibility are considered to be of major importance for an adequate interchangeability of the FWD fleet. If the fleet is not reproducible, the predicted remaining life will depend on the FWD used. This will result in a systematic over- or under-estimation of the overlay thickness in a given region of the state. It will also positively or negatively impact the reported quality of a district's pavement condition.

The primary objective of this project is to develop realistic field protocols and specifications, which in a rational manner will allow TxDOT personnel to quantify the repeatability and reproducibility of existing and future FWD devices. As a result of this activity, a more comprehensive calibration methodology will be developed. Some of the outcomes of the project will allow those who are involved in repairing and upgrading FWDs to decide more quantitatively when to replace components (such as buffers and sensor holders) to maintain a fully reproducible fleet.

The first two tasks of the project consisted of evaluating the reproducibility and repeatability of the fleet and study the impact of the components on the reproducibility and repeatability of a given FWD. This report contains a summary of the results from these two tasks.

Implementation Statement

The major outcome of this project is potentially a new test protocol, a replacement strategy and recommendations for a more rigorous maintenance schedule for the FWD fleet.

The new procedure not only will improve the precision and accuracy of the FWD readings, it will also assist TxDOT in extending the life of the fleet by replacing defective parts long before they cause failure in the system.

Table of Contents

ACKNOWLEDGEMENTS VII
ABSTRACT IX
EXECUTIVE SUMMARY XI
IMPLEMENTATION STATEMENT XIII
TABLE OF CONTENTS XV
LIST OF FIGURES XVII
LIST OF TABLES XIX
CHAPTER 1 INTRODUCTION 1
PROBLEM STATEMENT 1
OBJECTIVE 2
ORGANIZATION 2
CHAPTER 2 REVIEW OF LITERATURE 3
SHRP CALIBRATION METHOD 3
Relative Calibration Procedure 4
Reference Calibration Procedure 4
TXDOT PORTABLE CALIBRATION METHOD (PROJECT 913) 5
TXDOT CALIBRATION SYSTEM (PROJECT 2984) 5
CROW CALIBRATION METHOD 6
Protocol A: Relative Calibration Verification of Deflection Sensors 6
Protocol B: Short-term Repeatability Verification. 7
Protocol C: Long-term Repeatability Verification. 7
Protocol E: FWD Deflection Sensor Calibration Verification. 7
Protocol F: Group Field Calibration Procedure. 8
Protocol G: FWD Field Calibration 8
Protocol H: Reference Calibration of Load Cell 8
REPEATABILITY AND REPRODUCIBILITY 9
CHAPTER 3 REPEATABILITY AND REPRODUCIBILITY OF TXDOT FLEET 11
SELECTION OF FWDS 11
SITE SELECTION 12

SITE PREPARATION 12
TEST PROTOCOL 16
DATA ANALYSIS 16
Impact of External Factors *17*
Reproducibility *27*
CHAPTER 4 STATISTICAL ANALYSIS OF REPEATABILITY AND REPRODUCIBILITY 35
REPEATABILITY 36
Individual Sites *36*
Individual FWD *38*
Individual Drop Heights *38*
REPRODUCIBILITY 41
Individual Sites *41*
Individual Drop Heights *44*
Individual Sensors *46*
Impact of Calibration *46*
Similarity of Devices *47*
CHAPTER 5 CHARACTERISTICS OF FWD SYSTEM DURING LOADING 51
INSTRUMENTATION 51
Characteristics of Strike Plate *53*
Characteristics of Load Plate *56*
CHAPTER 6 IMPACT OF FWD COMPONENTS ON RESPONSE OF SENSORS 67
RUBBER BUFFERS 67
Laboratory Characterization of Buffers *68*
Field Characterization of Rubber Buffers *71*
GEOPHONE HOLDERS 74
CHAPTER 7 CLOSURE 79
SUMMARY 79
CONCLUSIONS 79
FUTURE DIRECTIONS 80
REFERENCES 81
APPENDIX A REPEATABILITY DISTRIBUTION CHARTS 83
APPENDIX B REPRODUCIBILITY DISTRIBUTION CHARTS 111

List of Figures

Figure 3.1 – Location of Test Site in Riverside Campus of Texas A&M University.....13
Figure 3.2 – A Typical Site Prepared for Testing (Site 1).....15
Figure 3.3 – Data Reduction Process for Evaluation Impact of External Parameters.....18
Figure 3.4 – Typical Results from Data Reduction Process for One Sensor.....19
Figure 3.5 – Influence of External Factor on Reproducibility on Site 1.....20
Figure 3.6 – Typical Coefficients of Variation Measured at Site 1 for Drop Height 2.....23
Figure 3.7 – Effect of Drop Height on Coefficients of Variation (After SHRP Calibration)...25
Figure 3.8 – Maximum Coefficients of Variation Observed for All Sites and All Drop Heights.....26
Figure 3.9 – Comparison of Repeatability of FWD Fleet Before and After SHRP Calibration.....27
Figure 3.10 - Data Reduction Process for Reproducibility Analysis.....28
Figure 3.11 - Variations in Average Difference from Mean (Grand Average of all FWDs for Drop Height 1.....30
Figure 3.12 - Impact of SHRP Calibration on Reproducibility of FWD Fleet.....32
Figure 3.13 - Comparison of Deviation from Grand Average from Before and After SHRP Calibration.....33
Figure 4.1 - Distribution of coefficients of Variation from all FWDs at Site 1.....36
Figure 4.2 - Comparison of Histograms of COVs from Before and After SHRP Calibration Process for FWD 024.....41
Figure 4.3 - Distribution of Coefficients of Variation from all FWDs at Site 1.....43
Figure 4.4 - Histograms of Deviation Indices from Before and After Calibration.....45
Figure 4.5 - Analysis of Variance on Difference from baseline measured at Three Sites with Six FWDs.....47
Figure 4.6 - Histograms of Difference from baseline from Two FWD Units.....49
Figure 5.1 - Typical Sensors Used in This Study.....51
Figure 5.2 - Schematic of Set up Used for Measuring Behavior of Strike Plate.....53
Figure 5.3 - Variation in Typical Strain Time Histories of Strike Plates.....54
Figure 5.4 - Schematic of Strike Plate Designs.....54
Figure 5.5 - Typical Load and Deflection Time Histories from Two Types of FWD Structures.....54
Figure 5.6 - Impact of Rotating Buffers from Same FWD.....56
Figure 5.7 - Installation of Strain Gauges on Load Plate.....57

Figure 5.8 - Typical Variations in Strain Time Histories along FWD Load Plate.....57
Figure 5.9 - Variations in Strain Time Histories along FWD Load Plate (Brand New Load Plate Assembly).....58
Figure 5.10 - Comparison of a Solid Plate Assembly and a Split Plate.....59
Figure 5.11 - Variation in Strain Time Histories along FWD Load Plate (Split Load Plate).....59
Figure 5.12 - Comparison of Load Time Histories Reported by FWD from Three Different Load Plates.....60
Figure 5.13 - Comparison of Deflection Time Histories Reported by FWD from Three Different Load Plates.....61
Figure 5.14 - Typical Placement of Accelerometers on Load Plate.....61
Figure 5.15 - Typical Motion of Load Plate.....62
Figure 5.16 - Instrumentation of Raise-Lower Bar.....63
Figure 5.17 - Typical Movement of Raise-Lower Bar.....63
Figure 5.18 - Instrumentation of FWD Trailer (Sergio add this Figure).....64
Figure 5.19 - One Type of Movement of FWD Trailer.....65
Figure 5.20 - Alternative Type of Movement of FWD Trailer.....65
Figure 6.1 - Laboratory Characterization of Load Buffers.....68
Figure 6.2 - Typical Load-Deformation Behavior of FWD Rubber Buffers.....69
Figure 6.3 - Typical Stress-Strain Relationship of Rubber Buffer.....70
Figure 6.4 - Effect of Temperature on Rubber Buffer Performance.....70
Figure 6.5 - Typical New and Old Buffers from FWD 024.....71
Figure 6.6 - Typical Load Cell Time Histories from New and Old Buffers.....73
Figure 6.7 - Typical Deflections Time Histories from New and Old Buffers.....73
Figure 6.8 - Typical Responses of FWD Sensor and Sensor Holder.....74
Figure 6.9 - Typical Sensor Holder Assembly.....75
Figure 6.10 - Comparison of Typical Responses of a FWD Sensor from Original and Brand New Holder.....75
Figure 6.11 - Typical Impact of Stiffness of Hold Down Springs on Measured Deflections....76
Figure 6.12 - Typical Deflection Time Histories from New and Old Neoprene Guides.....77

List of Tables

Table 2.1- Calibration Procedures Proposed by CROW 6
Table 3.1 – FWD Selected for Benchmark Reproducibility Evaluation 11
Table 3.2 – Layer Information of Selected Sites 12
Table 3.3 – Average Deflections from Three Sites Normalized to 9 kips 14
Table 3.4 – Maximum Deviation Index from Three Sites 21
Table 3.5 – Average Coefficients of Variation from Three Sites at a Nominal Load of 9 kips 30
Table 3.6 – Average Difference from Baseline Values from Three Sites at a Nominal Load of 9 kips 30
Table 4.1 – Statistical Information about Distribution of Coefficients of Variation from All FWDs at Three Sites Tested 37
Table 4.2 – Statistical Information about Distribution of Coefficients of Variation from All Sensors for Six FWDs 39
Table 4.3 – Statistical Information about Distribution of Coefficients of Variation from All Sensors for Six FWDs 39
Table 4.4 – Statistical Information about Distribution of Coefficients of Variation from All Sensors for Six FWDs 40
Table 4.5 – Impact of Calibration on Repeatability of FWD Fleet 43
Table 4.6 – Statistical Information about Distribution of Difference from baseline 43
from All FWDs at Three Sites Tested 43
Table 4.7 – Statistical Information about Distribution of Differences from baseline from All Sensors for Six FWDs 45
Table 4.8 – Statistical Information about Distribution of Differences from baseline from All Sensors for Six FWDs 45
Table 4.9 – Impact of SHRP Calibration on Improving Reproducibility of FWD Fleet 47
Table 4.10 – Statistical Evaluation of Reproducibility of Fleet at Each Site 48
Table 4.11 – Statistical Evaluation of Reproducibility of Fleet at Each Site 48
Table 4.12 – Statistical Evaluation of Interchangeability of Pairs of FWDs in Fleet 50
Table 6.1. – Test Results of Commercial and Dynatest Rubber Buffers 72

Chapter 1

Introduction

Problem Statement

Among a number of available nondestructive (NDT) methods, the Falling weight Deflectometer (FWD) is commonly considered to provide the estimates of material properties that are compatible with loads exerted by truck wheels. The FWD device has been extensively used by the Texas Department of Transportation (TxDOT) to support routine pavement design, to select rehabilitation strategies, to route super-heavy loads, to load zones, and to support other pavement management activities. A FWD primarily measures the pavement deflection at seven to nine points for a given load. The measured load and deflections along with pavement parameters are entered in a backcalculation program to obtain the stiffness profile of an existing pavement. These backcalculated moduli are then used to compute the strains at the interfaces of the pavement layers. The remaining life of the pavement is finally determined by using a semi-empirical relationship between the number of loads applied to the pavement and the critical strains at the interfaces of the different pavement layers.

The degree of accuracy of collected and analyzed FWD data has a direct impact on the conclusions drawn in many aspects of TxDOT operation. TxDOT owns 15 units, the largest FWD fleet of any single transportation agency in the world. TxDOT purchased its first unit in 1983 and has added additional FWDs on three- to four-year intervals over a span of 15 years. Although the same manufacturer has developed all FWDs, the performance of the fleet is not always comparable. Over time TxDOT has rebuilt a few of the FWDs in-house. Therefore, the current fleet consists of different vintage FWD units with different components. There is a concern that these differences may result in varying measured deflections among different FWDs. Some of the differences in equipment components include:

- At least two different designs for the outer and inner geophone holder;
- Variations in the inner geophone holder measuring rod lengths;
- At least two different designs for the load cell connection;
- Variation in electrical and hydraulic components;

- Variation in the design and condition of the rubber buffers;
- Variations in the design of buffer strike plates.

All of these components may impact the reproducibility of the parameters measured with the fifteen FWDs, and as such, the predicted remaining life of the pavements being studied.

Both good repeatability and reproducibility are considered to be of major importance for an adequate interchangeability of the FWD fleet. A fleet of FWDs is said to be reproducible if it measures almost identical deflection basins for a specific site under identical testing conditions. If the fleet is not reproducible, the predicted remaining life will depend on the FWD used. This will result in a systematic over- or under-estimation of the overlay thickness in a given region of the state. It will also positively or negatively impact the reported quality of a district's pavement condition. To evaluate the reproducibility of a FWD fleet, it is essential that each individual FWD is precise and accurate. A single FWD is repeatable if it yields almost identical deflection basins at a test site for multiple drops imposed under identical testing conditions.

Objective

The primary objective of this project is to develop realistic field protocols and specifications, which will allow TxDOT personnel to quantify the repeatability and reproducibility of existing and future FWD devices in an efficient manner. As a result of this activity, a more comprehensive calibration methodology will be developed. Additional outcome of the project will be new decision-making tools for maintaining a reproducible fleet. New tools will guide those who are involved in repairing and upgrading FWDs to decide more quantitatively when to replace components (such as buffers and sensor holders) to maintain a fully reproducible fleet.

The first two tasks of the project consisted of evaluating the reproducibility and repeatability of the fleet and study the impact of the components on the reproducibility and repeatability of a given FWD. This report contains a summary of the results from these two tasks.

Organization

The report consists of seven chapters. A review of literature focusing on efforts for calibrating and harmonizing the measurements with the FWDs by other agencies worldwide is included in Chapter 2. The protocols developed for determining the repeatability and reproducibility of the fleet is included in Chapter 3. In addition, the evaluation of the repeatability and reproducibility of the fleet are presented in Chapter 3. Comprehensive statistical analyses of the results presented in Chapter 3 are reported in Chapter 4. Chapter 5 is dedicated to the instrumentation used to measure the characteristics of the FWD device during field operation. The impact of the FWD components on the measured load and deflections are included in Chapter 6. Summary, conclusions and the future work plan are described in Chapter 7.

Chapter 2

Review of Literature

To maintain a reproducible FWD fleet, it is essential that all FWDs are accurate and precise. Thus, it is important that the reference or "absolute" calibration issues are addressed first, followed by the repeatability and then the reproducibility issues. It is critical to accurately determine the deflection basins and imparted loads in the field. Nazarian and Stokoe (1986) and Nazarian and Briggs (1989) have suggested that small errors in measured deflections may yield significantly erroneous modulus values. Hence, the use of a reliable method for evaluating the accuracy of the sensors used for determining deflections is essential.

Three different calibration systems for evaluating the accuracy and precision of the FWD sensors have been developed. One of them, developed by the Strategic Highway Research Program (SHRP), performs a relative as well as a reference calibration of the geophones. The second method is a so-called Texas Calibration Method, which was developed at UTEP for TxDOT (Project 913). Under Project 2984 a third procedure was proposed. Recently, Dutch Information and Technology Centre (CROW) have developed an extensive calibration standard that seems to be adapted by many highway agencies in Europe. Each method is briefly described next.

SHRP Calibration Method

Under the SHRP protocols, two types of calibrations are performed: 1) a reference calibration and 2) a relative calibration. In the SHRP reference calibration, deflections measured with a FWD are compared with those measured with an independent reference sensor that meets benchmarks traceable to the National Institute of Standards and Technology. On the other hand, the relative calibration ensures that the FWD sensors provide consistent results and function correctly. A brief description of these procedures is included here. A detailed description of them can be found in ASTM D4694.

Relative Calibration Procedure

The goal of the relative calibration procedure is to ensure that all sensors reproduce the same deflection under a given impact (i.e., the system is precise). The relative deflection calibration requires a sensor holding tower. The tower must have sufficient positions to accommodate all sensors used in a FWD. The sensors are stacked one above the other along a vertical axis. During the calibration, the sensors are rotated so that each sensor occupies every level in the tower. At each tower position, five deflections are recorded for each sensor. Deflections of about 15 mils are desired. Deflection ratio is determined for each sensor by dividing the average deflection of a specific sensor by the average deflection for all sensors. If any of the resulting ratios are greater than 1.003 or less than 0.997, all sensor calibration factors should be adjusted.

To ensure that small deflections are monitored to a reasonable degree of accuracy, the above procedure is also repeated for a deflection between 2 and 4 mils. If the average difference between any two-sensor readings is 0.08 mils or less, the calibration factors should not be altered. On the other hand, if the differences in average deflections are greater than 0.08 mils, the device should be repaired and recalibrated according to the manufacturer's recommendations.

Reference Calibration Procedure

The relative calibration ensures that all geophone readings are consistent. But it does not ensure that the deflections are accurate. The reference calibration is conducted to determine the accuracy of sensors. The SHRP reference calibration system uses a Liner Variable Differential Transformer (LVDT) as the reference deflection measurement device. The LVDT and a FWD geophone are mounted in special holders so that the magnetized tip of the LVDT core is always in contact with the top of the geophone holder, and hence is always subjected to the same movement as the geophone. The LVDT is mounted at the end of a wide-flange beam. The geophone holder is securely screwed to the pavement. During the calibration process, each geophone is taken out of the holder and placed in the fixed holder placed under the reference calibration beam. The geophone calibration data are collected at two deflection levels similar to that of the relative calibration procedure. Ten sets of deflection data are collected for each deflection level. The calibration factors are then calculated for each geophone.

The load cell is calibrated using a reference load cell. The reference load cell consists of an aluminum case, 11.8 in. (300 mm) in diameter, and 3.25 in. (83 mm) high, with four measuring links equally spaced on a 7.5 in. (190 mm) circle. A ribbed neoprene sheet, identical to that on the bottom of the FWD loading plate, is glued to the bottom of the reference load cell to ensure uniform pressure on the pavement surface. For each FWD, load cell calibration is performed at four load levels, with ten tests at each level. A relationship is developed between the FWD load cell and the reference load cell. The developed relationship can then be used for modifying the FWD load cell readings.

This method of calibration has two disadvantages. First, the geophone is taken out of the holder and placed in a rigid frame. As such, one does not calibrate the geophone system but only the geophone itself. It would be possible for the geophone to be working properly while the holding mechanism is worn out. In that situation, the calibration of the geophone will be accurate, but

the results obtained from the FWD system may not be accurate. Second, the accuracy of the system is determined at 15 mils and 2 mils. Deflections measured in the field can be as high as 100 mils. Therefore, potential problems at higher deflections cannot be identified with this method of calibration.

In recent years, highway agencies have started focusing on the issue of using the whole time history record of the geophone rather than using only peak deflections (Uzan, 1994). For accurate and precise measurement of the deflection time history, it is essential to evaluate the performance of the geophone over a range of frequencies and multiple deflection levels. SHRP protocol provides a means to calibrate for peak deflections.

TxDOT Portable Calibration Method (Project 913)

A portable reference calibration system, which can be used in the field, has also been developed at UTEP. This calibration system consists of two well-calibrated geophones, three load cells, a load-bearing plate, and a data acquisition system (Nazarian et al., 1991). The well-calibrated geophones are placed next to the FWD geophones with the help of modeling clay or vacuum grease. After the placement of the geophones, the load is dropped ten times from each drop height. Similar to the SHRP procedure, the deflection measured from the FWD and the calibration system geophones are compared to identify the accuracy of the individual geophone.

One advantage of this calibration system is that the FWD geophones are not removed from the FWD holders, therefore providing the calibration of the geophone system (not the geophone alone). The disadvantages of the system are that 1) similar to the SHRP method, this method can only calibrate for peak deflections, and 2) this method of calibration cannot be applied to the geophone located in the center of the loading plate.

The load cell calibration procedure is similar to the SHRP procedure except that the three dynamic load cells, sandwiched between two steel plates, are used in the Texas Calibration method. The load cells are affixed to the bottom plate, and the load is transferred to them through the top plate. The summation of peak loads obtained from the three load cells is compared with the load measured by the FWD load cell.

TxDOT Calibration System (Project 2984)

Based on the shortcomings of the two systems described, a more comprehensive calibration system has been developed under Project 2984. The system is capable of calibrating geophones over a wide range of frequencies and deflections such that the whole time history of a deflection basin can be obtained accurately and precisely. The modified calibration method is also capable of identifying the problems associated with the FWD holding system or the geophones. Thus, the highway agencies can determine when to replace the geophone holders or the geophones. A detailed discussion of the methodology is included in Research Report 2984-1.

Briefly, a 16 in. (410 mm) by 11.4 in. (290 mm) utility box is retrofitted into a 5 in. (140 mm) thick PCC slab. A shaker is placed in the utility box below the ground level such that the top of the shaker table is flush with the surface of the slab. In this manner, the FWD geophone holder can easily be placed on top of the shaker without any disassembly. The surface on which the shaker is placed is leveled to minimize any eccentric movement of the reference or the FWD geophone. A well-calibrated geophone is securely embedded in the shaker as a reference. The FWD geophone is then lowered onto the shaker in its holder using the FWD raise-lower mechanism. A signal can be sent to the shaker via an amplifier. The response of the FWD in-holder can be compared with the reference geophone to not only determine the accuracy of the peak deflection but also the variation of the calibration value with frequency. This distinction is of critical importance should TxDOT decide to implement a dynamic, full-waveform analysis method.

CROW Calibration Method

Dutch Information and Technology Centre (CROW) have recently developed an extensive calibration standard that seems to be adapted by many highway agencies in Europe (CROW, 1999). CROW advocates a two-level approach to reduce the calibration activities to a minimum. The first level consists of rather simple and fast relative calibrations and calibration verifications to be performed by each FWD user. The second level consists of reference calibration and calibration verification that is performed in a calibration facility. CROW has written seven calibration procedures for their two-level approach. These approaches, which are listed in Table 2.1, are summarized below.

Table 2.1- Calibration Procedures Proposed by CROW

Level	Protocol	Title	Remarks
1	A	RELATIVE CALIBRATION VERIFICATION OF DEFLECTION SENSORS	SIMILAR TO SHRP RELATIVE CALIBRATION
	B	SHORT-TERM REPEATABILITY VERIFICATION	Currently carried out by TxDOT FWD operators
	C	Long-term Repeatability Verification	
2	E*	Deflection Sensor Calibration Verification	Similar to TxDOT procedure
	F	Group Field Calibration Procedure	Currently not utilized in US
	G	Field Calibration Procedure	
	H	Reference Calibration of Load Cell	Similar to SHRP or TxDOT procedures

Note: Protocol D was withdrawn by CROW

Protocol A: Relative Calibration Verification of Deflection Sensors

Relative calibration verification of FWD deflection sensors is applied to ensure that all sensors on a given FWD are consistent with one another. In this procedure, all FWD deflection sensors are dismounted and stacked coaxially above each other in a deflection sensor stand, so that they all will

be exposed to the same deflection. The objective of the test is to verify similarity of the response of each of the deflection sensors. If one or more sensors generate different results, the deflection sensor gain factors should be adjusted. If large adjustments are required, the sensors should be subjected to closer investigation.

Protocol B: Short-term Repeatability Verification.

The objective of this procedure is to verify whether the FWD under test is capable of producing consistent results on a specific test site. In this procedure, the short-term repeatability of an FWD is verified by using a series of twelve successive drops without lifting the loading plate. The deflections are all normalized to a reference load level. The standard deviation of the load and normalized deflections should agree within specified limits. When the results do not meet the requirements, the test should be repeated. Cases of persistent non-compliance invalidate data collected by the instrument under test.

Protocol C: Long-term Repeatability Verification.

In this procedure, the long-term repeatability of the FWD under test is verified by using a series of eight successive drops. The deflections are all normalized to a target load. The mean of the normalized deflections is compared to results previously collected at the same location. This location should preferably be selected close to the FWD home base and protected from climatic influences as much as possible. The objective of this test is to detect any anomalies in the deflection output. Deflection results will not be constant over the year due to temperature and seasonal changes. For that reason the test provides only subjective results. It reveals whether unexpected absolute changes of deflection have occurred, whereas in the first step of this stage of calibration, only the relative deflections among deflection sensors were investigated. If the output does not seem reasonable, load cell and deflection sensors should be examined to identify the source of the problem.

Protocol E[1]: FWD Deflection Sensor Calibration Verification.

The objective of this procedure is to verify whether the FWD system is capable of producing correct peak values of deflection in cases of varying durations of deflection pulses. In this procedure, the FWD deflection sensor is dismounted and attached to a vibration table. The sensor is subjected to various series of single shock deflection pulses consisting of multiple combinations of displacement amplitude and deflection pulse rise time. The output of the sensor is compared to the output of a reference displacement transducer. When the variation and differences in output data are not within specified limits, the source of the problem should be identified. If the deflection pulse rise time happens to have a specific influence on the relationship between the deflection provided by the FWD deflection sensor and that provided by reference instrumentation, the sensors and the system processing electronics should be shipped to the FWD manufacturer for repair and recalibration. Also, presence of dispersion in the FWD deflection sensor data in excess of specified values necessitates shipping the equipment to the

[1] Note: Protocol D was withdrawn by CROW

FWD manufacturer for repair. When the FWD manufacturer has corrected the problem and returned the instrument, this calibration verification procedure should be performed again. In all other cases of non-compliance, gain factors are determined to adjust deflection sensor output to reference instrumentation output.

Protocol F: Group Field Calibration Procedure.

In this procedure, a group of FWDs is calibrated against a reference group of FWDs, which form a part of the entire FWD fleet under test. Prior to testing, CROW assigns which FWD entries form the eligible group of FWDs from which the reference group will be composed. This action is taken to ensure year-to-year consistency in reference deflections.

The FWD group field calibration procedure is conducted on various types of asphalt pavements on various subgrades with various degrees of load-carrying capabilities. A minimum of 30 test stations is required. Criteria are set to the distribution of the test stations over the various types of pavements and subgrades. Per station five drops (of which four are analyzed) using a target load level of 50 kN are imposed to collect the deflection data. Deflections are normalized to a load level of 50 kN and in the next step compared to the reference data. Corrective calibration factors are derived based on comparison of the reference deflections and the deflections measured by the FWD under test. Field calibration factors are given per FWD and not per FWD deflection sensor. If the variation in deflection data of the FWD under test is too large, or when the calibration factor is beyond tolerances, the FWD under tests fails to pass the specifications.

Protocol G: FWD Field Calibration.

In this procedure the output of the FWD under test is compared to the results of an FWD that holds a valid CROW FWD certificate. This FWD will be termed as the reference FWD. This procedure is conducted on various asphalt pavement structures with weak, medium and stiff subgrade. The same test station criteria as used in the FWD group field calibration apply to this procedure. All deflections are processed by statistical techniques for detecting significant differences between the results of the FWD under test and the reference FWD. A FWD calibration (multiplicative) factor is developed on the basis of the test data to make the deflections recorded by the FWD under test as identical as possible to the reference deflections. The procedure serves as an emergency procedure and is meant for FWDs failing to pass the FWD group field calibration criteria.

Protocol H: Reference Calibration of Load Cell.

Reference calibration of the FWD load cell is applied to ensure that the peak value of the FWD load is accurate. This peak value is frequently used in normalization of deflection data to reference load levels. In this process inaccurate and unreliable FWD load cells may cause wide deviations in normalized deflections, whereas the raw deflections may be subject to much smaller and acceptable variation in a series of multiple drops. In this procedure, the loading plate of the FWD is placed coaxially above a reference load platform. Three cycles of various drop height are used to record the peak value of the FWD load cell and the reference load platform. This test should be conducted at least twice. The ratio of the recordings of the two load recording

instruments is the new gain factor for the FWD load cell. Obviously, large adjustments and dispersion in the test data invalidate the test results.

Repeatability and Reproducibility

Realistically, one should understand that under the operational conditions it might not be practical to expect a 100% repeatable and reproducible fleet. One has to accept that, irrespective of the efforts placed on calibration, the fleet will contain a small systematic error and each individual FWD will be slightly out of calibration shortly after leaving the calibration facility. Accepting this reality, one has to define a threshold of tolerance above which the lack of accuracy and reproducibility is not acceptable. The acceptable thresholds for variations in deflections and load measured with the FWD not only depend on the level of sophistication of the analytical methods used to calculate the remaining lives, but they are also somewhat dependent on the institutional issue of how often the devices can be calibrated. Vanalaganti et al. (1994) somewhat address the technical aspects of this question using the Monte Carlo simulation with several existing remaining life algorithms.

Murphy (1998) contains an excellent overview of parameters that may contribute to the lack of reproducibility or repeatability of an FWD fleet. Not only Murphy provides a physical explanation of the behavior of the FWD, he also approaches the issue from the day-to-day operation and maintenance of the system. The reader is encouraged to refer to that document. Several groups have studied the reproducibility of various FWDs. Bensten et al. (1989) investigated the accuracy, reliability and repeatability of seven NDT devices. They found reasonable repeatability, but showed some concern with the reproducibility of different FWDs.

Van Gurp (1991) designed an experiment to determine the reproducibility of various types of FWDs such as Kuab, Phonix, and Dynatest. Van Gurp reported that most FWDs were repeatable. However, he also reported large variability (i.e., a coefficient of variation of up to 80%) amongst different makes of FWDs. He stated that the reproducibility of the three Dynatest FWDs used were about 10%. He also found good correlation between the load impulse energy and the deflection measured by the central sensor.

Lukanen (1992) studied the reproducibility of one FWD with three different sets of buffers. He concluded that the shape and size of buffers impact the rise time and the load pulse shape. As a consequence of change in the shape and rise time, the magnitude of the deflections changed. Depending on the pavement structure, the variation in deflection was from less than 2% to more than 10% with an average of about 6%.

Chen et al. (1999) conducted a study to investigate the impact of buffers on the response of the FWD. They studied the impact of the shape, size, age and stiffness of the buffers on the magnitude of peak load, load pulse duration and rise time, as well as the peak deflection. They concluded that the stiffness and shape of the buffers might impact the measured pavement response, especially when weaker flexible pavement sections are tested.

All these studies indicate that in order to improve the reproducibility and repeatability of a FWD fleet, a more sophisticated calibration process may be needed.

Chapter 3

Repeatability and Reproducibility of TxDOT Fleet

To evaluate the repeatability and reproducibility of the existing TxDOT FWD fleet, a preliminary investigation was performed. The FWD and site selection process along with the test protocol followed for this evaluation are described in this chapter. The results from this activity are also presented.

Selection of FWDs

The initial intention of the research team was to evaluate the reproducibility and repeatability of all fifteen FWDs. It was logistically impossible to have all FWDs available at one place at one time. In consultation with the project management committee (PMC), the number of FWDs evaluated was reduced to six. The six FWDs listed in Table 3.1 were selected in close interaction with TxDOT personnel in charge of operation and maintenance of the fleet. The selection criteria were based on the availability and the age of the devices. TxDOT fleet was primarily purchased in four time periods. At least one FWD from each time period was represented. This was desirable because of continuous modifications in the overall design and components of the FWD trailer by the manufacturer.

Table 3.1 – FWD Selected for Benchmark Reproducibility Evaluation

Serial No	District	Year of Acquisition	Last SHRP Calibration
024	Austin	1984	October 98
040	Amarillo	1986	December 98
047	Waco	1987	October 98
069	Dallas	1989	January 99
089	Odessa	1990	June 99
159	MLS	1998	September 99

TxDOT annually calibrates their entire FWD fleet annually using the SHRP procedure. During the calibration of each unit, the condition of the FWD trailer, the integrity of individual mechanical and electronic components, and the appropriateness of the electric system are also thoroughly checked. Since the most recent calibration of each of the six FWDs varied from about a year to about a month, the reproducibility and repeatability were investigated in two phases, just before SHRP calibration (conducted in early December 1999), and just after calibration (early January 2000).

Site Selection

Three pavement sections, two flexible and one rigid, were selected. The layering at each site is summarized in Table 3.2. All three sites, which were located in the Riverside Campus of Texas A&M University, have been well documented and studied. The general locations of the three sites are shown in Figure 3.1. The strong flexible site, located in front of Building 7181, was Section 9 of the Texas Transportation Institute experimental pavements section. The weak flexible pavement section was located along Avenue D (between 6^{th} and 7^{th} street). The rigid pavement site was part of the existing runway, and was located in front of Building 7098.

The overall average deflections (based on five drops and three attempts) from the three sites at a load level of 9 kips (40 KN) from before and after calibration are presented in Table 3.3. Significant differences exist between the deflections from the two flexible sites. This will allow us to observe the impact of the flexibility of the site on the reproducibility and repeatability of the results. The deflections from the rigid and strong flexible sites are fairly close. This information can be used to focus on the impact of the top pavement layer on the reproducibility.

Table 3.2 – Layer Information of Selected Sites

Site	Condition	Layer Information
1	Strong Flexible	5 in. (125 mm) ACP
		12 in. (300 mm) Stabilized Base
2	Weak Flexible	1.5 in. (37 mm) ACP
		10 in. (250 mm) Granular Base
3	Rigid	8 in. (200 mm) PCC

Site Preparation

At each site, the section was thoroughly inspected to ensure that the pavement was free of distress, i.e., no cracking or rutting was visible. The location of the load plate and the orientation of the sensors were clearly marked to ensure that same point is tested each time (Figure 3.2). To facilitate the precise positioning of the FWD at each test location, the site was striped with masking tape from about 30 ft (10 m) before the test location. This strategy was effective in minimizing the set up time and as such the overall test period.

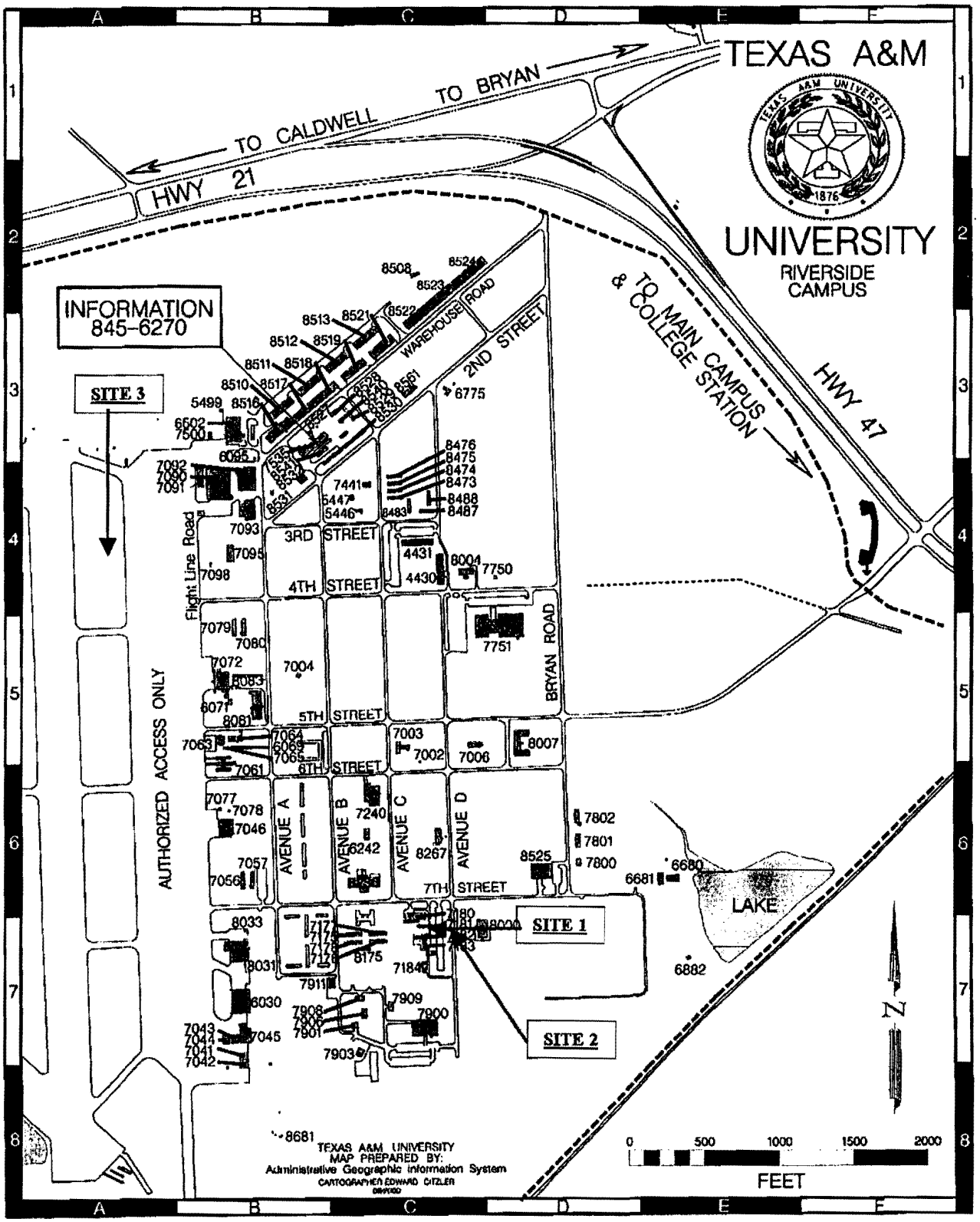

Figure 3.1 – Location of Test Site in Riverside Campus of Texas A&M University

Table 3.3 – Average Deflections from Three Sites Normalized to 9 kips

a) Site 1

Serial No.	Test* Period	Average Deflections Normalized to 9 kip Load, mils						
		D1	D2	D3	D4	D5	D6	D7
024	B/C	8.19	5.72	3.50	2.39	1.78	1.46	1.25
	A/C	8.02	5.78	3.58	2.40	1.77	1.43	1.17
040	B/C	7.61	5.17	3.03	2.03	1.50	1.24	1.02
	A/C	7.83	5.35	3.15	2.10	1.52	1.26	1.03
047	B/C	7.49	5.01	3.02	1.87	1.47	1.20	0.99
	A/C	7.59	5.20	3.13	2.06	1.52	1.22	1.00
069	B/C	7.24	4.90	2.94	1.95	1.45	1.22	0.99
	A/C	7.34	5.07	3.03	1.99	1.48	1.18	1.01
089	B/C	8.08	5.49	3.22	2.17	1.66	1.35	1.14
	A/C	8.34	5.75	3.46	2.24	1.72	1.43	1.12
159	B/C	8.04	5.28	3.13	2.03	1.65	1.33	1.07
	A/C	8.06	5.65	3.28	2.18	1.60	1.25	1.08

b) Site 2

Serial No.	Test* Period	Average Deflections Normalized to 9 kip Load, mils						
		D1	D2	D3	D4	D5	D6	D7
024	B/C	38.27	22.88	12.03	7.28	4.93	3.75	3.07
	A/C	39.50	23.32	11.68	7.04	4.82	3.69	2.92
040	B/C	41.53	23.55	11.80	7.10	4.75	3.69	3.01
	A/C	43.21	23.96	11.46	6.84	4.59	3.66	3.02
047	B/C	40.15	22.07	11.45	6.61	4.67	3.59	2.81
	A/C	43.14	22.94	11.47	6.84	4.73	3.62	2.91
069	B/C	39.92	21.96	11.54	6.76	4.77	3.56	2.88
	A/C	42.42	22.71	11.33	6.69	4.66	3.60	2.94
089	B/C	39.36	21.88	11.20	6.61	4.54	3.43	2.78
	A/C	42.80	23.49	11.48	6.66	4.61	3.53	2.86
159	B/C	39.21	21.42	11.03	6.50	4.55	3.36	2.82
	A/C	40.89	22.64	11.12	6.51	4.45	3.39	2.76

c) Site 3

Serial No.	Test* Period	Average Deflections Normalized to 9 kip Load, mils						
		D1	D2	D3	D4	D5	D6	D7
024	B/C	7.75	6.80	5.46	4.16	3.04	2.16	1.70
	A/C	7.36	6.55	5.24	3.99	2.80	1.85	1.43
040	B/C	6.98	6.28	4.91	3.63	2.58	1.84	1.43
	A/C	6.81	6.04	4.71	3.60	2.49	1.73	1.33
047	B/C	6.86	6.00	4.77	3.31	2.57	1.79	1.37
	A/C	6.72	5.84	4.61	3.49	2.45	1.61	1.24
069	B/C	6.66	5.80	4.63	3.50	2.53	1.73	1.34
	A/C	6.06	5.30	4.21	3.20	2.28	1.41	1.09
089	B/C	7.38	6.52	5.13	3.83	2.83	2.03	1.50
	A/C	7.38	6.52	5.17	3.82	2.71	1.89	1.39
159	B/C	7.20	6.20	4.88	3.74	2.79	1.88	1.44
	A/C	6.93	6.14	4.85	3.66	2.58	1.72	1.36

*** B/C denotes Before Calibration and A/C denotes After Calibration**

a) FWD Approaching Test Strip

b) FWD Aligned with Test Strip

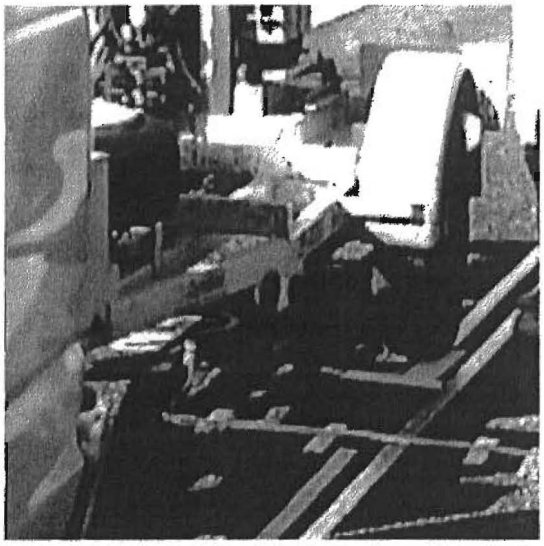

c) FWD Aligned with Test Spot

d) Load Plate Lowered for Test

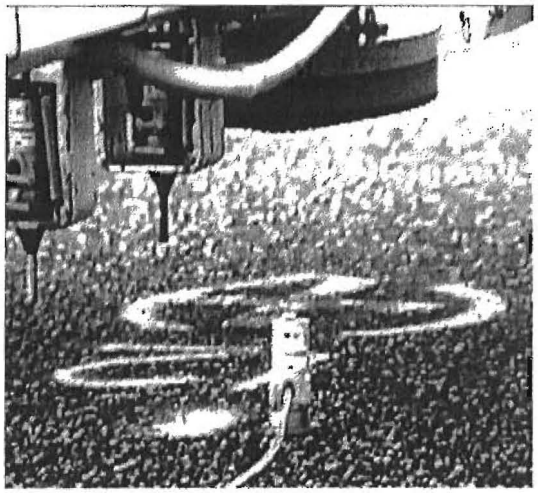

e) Close up of Load Plate Circle

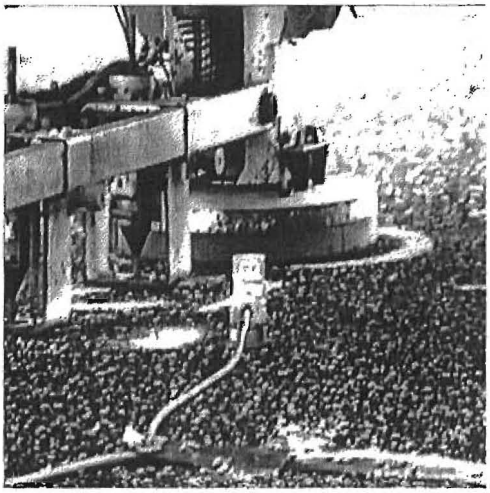

f) FWD Load Plate Within Circle

Figure 3.2 – A Typical Site Prepared for Testing (Site 1)

At each site, two thermocouples were installed to monitor the changes in pavement and air temperature during testing. The monitoring of temperature was essential in ensuring that the change in temperature would not impact our study. In addition, tests were carried out at or after sunset to minimize the change in temperature during testing. In general, the average change in pavement temperature from beginning to end of testing was less than 3°F (2°C) at each site.

To ensure that repeatedly impacting the pavement at one location would not affect this study, an independent well-calibrated geophone was securely placed on top of a washer glued to the pavement. The location of the washer was such that the FWD Sensor Number 4 (SD4) was side-by-side with the well-calibrated geophone.

Test Protocol

As indicated before, tests were carried out twice, before and after SHRP calibration. The repeatability of each FWD was evaluated by repeating the test three times and reproducibility was evaluated by testing same location with six FWDs. The following test protocol was followed at each site:

1) Measure Air and Pavement Temperature

2) Perform FWD tests
   a) Perform 2 seating drops at a nominal load level of 12 kip (53 KN).
   b) Drop load six times at four nominal load levels of 6 kip (27 KN), 9 kip (40 KN), 12 kip (53 KN) and 15 kip (67 KN). At each load level, record peak loads and peak deflections for first five drops and record load and deflection time history for the last (sixth) drop.
   c) Lift load plate and drive away

3) Perform Step 2 for each FWD

4) Repeat Steps 1 through 3 two additional times by driving away and repositioning FWD

The six FWDs followed one another for three repetitions. After each FWD was calibrated as per SHRP protocol, the above four steps were repeated at identical test points to evaluate the impact of calibration on the repeatability and reproducibility of the FWD fleet.

Data Analysis

An enormous amount of data was collected during the December and January test sessions. In total, 3456 deflection basin data sets were collected. As indicated before, the objective of this exercise was to establish the benchmark repeatability and reproducibility of the FWD fleet. The goal of the data analysis was to achieve the following objectives:

- to identify whether external factors (such as temperature) affected the repeatability and reproducibility of the data collected for this study;
- to establish the benchmark repeatability of individual FWD's;

- to establish the benchmark reproducibility of the TxDOT FWD fleet; and
- to identify the impact of the SHRP calibration procedure on the repeatability and reproducibility of the FWD fleet.

A single FWD is deemed repeatable if under identical testing conditions at a given test site, it provides loads and deflections from multiple drops that vary less than the tolerance suggested by the manufacturer (2% in this case). A fleet is said to be reproducible when all FWDs operated by various crews, produce similar deflection basins for a specific test site under identical testing conditions. Both high levels of repeatability and reproducibility are considered to be of major importance for a fully interchangeable FWD fleet.

The data reduction and analysis processes followed to achieve the four objectives are discussed in the following sections.

Impact of External Factors

A measured FWD deflection basin may vary with changes in temperature and other seasonal factors. The temperature of the surface layer was continuously monitored throughout the testing period. However, other parameters such as variations in base and subgrade moisture and depth to the water table were not taken into consideration. In addition, each site was impacted a number of times in a short period of time. Although the independent geophone did not exhibit any signs in change in the structure of the site, the repetitive application of the load might have changed the pavement structure. These factors may adversely impact the repeatability and reproducibility of the FWD fleet. Therefore, the collected data were analyzed to assess whether external factors impacted the results. The process followed is described below.

The data reduction process is explained in Figure 3.3a. The raw deflection data for each drop height was first normalized to their corresponding nominal loads of 6 kip (27 KN), 9 kip (40 KN), 12 kip (53 KN), or 15 kip (67 KN). Bentsen et al. (1989) indicated that the first deflection basin measured at each drop height is somewhat different than the deflections measured by the subsequent drops. Even though the results are not fully shown here, our data sets conformed to that pattern. As such, the result from the first drop from each set of data at each height was eliminated from the analysis[2]. The normalized deflections or loads from each attempt were then averaged. A grand average for each sensor was then calculated as shown in Figure 3.3b. The average of each attempt for the fleet was compared with the grand average using

$$Deviation\ Index = \frac{(Fleet\ Average\ for\ Attempt_i - Grand\ Average)}{Grand\ Average} * 100\% \qquad (3.1)$$

where index i corresponds to either the first, second or third attempt. The largest deviation index was defined to be the maximum deviation index (MDI). The MDI represents the worst-case scenario and was used to identify the influence of external factors on reproducibility of individual sensors at each site. This process was repeated for three sites, eight sensors, and four

[2] The practical implication of this observation is that instead of applying seating drops at a site at the beginning of a test sequence, it may be more appropriate to add one seating drop before each new drop height.

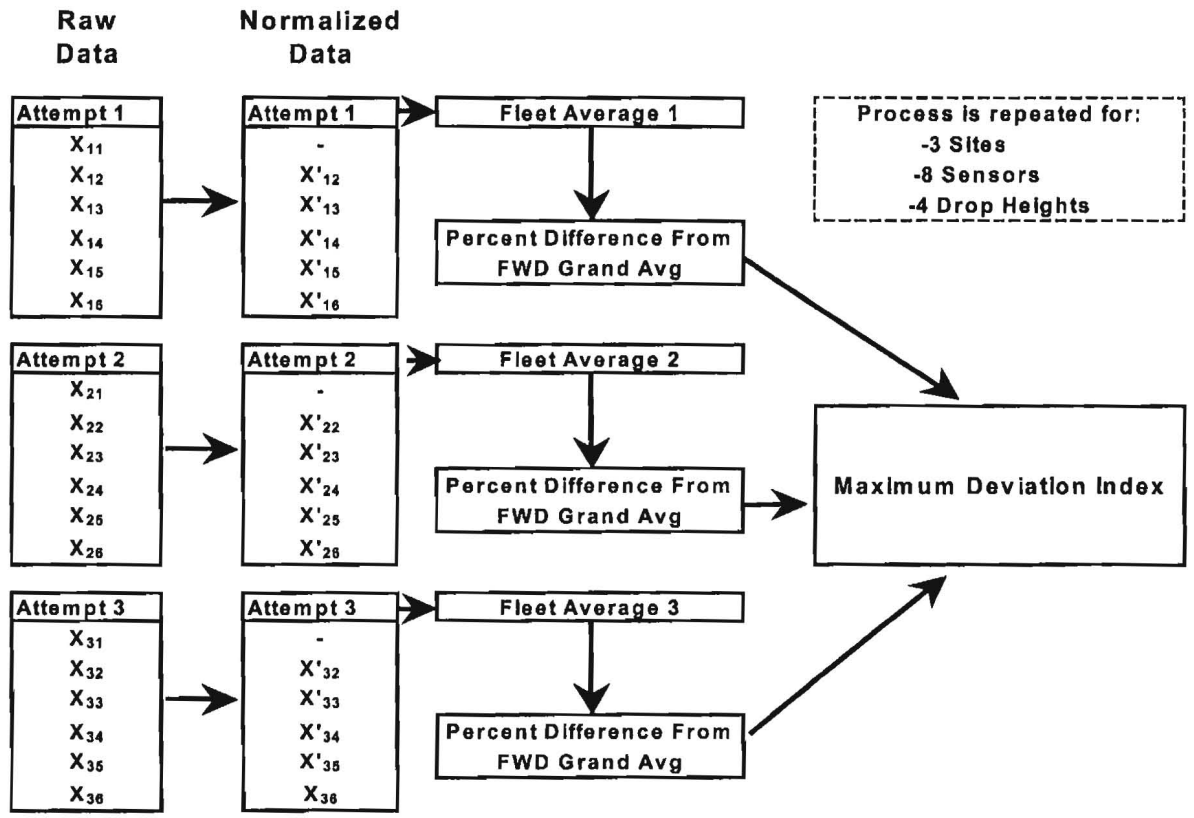

a) Data Reduction Process

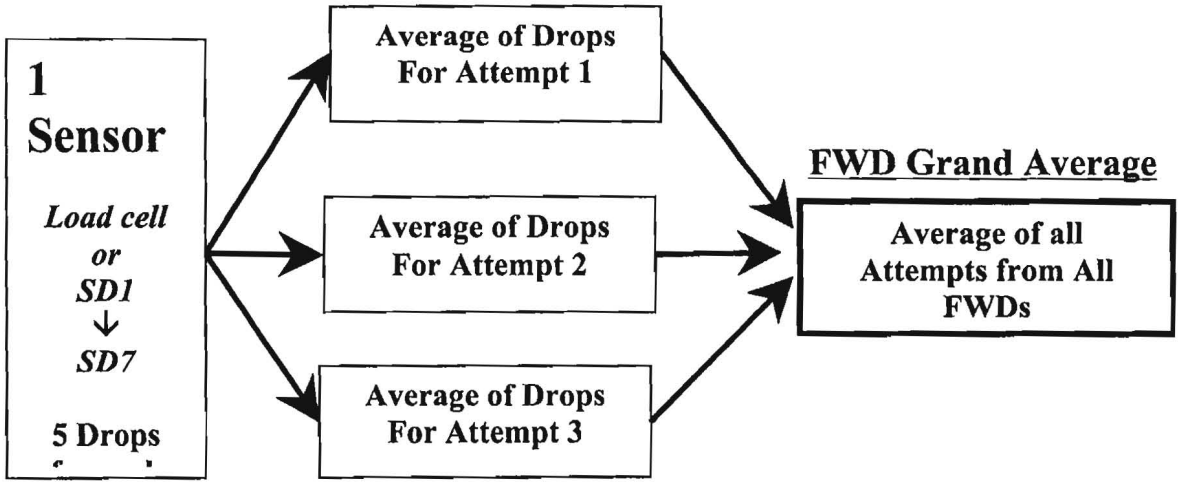

b) FWD Grand Average Calculations

Figure 3.3 – Data Reduction Process for Evaluating Impact of External Parameters

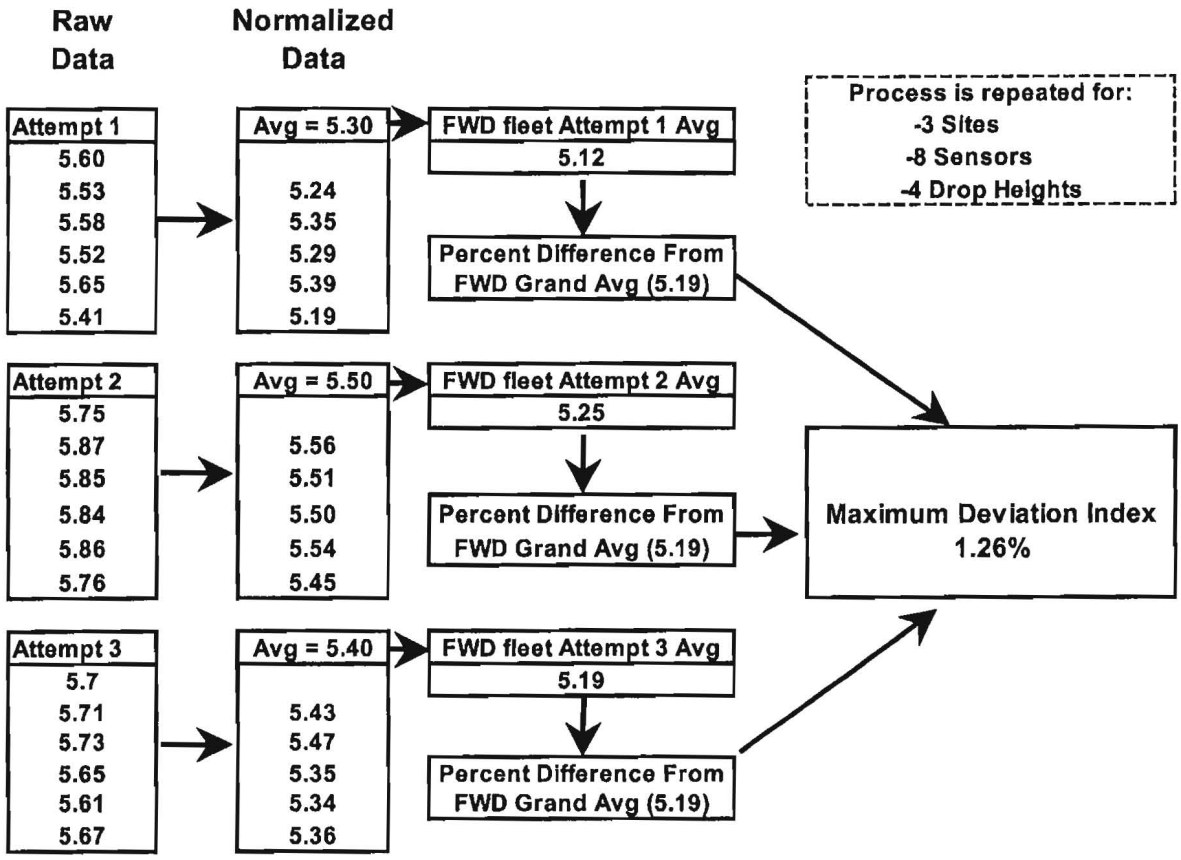

Figure 3.4 – Typical Results from Data Reduction Process for One Sensor

drop heights. A typical calculation for Site 1, Drop Height 1, and Sensor SD1 is shown in Figure 3.4. A maximum deviation from the grand average of 1.26% was observed for this particular sensor. Since this value is well within the 2% repeatability specified by the manufacturer, one can state that the influence of external factors on the repeatability and reproducibility of sensor SD1 at Site 1 (strong flexible site) is minimal.

The maximum deviation index for eight sensors and four different drop heights for Site 1 (before and after SHRP calibration) are shown in Figure 3.5. Before calibration, the MDIs from all but six sensors are within the 2% tolerance defined by the manufacturer. In any case, none of the sensors demonstrate a MDI greater than 2.5%. After the calibration process, the MDIs are all within 2% except for SD 7 for Drop Height 1. As such, the data set collected after calibration is less impacted by external parameters.

The results from all three sites and the four different drop heights are summarized in Table 3.3. The values that exceed 2% are highlighted for convenience. As indicated before, the MDIs for six sensors were barely above 2% for Site 1. For Site 2 and Site 3, only 2 points in each case are above 2%. But even these values are very close to 2%. Based on the results presented, we concluded that the impact of the external parameters was minimal.

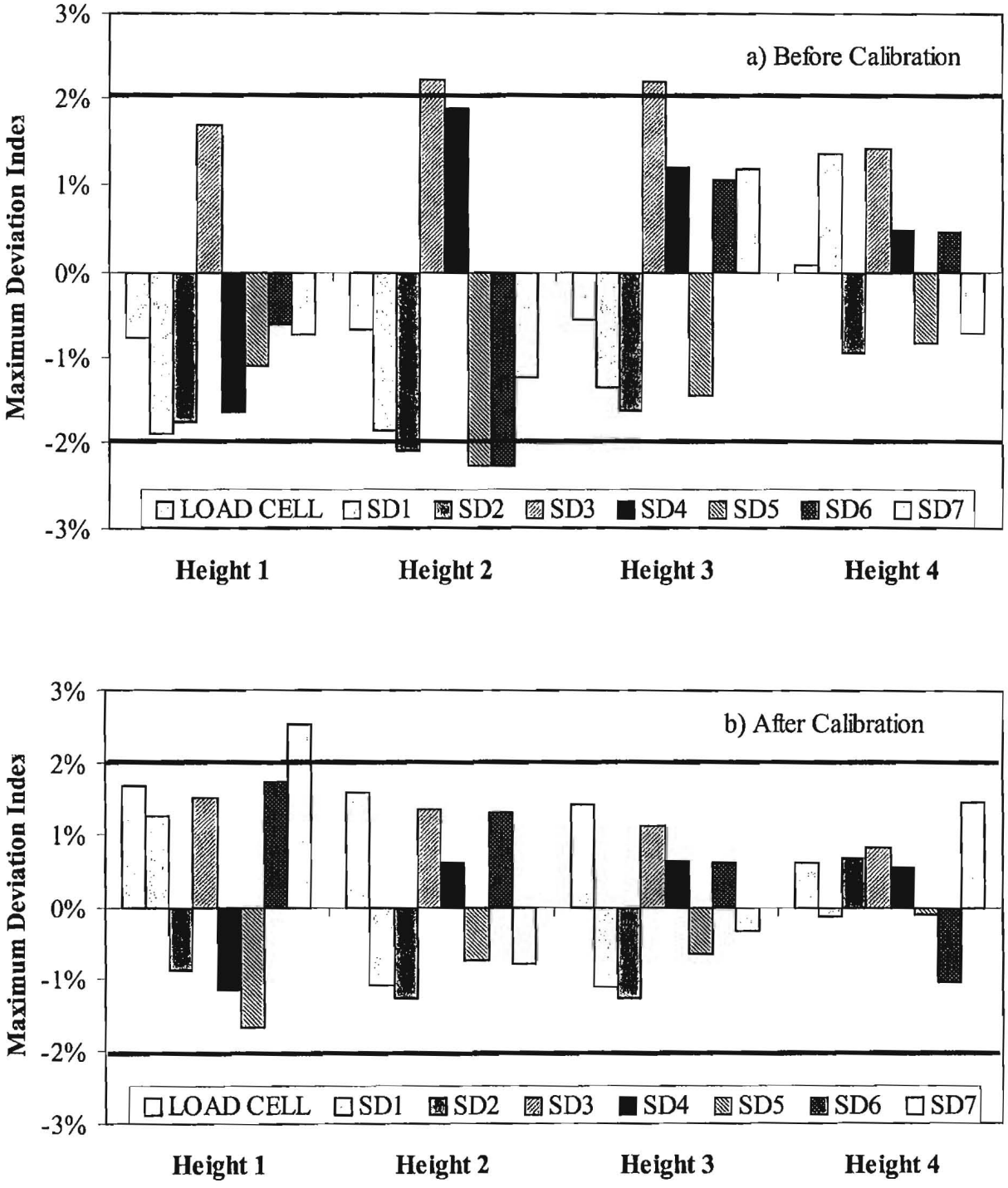

Figure 3.5 – Influence of External Factor on Reproducibility on Site 1

Table 3.4 – Maximum Deviation Index from Three Sites

a) Site 1

Drop Height	Test* Period	Maximum Deviation Index							
		Load	SD1	SD2	SD3	SD4	SD5	SD6	SD7
1	B/C	-0.77%	-1.90%	-1.77%	1.70%	-1.65%	-1.10%	-0.62%	-0.72%
	A/C	1.67%	1.26%	-0.90%	1.52%	-1.17%	-1.68%	1.75%	**2.55%**
2	B/C	-0.68%	-1.86%	**-2.10%**	**2.22%**	1.89%	**-2.27%**	**-2.27%**	-1.25%
	A/C	1.59%	-1.10%	-1.29%	1.35%	0.61%	-0.75%	1.31%	-0.81%
3	B/C	-0.55%	-1.35%	-1.63%	**2.20%**	1.20%	-1.45%	1.06%	1.18%
	A/C	1.42%	-1.11%	-1.27%	1.13%	0.63%	-0.65%	0.61%	-0.33%
4	B/C	0.09%	1.37%	-0.95%	1.41%	0.48%	-0.84%	0.46%	-0.71%
	A/C	0.62%	-0.13%	0.69%	0.83%	0.54%	-0.10%	-1.05%	1.44%

b) Site 2

Drop Height	Test* Period	Maximum Deviation Index							
		Load	SD1	SD2	SD3	SD4	SD5	SD6	SD7
1	B/C	-0.21%	-1.94%	**-2.07%**	-1.48%	-1.07%	0.43%	0.84%	-1.20%
	A/C	1.09%	-0.95%	-1.69%	-1.66%	-1.77%	-0.64%	1.07%	1.65%
2	B/C	-0.42%	-1.62%	-1.68%	-0.97%	-1.04%	0.31%	-0.58%	0.55%
	A/C	-0.44%	-0.88%	-1.75%	-1.50%	-0.90%	-0.70%	-0.97%	-0.84%
3	B/C	-0.17%	**-2.17%**	-1.60%	-0.98%	-1.00%	-0.91%	-0.60%	-0.45%
	A/C	-0.22%	1.86%	1.32%	-1.33%	-0.75%	-0.66%	-0.80%	-0.70%
4	B/C	0.06%	-1.34%	-1.35%	-1.05%	-0.77%	-0.35%	-1.07%	-0.41%
	A/C	-0.28%	-0.21%	-1.12%	-0.50%	-0.38%	0.09%	-0.29%	0.45%

c) Site 3

Drop Height	Test* Period	Maximum Deviation Index							
		Load	SD1	SD2	SD3	SD4	SD5	SD6	SD7
1	B/C	0.39%	0.66%	-0.65%	1.14%	0.82%	-1.08%	-0.89%	**-2.06%**
	A/C	-0.61%	-0.84%	-0.43%	0.59%	0.89%	0.70%	1.02%	**2.02%**
2	B/C	-0.20%	0.41%	0.55%	-0.95%	-0.36%	-0.48%	-1.06%	-0.31%
	A/C	-0.49%	-0.56%	0.30%	-0.09%	-0.36%	-0.12%	-1.12%	1.24%
3	B/C	-0.21%	0.39%	0.67%	-0.64%	-0.42%	-0.38%	-0.59%	0.44%
	A/C	-0.50%	-0.29%	0.19%	-0.08%	-0.16%	0.14%	-0.79%	1.06%
4	B/C	-0.06%	0.31%	0.47%	0.37%	-0.24%	-0.34%	-0.12%	0.44%
	A/C	-0.56%	-0.22%	0.16%	-0.28%	0.46%	-0.28%	-0.73%	1.15%

*** B/C denotes Before Calibration and A/C denotes After Calibration**

Repeatability

To identify the repeatability of each FWD, the coefficients of variation (COV) of the measured deflections or loads for the last five drops of each attempt were calculated. To determine the COVs from deflections, the deflections were first normalized to their appropriate nominal load levels i.e., 6 kip, 9 kip, 12 kip and 15 kip (27 KN, 40 KN, 53 KN, and 67 KN). For each load level, the average and maximum COVs from the three attempts were then determined. These values were used to assess the repeatability of each sensor. The average COV corresponds to the

overall repeatability anticipated for a given device. On the other hand, the maximum of the three COVs corresponds to the worst-case scenario associated with a given device. To further summarize the results, the maximum COVs from all drops heights and all attempts were calculated to represent the repeatability of a given sensor.

Typical results for Drop Height 2 (nominal load of 9 kip, 40 KN) at Site 1 are shown in Figure 3.6. Figure 3.6a contains the average COVs of the measured parameters before the FWDs were calibrated as per SHRP protocol. Figure 3.6b provides the same information after calibration. In each graph, a horizontal line corresponding to a 2% COV is included to demonstrate the acceptable level as per the FWD manufacturer. In general, the average COVs were less than 2% for almost all sensors. Before calibration, the COVs for SD6 of FWDs 069 and 159 were greater than 2%, but less than 3%. After the calibration process, the COV for sensor 6 of FWD 069 became significantly smaller, indicating improved repeatability. The repeatability of SD 6 of FWD 159, as judged by the average COV, was essentially the same from tests before and after calibration.

The average COVs for all sites are summarized in Table 3.5. Similar trends are observed in all cases. In a number of cases, the system is less repeatable after calibration as compared to before calibration. In almost all these cases, the differences are so small that they can be attributed to random errors associated with data analysis.

Another example is shown in Figure 3.7 where the COVs for different measured parameters are compared as a function of drop height. As anticipated, the COVs are smaller for greater drop heights. Since the measured deflections are greater for higher drop heights, random system errors are less significant. For Drop Height 1, a number of outer sensors exhibit COVs that are greater than 2%; whereas for Drop Height 4 all COVs are significantly less than 2%.

As indicated before, the maximum COVs associated with all measured parameters were also considered. The maximum COVs from the three attempts and from the four different drop heights for each FWD are summarized in Figure 3.8. Results from both before and after calibration are shown. As a result of the SHRP calibration, the maximum COVs decreased for a number of sensors. Unfortunately, some sensors also exhibited larger COVs after the calibration. Using the maximum COV criteria, the repeatability of FWDs 024, 040, and 047 seems to improve after SHRP calibration. The impact of SHRP calibration was mixed for FWD 069. The maximum COV for SD1 and SD7 increased after the calibration process while it decreased for the other sensors. The repeatability of FWD 159 did not change significantly after the SHRP calibration. FWD 159 is the newest FWD in the fleet and was calibrated in September 1999.

To evaluate the impact of the SHRP calibration on the repeatability of the FWD fleet, the COVs from before and after calibration are compared for all sensors, sites, attempts, and FWDs in Figure 3.9. Most of the COVs from different sensors of the FWD fleet fall within the 2% limit recommended by the manufacturer even before calibration. The data also suggests that in general the SHRP calibration procedure improves the repeatability of the fleet by decreasing the COVs for a number of parameters.

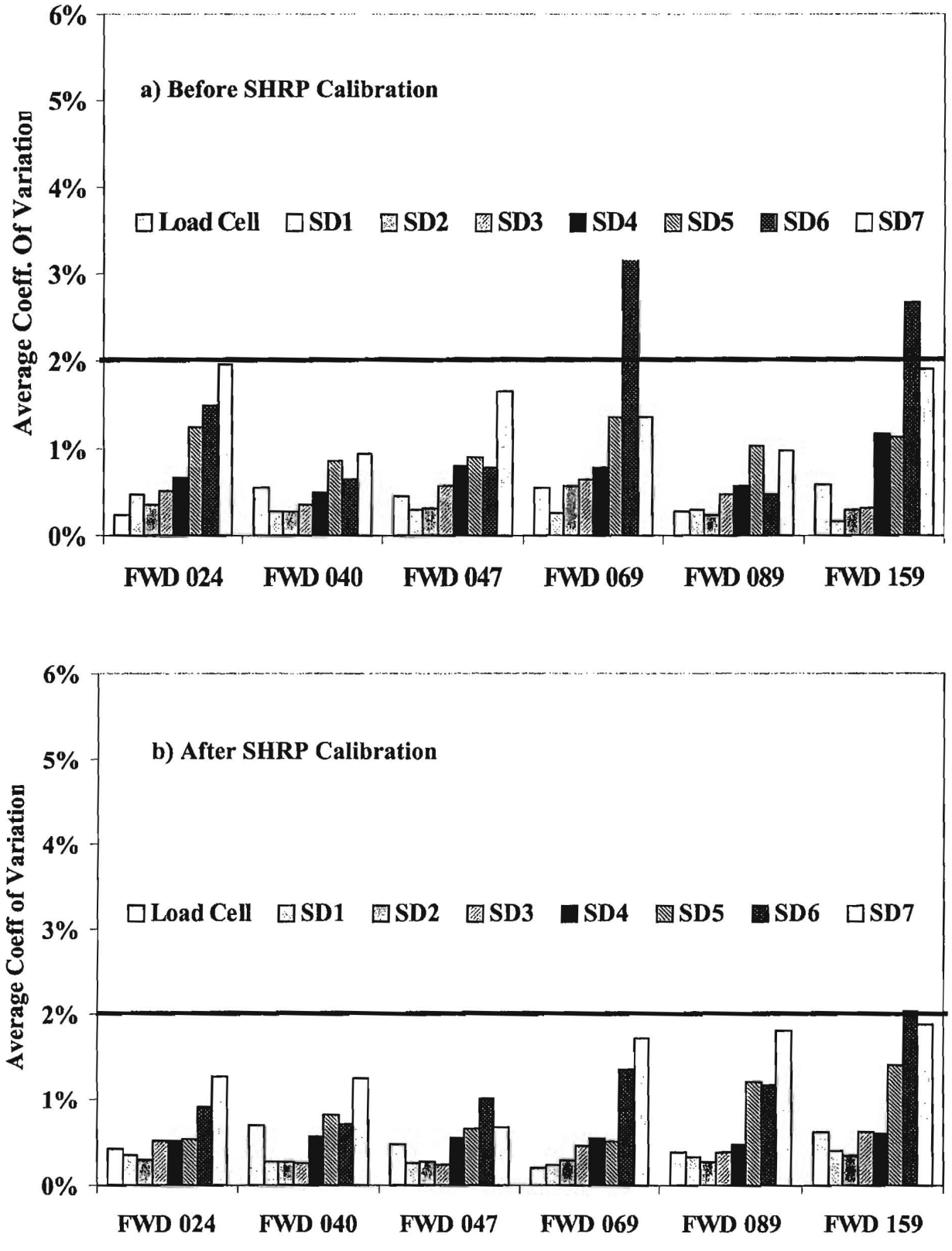

Figure 3.6 – Typical Coefficients of Variation Measured at Site 1 for Drop Height 2

Table 3.5 – Average Coefficients of Variation from Three Sites at a Nominal Load of 9 kips

a) Site 1

Serial No.	Test * Period	Average Coefficient of Variation							
		Load	D1	D2	D3	D4	D5	D6	D7
024	B/C	0.23%	0.47%	0.35%	0.51%	0.66%	1.25%	1.50%	1.96%
	A/C	0.41%	0.35%	0.30%	0.50%	0.51%	0.53%	0.91%	1.27%
040	B/C	0.55%	0.26%	0.28%	0.35%	0.49%	0.86%	0.64%	0.93%
	A/C	0.70%	0.27%	0.27%	0.26%	0.57%	0.81%	0.72%	1.25%
047	B/C	0.45%	0.28%	0.32%	0.57%	0.79%	0.89%	0.79%	1.65%
	A/C	0.48%	0.25%	0.28%	0.24%	0.54%	0.65%	1.02%	0.67%
069	B/C	0.54%	0.26%	0.56%	0.64%	0.77%	1.36%	3.20%	1.36%
	A/C	0.20%	0.24%	0.30%	0.46%	0.55%	0.51%	1.37%	1.74%
089	B/C	0.28%	0.30%	0.24%	0.47%	0.56%	1.04%	0.47%	0.98%
	A/C	0.38%	0.32%	0.27%	0.39%	0.48%	1.23%	1.18%	1.82%
159	B/C	0.59%	0.16%	0.30%	0.31%	1.18%	1.13%	2.68%	1.90%
	A/C	0.61%	0.40%	0.35%	0.63%	0.59%	1.42%	2.05%	2.42%

b) Site 2

Serial No.	Test * Period	Average Coefficient of Variation							
		Load	D1	D2	D3	D4	D5	D6	D7
024	B/C	0.57%	0.33%	0.39%	0.39%	0.50%	0.62%	0.59%	1.29%
	A/C	0.48%	0.25%	0.33%	0.28%	0.30%	0.44%	0.35%	1.18%
040	B/C	0.26%	0.21%	0.22%	0.21%	0.23%	0.24%	0.42%	0.58%
	A/C	0.49%	0.29%	0.32%	0.26%	0.59%	1.01%	0.87%	1.01%
047	B/C	0.51%	0.57%	0.48%	0.51%	0.79%	0.79%	0.56%	0.69%
	A/C	0.40%	0.28%	0.38%	0.56%	0.56%	0.60%	0.72%	1.06%
069	B/C	0.37%	0.31%	0.40%	0.38%	0.51%	1.77%	0.66%	2.98%
	A/C	0.39%	0.38%	0.51%	0.42%	0.70%	0.86%	2.11%	1.80%
089	B/C	0.34%	0.24%	0.21%	0.31%	0.24%	0.52%	0.25%	0.48%
	A/C	0.29%	0.16%	0.14%	0.16%	0.48%	0.64%	0.50%	0.38%
159	B/C	0.57%	0.16%	0.19%	0.18%	0.45%	0.38%	1.11%	2.44%
	A/C	0.64%	0.20%	0.28%	0.42%	0.46%	0.53%	1.36%	1.19%

c) Site 3

Serial No.	Test * Period	Average Coefficient of Variation							
		Load	D1	D2	D3	D4	D5	D6	D7
024	B/C	0.22%	0.81%	0.43%	0.49%	0.60%	1.00%	0.72%	1.86%
	A/C	0.38%	0.26%	0.30%	0.25%	0.38%	0.25%	0.70%	1.48%
040	B/C	0.60%	0.41%	0.55%	0.73%	0.49%	0.56%	0.61%	1.26%
	A/C	0.55%	0.46%	0.39%	0.46%	0.44%	0.53%	0.89%	1.20%
047	B/C	0.43%	0.27%	0.22%	0.28%	0.91%	0.42%	0.40%	1.52%
	A/C	0.46%	0.51%	0.59%	0.56%	0.71%	0.50%	0.77%	1.15%
069	B/C	0.52%	0.30%	0.45%	0.79%	0.65%	0.93%	0.91%	2.07%
	A/C	0.57%	0.50%	0.52%	0.63%	0.62%	0.68%	0.81%	1.07%
089	B/C	0.33%	0.34%	0.23%	0.24%	0.24%	0.43%	0.52%	0.79%
	A/C	0.48%	0.30%	0.27%	0.21%	0.72%	0.31%	0.64%	0.69%
159	B/C	0.47%	0.19%	0.36%	0.22%	0.60%	0.83%	0.80%	0.72%
	A/C	0.76%	0.22%	0.21%	0.29%	0.33%	0.70%	1.14%	1.47%

* B/C denotes Before Calibration and A/C denotes After Calibration

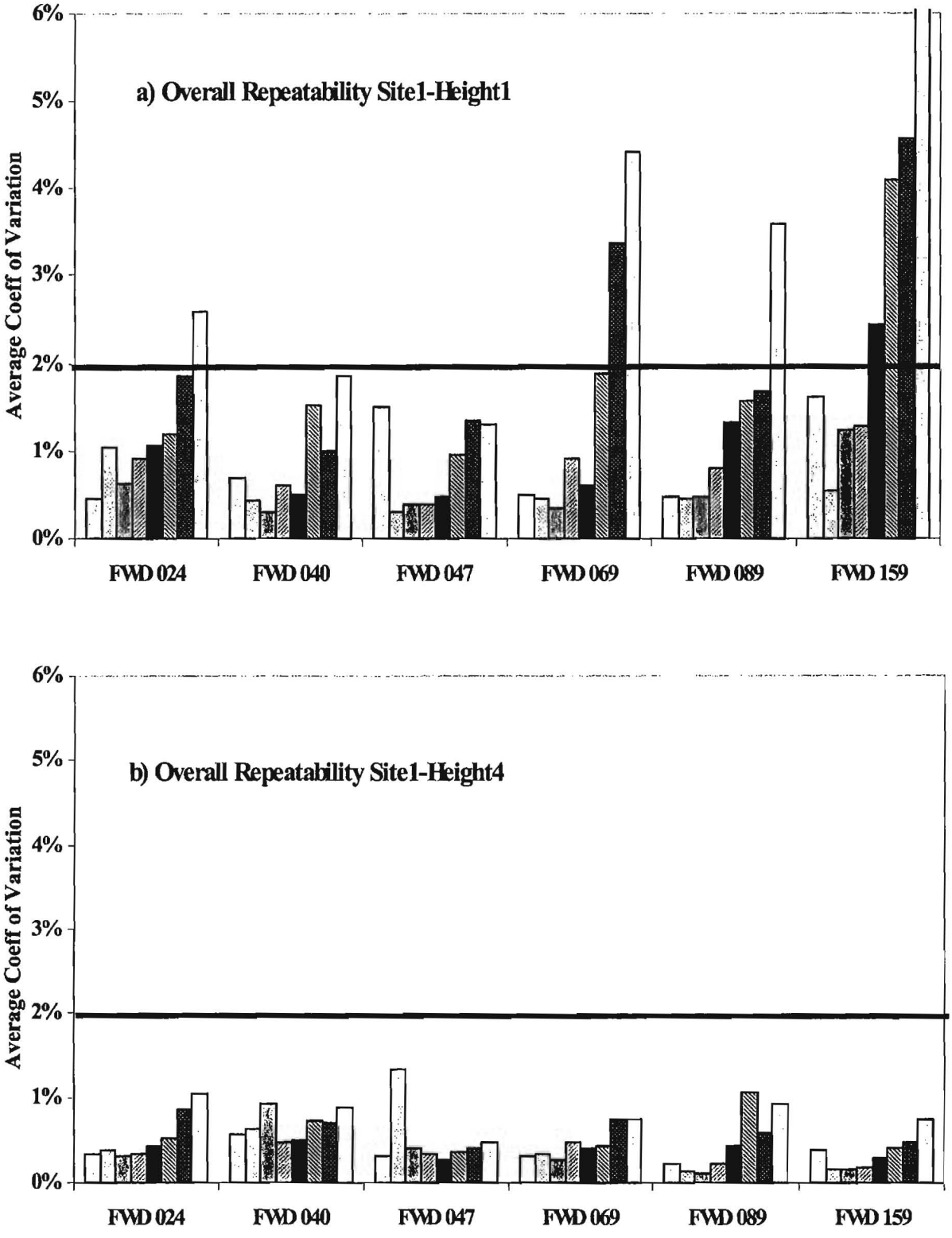

Figure 3.7 – Effect of Drop Height on Coefficients of Variation (After SHRP Calibration)

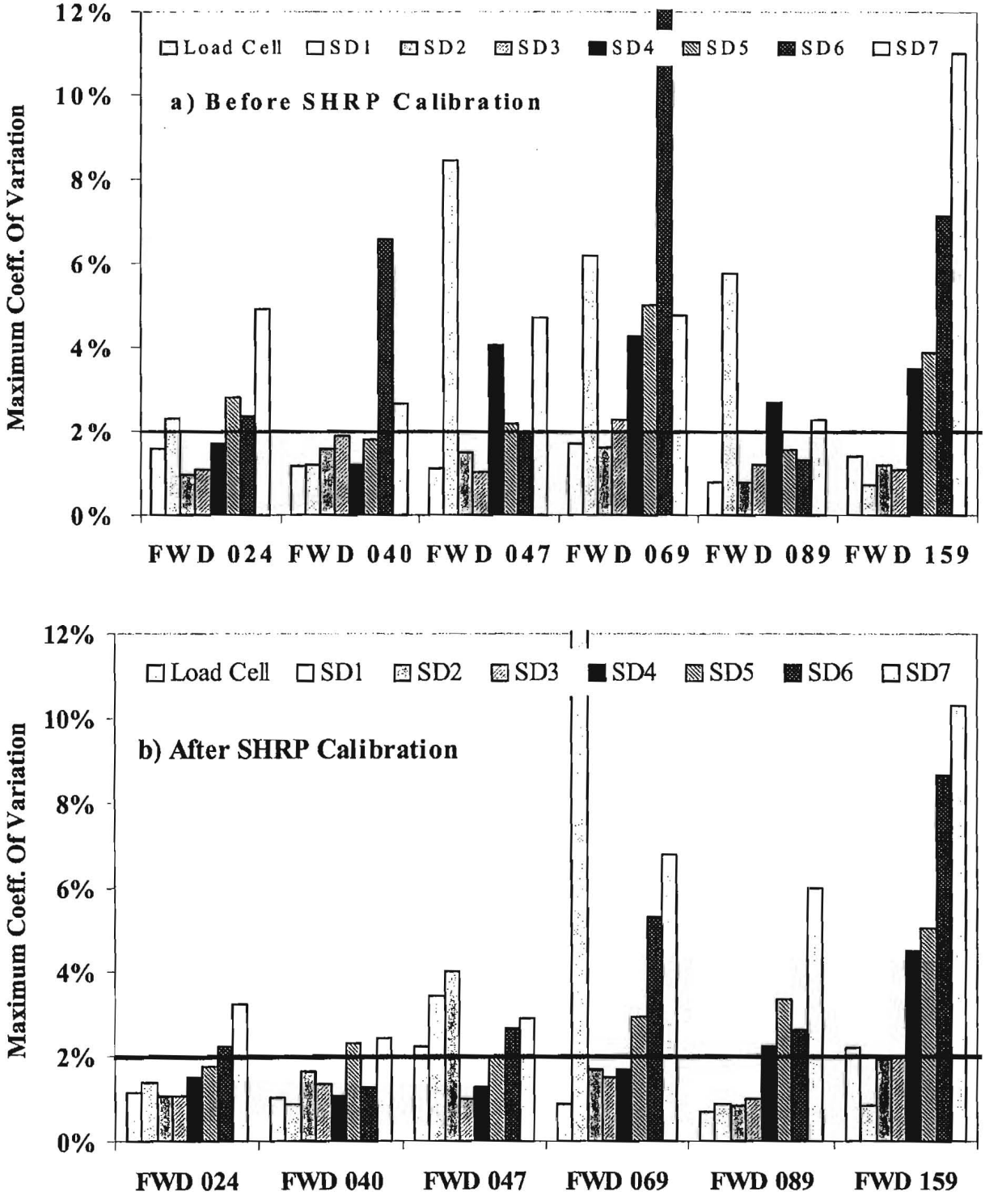

Figure 3.8 – Maximum Coefficients of Variation Observed for All Sites and All Drop Heights

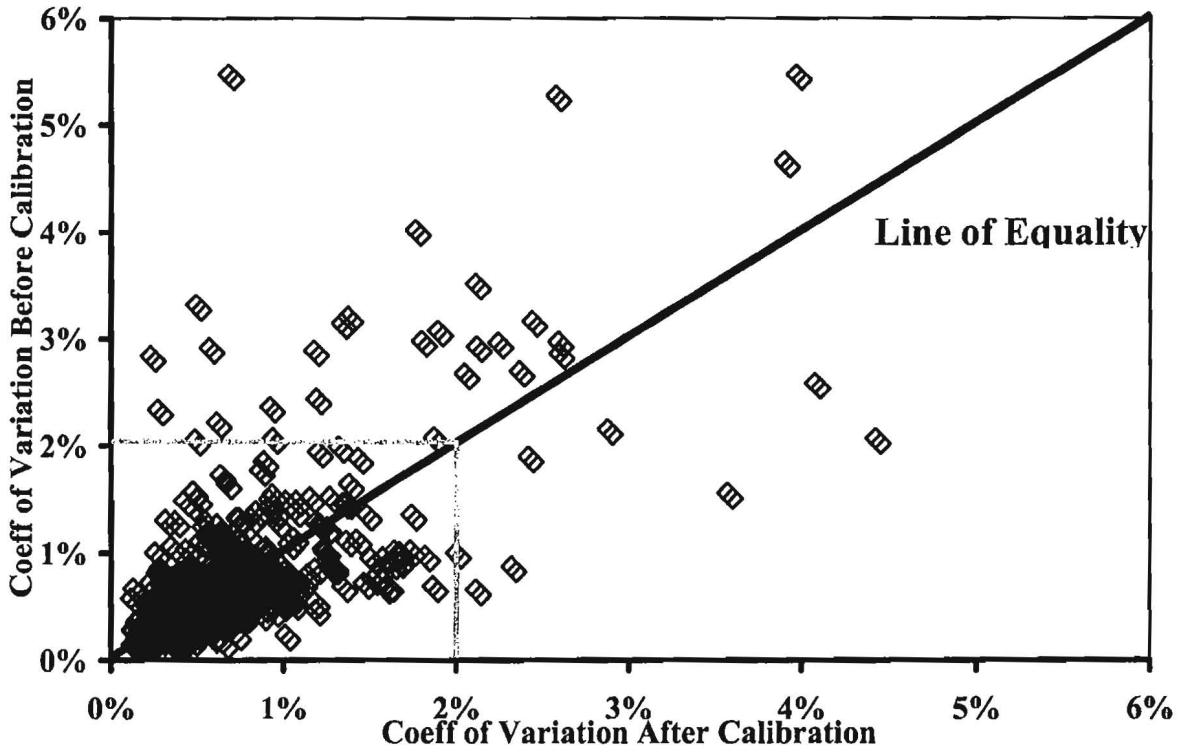

Figure 3.9 – Comparison of Repeatability of FWD Fleet Before and After SHRP Calibration

Reproducibility

To evaluate the reproducibility of the FWD fleet, the data reduction process shown in Figure 3.10 was followed. At each site, for each drop height and for each sensor (either geophone or load cell), the average value from the last five drops for each attempt and each device was determined separately[3]. In addition, an overall average that included all sites and all FWDs was determined. Considering this grand average as the "baseline" value, the percent difference between each average and the baseline value was calculated from:

$$Difference = \frac{AvgValue - BaselineAvg}{BaselineAvg} * 100\% \qquad (3.2)$$

To summarize the results further, the differences measured from the three attempts for each FWD were averaged. In addition, the largest of the three values was also noted. For a reproducible fleet, all FWDs should measure deflections and loads that are close to the baseline. In that case, the average and maximum deviation from the baseline will be rather small. Based on an uncertainty study performed under Project 0-1735 (See Nazarian et al., 1998), a limit of 5% for average deviation from baseline was adapted as the acceptable limit.

[3] This corresponds to 24 average values per sensor, per drop height per site.

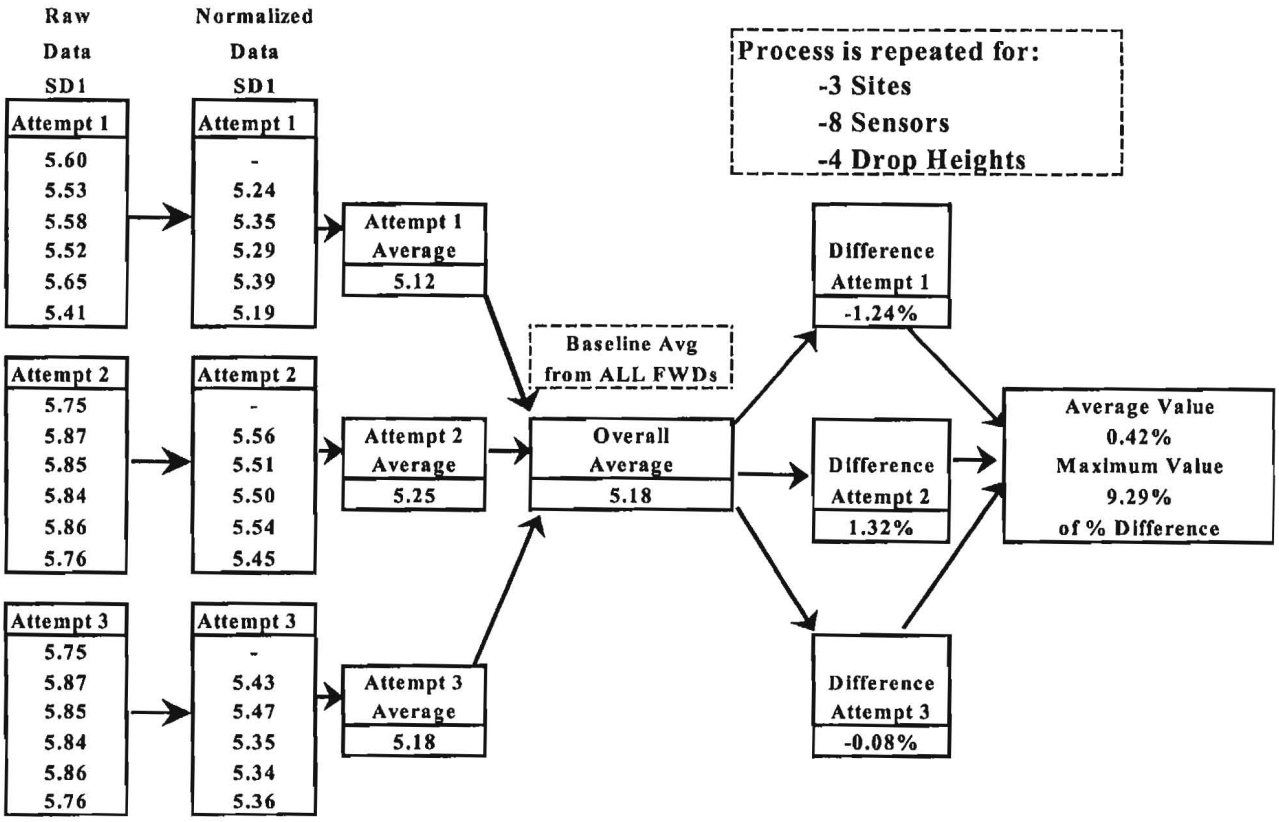

Figure 3.10 – Data Reduction Process for Reproducibility Analysis

This level translates to an uncertainty of about 20% in the remaining life of a typical flexible pavement in Texas. The process was repeated for three sites, eight sensors, and four drop heights. The average deviations from the baseline for Drop Height 2 are summarized in Table 3.6. Large variations are observed between different devices.

As an example, the average differences from the baseline values at Drop Height 1 for all sensors at the three sites are shown in Figure 3.11. The results correspond to the data collected before the devices were calibrated. Based on average deviations from the baseline value, the reproducibility of the fleet is site dependent. The fleet is more reproducible for Site 2 in comparison to Site 1 or Site 3. In general, FWD 159 seems to measure loads and deflections that are closest to the baseline value. In contrast, FWD 024 showed the largest differences from the baseline values at all three sites, and consistently measured higher deflections than others.

The most variability in the measured deflections occurred at Site 3 and Site 1, i.e. the rigid and the strong flexible pavement sections. Assuming that the random errors are constant, this variability can be attributed to the smaller deflections that were measured at these two sites. As reflected in Table 3.3, these two sites produce similar deflections.

Table 3.6 – Average Difference from Baseline Values from Three Sites at a Nominal Load of 9 kips

a) Site 1

Serial No.	Test* Period	Average Difference from Baseline Value							
		Load	D1	D2	D3	D4	D5	D6	D7
024	B/C	-5.04%	5.42%	8.69%	11.57%	15.23%	12.45%	12.40%	15.99%
	A/C	2.10%	1.97%	5.72%	9.46%	11.05%	10.45%	10.27%	9.42%
040	B/C	0.88%	-2.15%	-1.78%	-3.65%	-2.22%	-5.51%	-4.65%	-5.52%
	A/C	3.43%	-0.34%	-2.04%	-3.67%	-2.69%	-4.86%	-2.51%	-3.41%
047	B/C	2.76%	-3.67%	-4.74%	-3.80%	-9.63%	-7.13%	-8.03%	-8.35%
	A/C	1.85%	-3.46%	-5.02%	-4.41%	-5.01%	-4.93%	-5.69%	-6.47%
069	B/C	3.47%	-6.91%	-6.94%	-6.37%	-5.86%	-8.41%	-5.99%	-7.77%
	A/C	-2.85%	-6.67%	-7.19%	-7.49%	-8.09%	-7.55%	-9.22%	-5.72%
089	B/C	-0.79%	3.92%	4.34%	2.64%	4.57%	4.68%	3.71%	5.94%
	A/C	-3.89%	5.99%	5.09%	5.89%	3.83%	7.36%	10.38%	4.81%
159	B/C	-1.29%	3.40%	0.43%	-0.38%	-2.09%	3.93%	2.56%	-0.29%
	A/C	-0.63%	2.52%	3.44%	0.23%	0.91%	-0.47%	-3.22%	1.37%

b) Site 2

Serial No.	Test * Period	Average Difference from Baseline Value							
		Load	D1	D2	D3	D4	D5	D6	D7
024	B/C	3.63%	-3.70%	2.62%	4.53%	6.88%	4.82%	5.11%	6.07%
	A/C	8.49%	-5.91%	0.61%	2.27%	4.11%	3.78%	3.18%	0.75%
040	B/C	-6.18%	4.50%	5.64%	2.53%	4.19%	1.17%	3.60%	4.01%
	A/C	-1.42%	2.93%	3.48%	0.42%	1.11%	-1.10%	2.07%	4.08%
047	B/C	-2.70%	1.03%	-0.98%	-0.48%	-2.94%	-0.67%	0.81%	-2.88%
	A/C	-4.57%	2.70%	-1.08%	0.33%	1.14%	1.86%	1.06%	0.26%
069	B/C	-3.31%	0.45%	-1.48%	0.28%	-0.67%	1.43%	-0.08%	-0.51%
	A/C	-7.76%	0.95%	-2.05%	-0.82%	-1.19%	0.35%	0.49%	1.35%
089	B/C	5.84%	-0.96%	-1.87%	-2.70%	-2.97%	-3.48%	-3.71%	-4.05%
	A/C	1.70%	1.98%	1.37%	0.55%	-1.41%	-0.83%	-1.50%	-1.39%
159	B/C	2.72%	-1.33%	-3.93%	-4.15%	-4.49%	-3.27%	-5.73%	-2.65%
	A/C	3.57%	-2.65%	-2.34%	-2.75%	-3.76%	-4.06%	-5.30%	-5.05%

c) Site 3

Serial No.	Test * Period	Average Difference from Baseline Value							
		Load	D1	D2	D3	D4	D5	D6	D7
024	B/C	-3.23%	8.51%	8.54%	9.92%	12.56%	11.52%	13.47%	16.14%
	A/C	2.57%	7.09%	7.96%	9.20%	10.10%	9.76%	8.78%	9.77%
040	B/C	-1.22%	-2.18%	0.26%	-1.11%	-1.84%	-5.24%	-3.52%	-2.28%
	A/C	0.94%	-0.97%	-0.39%	-1.82%	-0.63%	-2.31%	1.54%	1.80%
047	B/C	1.56%	-3.84%	-4.27%	-3.81%	-10.32%	-5.64%	-6.26%	-6.25%
	A/C	-0.92%	-2.33%	-3.73%	-4.01%	-3.92%	-3.99%	-5.48%	-5.14%
069	B/C	1.24%	-6.76%	-7.48%	-6.64%	-5.31%	-7.23%	-9.11%	-8.65%
	A/C	2.67%	-11.94%	-12.71%	-12.29%	-11.91%	-10.77%	-17.10%	-16.79%
089	B/C	1.22%	3.39%	3.99%	3.25%	3.74%	4.07%	6.53%	2.57%
	A/C	-5.27%	7.36%	7.56%	7.76%	5.41%	6.21%	11.27%	6.55%
159	B/C	0.42%	0.88%	-1.04%	-1.61%	1.17%	2.53%	-1.11%	-1.54%
	A/C	0.02%	0.80%	1.32%	1.16%	0.95%	1.10%	1.00%	3.81%

*** B/C denotes Before Calibration and A/C denotes After Calibration**

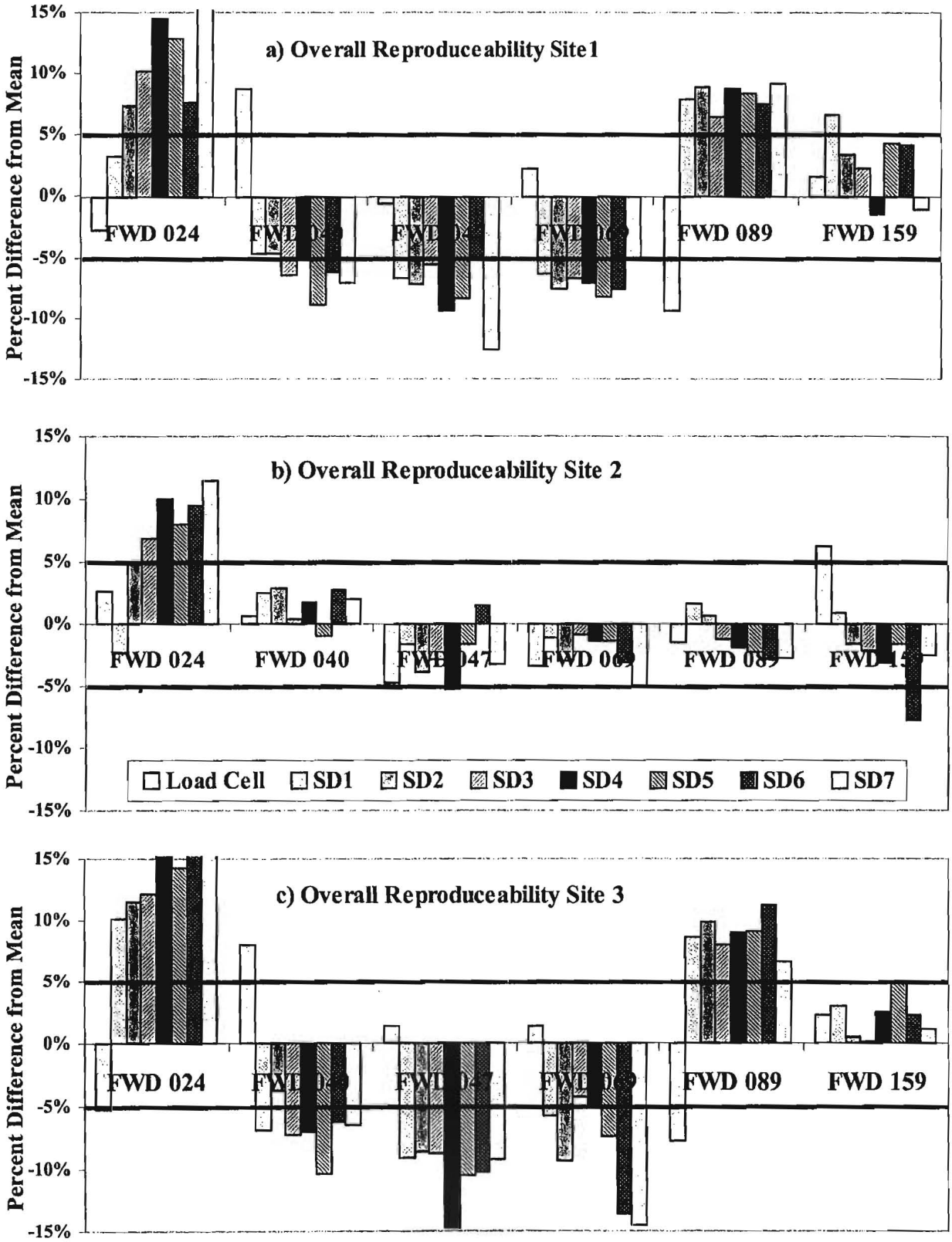

Figure 3.11 – Variations in Average Difference from Mean (Grand Average of all FWDs) for Drop Height 1

Typical deviations in the measured parameters from baseline are shown in Figure 3.12 (both before and after calibration). The impact of the SHRP calibration on improving the reproducibility is not evident. FWD 047 measured deflections that are closer to the baseline after the SHRP calibration. All other FWDs more or less maintained the same level of reproducibility.

To further establish the benchmark reproducibility of the fleet, differences from the baseline from before and after calibration (from all sensors, all sites and all drop heights) are compared in Figure 3.13. Most of the measurements reside within the 5% difference defined as acceptable. A number of sensors also measure deflections or loads that vary from the average by more than 5%. A systematic decrease in the difference from the baseline after the calibration is not evident in the data, suggesting that the SHRP calibration procedure does not necessarily improve the reproducibility of the FWD fleet.

The data points are concentrated along the line of equality in Figure 3.13. This may indicate that the lack of reproducibility is not related to the behavior of the sensor itself but it may depend on the movement of the system as a whole. This will be further elaborated in Chapter 5.

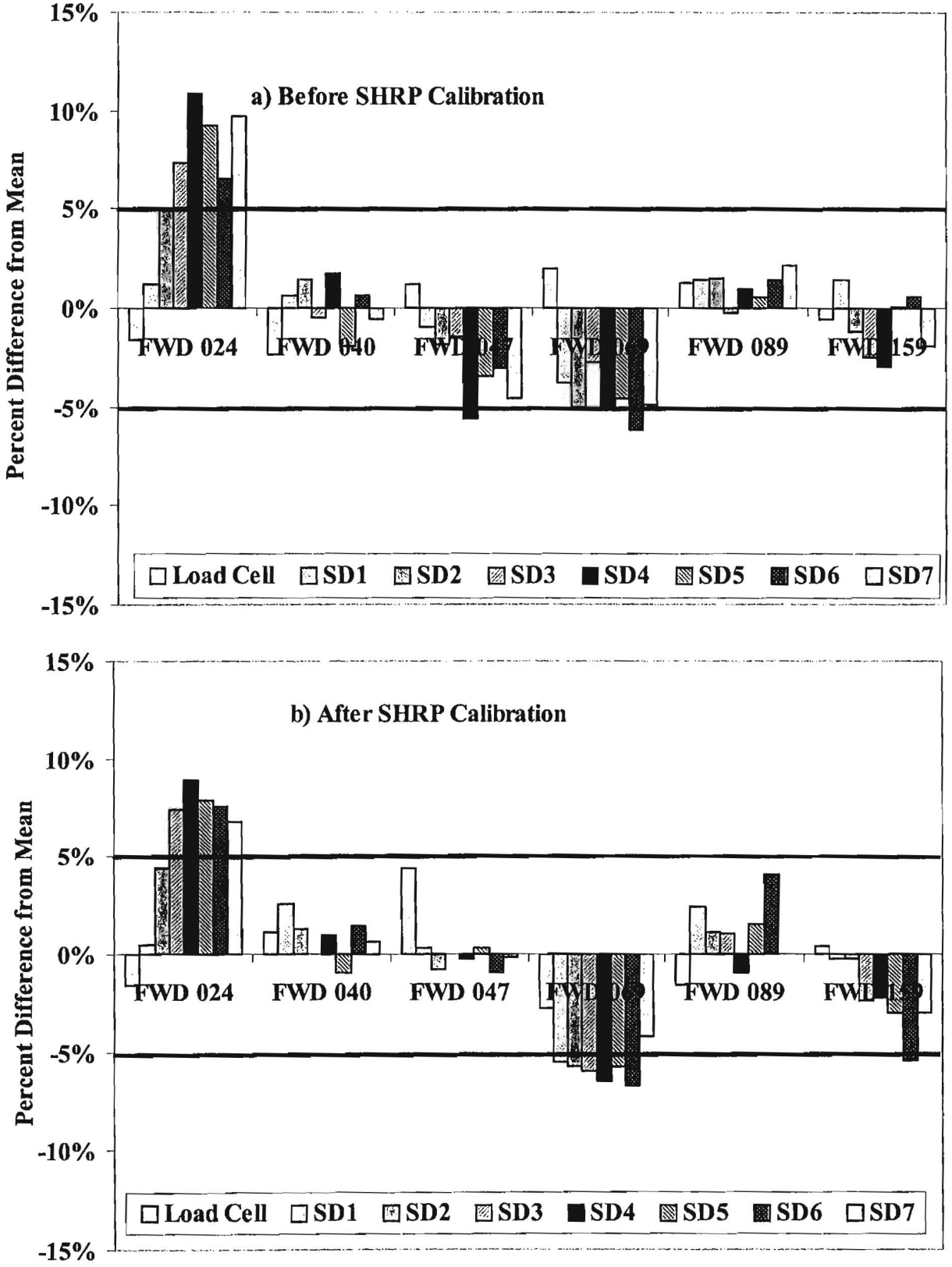

Figure 3.12 – Impact of SHRP Calibration on Reproducibility of FWD Fleet

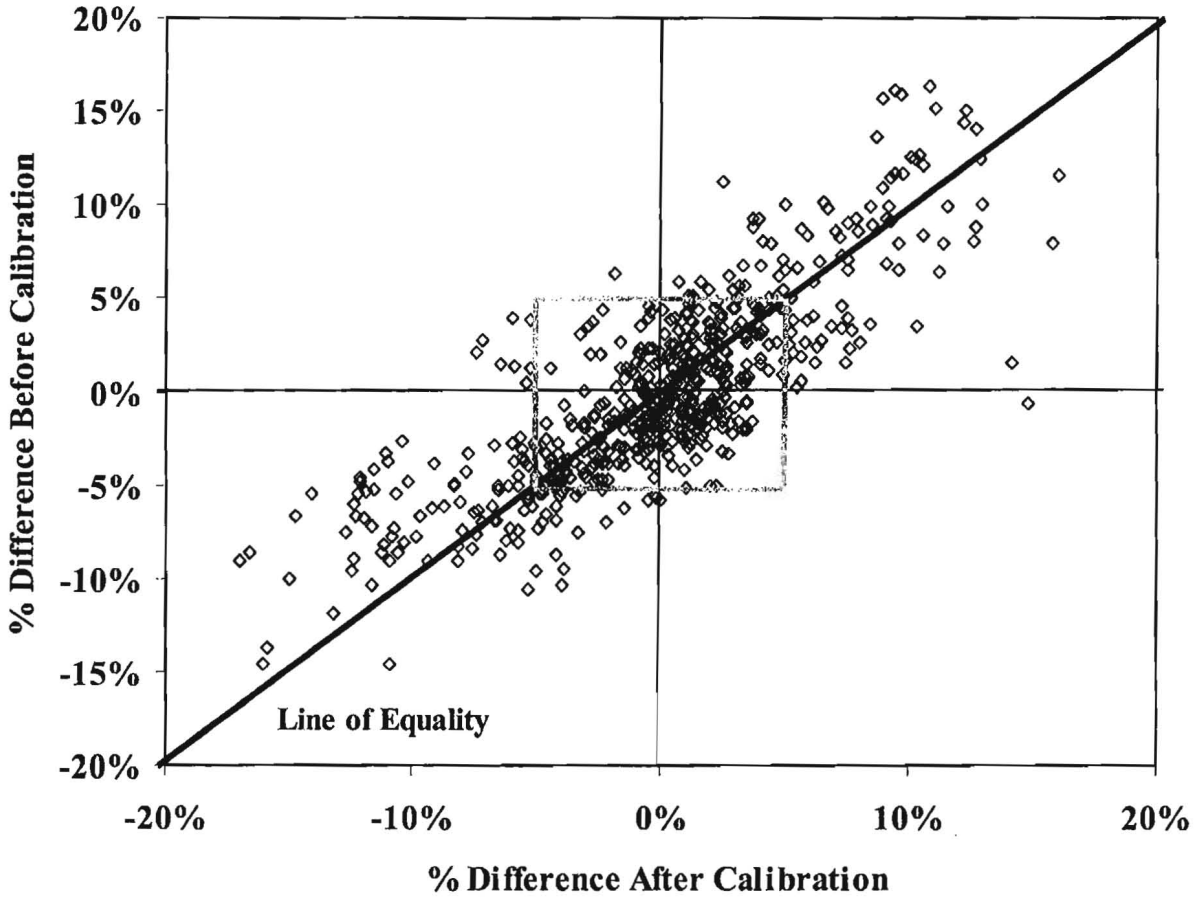

Figure 3.13 – Comparison of Deviation from Grand Average from Before and After SHRP Calibration.

Chapter 4

Statistical Analysis of Repeatability and Reproducibility

To further quantify the repeatability and reproducibility of the FWDs, extensive statistical analyses were performed. The main goals of these analyses were to assess systematically the impacts of the pavement structure, individual FWDs, individual sensors and drop heights on the repeatability and reproducibility of the fleet. The other goal of this study was to statistically assess the impact of the SHRP calibration on improving the reproducibility and repeatability of the fleet.

The procedure followed was similar for each parameter. First appropriate sub-databases were developed from the main database containing all of the collected data. The distribution of the data for each sub-database was determined. The reason for describing the best distribution is to provide a realistic means of incorporating the uncertainty analysis in the future pavement design procedures.

Computer software BESTFIT was used for this purpose. This program has the capability of fitting more than two dozens distributions to the data. For the sake of practicality, only the most popular distributions were considered. These distributions were mostly the normal and the log-normal. As a reminder, the normal distribution can be described as:

$$f(x) = \frac{1}{\sqrt{2\pi\sigma^2}} e^{\frac{-(x-\mu)^2}{2\sigma^2}} \tag{4.1}$$

where μ and σ are the mean and the standard deviation of the variate, respectively.

Similarly, the log-normal distribution can be defined as

$$f(x) = \frac{1}{x\sqrt{2\pi\sigma_1^2}} e^{\frac{-[\ln(x)-\mu_1]^2}{2\sigma_1^2}}$$

where (4.2)

$$\mu_1 = \ln\left[\frac{\mu^2}{\sqrt{\sigma^2+\mu^2}}\right], \sigma_1 = \sqrt{\ln\left[\frac{\sigma^2+\mu^2}{\mu^2}\right]}$$

Repeatability

The impacts of several FWD elements on the repeatability of the measured parameters were studied. These studies are summarized below.

Individual Sites

The actual distribution of coefficients of variation measured from each attempt, each FWD and each sensor for Site 1 is shown in Figure 4.1. The most widely used distribution that best described this data was the log-normal distribution. The statistical information for this and other sites are summarized in Table 4.1. For Site 1, the average coefficient of variation from all attempts with all FWDs is about 0.87, which translates to an average repeatability of less than 1% for individual sensors. After calibration, this value slightly decreased indicating further improvement in the repeatability. As reflected in the table, the standard deviation is rather large for Site 1. This occurs because of occasional instances where a sensor did not provide repeatable results. Before calibration, in one occasion the repeatability is about 9%. After calibration, the maximum variability is less than 4%. Similar results were obtained for sites 2 and 3, as shown in Table 4.1[4]. After calibration, the maximum variability is less than 4%. Similar results were obtained for sites 2 and 3, as shown in Table 4.1.

As discussed in previous sections, for all three sites, the mean repeatability is less than 1%. For all three sites, the repeatability slightly improves, as judged by the decrease in the mean values in Table 4.1. Given the standard deviations, the improvement is statistically insignificant. This should not be of any practical concern since all the FWDs were very repeatable before calibration to begin with.

To judge the appropriateness of the fitted distribution to the actual data, the χ^2 (chi-square) value was used (Ang and Tang, 1975). Chi-square test considers a sample of n observed values of a random variable. The χ^2 goodness-of-fit test compares the observed frequencies n_1, n_2, n_k of k values (or in k intervals) of the variate with the corresponding frequencies e_1, e_2, , e_k from an

[4] All distributions are included in Appendix A.

Table 4.1 – Statistical Information about Distribution of Coefficients of Variation from All FWDs at Three Sites Tested

Site	Test* Period	Statistical Information		
		Mean	Standard Deviation	χ^2
1	B/C	0.87	0.76	55.1
	A/C	0.74	0.62	32.2
2	B/C	0.67	0.49	147.1
	A/C	0.62	0.39	23.3
3	B/C	0.67	0.46	40.0
	A/C	0.59	0.41	12.8

*** B/C denotes Before Calibration and A/C denotes After Calibration**

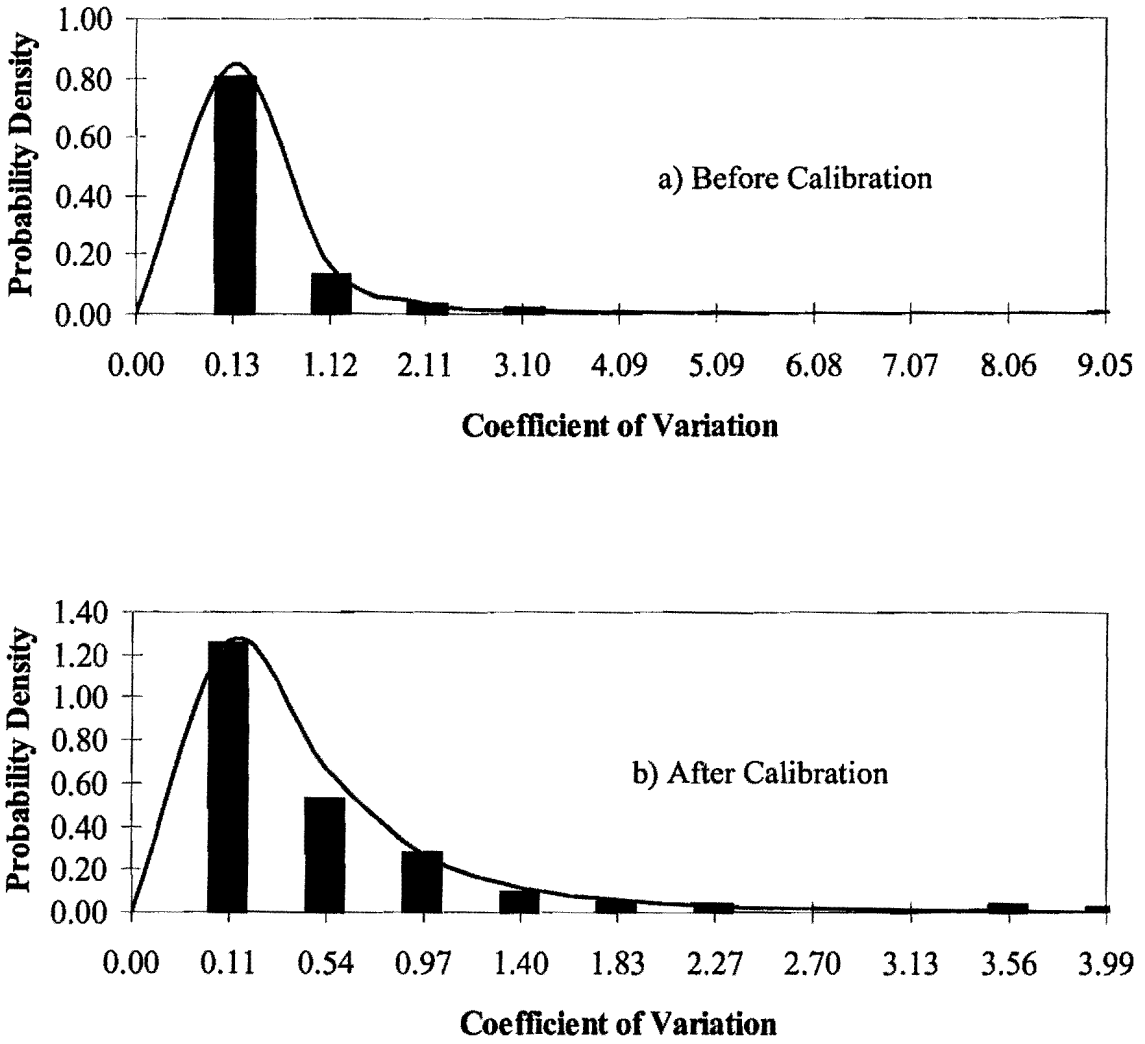

Figure 4.1 – Distribution of Coefficients of Variation from all FWDs at Site 1

assumed theoretical distribution. The basis for appraising the goodness of this comparison is the distribution of the quantity

$$\chi^2 = \sum_{i=1}^{k} \frac{(n_i - e_i)^2}{e_i} \tag{4.3}$$

The assumed theoretical distribution is an acceptable model, at the significance level α, when χ^2 is less than a value of $C_{1-\alpha,k-1}$. The $C_{1-\alpha,k-1}$ is the value of the appropriate χ^2 distribution at the cumulative probability of $(1-\alpha)$. For a confidence level of 95%, a $C_{1-\alpha,k-1}$ value of 16.90 was identified from a standard table for χ^2 distribution. As such, a χ^2 of less than 16.90 indicates that the fit is reasonable. As reflected in Table 4.1, in some cases, these values are larger than 16.90. Nevertheless, no other distribution provided a better fit.

Individual FWD

Similar process was carried out to determine the distribution of the COVs related to each FWD. Once again, the most practical distribution was log-normal. The results are shown in detail in Appendix A and are summarized in Table 4.2. For most FWDs the mean COVs were less than 1%, indicating fairly repeatable fleet. Once again, the calibration process had a minimal, and usually adverse, impact on improving the repeatability of each individual FWD. However, all values are well within the acceptable limit of 2%.

Individual Drop Heights

The most practical distribution for explaining the distribution of the COV from different drop heights was again log-normal. The results are shown in detail in Appendix A and are summarized in Table 4.3. As anticipated, the mean COV was largest for Drop Height 1 (lowest force imparted to the pavement). For the other three drop heights, the mean COVs were less than 1%, indicating fairly repeatable fleet. The calibration process marginally improves the repeatability of the fleet. For a confidence level of 95%, the theoretical distributions reasonably describe the data in many cases.

Individual Sensors

Finally, the distribution of COVs from data for each individual sensor was studied. Even though a gamma distribution provided a better fit to the data, we decided to recommend the log-normal distribution (the second best fit) as representative of the data. This was done for the sake of uniformity. Table 4.4 summarizes these results, while more extensive values are presented in Appendix A. The most repeatable sensors, per attempt before calibration, were the load cell and sensor SD5 whereas theand load cell as well as sensors SD1, SD3 and SD4 were more repeatable after calibration. In this case, the calibration seems to improve the repeatability.

Table 4.2 – Statistical Information about Distribution of Coefficients of Variation from All Sensors for Six FWDs

FWD Serial No.	Test* Period	Statistical Information		
		Mean	Standard Deviation	χ^2
024	B/C	0.74	0.45	19.8
	A/C	0.73	0.44	24.6
040	B/C	0.62	0.42	218.6
	A/C	0.83	0.43	21.8
047	B/C	0.76	0.52	30.6
	A/C	0.88	0.58	35.2
069	B/C	0.97	0.71	240.7
	A/C	1.16	0.78	14.6
089	B/C	0.52	0.33	20.8
	A/C	1.14	1.26	55.4
159	B/C	0.80	0.86	32.8
	A/C	1.34	1.32	42.6

*** B/C denotes Before Calibration and A/C denotes After Calibration**

Table 4.3 – Statistical Information about Distribution of Coefficients of Variation from All Sensors for Six FWDs

Drop Height	Test* Period	Statistical Information		
		Mean	Standard Deviation	χ^2
1	B/C	1.16	0.81	105.6
	A/C	1.08	0.72	16.5
2	B/C	0.64	0.46	17.8
	A/C	0.62	0.40	13.5
3	B/C	0.51	0.36	37.8
	A/C	0.45	0.26	17.8
4	B/C	0.63	0.37	52.5
	A/C	0.47	0.26	7.3

*** B/C denotes Before Calibration and A/C denotes After Calibration**

Table 4.4 – Statistical Information about Distribution of Coefficients of Variation from All Sensors for Six FWDs

Sensor	Test* Period	Statistical Information		
		Mean	Standard Deviation	χ^2
Load Cell	B/C	0.87	0.82	44.7
	A/C	0.51	0.29	21.3
SD 1	B/C	0.98	1.14	21.0
	A/C	0.41	0.24	4.8
SD 2	B/C	0.94	1.04	30.3
	A/C	1.38	1.33	48.4
SD 3	B/C	0.98	1.05	24.2
	A/C	0.44	0.27	13.0
SD 4	B/C	1.17	1.10	6.7
	A/C	0.53	0.28	8.2
SD 5	B/C	0.78	0.47	11.8
	A/C	0.72	0.43	46.2
SD 6	B/C	1.06	0.89	90.0
	A/C	0.91	0.33	37.2
SD 7	B/C	1.35	0.86	10.1
	A/C	1.25	0.86	14.5

*** B/C denotes Before Calibration and A/C denotes After Calibration**

Impact of Calibration

In the previous section, appropriate distributions for the COVs associated with repeating each test six times at a given point by each device were demonstrated. Informal observations with respect to the impact of calibration on repeatability were also made. In this section, a formal statistical analysis of the impact of calibration is provided.

The χ^2 analysis used for determining the appropriateness of the fit of the distribution to the measured data can also be used to determine whether the distributions of the COVs from before and after calibrations are significantly different. Equation 4.4 has to be slightly modified. Parameters n_i (deviates from observed distribution) and e_i (deviates from theoretical distribution) should be replaced by B_i (deviates from distribution before calibration) and A_i (deviates from after calibration). As such, Equation 4.3 can be written as

$$\chi^2 = \sum_{i=1}^{k} \frac{(B_i - A_i)^2}{A_i} \tag{4.4}$$

In this equation, if χ^2 is less than 16.90, one can conclude that the calibration does not significantly improve repeatability. In contrast, if χ^2 is greater than 16.90, the calibration either positively or

negatively impacts repeatability. It should be mentioned that although other methods, such as the analysis of variance (ANOVA), are typically used in engineering circles for this purpose, the χ^2 analysis is more appropriate especially when the distribution is not normal Cheremisinoff (1987).

Typical COV distributions for FWD 024 at two sites from before and after the calibration process are compared in Figure 4.2. The two distributions for Site 2 (weak flexible site) are shown in Figure 4.2a, and for Site 3 (rigid site) in Figure 4.2b. The observed χ^2 value for Site 2 was 1.6 and for Site 3 was 18.3. As such, the calibration process did not significantly impact the repeatability of FWD 024 at Site 2, but it impacted that of Site 3. To determine whether the impact of the calibration is favorable or not, one should compare the mean COVs from before and after calibration. From Figure 4.2b, the mean COV after calibration is smaller as compared to before calibration. This indicates that the calibration has improved the repeatability of FWD 024 at Site 3.

The results from similar analyses performed on data from the three sites for all FWDs are summarized in Table 4.5. The improvement in FWD repeatability is site dependent. At Site 1 (strong flexible site) for example, SHRP calibration seemed to have a positive impact on the repeatability of three of the FWDs. In this case, the impact was rather small because the χ^2 values were close to 16.90. For Site 2 (weak flexible site) however, the calibration process did not significantly improve the repeatability, since all χ^2 values were much less than 16.90. And again, for Site 3 (rigid site), the repeatability of only two FWDs was marginally impacted by calibration (one positively and one negatively).

Reproducibility[5]

Similar to the previous section, the impacts of several parameters on the reproducibility of the fleet were studied. In this section, the major parameter is the deviation index as described in Equation 3.1. These studies are summarized below.

Individual Sites

The actual distribution of differences from baseline measured for each attempt, each FWD and each sensor are demonstrated for Site 1 in Figure 4.3. The statistical information for this and other sites are summarized in Table 4.6. The normal distribution described this data adequately since most χ^2 values were 16.90. The mean values were in all cases close to zero. A study of Equation 3.2 indicated that these values should be close to zero. The standard deviation varies between 3% and 7%. The FWD fleet is least reproducible on the weak flexible pavement. Comparing the standard deviations from before and after calibration, the reproducibility is either not impacted or slightly negatively impacted.

[5] Detailed results can be inspected in Appendix B.

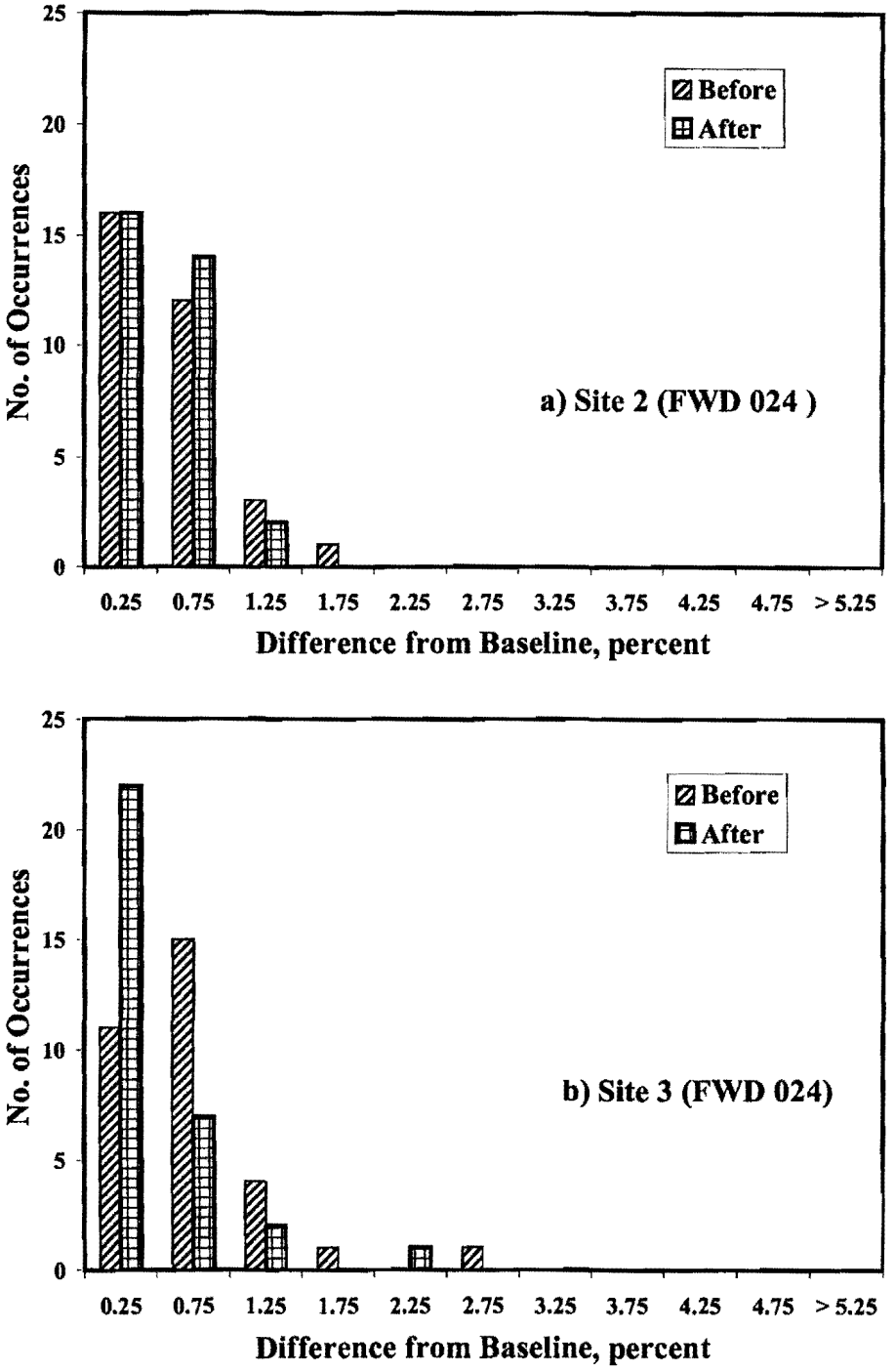

Figure 4.2 – Comparison of Histograms of COVs from Before and After SHRP Calibration Process for FWD 024

Table 4.5 – Impact of Calibration on Repeatability of FWD Fleet

Site	FWD Number	χ^2	Significance*
1	024	3.88	NS
	040	1.75	NS
	047	23.84	S (P)
	069	26.74	S (P)
	089	18.55	S (P)
	159	6.23	NS
2	024	1.57	NS
	040	9.02	NS
	047	7.39	NS
	069	2.96	NS
	089	3.62	NS
	159	4.00	NS
3	024	18.37	S (P)
	040	1.58	NS
	047	3.16	NS
	069	22.74	S (N)
	089	1.61	NS
	159	10.15	NS

*** NS = not significant, S (N) = significant but the impact is negative, S (P) = significant but the impact is positive**

Table 4.6 – Statistical Information about Distribution of Difference from baseline from All FWDs at Three Sites Tested

Site	Test* Period	Statistical Information		
		Mean	Standard Deviation	χ^2
1	B/C	0	5.58	20.1
	A/C	0	5.64	21.7
2	B/C	0	3.47	15.3
	A/C	0	2.95	16.7
3	B/C	0	6.13	15.3
	A/C	0	7.02	39.2

*** B/C denotes Before Calibration and A/C denotes After Calibration**

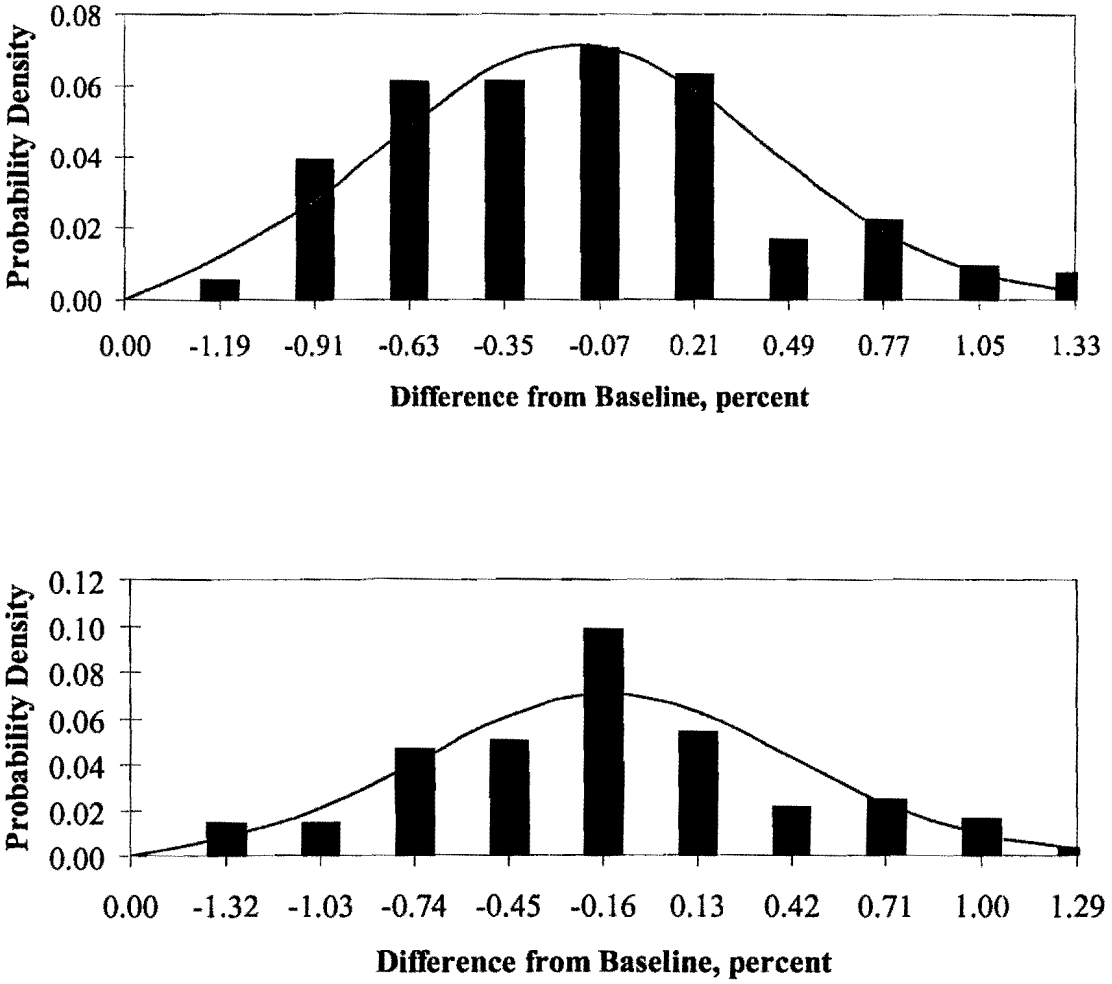

Figure 4.3 – Distribution of Coefficients of Variation from all FWDs at Site 1

Individual Drop Heights

The normal distribution was again the most fitting in describing the distribution patterns of the difference from baseline values for different drop heights. The results are shown in detail in Appendix B and are summarized in Table 4.7. Once again, the means are equal to zero as they should be. As judged from the standard deviations in Table 4.7, the fleet is most reproducible for larger drop heights. For Drop Height 1, the standard deviation is about 7% and for Drop Height 4 about 3%. Comparing the standard deviations from before and after calibration, the reproducibility is either not impacted or slightly negatively impacted.

Table 4.7 – Statistical Information about Distribution of Differences from baseline from All Sensors for Six FWDs

Drop Height	Test Period	Statistical Information		
		Mean	Standard Deviation	χ^2
1	B/C	0	7.25	18.3
	A/C	0	7.79	15.9
2	B/C	0	5.59	17.8
	A/C	0	5.59	23.2
3	B/C	0	3.70	23.8
	A/C	0	4.26	34.8
4	B/C	0	3.23	10.2
	A/C	0	3.17	49.7

Table 4.8 – Statistical Information about Distribution of Differences from baseline from All Sensors for Six FWDs

Sensor	Test Period	Statistical Information		
		Mean	Standard Deviation	χ^2
Load Cell	B/C	2.20	4.60	62.3
	A/C	2.20	4.60	62.3
SD 1	B/C	2.87	4.62	52.4
	A/C	3.20	4.76	57.3
SD 2	B/C	3.30	4.84	22.5
	A/C	3.57	4.96	75.9
SD 3	B/C	3.71	4.90	9.7
	A/C	3.89	5.11	48.6
SD 4	B/C	4.04	5.60	18.3
	A/C	4.25	5.27	33.9
SD 5	B/C	4.54	5.63	33.1
	A/C	4.58	5.37	31.2
SD 6	B/C	4.88	5.88	27.4
	A/C	4.88	6.06	119.9
SD 7	B/C	5.21	6.33	31.3
	A/C	5.24	5.98	84.1

Individual Sensors

The distribution of the difference from baseline for individual sensors was also considered. Once again, the normal distribution gave us the best results; those are summarized in Table 4.8. The mean values showed a bias towards over-prediction. This bias, which is more or less independent of the calibration, increases as the distance from the load increases. As it will be discussed later, this bias can partially be attributed to the method used for normalizing the deflections. A decreasing reproducibility trend, as indicated by the standard deviation increase in Table 4.8, can be linked to the distance from the load.

Impact of Calibration

To assess the impact of the calibration process on fleet reproducibility, the differences from baseline from all FWDs were combined and analyzed for each site. A typical result for Site 3 is shown in Figure 4.4. The reproducibility of the FWD fleet at this site after the sensors were calibrated is slightly less desirable as compared to the before condition. The number of cases where the differences from baseline were less than 0.5% after calibration was less than that before calibration. At the same time, the number of cases with differences from baseline greater than 5% increased.

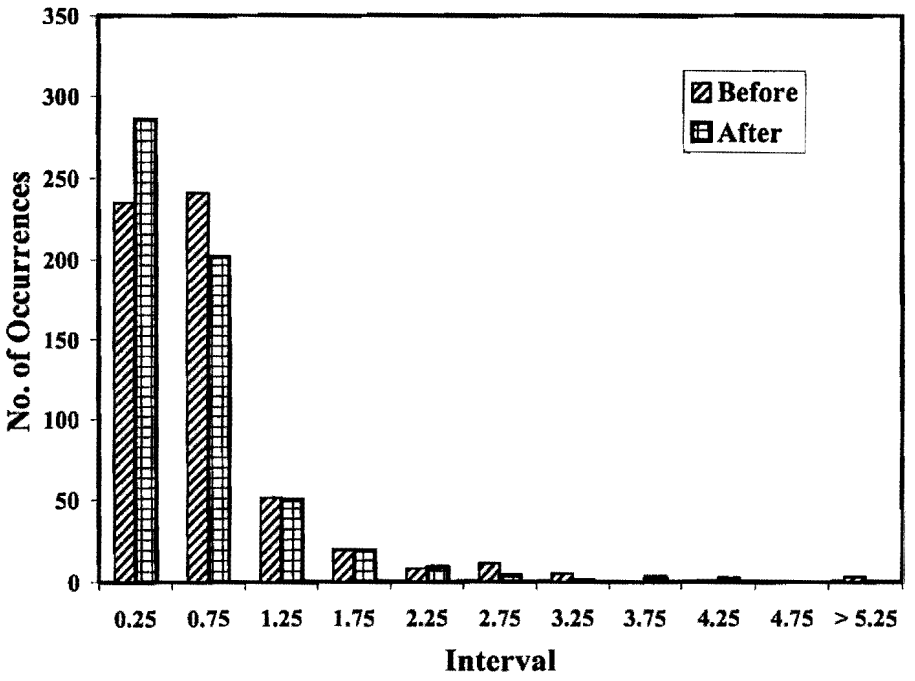

Figure 4.4 – Histograms of Deviation Indices from Before and After Calibration

The χ^2 values from the three sites are shown in Table 4.9. The reproducibility of the FWD fleet decreased slightly for Sites 2 and 3 after SHRP calibration, but did not significantly change for Site 1.

Table 4.9 – Impact of SHRP Calibration on Improving Reproducibility of FWD Fleet

Site	χ^2	Significance
1	10.7	Not Significant
2	64.9	Significant (Negative Impact)
3	23.3	Significant (Negative Impact)

Similarity of Devices

The final practical question to address is whether the six FWDs tested, in general, or different sensors, in particular, measure parameters that are statistically similar. A series of analysis of variance (ANOVA) were carried out to respond to these concerns.

The first analysis consisted of determining whether the six FWDs statistically provide similar results, independent of the site or sensor. To test this hypothesis, the differences from baseline from all drop heights and all sensors at all sites for each FWD were separated. This provided 96 data points per FWD. A sample calculation from data collected before calibration is shown in Figure 4.5. Two parameters of importance in this figure are F and F_{crit}. The F value is the ratio MS (between groups) and MS (within group). MS (within) is an estimate of the population variance based upon the deviation of scores about their respective group means. MS (between groups) is also an estimate of the population variance and is based upon the deviations of group means about the grand mean. The F_{crit} is directly obtained from a table of F statistics, which is based on confidence level and number of variables. If the observed F ratio is very large such that the probability is quite small that an F of this size should be obtained merely by chance, then perhaps the readings (sensor readings) do not belong to the same population. For a confidence level of 95% and the number of variables, F_{crit} is approximately 2.23. When F is less than F_{crit} one can assume that the sensor readings from all six FWDs belong to the same population (i.e. the FWDs are interchangeable). From Figure 4.5, the value of F is about 72 indicating that the probability of the FWDs being interchangeable is very small. Even though not shown here, after the calibration process, the F value was about 71, indicating no improvement.

To evaluate the impact of the site on the ANOVA results, the analysis was carried out at each site separately. The F values from all cases are reported in Table 4.10. Even though the F values are closer to F_{crit}, the probability of the fleet being interchangeable is still extremely small. For all three sites, the calibration was not enough to provide a reproducible fleet.

We further statistically examined the reproducibility of the sensors. The F values are shown in Table 4.11. According to the ANOVA test, the load cell is the most reproducible sensor. The F value before calibration is quite close to F_{crit} indicating that this sensor is almost interchangeable amongst the FWDs in the fleet. After calibration, the F value is way less than F_{crit}. As such, this

sensor can be considered as fully interchangeable. This trend is supported with some of the component studies we will report in Chapter 5.

SUMMARY

Groups	*Count*	*Sum*	*Average*	*Variance*
FWD 024	96	5.7839691	0.0602497	0.0029683
FWD 040	96	0.0390725	0.0004070	0.0016935
FWD 047	96	-2.8813619	-0.0300142	0.0013413
FWD 069	96	-3.8219982	-0.0398125	0.0012724
FWD 089	96	1.0996400	0.0114546	0.0018468
FWD 159	96	-0.2193215	-0.0022846	0.0008060

ANOVA

Source of Variation	*SS*	*df*	*MS*	*F*	*P-value*	*F crit*
Between Groups	0.60024012	5	0.120048024	72.54848556	9.81863E-59	2.229832319
Within Groups	0.943195067	570	0.001654728			
Total	1.543435186	575				

Figure 4.5 – Analysis of Variance on Difference from baseline measured at Three Sites with Six FWDs

Table 4.10 – Statistical Evaluation of Reproducibility of Fleet at Each Site

Site	F-Value*	
	Before Calibration	After Calibration
1	36.2	38.7
2	22.9	10.2
3	39.7	47.1

*** Fcrit = 2.26**

Table 4.11 – Statistical Evaluation of Reproducibility of Fleet at Each Site

Sensor	F-Value*	
	Before Calibration	After Calibration
Load Cell	2.9	0.5
SD1	8.1	4.9
SD2	18.5	15.4
SD3	18.3	15.5
SD4	19.5	28.0
SD5	15.5	16.0
SD6	16.7	15.0
SD7	10.6	20.5

*** Fcrit = 2.35**

Finally, we studied the possibility of any two FWDs in the fleet being statistically interchangeable. To do so, we utilized a χ^2 test to determine whether the distributions from any two difference from baseline calculated from two FWDs belong to the same population using Equation 4.4. In this case, A_is and B_is in Equation 4.4 are the histograms from two FWDs. An example of the histograms is shown in Figure 4.6. The two histograms are different resulting in a large χ^2 value of 254. The results from other pairs before and after calibration are summarized in Table 4.12. Almost all χ^2 values are greater than the critical value of about 16.90.

Table 4.12 – Statistical Evaluation of Interchangeability of Pairs of FWDs in Fleet

a) Before Calibration

Device	FWD 024	FWD 040	FWD 047	FWD 069	FWD 089
FWD 040	164.7				
FWD 047	117.8	147.9			
FWD 069	374.0	211.1	60.6		
FWD 089	241.9	169.2	213.7	969.9	
FWD 159	200.2	109.8	40.8	389.4	38.2

b) After Calibration

Device	FWD 024	FWD 040	FWD 047	FWD 069	FWD 089
FWD 040	78.9				
FWD 047	232.3	68.0			
FWD 069	391.2	169.7	76.4		
FWD 089	38.9	34.1	90.8	160.3	
FWD 159	236.4	15.3	39.4	116.7	75.0

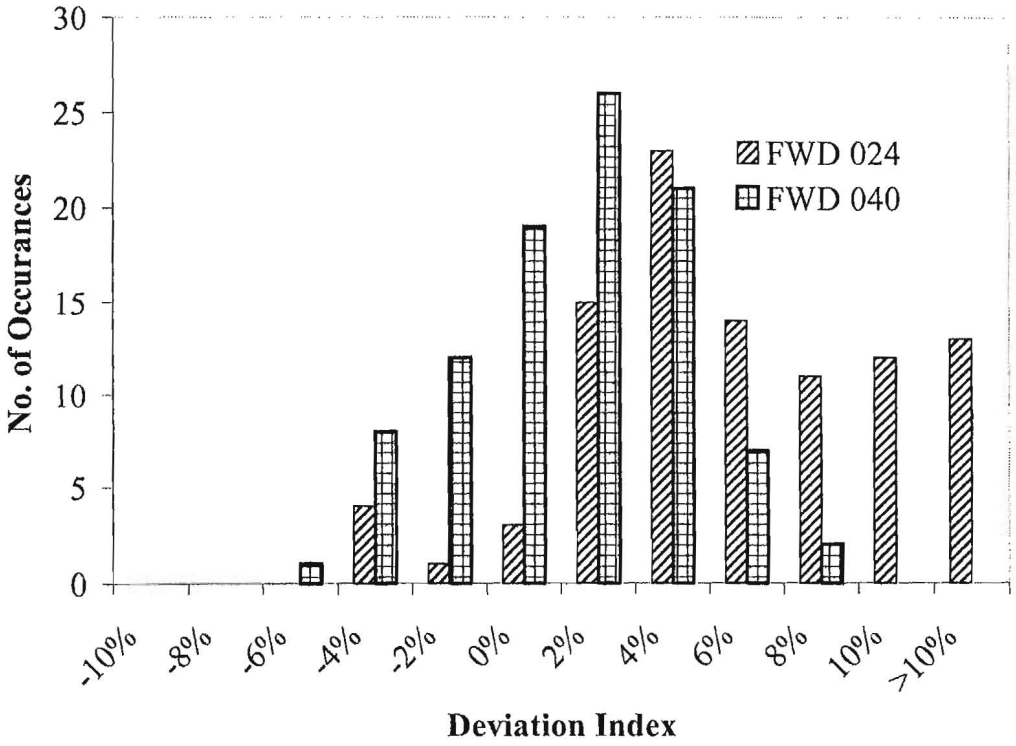

Figure 4.6 – Histograms of Difference from baseline from Two FWD Units

Chapter 5

Characteristics of FWD System During Loading

One of the major parameters that could contribute to a lack of reproducibility of the FWD is the movement of the FWD trailer during the impulse. If the sensors are not fully decoupled from the trailer, this motion can adversely impact the measured deflections. The movement of the trailer is related to the characteristics of the loading sub-assembly, the condition of the sensor holders, and the raise-lower system. Depending on the frequency and thoroughness of the trailer maintenance, the interaction between the trailer and sensor would change. To understand the nature of this interaction, three FWDs were instrumented in several manners. The movements of the strike plate (the plate that the buffers hit), the load plate (the plate that is in contact with pavement), the raise-lower bars, and the trailer itself were investigated.

Tests were typically carried out on a rigid and a flexible pavement on UTEP campus. The rigid pavement consisted of about 6 in. (150 mm) of PCCP over a stiff subgrade. The flexible pavement section consisted of about 2 in. (50 mm) of ACP over 6 in. (150 mm) of granular base, over a soft subgrade.

In this chapter, the instrumentation used is described, the experimental procedures are detailed, and typical results are presented.

Instrumentation

The main transducers used for this purpose were geophones, accelerometers and dynamic strain gauges (see Figure 5.1). Four well-calibrated geophones were used throughout this study. A detailed explanation of the characteristics of a geophone and the mechanical and electrical model that describes its function can be found in Nazarian and Bush (1989). Geophones are basically coil-magnet systems. When subjected to motion, the relative motion between the coil and the magnet generates a voltage that is proportional to the particle velocity of the materials underneath it. Therefore, in principle to obtain the displacement, the response of the geophone has to be integrated. The calibration of geophones is discussed in Tandon and Nazarian (2000).

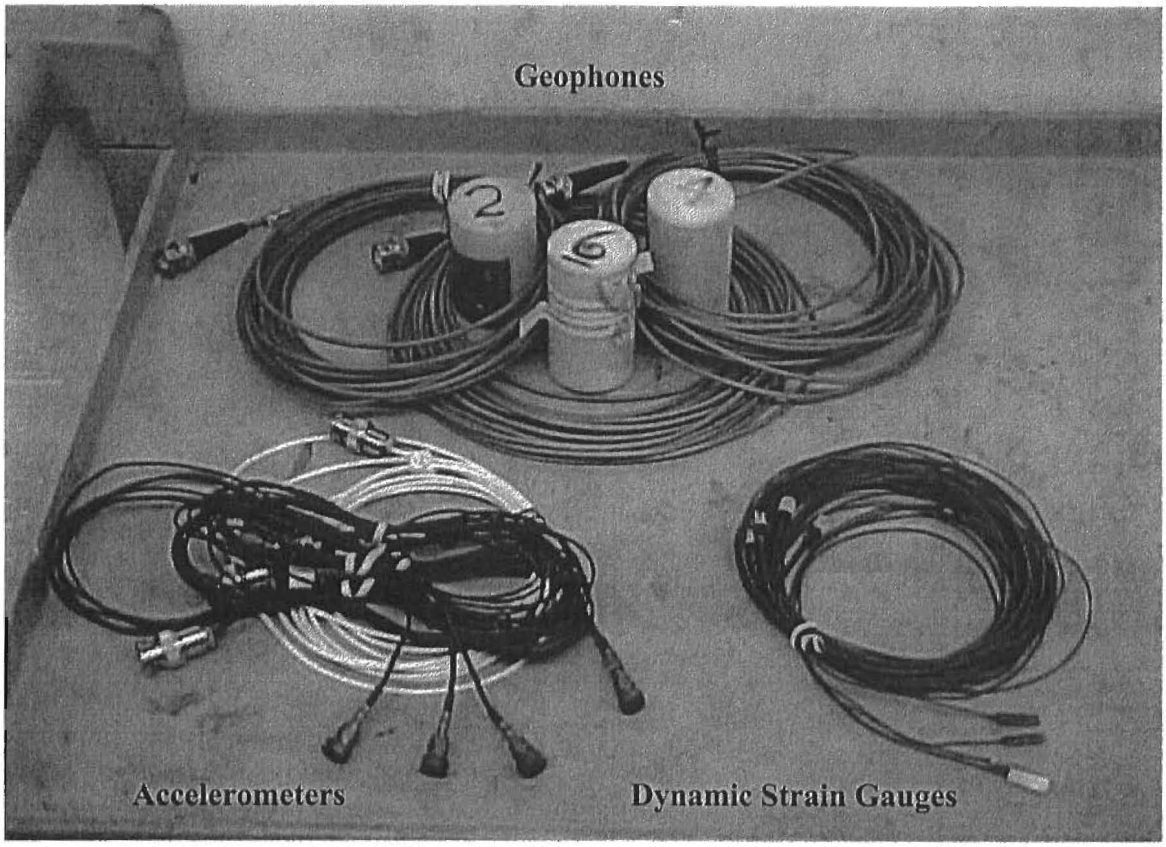

Figure 5.1 – Typical Sensors Used in This Study

The geophones used here have a natural frequency of 4.5 Hz, with a nominal sensitivity of 0.8 volt/in./sec (31.5 mV/mm/sec) and a damping ratio of about 0.7.

Four piezoelectric accelerometers were used to monitor some of the relevant motions of the FWD system. Tandon (1990) describe the conceptual design of such accelerometers. In principle, an accelerometer transmits output voltage that is proportional to the acceleration of the mass it is attached to. Once again, the calibration of accelerometers is discussed in Tandon and Nazarian (2000). To obtain displacement, the response of the accelerometer has to be integrated twice. Mathematically this is a simple task. However, because of practical complications of this operation in the presence of noise in data, double integration should be avoided except for high quality accelerometers. As such, the accelerometers were used to compare relative motion between different components. The nominal sensitivity of the accelerometers used is 100 mV/g (i.e., 0.26 mV/in./sec^2 or 10.2 μV/mm/sec^2).

Because of their small size (less than 1 in., 25 mm) and ease of installation, dynamic strain gauges are ideal for the type of instrumentation required for this project. The dynamic strain gauges are piezoelectric in nature, similar to the accelerometers described above. They incorporate quartz sensing elements and built-in microelectronic signal conditioning circuitry to generate an output signal that is proportional to dynamic strain influences. Since these sensors only respond to dynamic strains, they may be used to detect low-level dynamic strains that are superimposed on a large static load. The nominal sensitivity of the strain gauges used is 50 mV/μstrain.

Characteristics of Strike Plate

As indicated before, a total decoupling of the FWD geophones from the load subassembly is not practical. As such, it is desirable to minimize any vibration of the trailer, especially horizontal deformations. The strike plate is impacted directly by four buffers. The main function of this plate is to convert the potential energy, stored when the weights are raised, to kinematic force to be transmitted through the load sub-assembly to the load plate. It is desirable that the buffers impact the strike plate uniformly and simultaneously. In that manner, the load is transferred vertically minimizing the horizontal or torsional movement of the trailer during the impact. Aside from minimizing horizontal and torsional motions of the trailer, vertical impact will provide load time histories that are similar in shape and magnitude.

The typical set up used for this purpose is shown in Figure 5.2. Four dynamic strain gauges were placed symmetrically on the strike plate. To install the sensors, the strike plate was thoroughly cleaned and the sensors were glued using fast setting super glue.

Typical behaviors of the strike plate observed during our test program are shown in Figure 5.3. For one of the older FWDs the trend shown in Figure 5.3a was observed. In this case, three of the buffers struck the plate at almost the same time, with the fourth one about 3 msec later. The loads applied to the plate, and as a result the strains, were not symmetrical. The least load was applied by Buffer 3, and the most by Buffer 4. The nominal capacity of the strain gauges used is 100 μstrain. The flat response of Strain Gauge 4 near the maximum strain occurs because the strains exceed the capacity of the gauge. A set of less sensitive strain gauges is acquired for future tests. Based on these records, this FWD would exert a movement towards the general direction of the line connecting Buffers 2 and 4. The second trend, which was observed on the newer FWDs, is shown in Figure 5.3b. For ease of comparison, Figures 5.3a and 5.3b are plotted with the same scale. In this case, the strike plate experiences much less deformation. Nevertheless, sensors near Buffers 2 and 4 experience higher deformations than the other two, with sensor one recording a small strain in the opposite direction of the other three.

The reason for such a different behavior was further investigated. It was found that the location and shape of the stiffeners supporting the strike plate could contribute to such differences. The schematic of the strike plates along with the location of the stiffeners are shown in Figure 5.4. In the figure, the dashed circles represent the locations where the buffers strike the plate. For the newer FWDs, the stiffeners are aligned with the location of the buffers, whereas for the older one this is not the case.

The implication of differences in the structure is demonstrated in Figure 5.5a. The load pulse from the older FWD contains two peaks that more or less coincide with the peaks from the two sets of buffers. The load pulse from the newer FWD is smoother, but hints of localized peaks that coincide with the peaks of the strain records from different buffers are still evident. The deflections of SD 4, measured simultaneously from the two FWDs, are shown in Figure 5.5b. The two deflection time histories are similar. As it will be discussed later, these localized peaks may contribute to some of the variations in the normalized deflections.

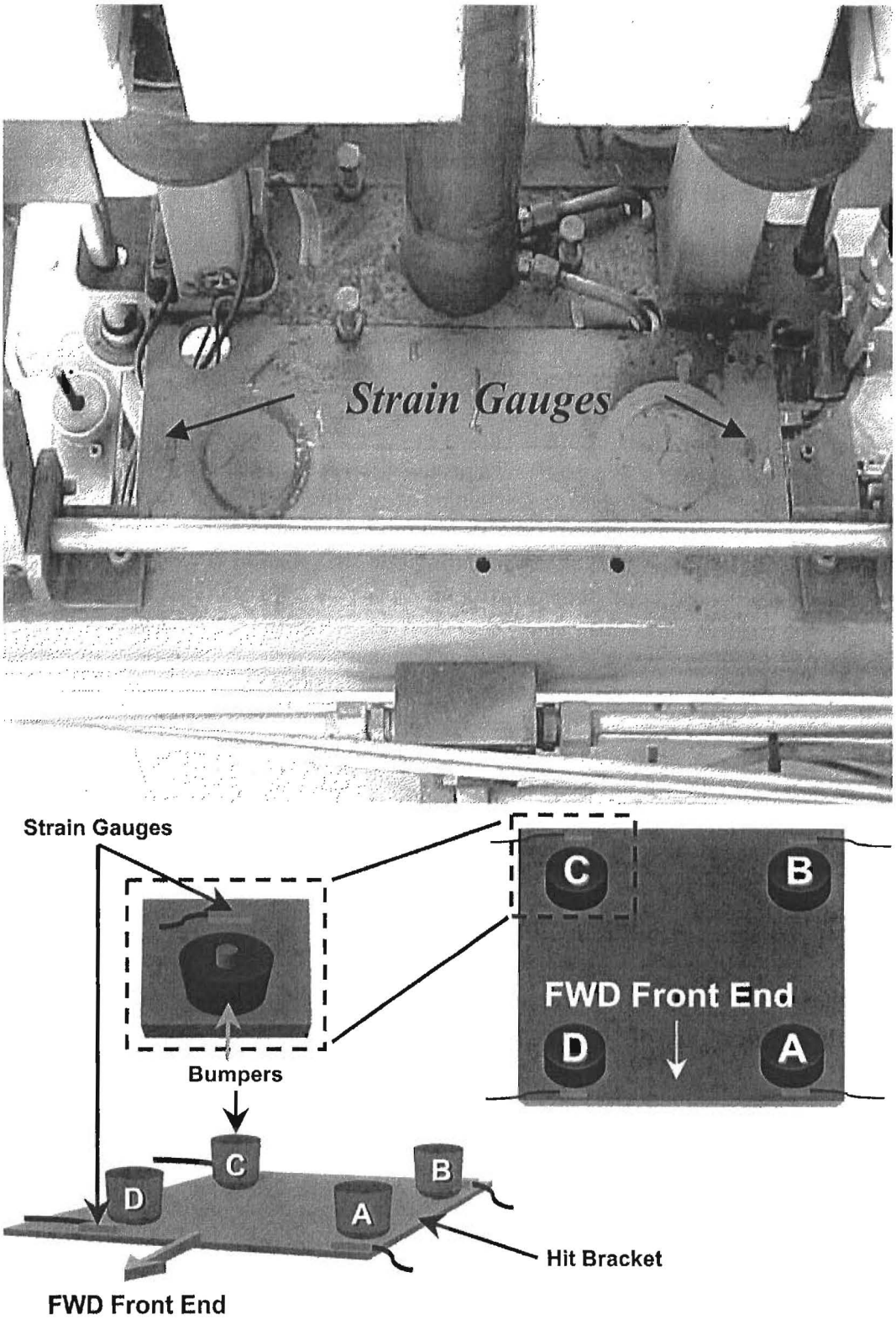

Figure 5.2 – Schematic of Set up Used for Measuring Behavior of Strike Plate

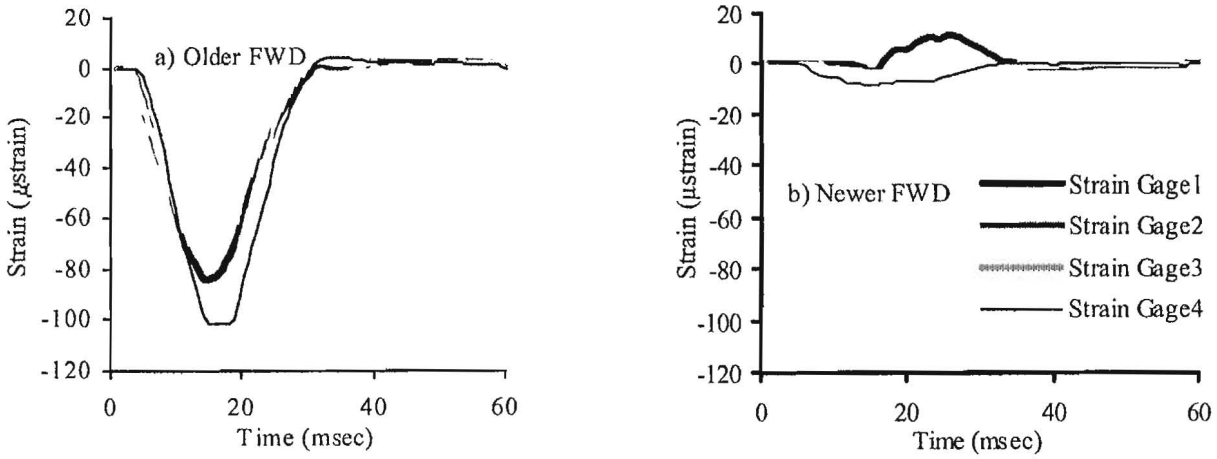

Figure 5.3 – Variations in Typical Strain Time Histories of Strike Plates

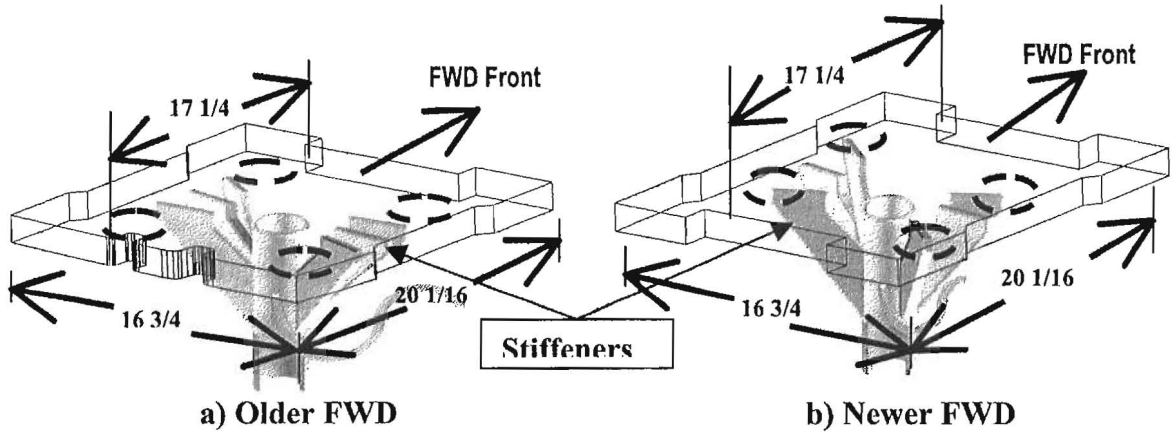

Figure 5.4 – Schematic of Strike Plate Designs

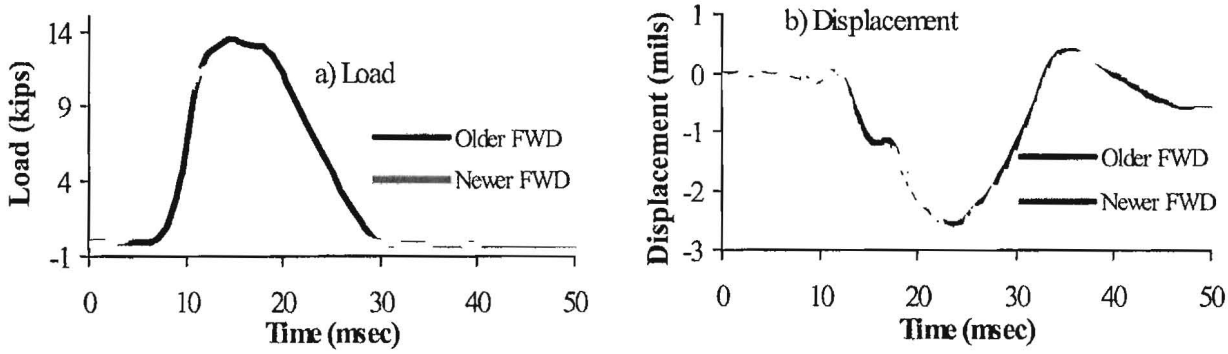

Figure 5.5 – Typical Load and Deflection Time Histories from Two Types of FWD Structures

One of the questions typically asked is whether rotating the buffers will impact the response of the FWD. Even though not shown here, mixing new and old buffers, especially when they are different shapes significantly impact the behavior of the FWD. Extremely high and non-symmetrical strains are measured on the strike plate. In these cases, excessive trailer vibration was obvious to the naked eye. However, when buffers of the same age from the same FWD were rotated, the differences in the deflections measured were small. Typical variation in deflections as a function of the position of the buffers is shown in Figure 5.6. Typically the differences in deflection from different buffer arrangements are less than 2%.

After quite a few drop tests, a relationship between the load cell pulse shape and the geophone deflections can be observed. It is therefore reasonable to assume that anything that affects the shape of the load cell pulse will in turn have an effect on the geophone deflections. The rotation of the buffers is not the exception. While rotating a new set of buffers creates little differences in the load cell pulse shape and geophone deflections, the same cannot be said when different types of buffers are mixed, or even when new and old buffers make up the set. In the latter instance, the geophone deflections show striking differences as the buffers are positioned at different corners. This can be attributed to the fact that different buffer types may have different heights and different coefficients of stiffness. The difference in buffer strikes can even be heard, as the buffers hit the bracket at different times. This creates a double-peak effect on the load cell pulse, which is then detected by the geophones. These double peaks can diminish the repeatability of an FWD because there could be cases when the first peak of the time history detected by the geophone is greater and other cases when the second is greater. This is important because the time from zero to peak of the signal should remain as constant as possible for repeatable measurements.

It should be mentioned that such repeatable results were possible only when the buffers were secured and tightened using a torque wrench. It is highly recommended that all four buffers be tightened using a torque of about 30 lb-in. (3 KN-mm).

Characteristics of Load Plate

The next step consisted of documenting the movement of the load plate. The load plate transfers the applied load to the pavement through a multi-layered plate. The plate typically consists of a 3/4-in. (19-mm) thick steel plate connected to a 7/8-in. (22-mm) thick PVC plate. A ribbed neoprene plate, glued to the PVC plate, is in contact with the pavement to provide a uniform load distribution. To study the characteristics of the load plate, it was instrumented with accelerometers and strain gauges. The typical arrangement of strain gauges is shown in Figure 5.7. The four strain gauges where placed along a radius of the plate to measure the strain experienced by the plate. The nominal locations of the strain gauges from the center of the plate were 3-7/8 in. (98 mm), 4-5/8 in. (118 mm), 5-3/8 in. (137 mm) and 6-1/8 in. (156 mm).

Typical response of the load plate on a concrete slab is shown in Figure 5.8. The highest strain is experienced by the strain gauge closest to the load. The strain decreases as the radial distance increases. Typically the strain measured by the first strain gauge was three to four times that of the fourth strain gauge. Similar results for testing on flexible pavement were obtained. While the strain patterns observed on both the load and strike plates were similar in shape, the amount of strain, particularly on the strike plate, was of such magnitude on the flexible surface that it only allowed us

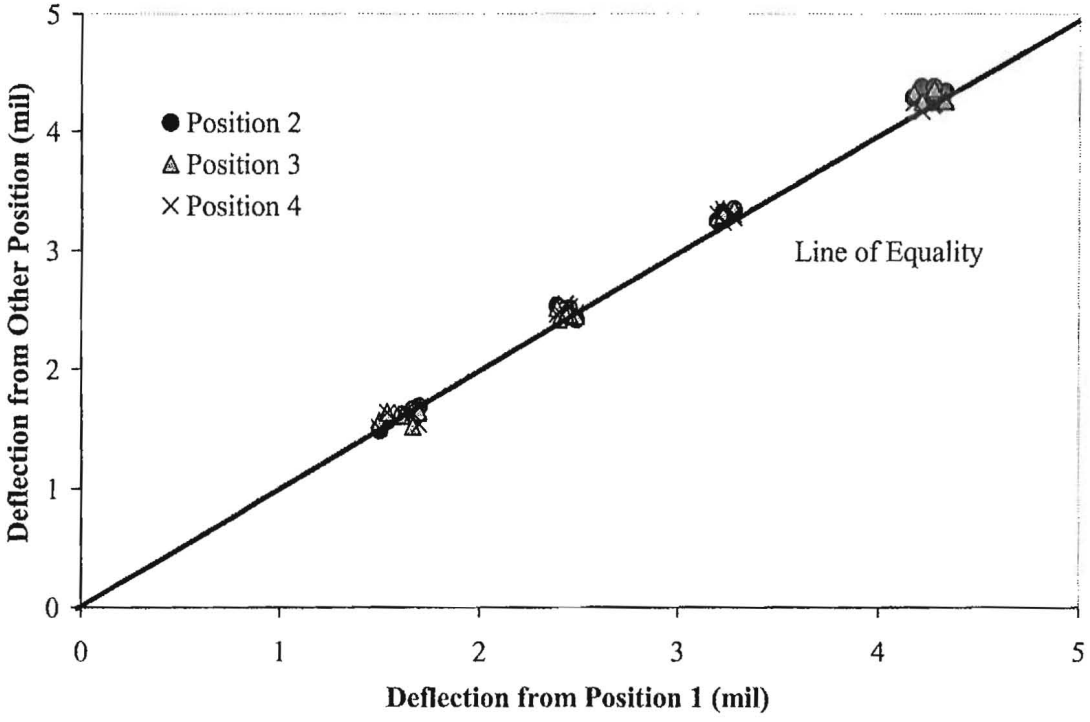

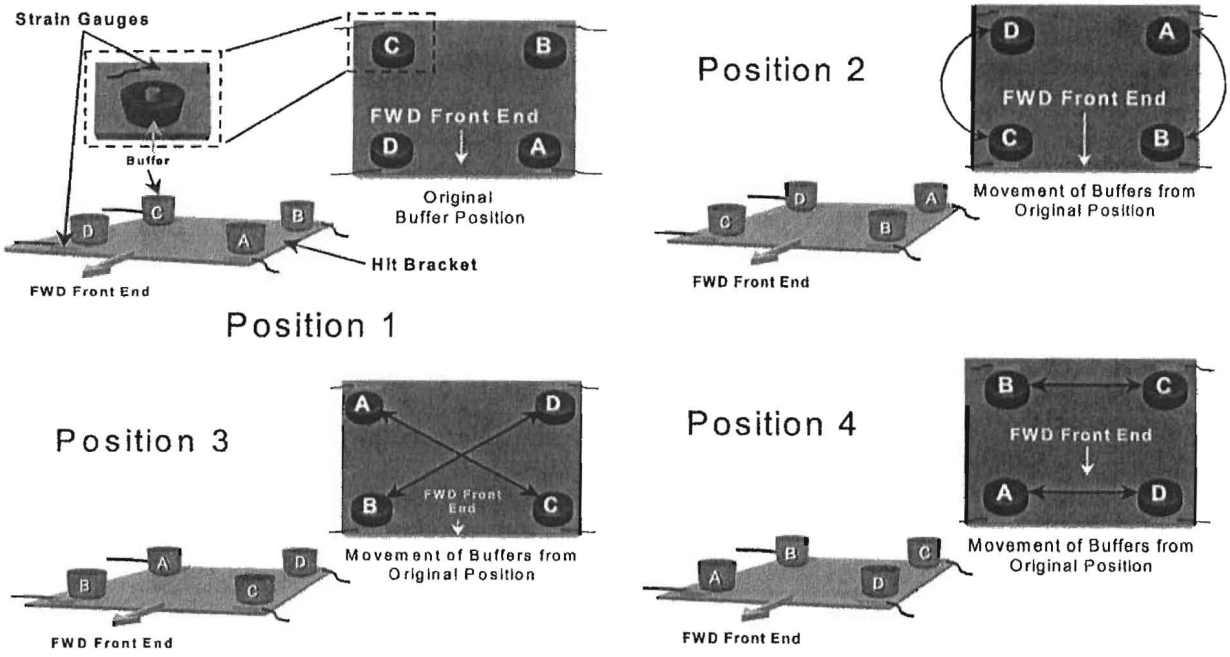

Figure 5.6 – Impact of Rotating Buffers from Same FWD

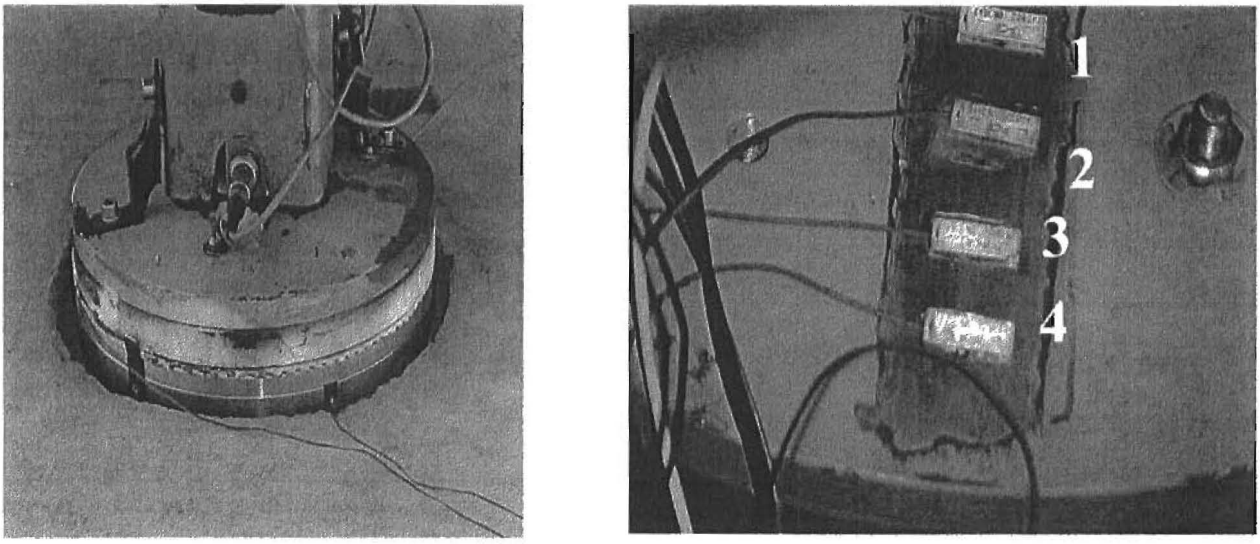

Figure 5.7 – Installation of Strain Gauges on Load Plate

to measure strains at Drop Height 1. On all other heights, the strain signals exceeded the limits of the strain gauge.

To investigate the impact of the condition of the load assembly on the response of the load cell, the old load plate assembly was replaced with a brand new one, without altering any other components. The distribution of strain along the new plate is shown in Figure 5.9. In this case, the strains are smaller than those shown in Figure 5.8. Strain Gauge 4, which is farthest from the load experiences negligible strain.

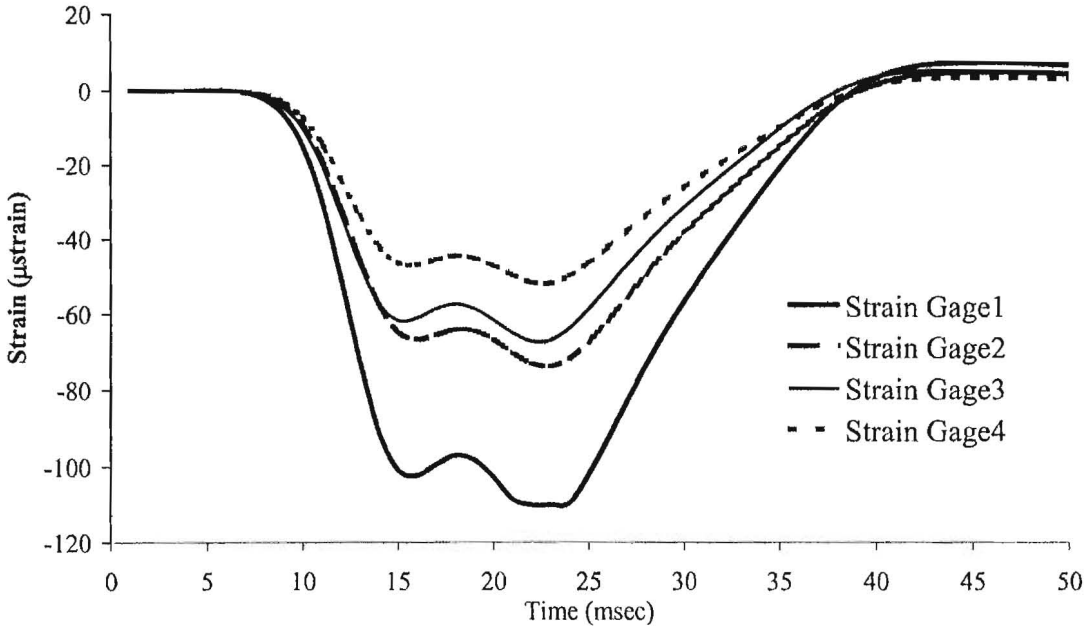

Figure 5.8 – Typical Variations in Strain Time Histories along FWD Load Plate

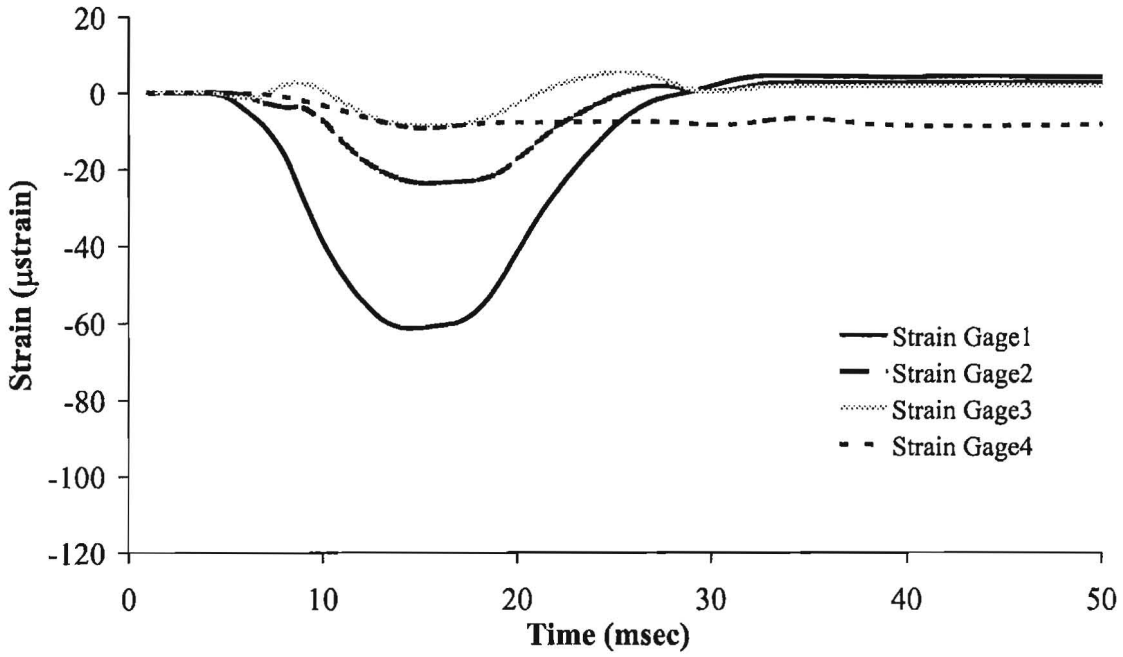

Figure 5.9 – Variations in Strain Time Histories along FWD Load Plate (Brand New Load Plate Assembly)

A comparison of Figures 5.8 and 5.9 indicates that changing the load plate assembly also changes the load pulse shape. This was a surprising finding. However, a closer inspection of the old load assembly revealed that accumulation of dirt and lack of lubrication could be the reason for this phenomenon. When the old assembly was cleaned, lubricated and reinstalled, the load pulse shape was similar to the one obtained from the new one.

A split plate assembly was also mounted on the FWD. The solid and split plates are shown in Figure 5.10. Because of the shape of the plate, Strain Gauges 1 and 2 could not be placed on the load plate. The strain time histories for gauges 3 and 4 using a split plate are shown in Figure 5.11. As seen in Figure 5.10, the load is transferred through an intermediate plate to the split load plate. In this case, the load plate experiences small strains, but in the opposite direction of those measured on the two solid plates.

The time histories measured at one point on the slab are compared in Figure 5.12 for the same drop height. The split plate and the new solid plate provide similar pulse shapes. However, the pulse shape from the original load plate was somewhat different. For the two solid plates, the load pulse shape and the responses from the strain gauges are quite similar. The measured peak loads reported by the FWD varied by about 3%.

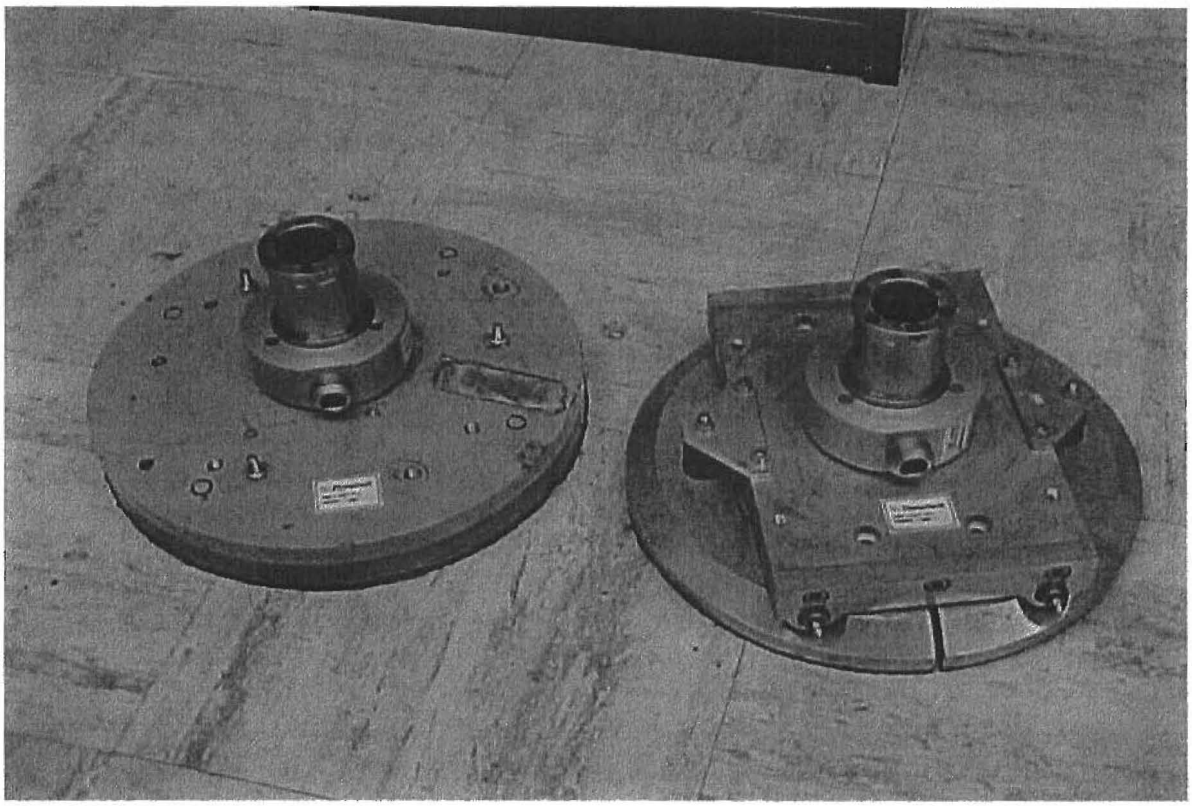

Figure 5.10 – Comparison of a Solid Plate Assembly and a Split Plate

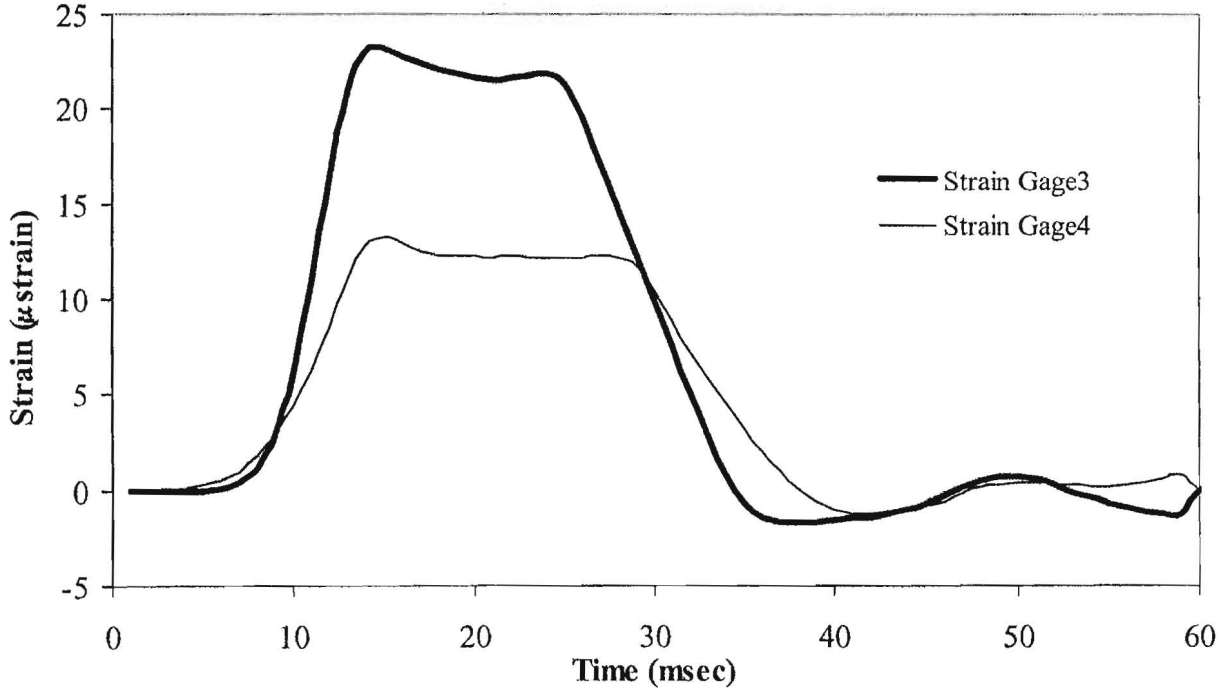

Figure 5.11 - Variations in Strain Time Histories along FWD Load Plate (Split Load Plate)

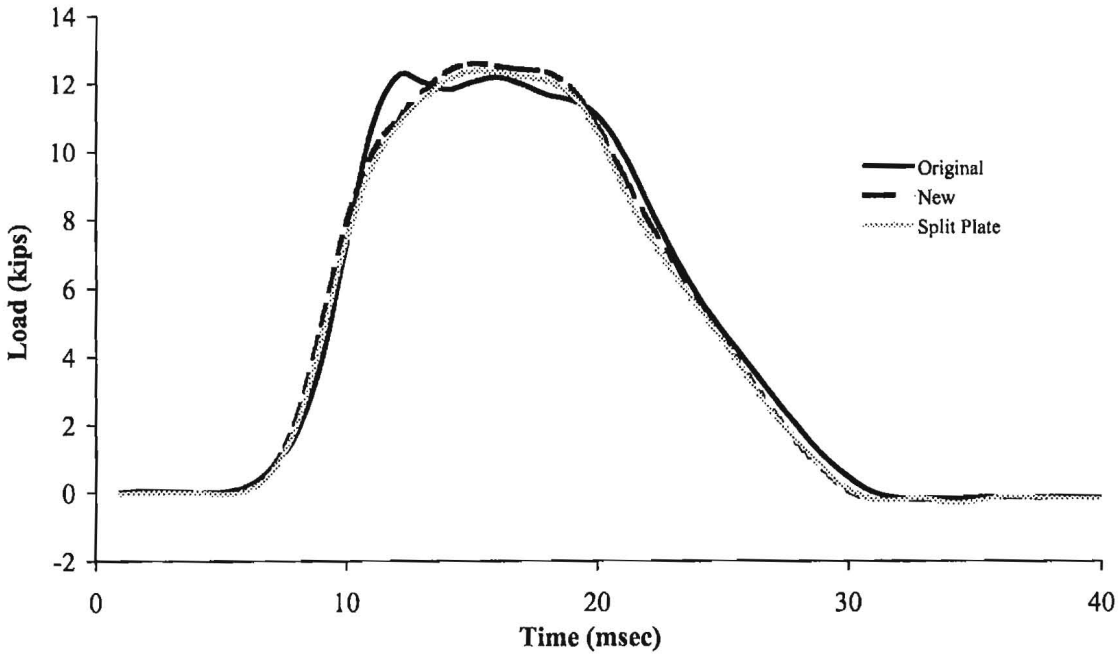

Figure 5.12 – Comparison of Load Time Histories Reported by FWD from Three Different Load Plates

Similarly, the deflections time histories reported by the FWD (simultaneous with the loads shown in Figure 5.12) are demonstrated in Figure 5.13 for one sensor. In this case, the time histories are very similar in shape; however, the differences in peak values are around 5%. Based on studies similar to this, one can conclude that the condition of the load plate assembly may impact reproducibility of the FWD fleet. The condition of the load plate should be included as part of FWD evaluation in new calibration protocols.

To monitor the motion of the load plate, four accelerometers were placed about 6-3/8 in. (160 mm) from the center of the plate along two mutually perpendicular radii (see Figure 5.14). Typical responses from the accelerometers are shown in Figure 5.15. The motion of the plate measured at three locations is very similar. With the motion from the fourth location somewhat more exaggerated.

Characteristics of Raise-Lower Bars

The raise-lower bars contain a mechanism to place the deflection sensors automatically and securely onto the pavement. As schematically shown in Figure 5.16, one side of each bar is secured to the FWD near the loading system, while the other side is free-floating. Given this design, one would anticipate these bars to experience motion during the FWD load impulse.

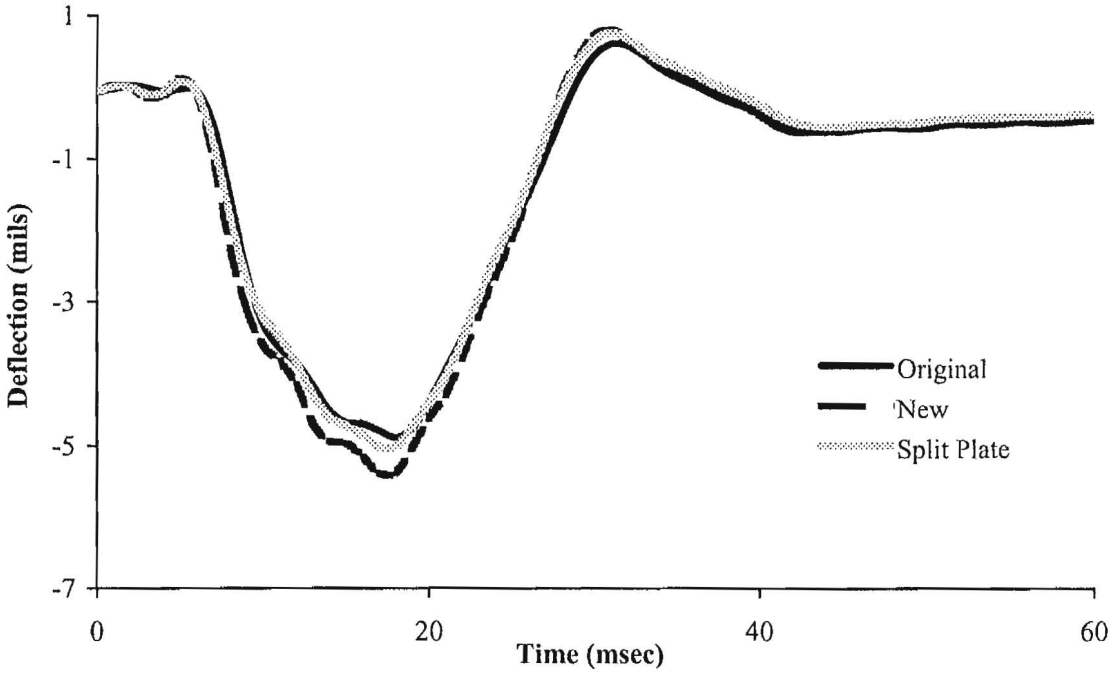

Figure 5.13 - Comparison of Deflection Time Histories Reported by FWD from Three Different Load Plates

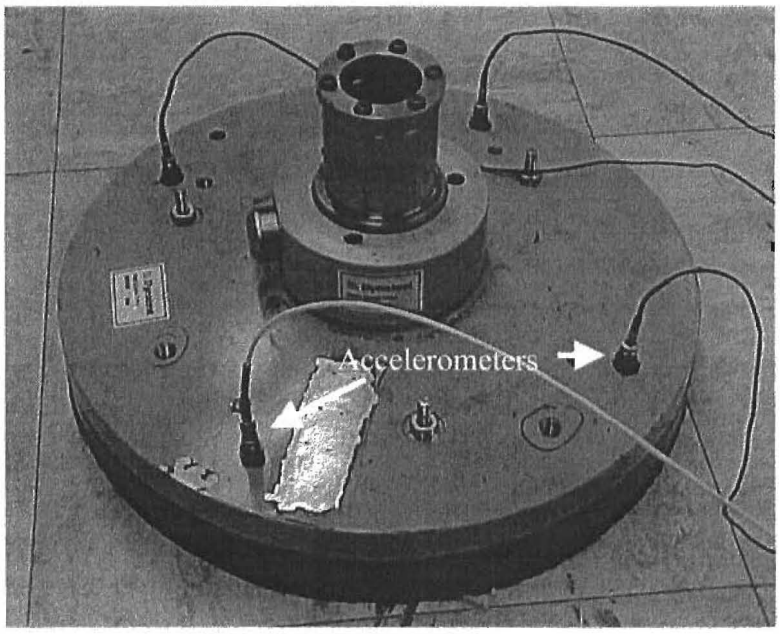

Figure 5.14 – Typical Placement of Accelerometers on Load Plate

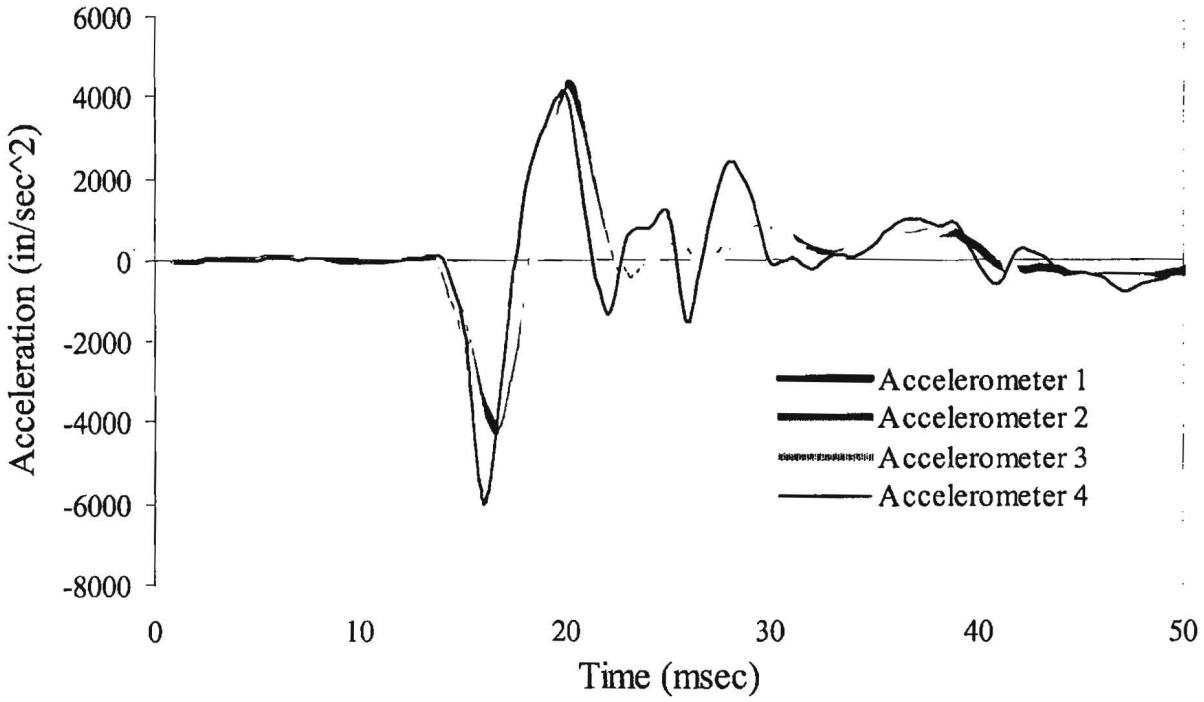

Figure 5.15 – Typical Motion of Load Plate

Typical movement of one raise-lower bar at three locations (at SD2, SD4 and SD6) is shown in Figure 5.17. The deflection from SD4 is also shown in the figure as a reference. The beam experiences movement that in some instances is greater than the deflection measured on the pavement itself. The largest motion is measured near the load plate, and the least closer to the pivot end of the bar near SD7. The time histories from the three locations experience peaks and valleys at almost the same time. From the last two statements, the raise-lower bar vibrates similar to a rigid beam with the pivot point near SD7. The large amplitude steady-state vibration of the beam occurs past the peak deflection measured on the pavement. As such, the impact on peak deflections should not be significant. Should TxDOT decide to implement the so-called full-waveform analysis on the FWD responses, this matter should be revisited.

Comparing the deflection time history measured with SD4 and the deflection of the raise-lower beam near SD4, one observes that some of the motion of the beam occurs during the peak deflection of the pavement. One should not automatically assume that such a movement would necessarily significantly and adversely impact the recorded deflections. However, excessive movement of these bars may be a reason for more careful inspection of the loading system and the geophone holders. The overall movement of the bars can be minimized by ensuring that the buffers, strike plate and the load plate system of the FWD are functioning well. The geophone holders, as it will be discussed in the next section, are designed to minimize the interaction between the sensors and the other components of the FWD.

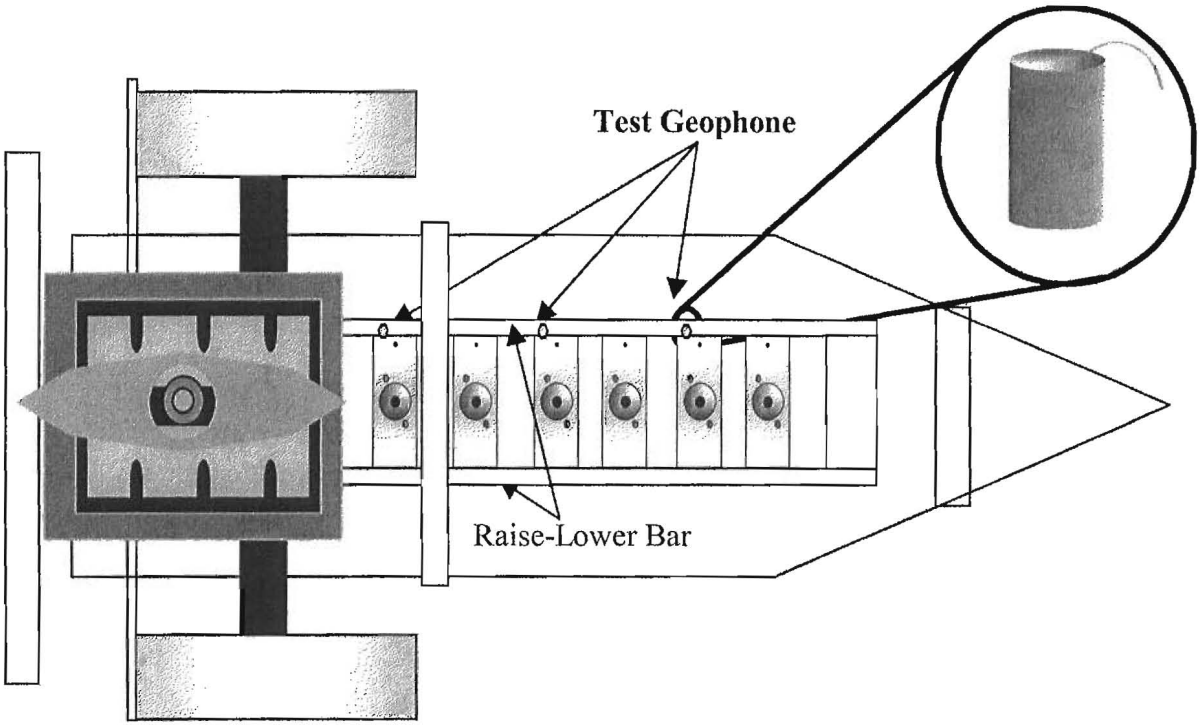

Figure 5.16- Instrumentation of Raise-Lower Bar

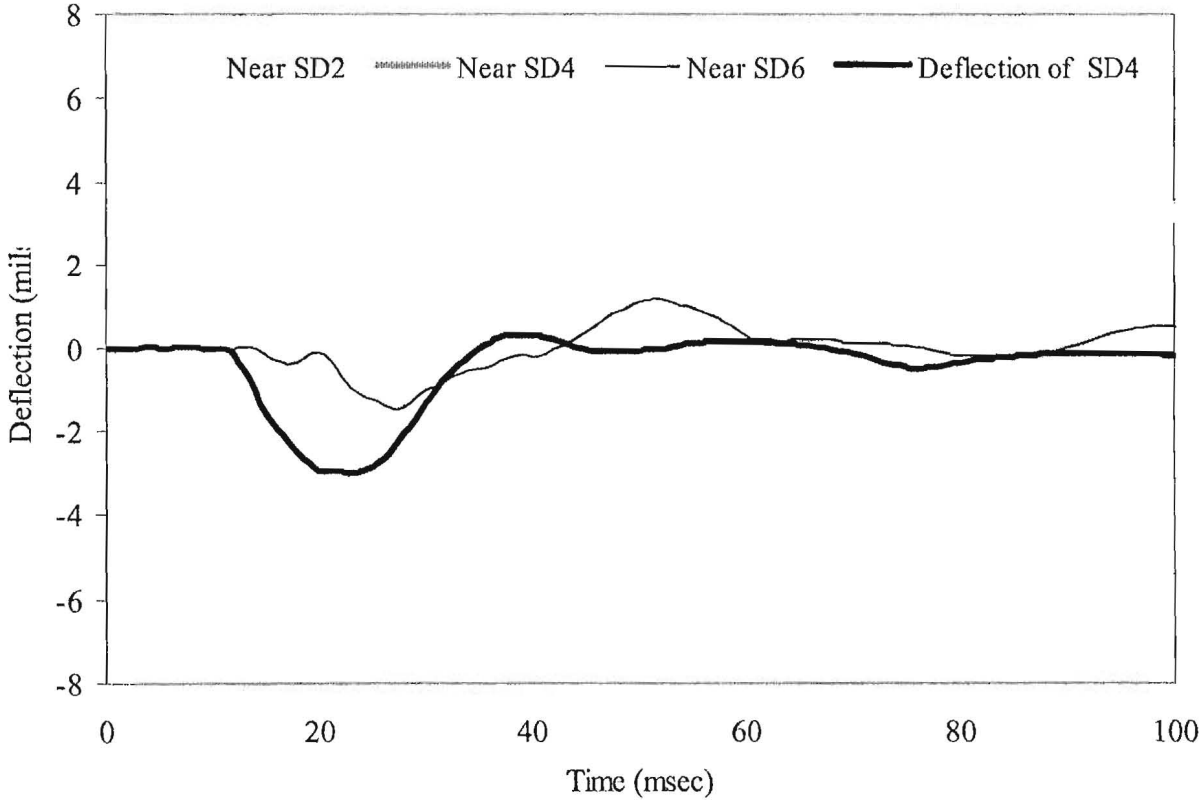

Figure 5.17 - Typical Movement of Raise-Lower Bar

Characteristics of FWD Trailer

The main purpose of the FWD trailer is to transport the different FWD components as one unit. As such, one would anticipate that its impact on the deflection and load measuring components should be small. Excessive motion of the FWD trailer and its mode of vibration are quite important to the overall health, and the long-term performance of the system. A trailer with little movement would indicate a well-maintained loading system.

To determine the movement of the trailer, six measurements were made by placing geophones along the railing of the trailer as shown in Figure 5.18. The sensors were aligned with SD2, SD4 and SD6 on the FWD. The motion experienced by one side of the FWD trailer is shown in Figure 5.19. The motion of the sensors aligned with SD6 is the smallest while the motion from the sensor aligned with SD2 is the largest. Also the motion detected by these two sensors is out of phase (i.e., the peak from one sensor is aligned with the trough of the other). This indicates a swaying motion. In addition, the relative motions are small and are in the order of the motion measured by the FWD sensor 4.

Another type of motion is shown in Figure 5.20. In this case, the three sensors measure motions that are in synchronization since the peaks and troughs are aligned. The maximum motion is somewhat large and delayed between the sensor aligned with SD2 and that aligned with SD6. The deflections are also much larger. Large deformations of the trailer should not be automatically inferred as a source of the problem in terms of measuring accurate deflections. The quality of the sensor holding assembly dictates the amount of the change in deflection. However, it may be a good practice to minimize this vibration to increase the life of the device.

In general, it can be concluded that the characteristics of the movement of the FWD system during loading may influence measurements made with the system. As designed by the manufacturer, these systems are well isolated so that their impact on the measurements made may be small. With time and wear and tear the interaction of these parameters may contribute to slightly less accurate measurements. Since current calibration processes do not consider these parameters, one may suspect that they may contribute to the lack of reproducibility of the fleet.

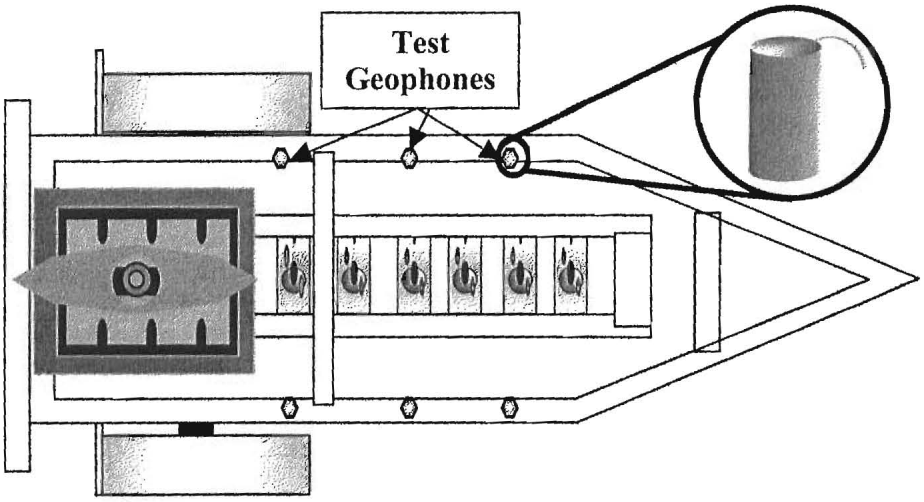

Figure 5.18 - Instrumentation of FWD Trailer

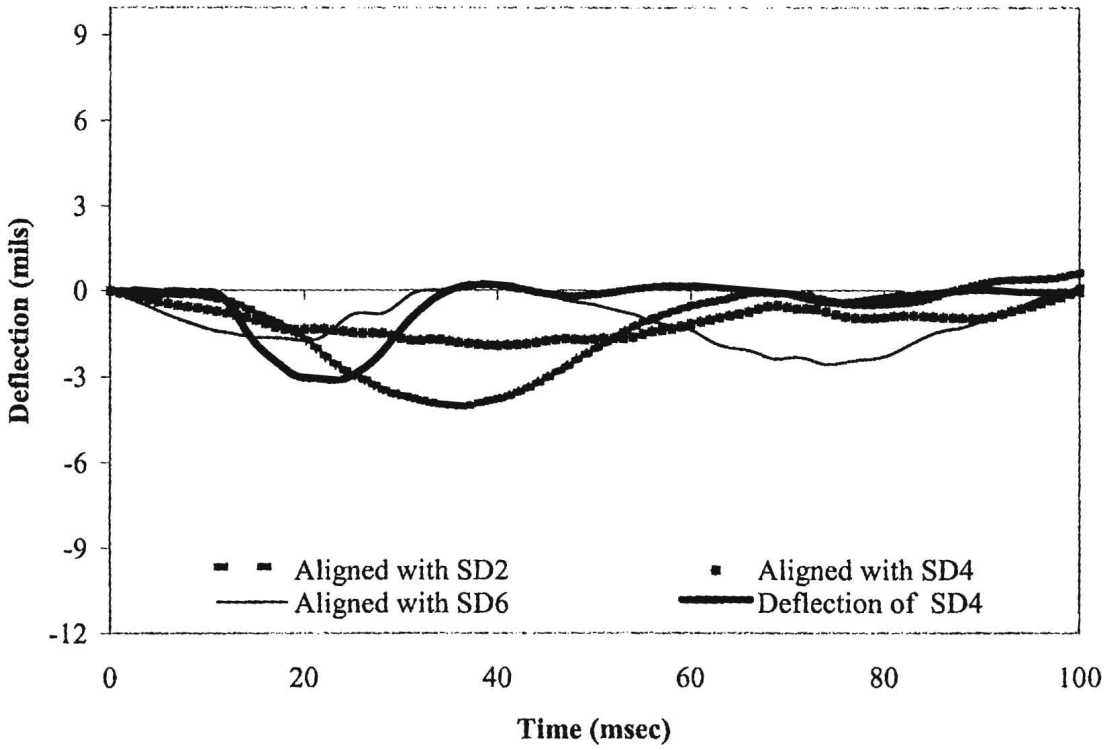

Figure 5.19 – One Type of Movement of FWD Trailer

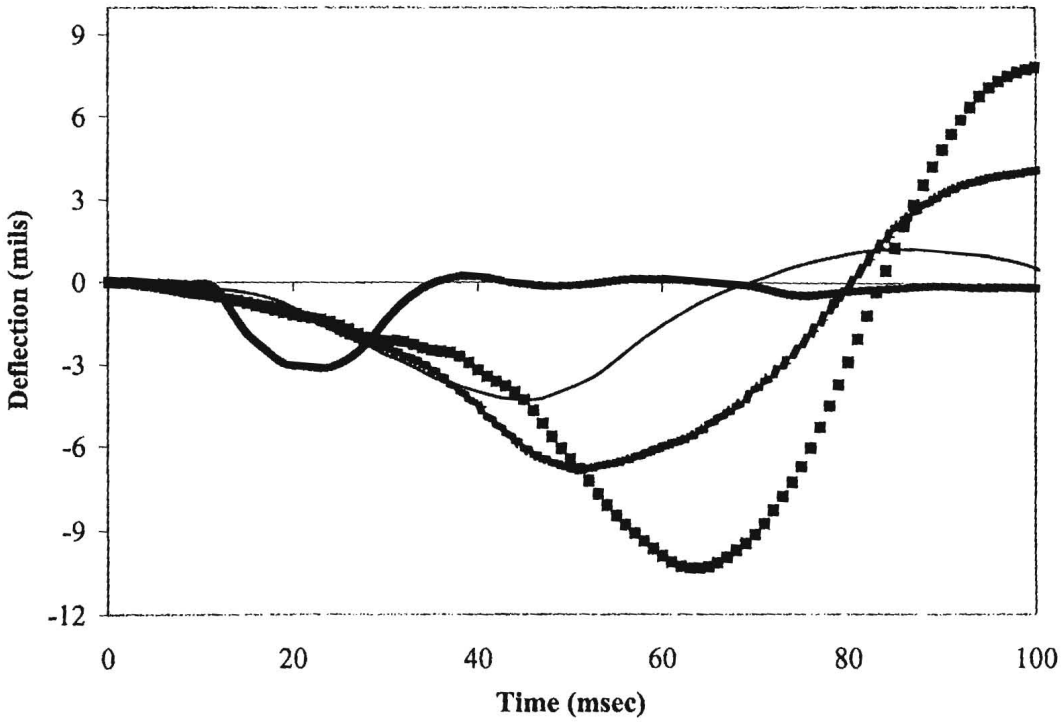

Figure 5.20 –Alternative Type of Movement of FWD Trailer

Chapter 6

Impact of FWD Components on Response of Sensors

Tandon and Nazarian (1998) and Chen et al. (1999) have identified several FWD components that can impact the response of FWD sensors (load cell and geophones). In this chapter, the effect each of the components has on sensor performance is described. The items under study were the rubber buffers, geophone holder elements and the load plates. The impact of the load plate (solid vs split) and their components were reported in the previous chapter.

Rubber Buffers

The rubber buffers act as a spring set between the falling mass and the hit bracket. This spring set assists in decelerating the mass as it impacts the bracket. As such, the rubber buffers are used in the FWD for a smooth transfer of loads from the falling weight to the load plate through the hit bracket. The falling weight energy is distributed to three sections of the loading mechanism: a) energy transferred to the hit bracket, b) energy transferred back to the falling weight, and c) energy absorbed by the buffers due to dampening or frictional losses. The stiffness or spring constant of the buffers will dictate the shape of the load pulse, i.e., rise time, pulse width, and impulse loads. A stiffer buffer will reduce the pulse width, increase the impulse load and decrease the rise time (Lukanen, 1992). The rate and level of loading does not change the response of an elastic material, however, the response of a visco-elastic material is dependent on the rate and level of loadings. A pavement will deflect more when the load is applied over a longer period, thus exhibiting lower stiffness. Lukanen (1992) and Chen et al. (1999) have shown that the effects of buffer stiffness are more significant in the case of weaker structures, perhaps due to the visco-elastic response of the structure.

The shape of the buffer also changes the rate of loading (Lukanen, 1992; and Chen et al., 1999). Flat buffers seem to produce shorter pulse widths; hence, a higher rate of loading in comparison to rounded buffers. The rounded buffers create a variable spring rate. The spring constant is lower at the initial drop heights and increases at higher drop heights due to an increase in the contact area. Ideally, flat buffers are better because the pulse width does change with drop heights. To evaluate

the impact buffers have on load pulse shape and magnitude, it was decided to identify buffer characteristics in a laboratory setting followed by field-testing.

Laboratory Characterization of Buffers

The laboratory characterization of buffers was performed using an MTS device. The test setup used in this study is shown in Figure 6.1. The buffer was placed between two loading platens and plaster of Paris was used to securely attach the buffer to the platens. After the plaster of Paris was cured, a static load of 100 ± 2.5 lb (450 ± 15 N) was applied as a seating load. A haversine dynamic load, with duration of 0.1 seconds and rest period of 0.9 sec was then applied to the buffer. Attempts to reduce the duration of the load pulse to 30 msec were not successful because it would exceed the capabilities of the MTS system. This could have been overcome, but given the comparative nature of this study, the cost of modifications could not be justified.

The dynamic load was varied from a minimum of 1 kip (4.5 KN) to a maximum of 3.75 kips (17 KN) to generate different stress levels. The maximum load level, which was selected to be similar to the ones observed in the field, could not always be achieved for several reasons. The tendency of a buffer is to bounce back rapidly during unloading and this would adversely impact the proper operation of the MTS's closed-loop control system, resulting in invalid load and deformation measurements. For softer buffers, the displacements attained exceeded the capacity of the transducers.

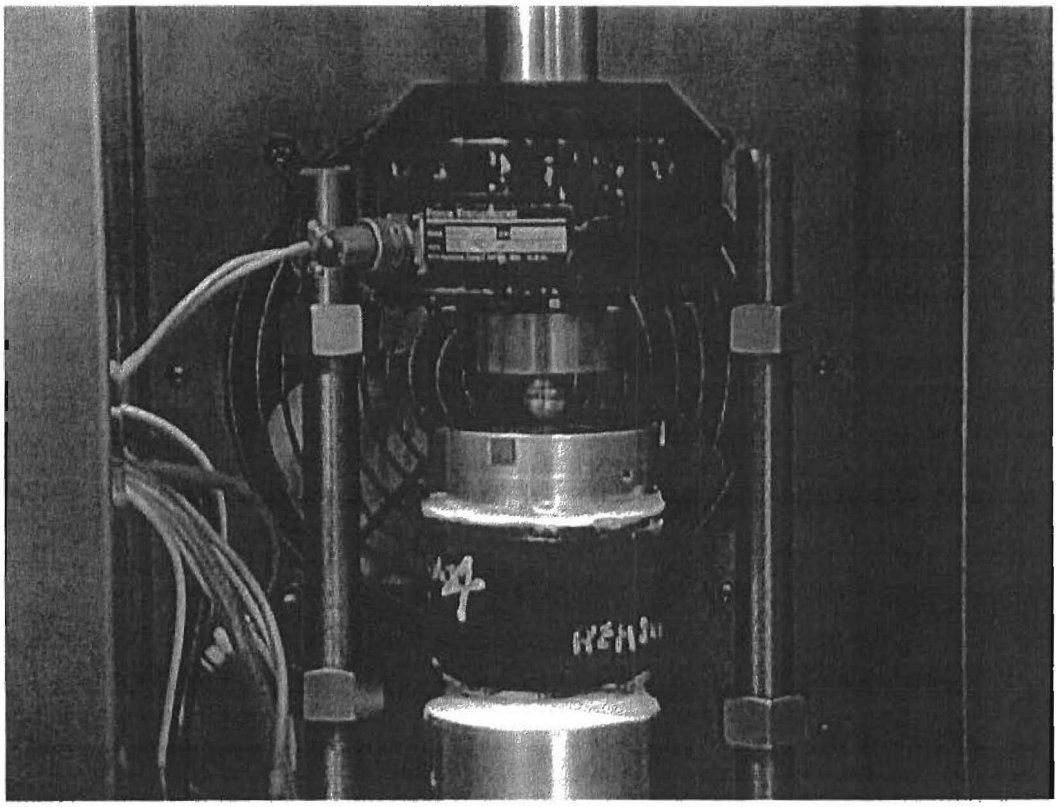

Figure 6.1 – Laboratory Characterization of Load Buffers

Typical variations of load with deformation for one loading-unloading cycle for a buffer are shown in Figure 6.2. Tests were performed at three different temperatures, namely 75 °F (24 °C), 100 °F (38 °C), and 125 °F (52 °C). At each temperature, both the loading and unloading patterns deviate from a straight line, indicating that the behavior of the buffer is nonlinear. The area between the loading and unloading curves depicts the energy absorbing characteristics of the buffer. While the area between a curve and the x-axis depicts the strain energy. The ratio of the area between the curves and the strain energy is proportional to the damping ratio of the buffer.

Typical stress-strain curves for one of the buffers are shown in Figure 6.3. Each data point corresponds to the tip of the loading-unloading curve shown in Figure 6.2. The curve yields a modulus of elasticity of 1.5 ksi (10 MPa) for a temperature of 75°F (24°C), which slightly decreases with an increase in temperature.

The areas between the loading and unloading curves as a function of load amplitude and temperature are shown in Figure 6.4. With increase in temperature, the rubber buffers absorb more energy. That indicates that during the FWD testing, less energy is transferred to the pavement during warmer temperatures. This may explain why the load imparted to the pavement during FWD testing in the summer is less than the nominal values obtained on the other seasons.

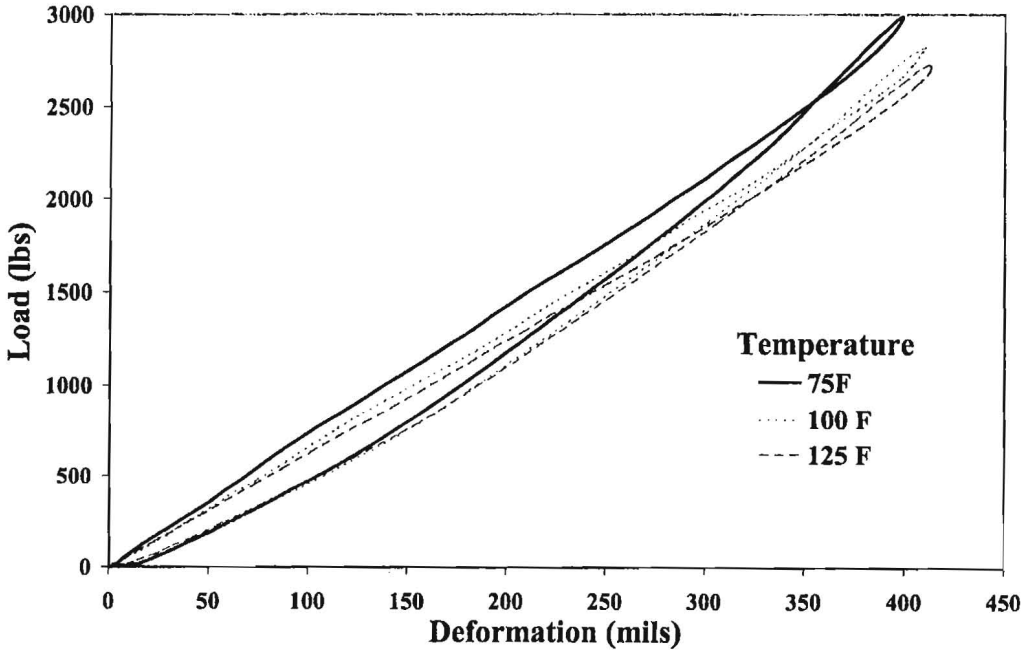

Figure 6.2 – Typical Load-Deformation Behavior of FWD Rubber Buffers

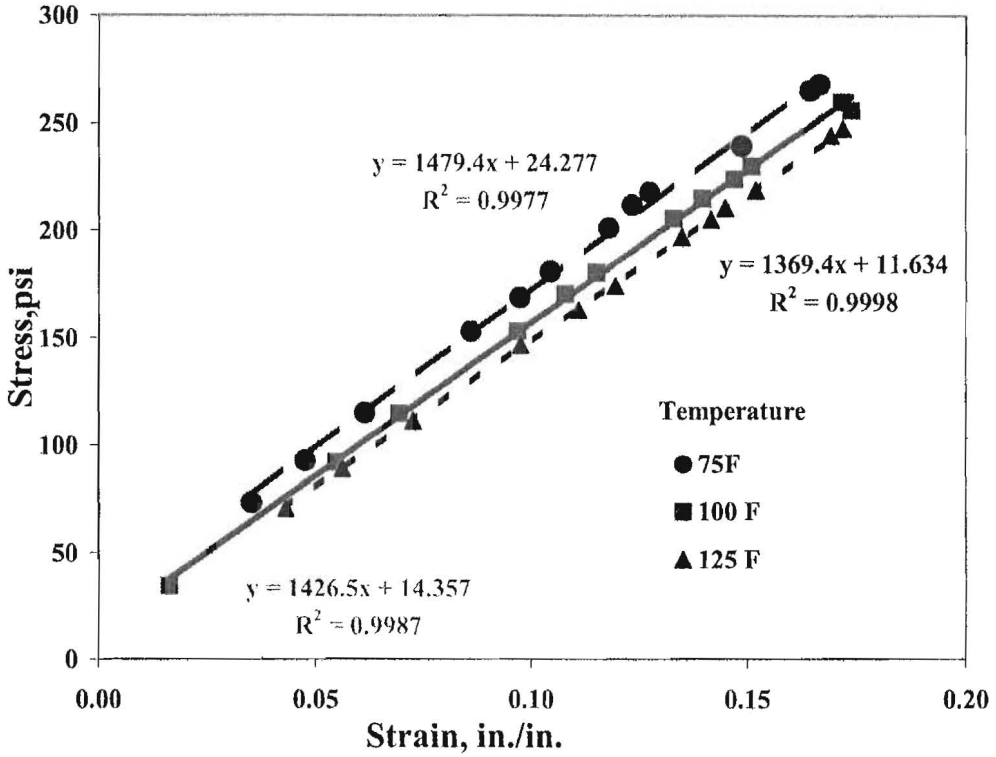

Figure 6.3 – Typical Stress-Strain Relationship of Rubber Buffer

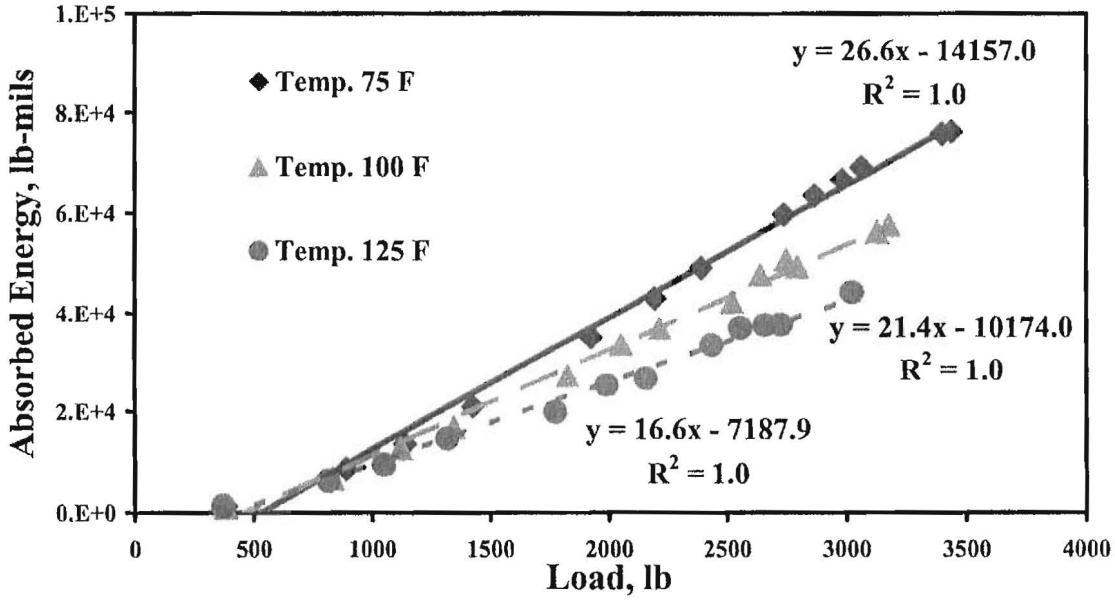

Figure 6.4 – Effect of Temperature on Rubber Buffer Performance

In this study, many rubber buffers were evaluated, but results from only a few are included here for the sake of brevity. Used buffers from different FWDs as well as new set of buffers were tested. The new buffers were the same as those that are currently provided by the FWD supplier. The test results from a new buffer and typical results from an old buffer are summarized in Table 6.1. The differences in shape and size between an old buffer from FWD 024 and a newly acquired buffer are evidenced in Figure 6.5. The moduli of the aged buffers were significantly higher than those of the new buffer, especially at lower temperature. This in turn, caused the damping of the used buffer to have a much greater change over the range of loads and temperatures as compared to the new buffer.

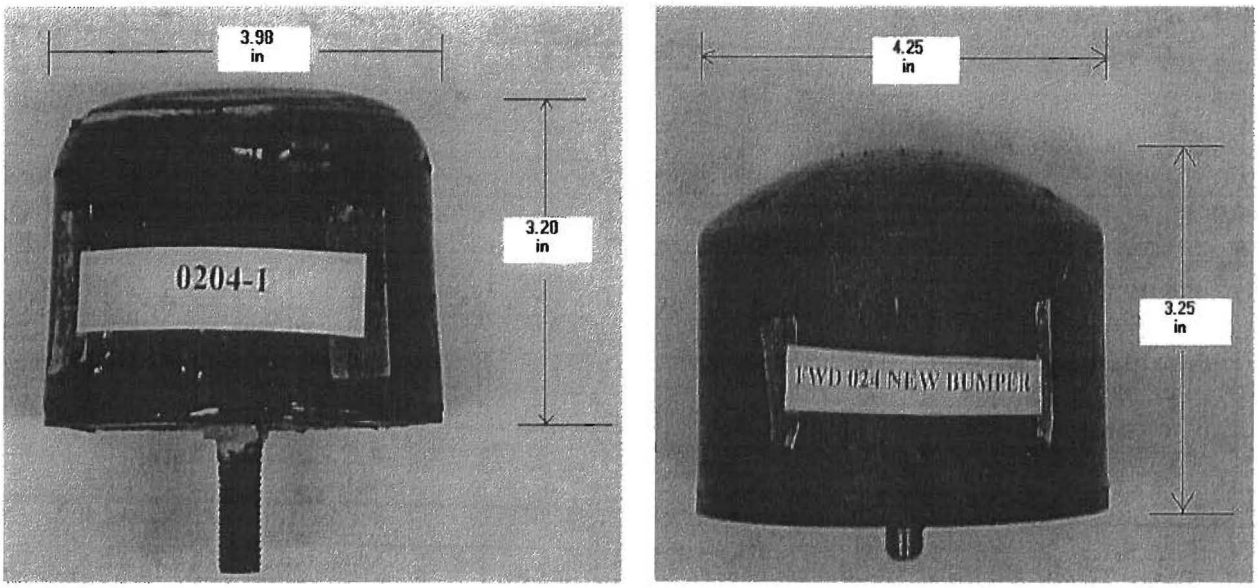

a) Old Buffer **b) New Buffer**

Figure 6.5 – Typical New and Old Buffers from FWD 024

Field Characterization of Rubber Buffers

The original buffers from three of the FWD's used in the repeatability and reproducibility study were replaced with a set of new buffers after several deflection basins where measured. Identical set of data was also collected with the new buffers within a short period of time after the data with the old buffers were collected. Typical findings are summarized here.

Typical differences in the load pulse time histories are shown in Figure 6.6. With the new buffers having on the average an increase in the peak load of about 6%. Similarly, geophone deflection time histories were somewhat different (see Figure 6.7). The measured deflections were also typically greater with the new buffers. However, the increase was about zero to 7% (average 3%). This clearly demonstrates that the stiffness of the buffer is an important parameter that should be considered.

Table 6.1. – Test Results of Commercial and Dynatest Rubber Buffers

Buffer Type	Temperature Tested (F)	Load (kips)	Modulus (kips/in^2)	Damping (%)
FWD Manufacturer (New)	75	1.1	7.8	25.1
		2.0	6.6	22.9
		2.5	6.3	21.8
		2.8	6.1	22.7
	100	0.9	5.7	21.9
		1.5	5.2	19.9
		2.0	5.1	22.0
		2.4	5.2	18.7
	125	1.1	4.8	17.1
		1.6	4.6	15.5
		2.0	4.6	16.1
		2.2	4.6	15.4
FWD Manufacturer (Old)	75	1.0	12.5	34.8
		2.1	12.3	35.8
		2.3	12.1	35.5
		2.8	13.1	32.8
	100	0.9	11.1	25.0
		2.0	11.3	23.2
		2.2	11.5	23.6
		2.5	10.6	20.0
	125	1.1	4.4	5.5
		1.5	4.4	4.8
		2.0	4.6	6.6
		2.4	5.0	7.0

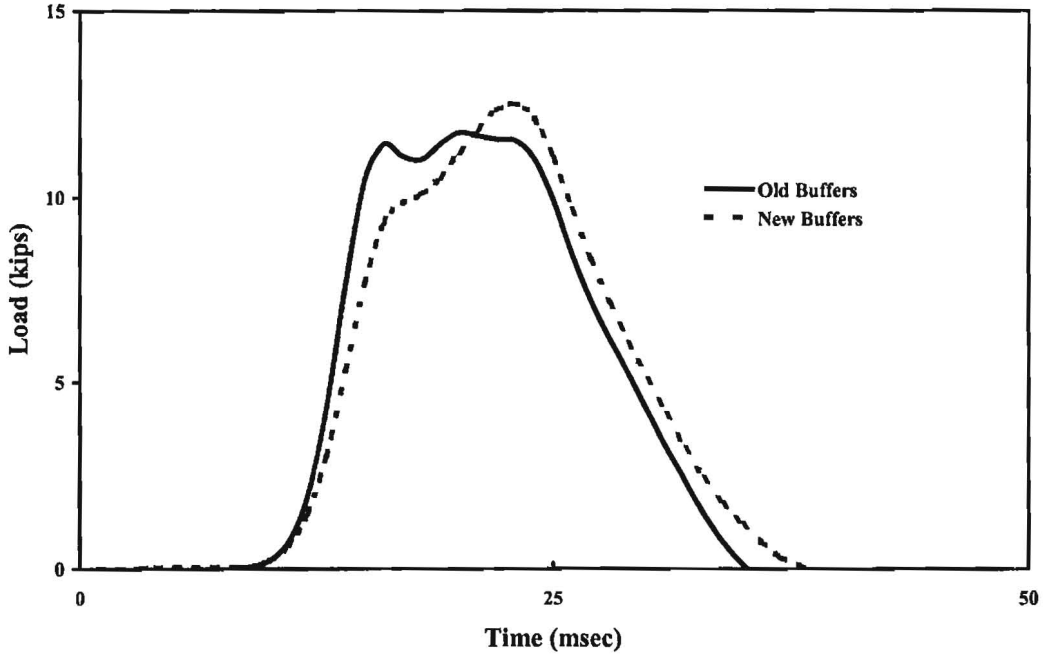

Figure 6.6 – Typical Load Cell Time Histories from New and Old Buffers

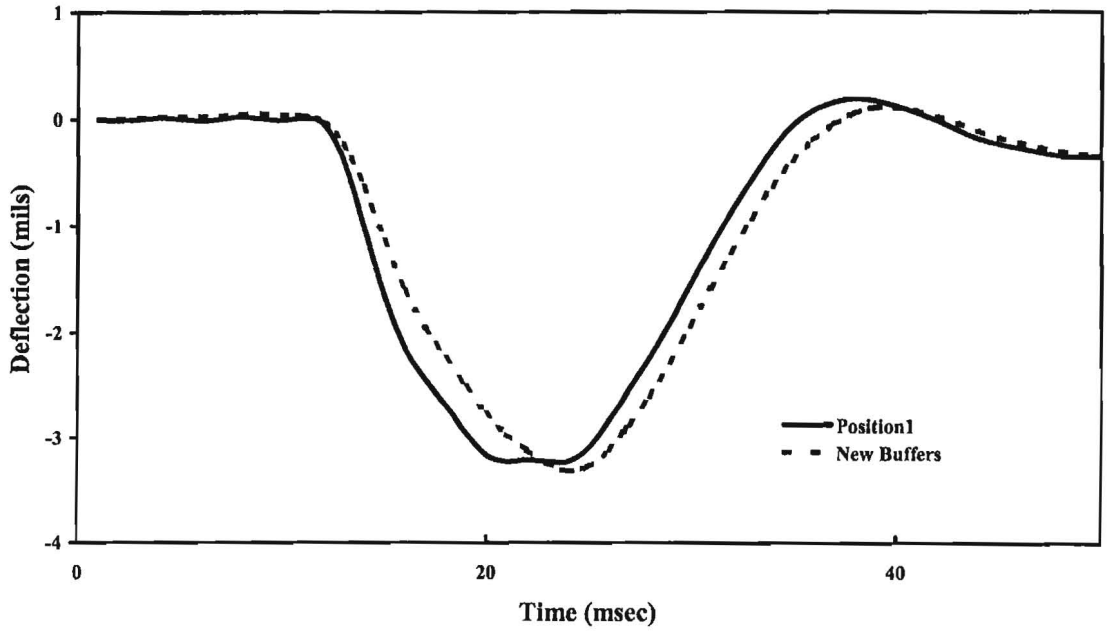

Figure 6.7 – Typical Deflection Time Histories from New and Old Buffers

Geophone Holders

The next step consisted of studying the impact of the geophone holders. The reason for focusing on the components of the geophone holder is best described by inspecting Figure 6.8. The deflection time history of a geophone in a brand new sensor holder and the response of the corresponding holding assembly are shown in the figure. The FWD sensor's response is as typically observed. The sensor holder does not experience any significant motion until the peak motion of the FWD sensor is registered. After the peak deflection of the FWD sensor, the holder demonstrates a large amplitude steady-state motion. A careful inspection of the sensor deflection reveals a small hint of the impact of such a steady state motion. For example, the sensor record between 40 msec and 60 msec demonstrates that when the holder experiences a peak, the FWD deflection demonstrates a slight trough. This example indicates that the holder assembly is well designed to minimize the impact of the external vibrations. However, when the components of the sensor assembly such as the neoprene guides or the springs are worn out or damaged, this vibration isolation may not be as effective.

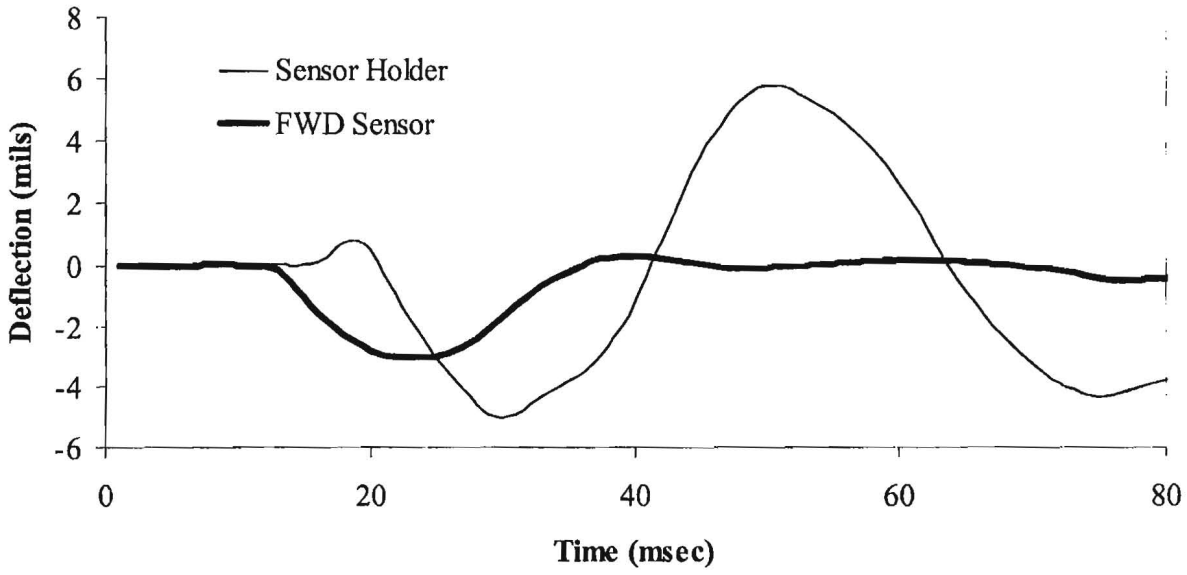

Figure 6.8 – Typical Responses of FWD Sensor and Sensor Holder

In the first step, we studied the impact of completely replacing used holders with brand new holders. A typical sensor holder is shown in Figure 6.9 as a reminder. For this exercise, we concentrated on holders that visually showed no signs of damage or wear. The results of a typical comparison between the deflections from a new and an old holders at four drop heights and five repeats are shown in Figure 6.10. Typically a difference of about or less than 2% observed. As such, it may not be a financially feasible practice to simply replace the geophone holders.

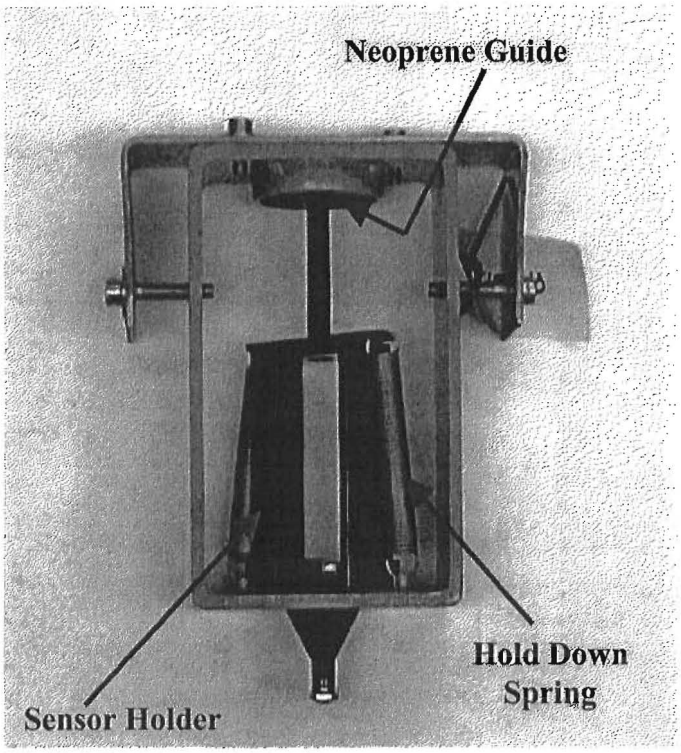

Figure 6.9 – Typical Sensor Holder Assembly

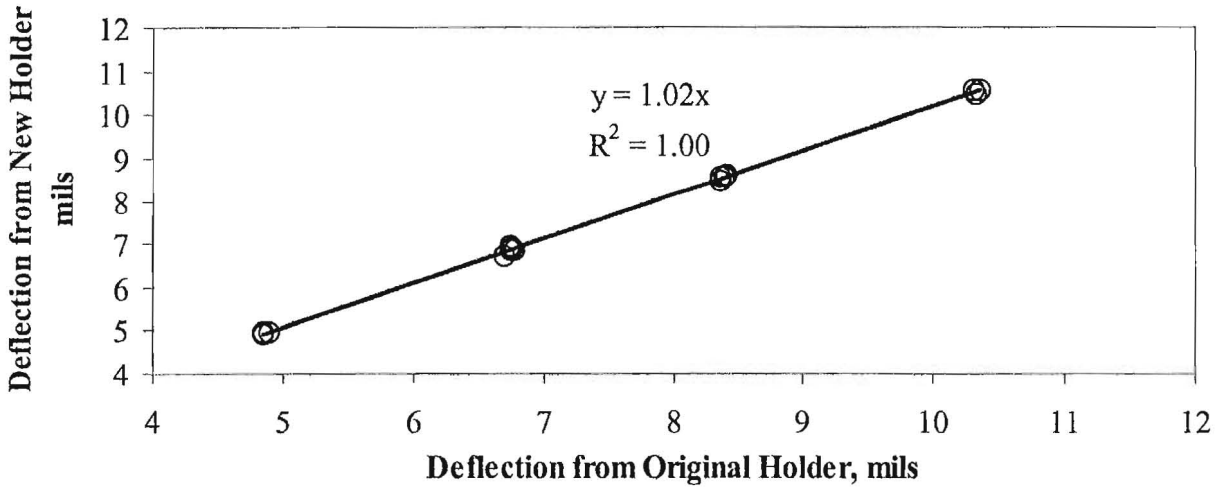

Figure 6.10 – Comparison of Typical Responses of a FWD Sensor from Original and Brand New Holder

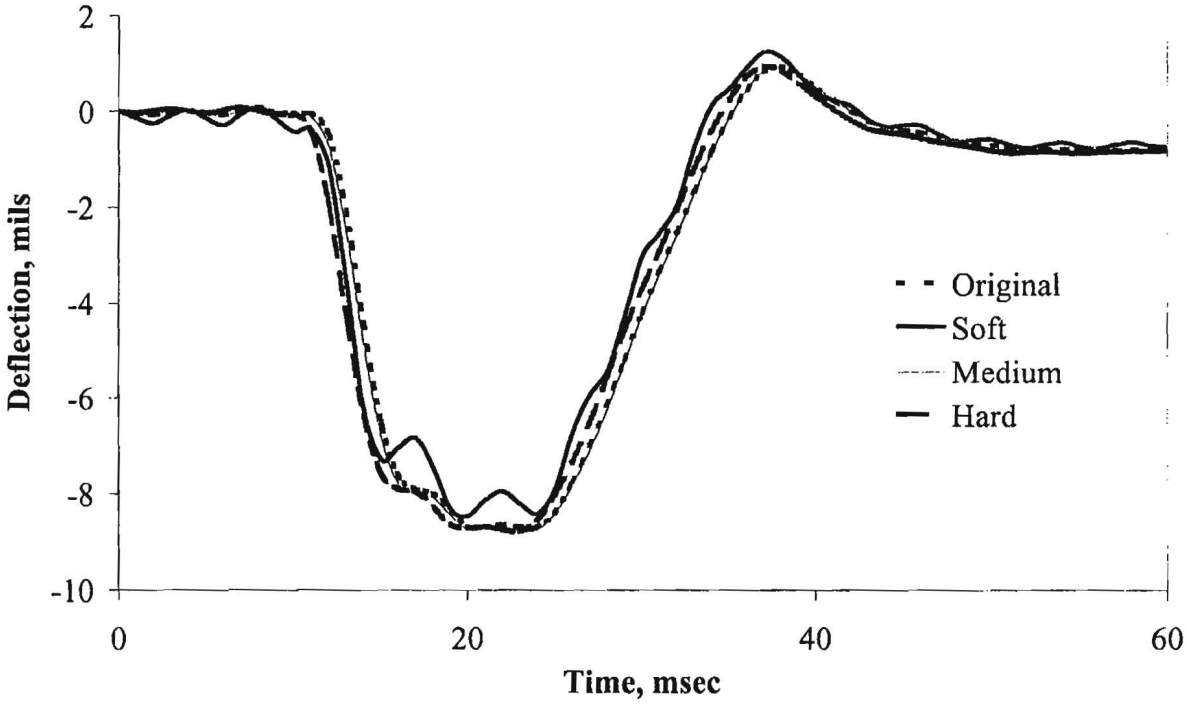

Figure 6.11 – Typical Impact of Stiffness of Hold Down Springs on Measured Deflections

In the next step we focused on the impact of the springs. We replaced the two hold down springs with three sets of springs with different stiffness. A comparison of the deflections measured with the original and the three other springs are included in Figure 6.11. The stiffness of the spring seems to impact the peak deflection. A soft (or over-stretched) spring will generate a signal that can be visibly distinguished from the responses from the other springs. However, the original, medium and hard springs do not seem to generate appreciably different responses. However, the registered deflections may be different by several percentage points. Given the low cost of springs, we recommend that TxDOT replace the springs annually as part of the calibration process. Given the manpower required to determine the condition of the springs, it is economically more feasible to simply replace them without any inspection.

Finally we studied the impact of the neoprene guide on top of the sensor holder. The main function of this guide is to maintain the position of the sensors. The hole in the middle of this guide becomes larger with use. When the diameter of the hole is increased significantly, the geophone cannot maintain its verticality and the holding mechanism may touch the assembly. In these cases the results will be significantly affected. However, the operator or the person in charge of calibrating the FWD will notice this case and can replace the component. The challenge is when the wear and tear of this component is small such that the sensor holder can move in it. We measured this behavior, by replacing used neoprene guides with brand new ones. As shown in Figure 6.12, this action changed the pick deflection measured by the sensor by as much as 3%. Once again, this demonstrates that perhaps it would be reasonable to replace these guides periodically to ensure that they maintain their shape.

As shown in the last two chapters, even though the FWD is well designed to provide repeatable and reproducible results, the current calibration procedure used by TxDOT may not be able to detect or address all these parameters. Therefore a more rigorous calibration process may be necessary. This report only contains a brief summary of the results to demonstrate this point.

A new calibration process is being developed that should consider the impacts of many of the parameters that are discussed here.

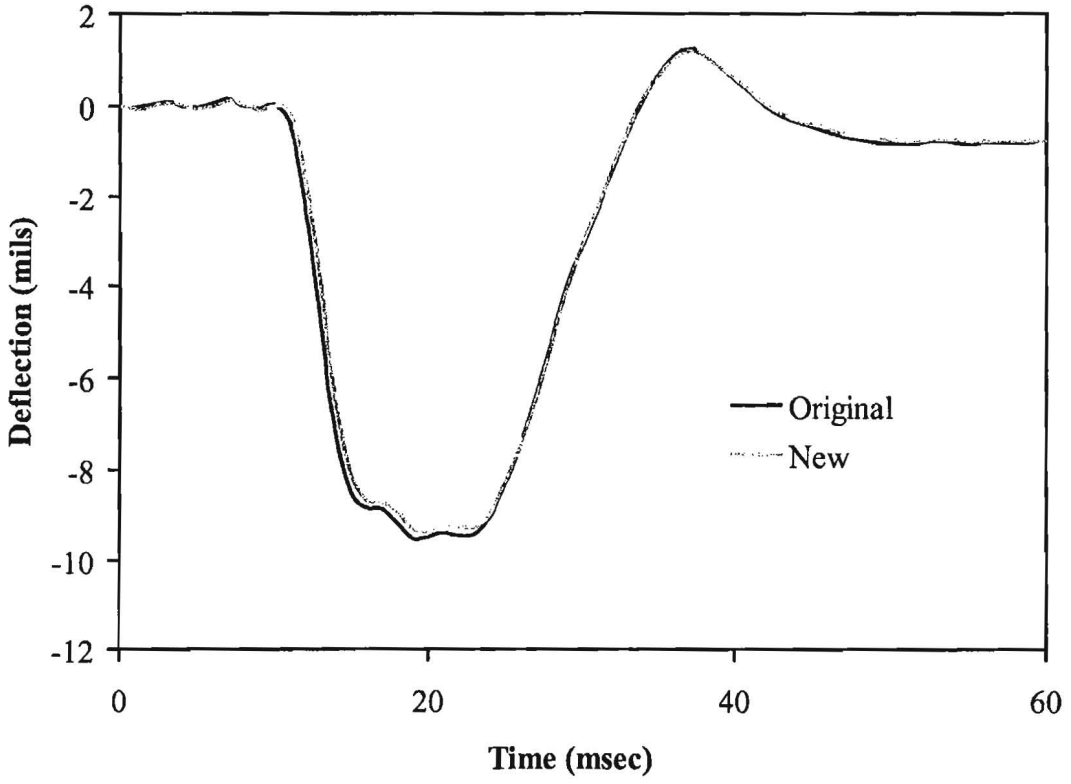

Figure 6.12 – Typical Deflection Time Histories from New and Old Neoprene Guides

Chapter 7

Closure

Summary

The current fifteen-unit FWD fleet is of different vintages, and as such is manufactured from different components. Both good repeatability and reproducibility are considered to be of major importance for an adequate interchangeability of the FWD fleet. If the fleet is not reproducible, the predicted remaining life will depend on the FWD used. This will result in a systematic over- or under-estimation of the overlay thickness in a given region of the state. It will also positively or negatively impact the reported quality of a district's pavement condition.

The primary objective of this project is to develop realistic field protocols and specifications, which in a rational manner will allow TxDOT personnel to quantify the repeatability and reproducibility of existing and future FWD devices. As a result of this activity, a more comprehensive calibration methodology will be developed. Additional outcome of the project will be new decision-making tools for maintaining a reproducible fleet. These new tools will give those who are involved in repairing and upgrading FWDs to decide more quantitatively when to replace components (such as buffers and sensor holders) to maintain a fully reproducible fleet.

The first two tasks of the project consisted of evaluating the reproducibility and repeatability of the fleet and study the impact of the components on the reproducibility and repeatability of a given FWD. This report contains a summary of the results from these two tasks.

Conclusions

Based on the results presented here, the following can be concluded:

- Individual FWDs owned by TxDOT are quite repeatable. The current SHRP calibration procedure seems to improve the repeatability even further.

- The reproducibility of the fleet should be improved for effective interchangeability of the fleet. The current calibration procedure should be modified to address this issue.

- The transient motions in the FWD during the loading seem to impact the measured peak loads and deflections from the FWD. These transient motions seem to be a function of the structural design of the trailer and the condition of the buffers and the load plates.

- The stiffness and age of the buffers as well as the condition of the components of the geophone holding assembly would also impact the measured loads and deflections.

Future Directions

At this time a new calibration protocol is being developed. The new protocol contains up to four steps. These steps include:

1. Monthly Observations by FWD Operators: This step includes a monthly inspection of the FWD by the operator to replace the worn out components, ensuring appropriate tension in bolts and screws and the lubrication and cleaning of the load cell assembly and sensor holding assembly.

2. Preventative Maintenance by FWD Calibration Staff: This step includes a thorough check of the electrical and electronic components, replacement of mechanical components (e.g., geophone hold down springs, neoprene guides etc.), tune-up of the FWD to minimize excessive trailer movement and sensor bar movement, ensure smooth and centered load application. These steps not only contribute to better reproducibility of the fleet, it will also extend the life of the fleet.

3. Conduct Stage I Calibration by FWD Calibration Staff: Compare deflections and load measured with the FWD with those of well-calibrated sensors embedded in a calibration slab. This step will provide a calibration procedure very similar to the SHRP calibration. The only difference is that all deflection sensors are calibrated simultaneously and in place within their sensor holders. If the FWD system passes the calibration process. It would be ready for operation. For the sensors that fail, a second stage calibration and diagnostic process is needed.

4. Conduct Stage II Calibration for Diagnosis by FWD Calibration Staff: In this stage the sensors that failed will go through a thorough calibration somewhat similar to those recommended by Tandon and Nazarian (2000) as briefly discussed in Chapter 2.

References

1. Ang, A. H-S and Tang, W.H. (1975), "Probability Concepts In Engineering Planning & Design, Volume-I Basic Principles, John Wiley & Sons.

2. Bentsen, R. A., Nazarian, S., Harrison, J.A.(1989), "Reliability Testing of Seven Nondestructive Pavement Testing Devices," Nondestructive Testing of Pavements and Backcalculation of Moduli, ASTM STP 1026, American Society of Testing Materials, Philadelphia, pp. 41-58.

3. Boddapati, K.M., and Nazarian, S. (1994), "Effects of Pavement Falling Weight Deflectometer Interaction on Measured Pavement Response," Nondestructive Testing of Pavements and Backcalculation of Moduli (Second Volume), ASTM STP 1198, American Society of Testing and Materials Philadelphia, pp. 326-340.

4. Chen, D., Bilyeu, J., He, R., and Murphy, M. (1999), "Effects of Buffers on Falling Weight Deflectometer Measurements," Internal Technical Memo, Design Pavement Section, TxDOT, Austin, Texas.

5. Cheremisinoff N.P. (1987), Practical Statistics for Engineers and Scientists, Technomic Publishing Co., Lancaster, PA, 211 p.

6. COST 336 (1998), "State of the Art on Calibration of Falling Weight Deflectometers," Final Draft Approved by the Management Committee Meeting of COST 336, Athens, Greece.

7. Crovetti, J.A., and Shahin, M.Y. (1994), "The Effect of Annular Load Distributions on the Backcalculated Moduli of Asphalt Pavement Layers," Nondestructive Testing of Pavements and Backcalculation of Moduli (Second Volume), ASTM STP 1198, American Society of Testing and Materials Philadelphia, PA, pp. 309-325.

8. Lukanen, E.O. (1992)," Effects of Buffers on Falling Weight Deflectometer Loadings and Deflection," TRR No. 1355, Transportation Research Board, National Research Council, Washington, D.C.

9. Murphy, M. (1998), "A Mechanistic-Empirical Approach to Characterizing Subgrade Support and Pavement Structural Condition for Network-level Application," Ph.D. Dissertation, The University of Texas at Austin, December.

10. Nazarian, S. and Briggs, R.C. (1990), "Determination of Structural Integrity of Secondary Roads Using Falling Weight Deflectometer. Proc., 2nd International Conference on Bearing Capacity of Roads and Airfields, Trondheim, Norway.

11. Nazarian S. and Bush A.J. (1989) "Determination of Deflection of Pavement Systems Using Velocity Transducers," Transportation Research Record 1227, Washington, DC, pp. 147-158.

12. Nazarian S., Stokoe, K.H., II (1987), "A Theoretical Sensitivity Study of the Falling Weight Deflectometer Device on Determining Moduli of Farm-to-Market Roads," Technical Memorandum IAC936-4, Center for Transportation Research, The University of Texas at Austin.

13. Nazarian S., Yuan D. and Nazarian S. (1998), "Specifications for Tools Used in Structural Field Testing of Flexible Pavement Layers," Research Report 1735-1, Center for Highway Materials Research, UTEP.

14. Tandon, V. (1990), "Development of an Absolute Calibration System for Nondestructive Testing Devices," Master of Science Thesis, Department of Civil Engineering, The University of Texas at El Paso.

15. Tandon, V. and Nazarian, S. (2000), " Calibration Procedures for Seismic and Deflection-Based Devices," Report No. TX-00 2984-2F, Texas Department of Transportation, Texas.

16. Touma, B.E., Crovetti, J.A., and Shahin, M.Y. (1991), "Effects of Various Load Distributions of Backcalculated Moduli Values in Flexible Pavements," TRR No. 1293, Transportation Research Board, National Research Council, Washington, D.C.

17. Uzan, J. (1994), "Advanced Backcalculation Techniques," Nondestructive Testing of Pavements and Backcalculation of Moduli (Second Volume), ASTM STP 1198, American Society of Testing and Materials Philadelphia, pp. 3-37.

18. Van Gurp, C. (1991), "Consistency and Reproducibility of Falling Weight Deflections," Road and Airport Pavement Response Monitoring Systems-Conference Proceedings, Sponsored by the US Army Cold Regions Research & Engineering Laboratory, September, pp. 291-305.

19. Vennalaganti, K.M., Ferregut, C., and Nazarian, S. (1994), "Stochastic Analysis of Errors in Remaining Life due to Misestimation of Pavement Parameters in NDT," Nondestructive Testing of Pavements and Backcalculation of Moduli (Second Volume), ASTM STP 1198, American Society of Testing and Materials Philadelphia, pp. 261-276.

Appendix A

Repeatability Distribution Charts

Overall Statistical Distribution Before SHRP Calibration

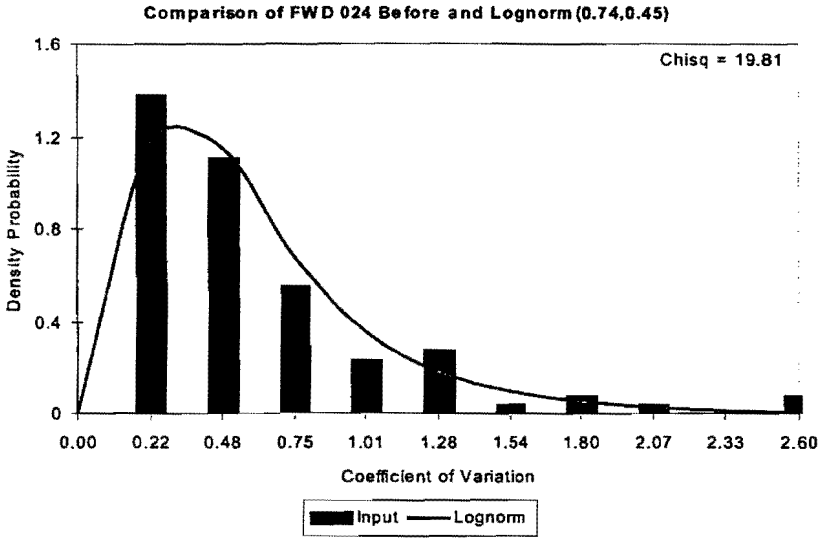

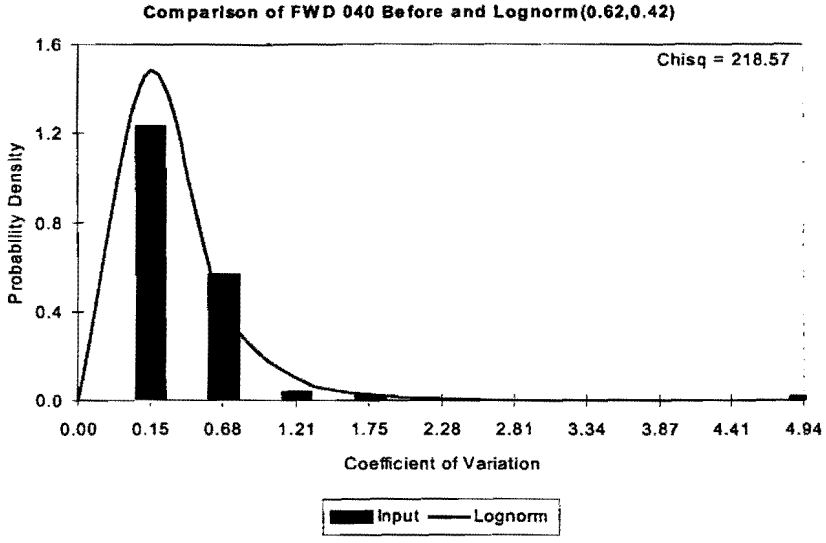

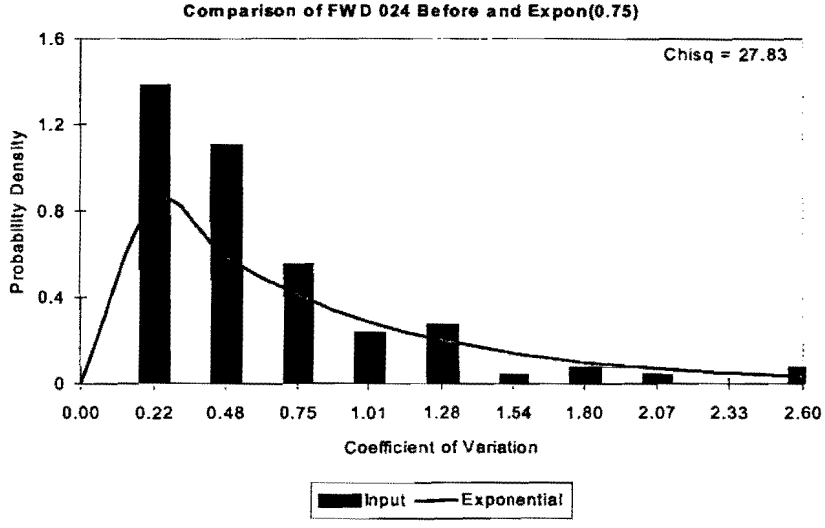

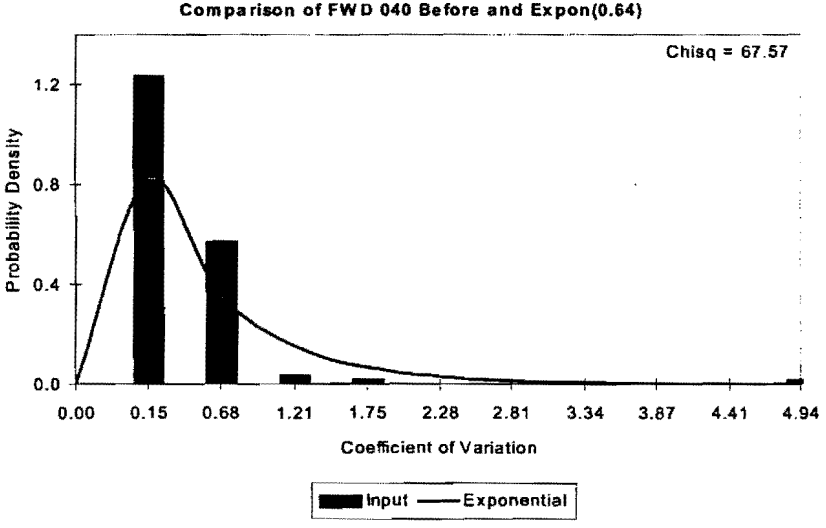

Overall Statistical Distribution Before SHRP Calibration

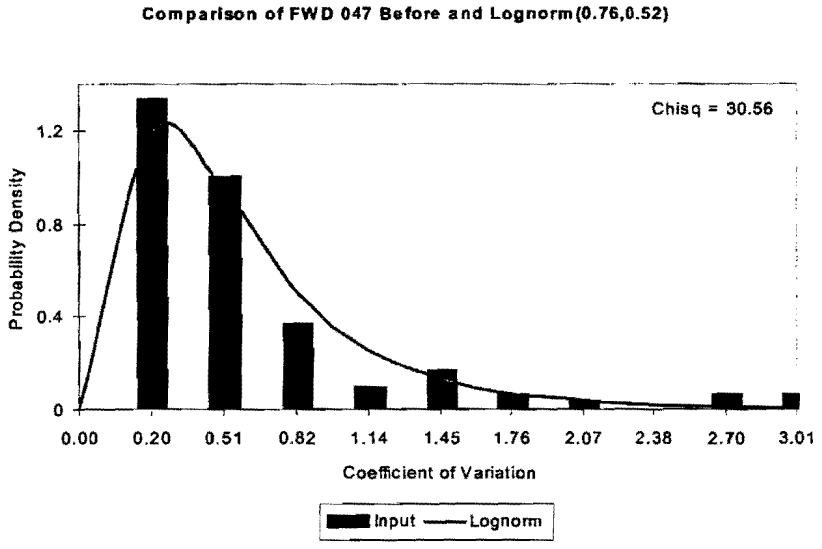

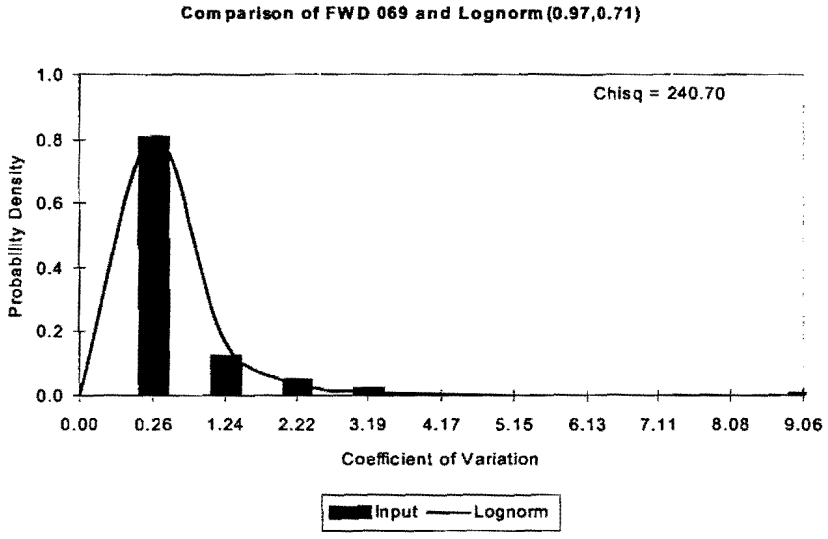

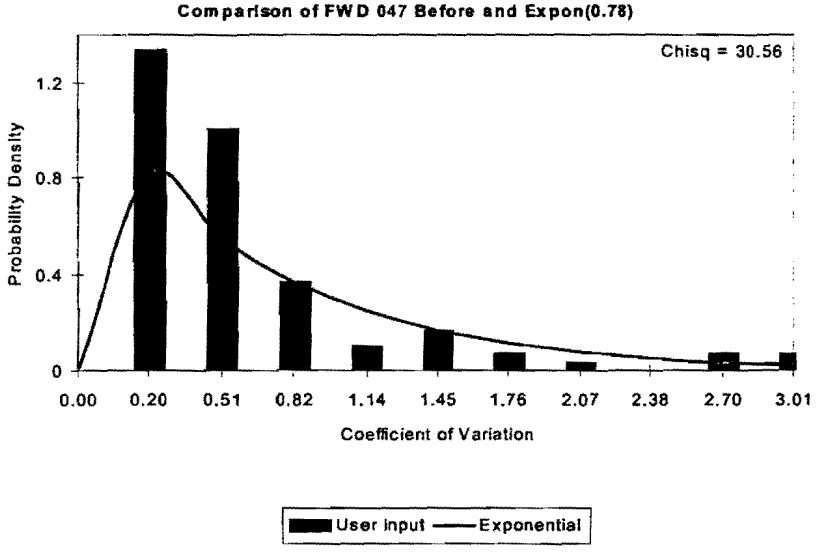

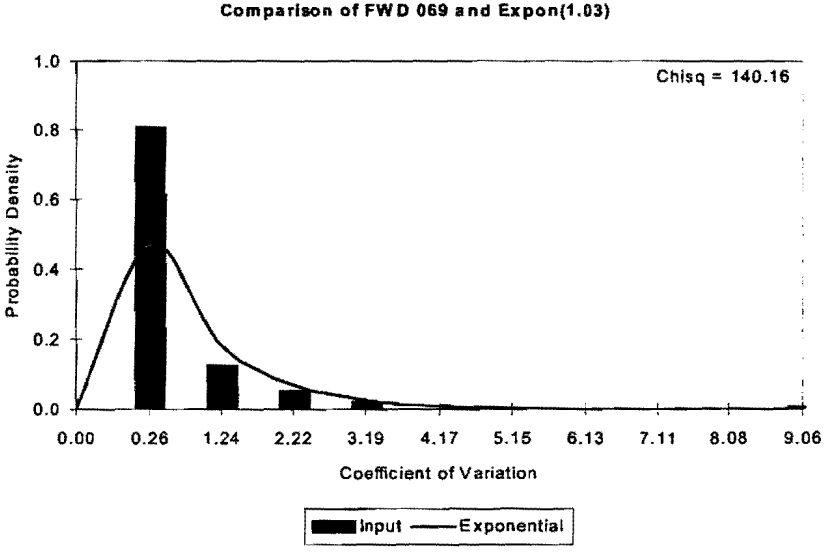

Overall Statistical Distribution Before SHRP Calibration

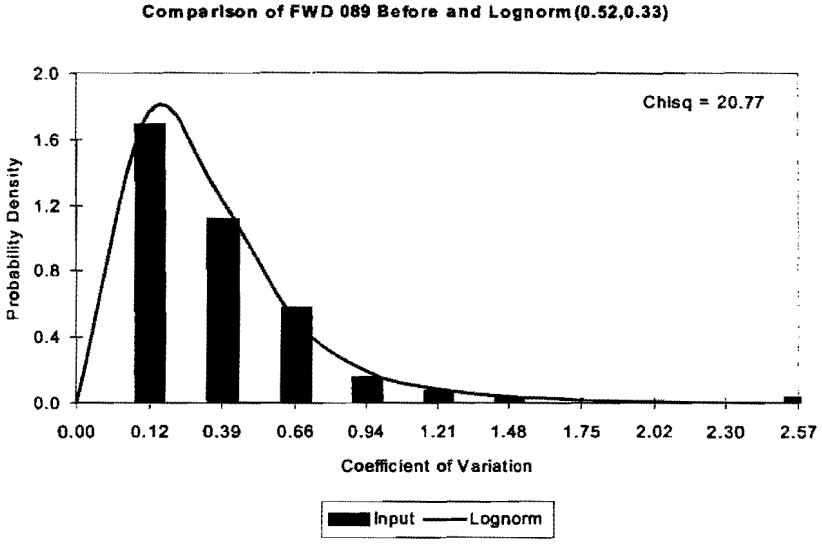

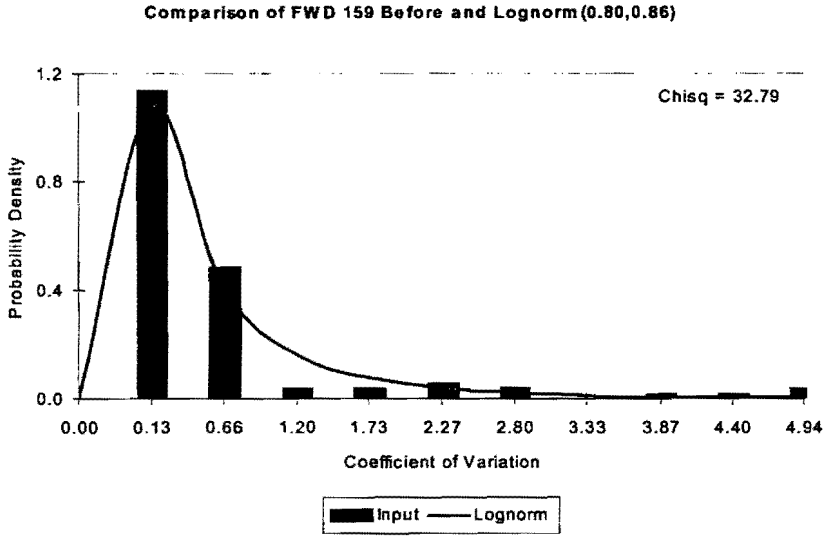

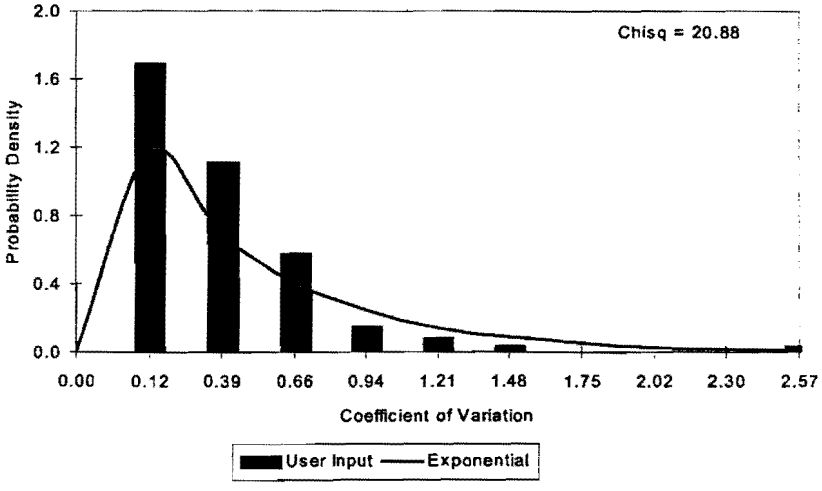

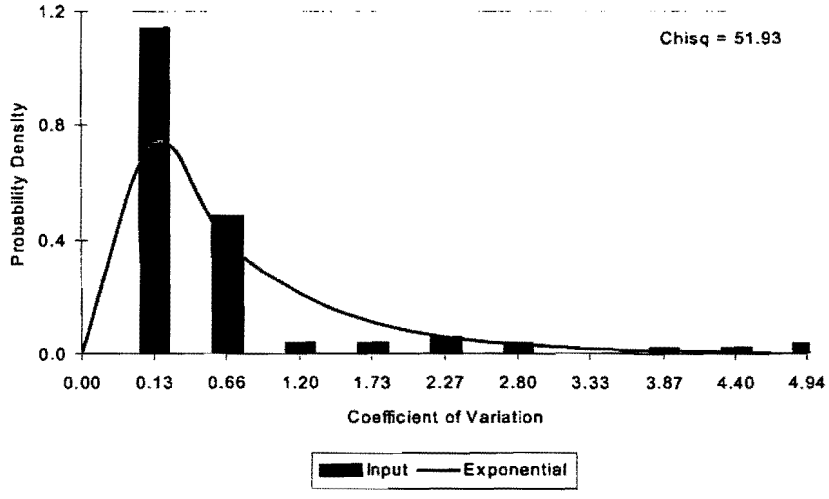

Overall Statistical Distribution After SHRP Calibration

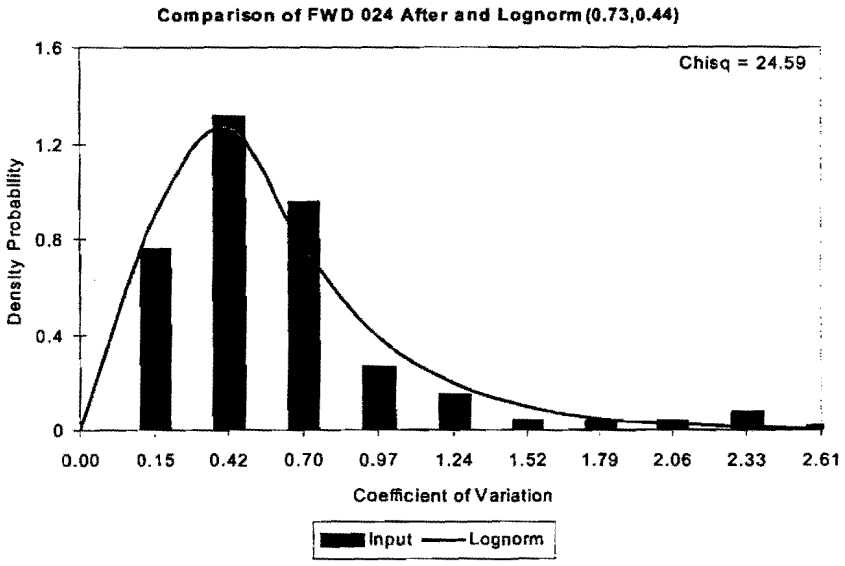

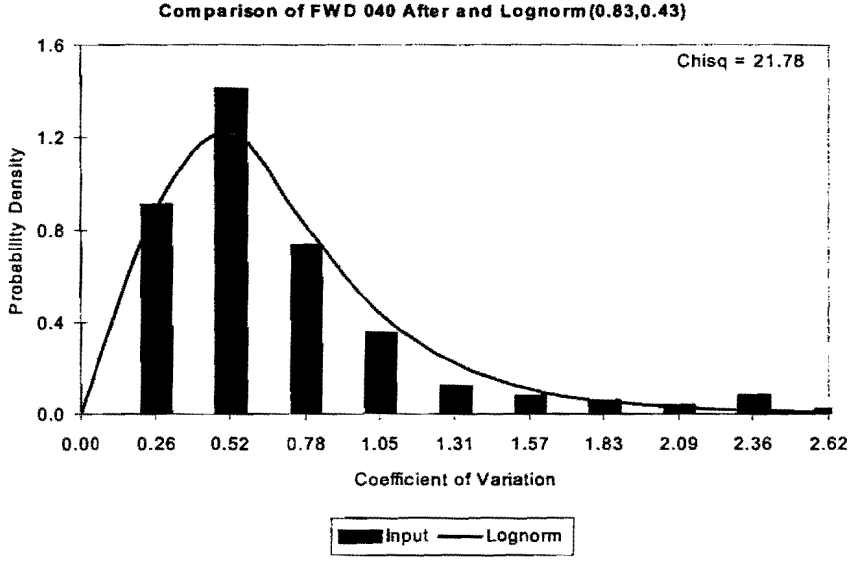

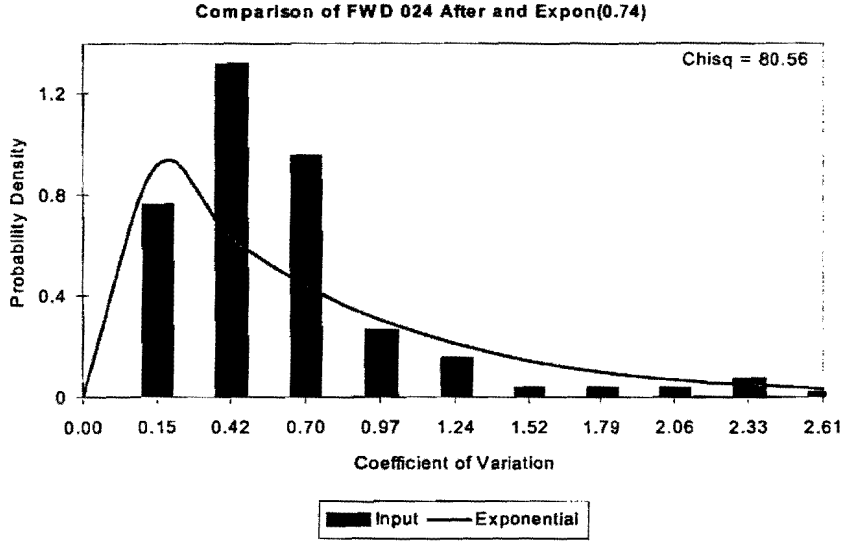

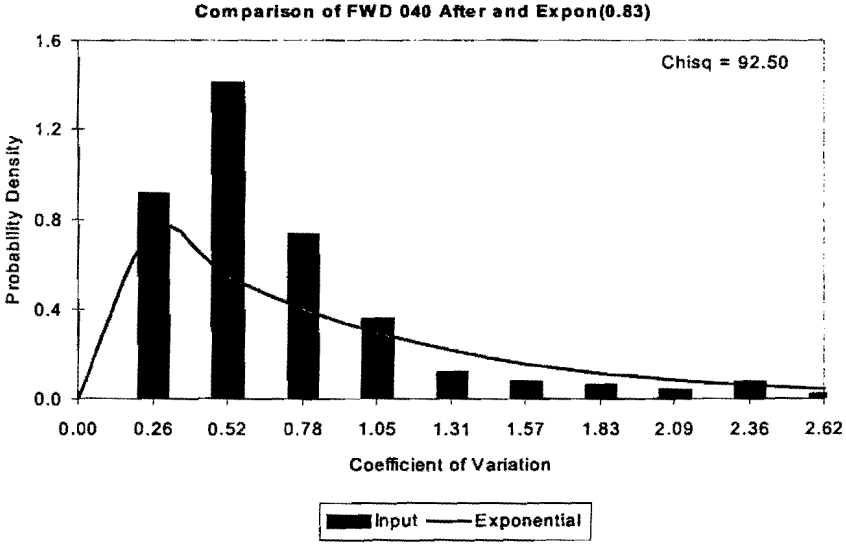

Overall Statistical Distribution After SHRP Calibration

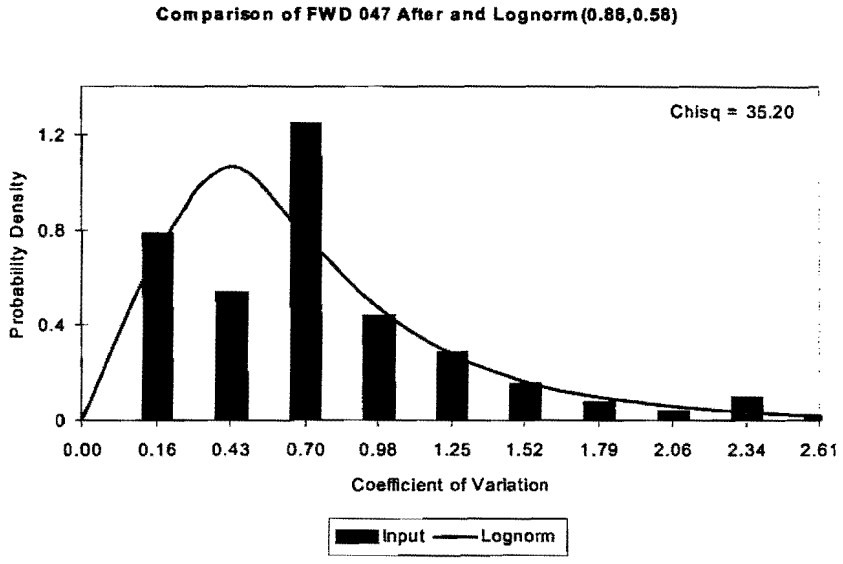

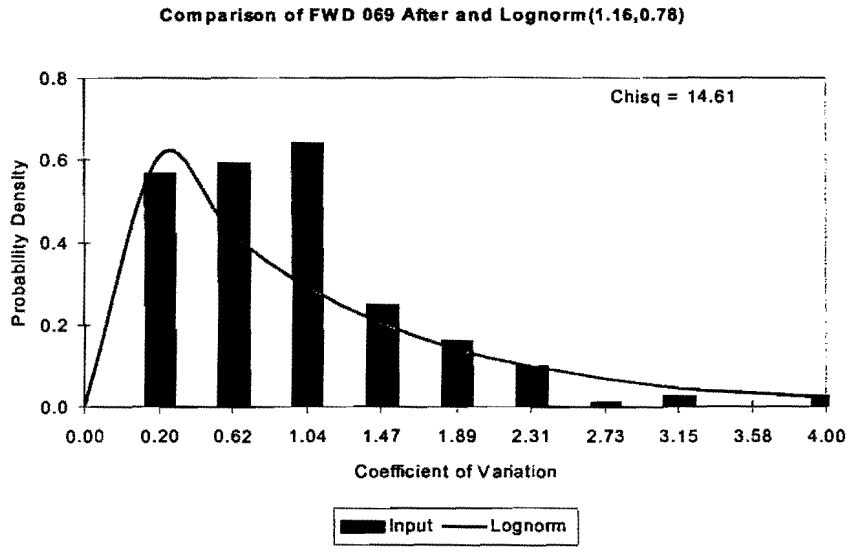

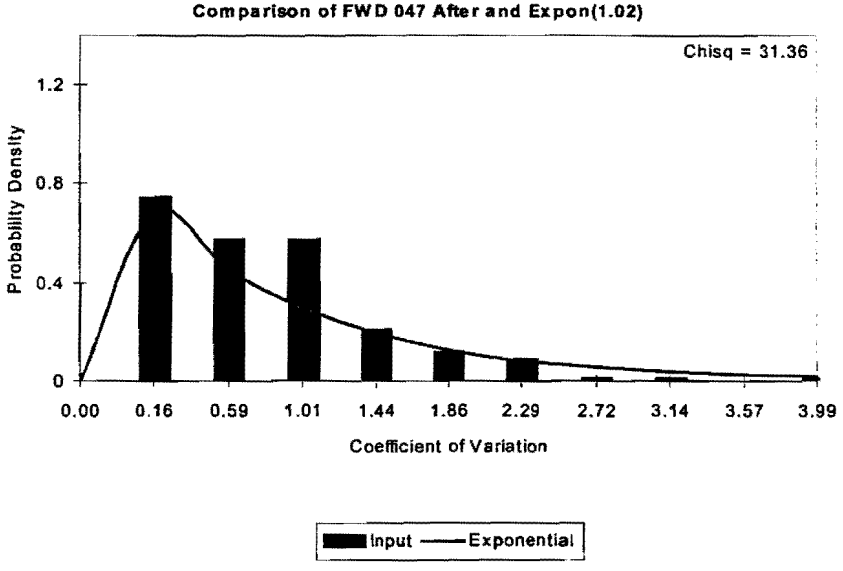

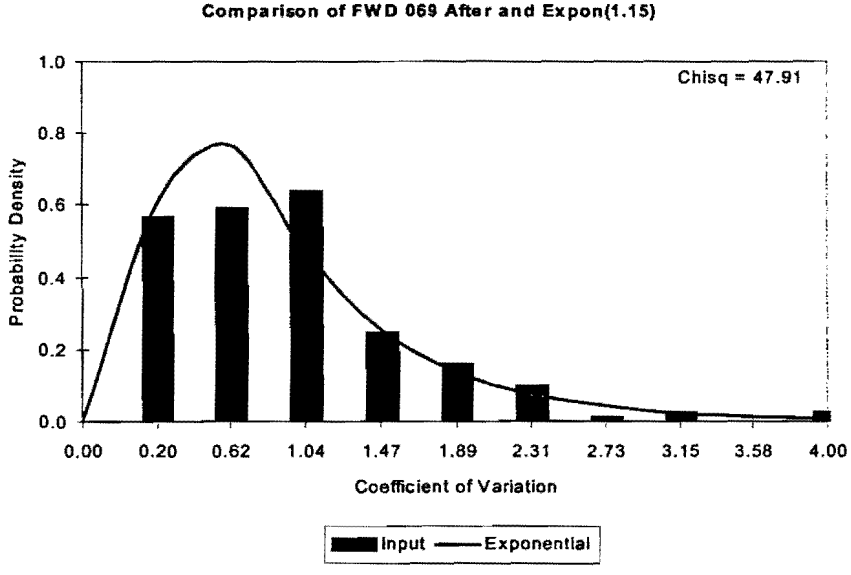

Overall Statistical Distribution After SHRP Calibration

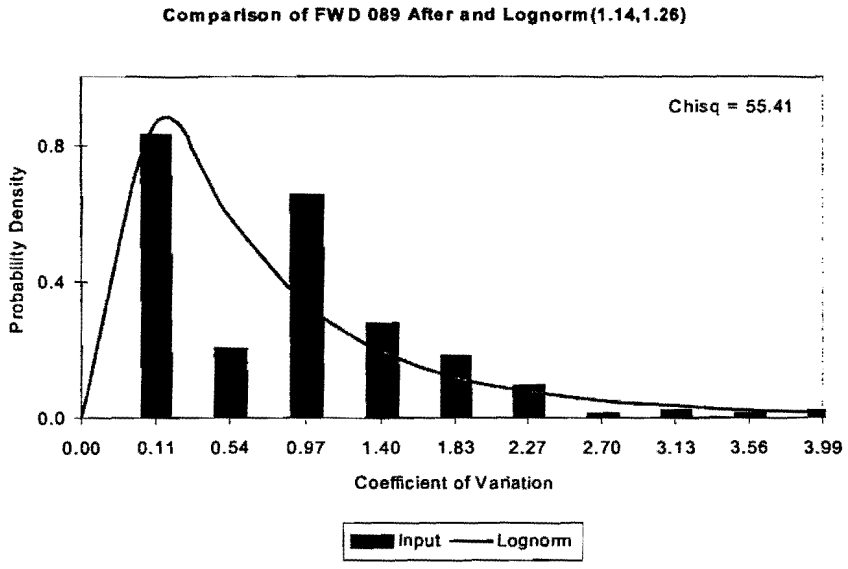

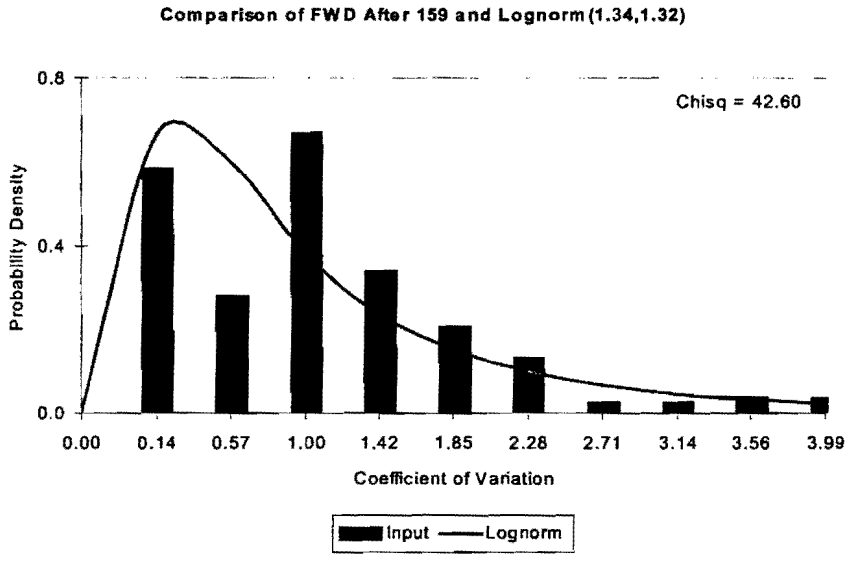

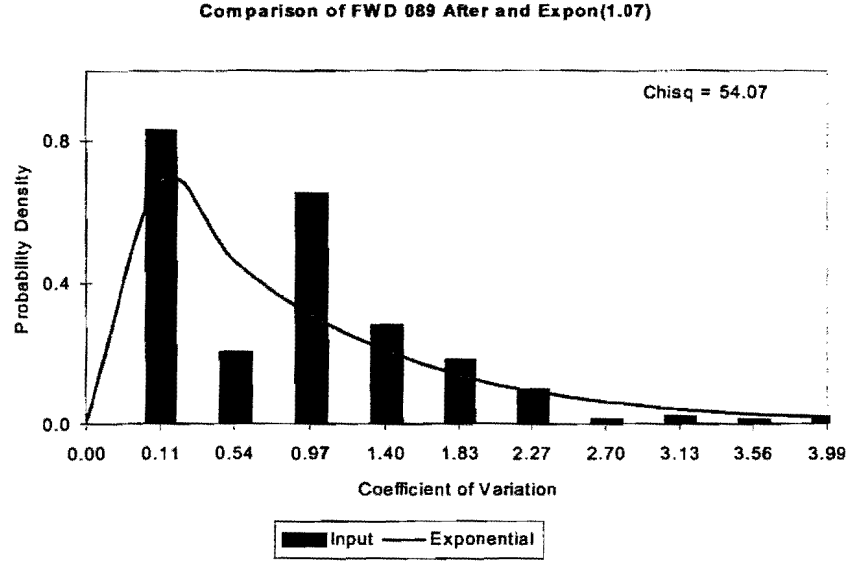

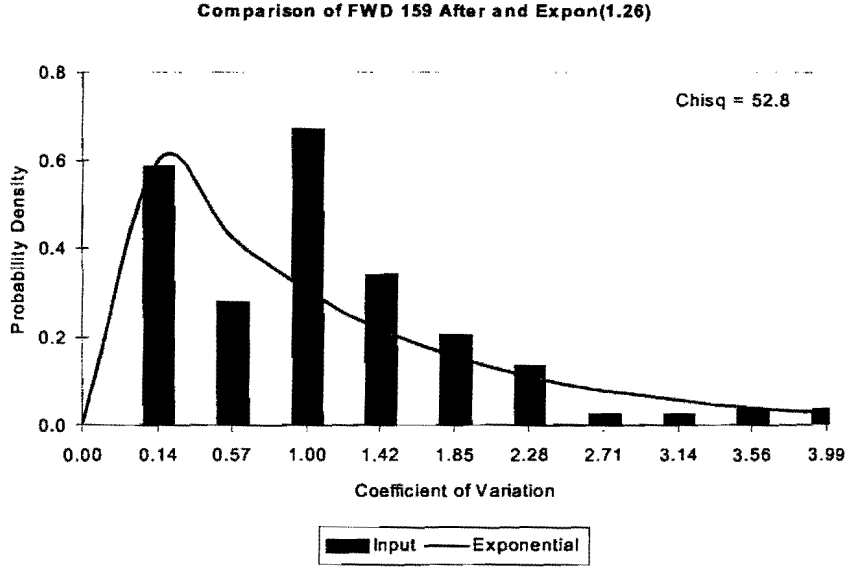

Statistical Distribution By Height Before SHRP Calibration

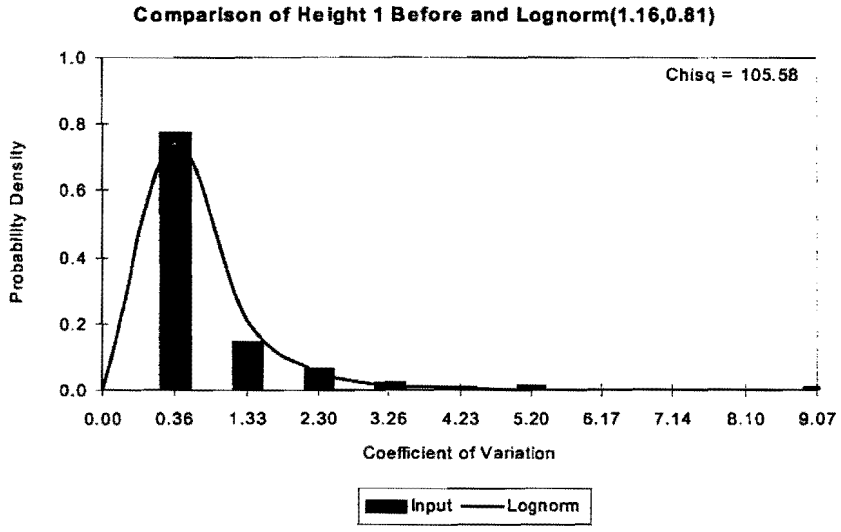

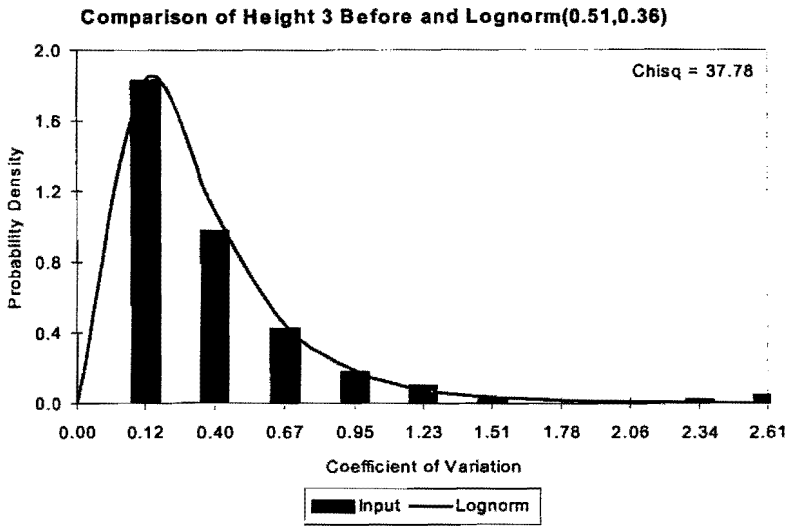

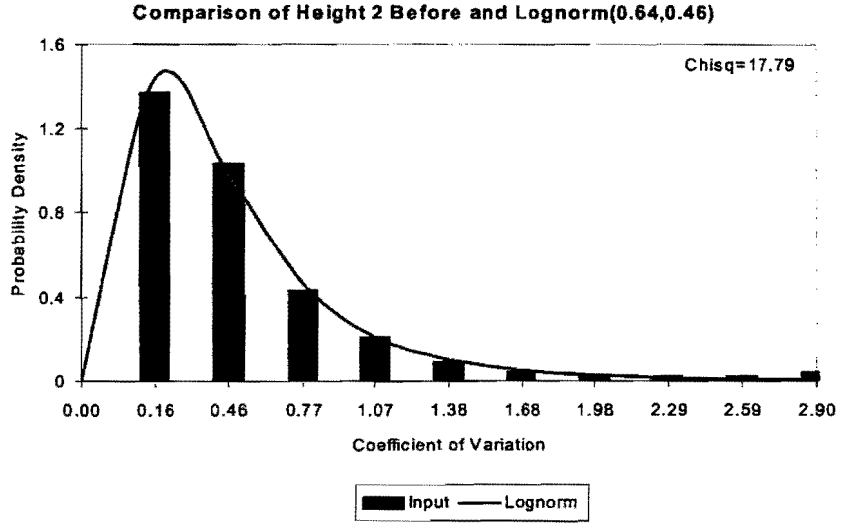

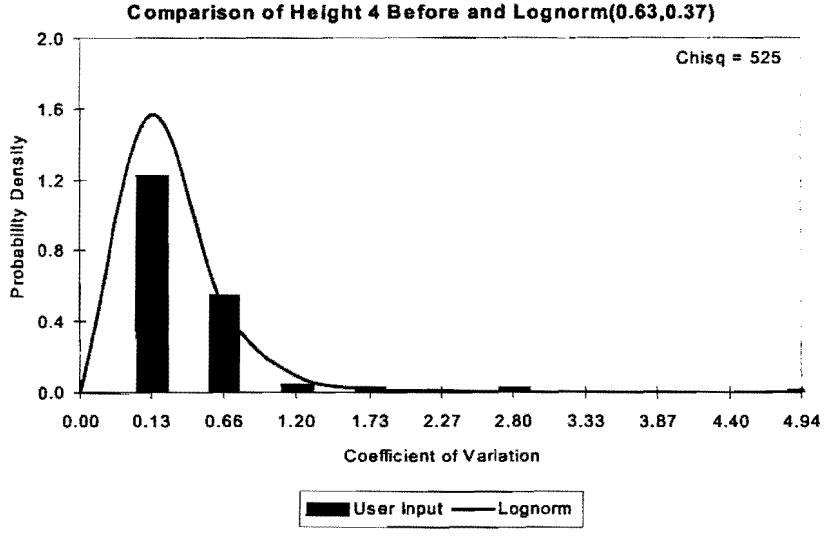

Statistical Distribution By Height After SHRP Calibration

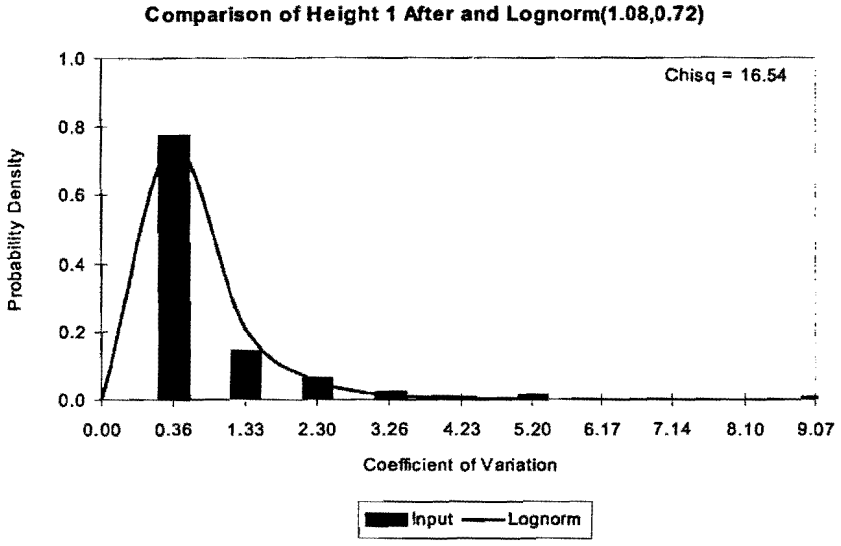

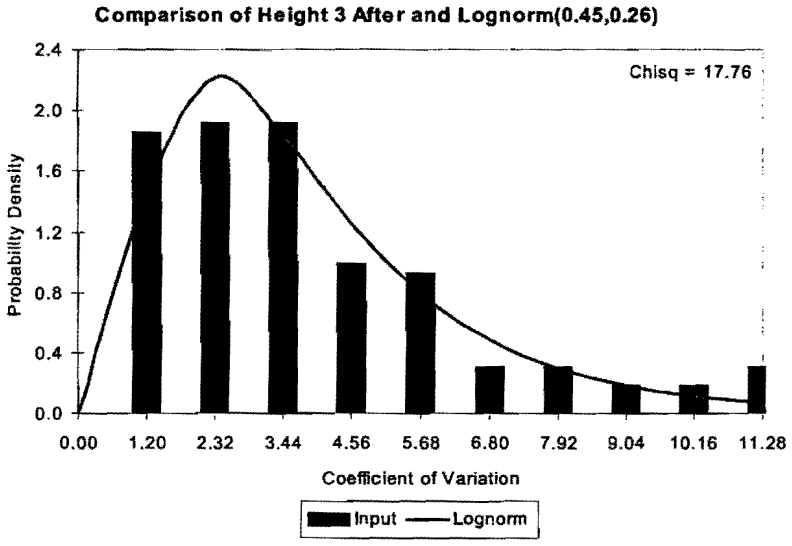

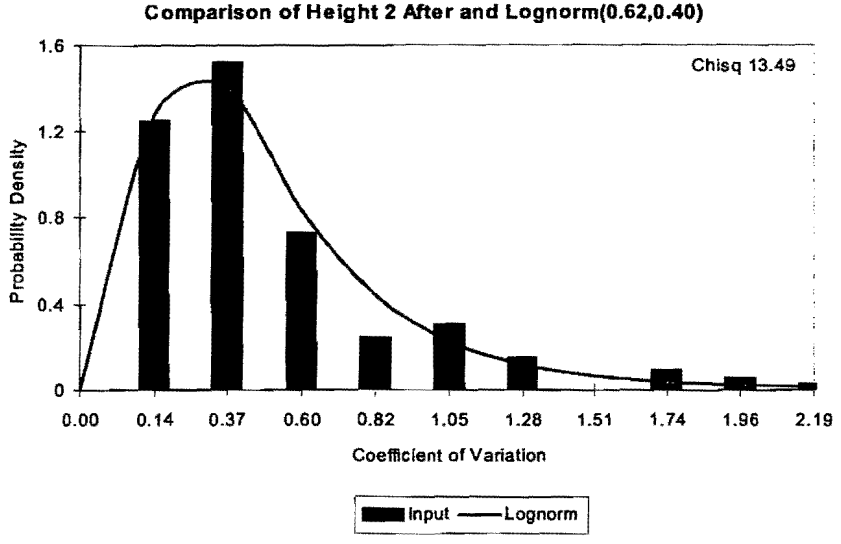

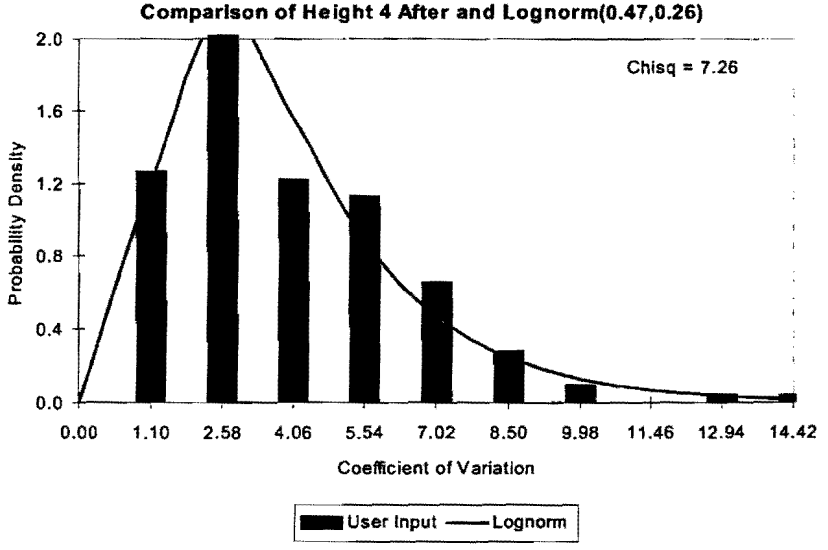

Statistical Distribution By Site Before SHRP Calibration

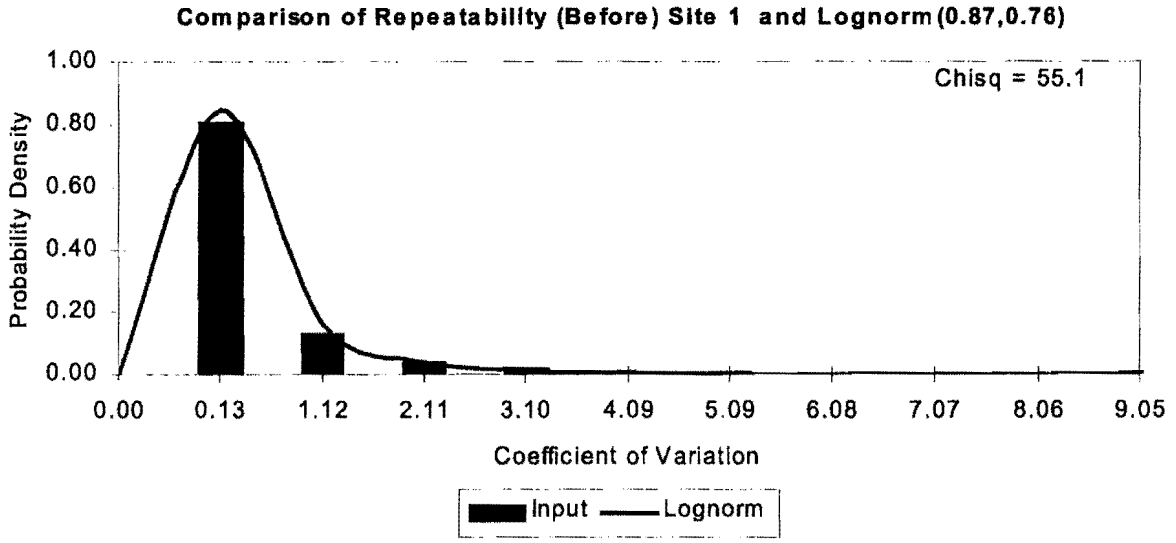

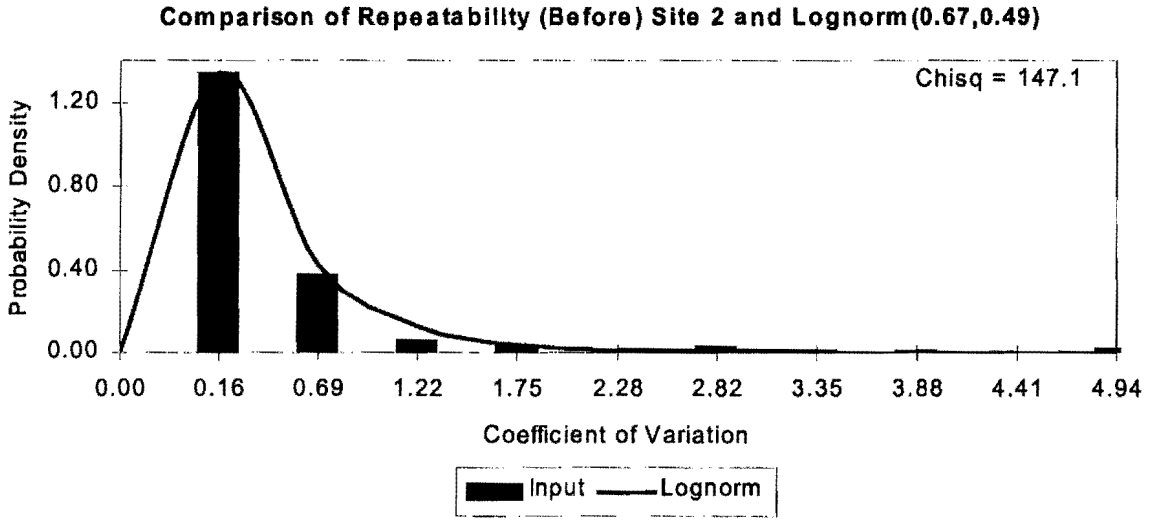

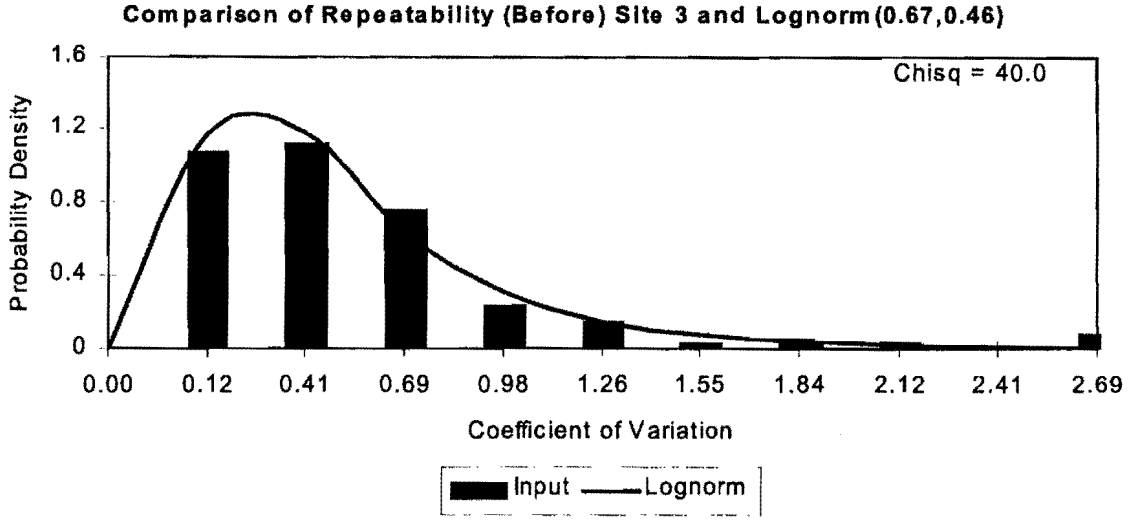

Statistical Distribution By Site After SHRP Calibration

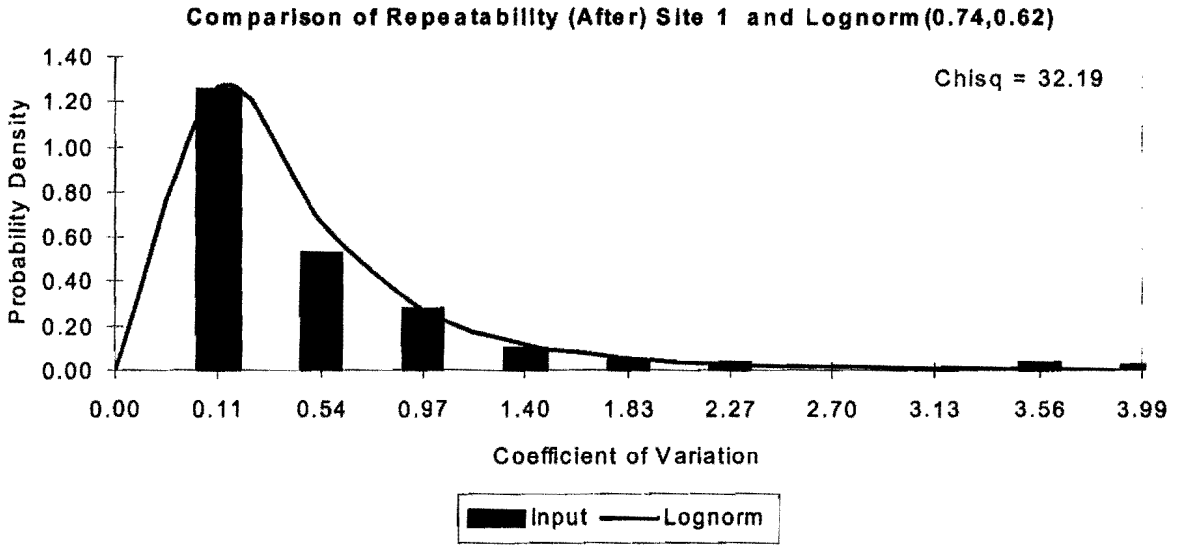

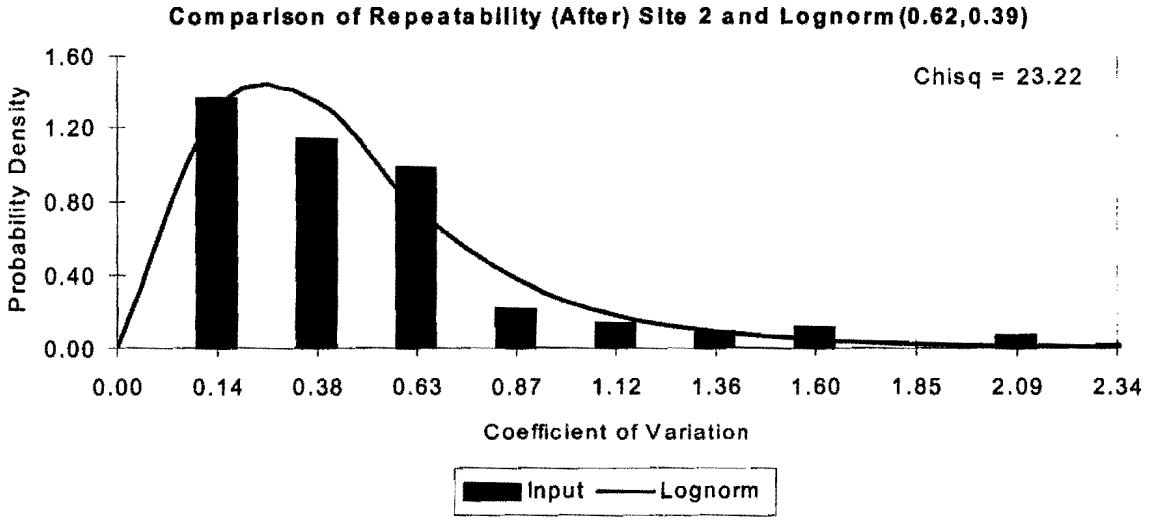

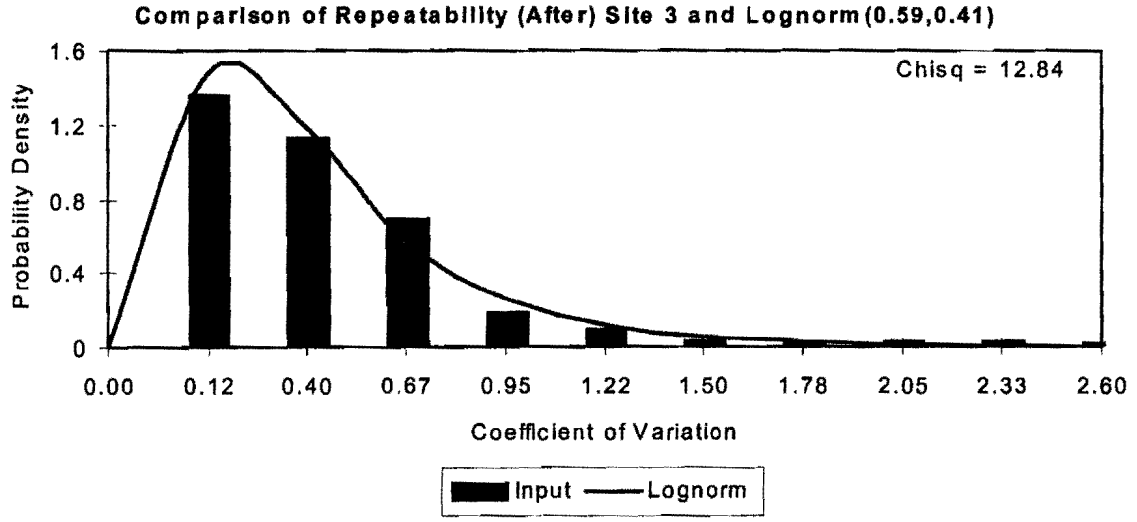

Statistical Distribution By Sensor Before SHRP Calibration

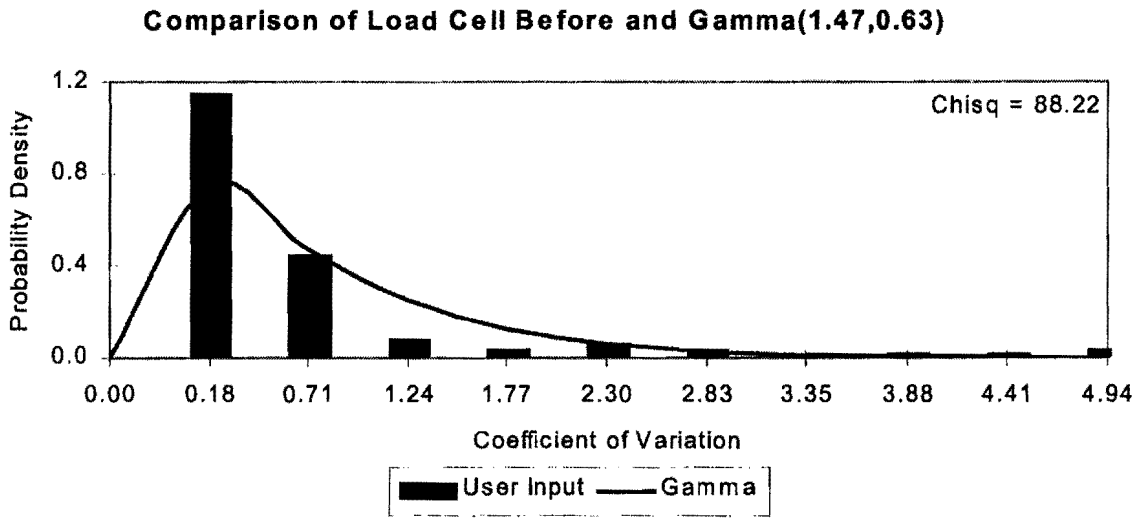

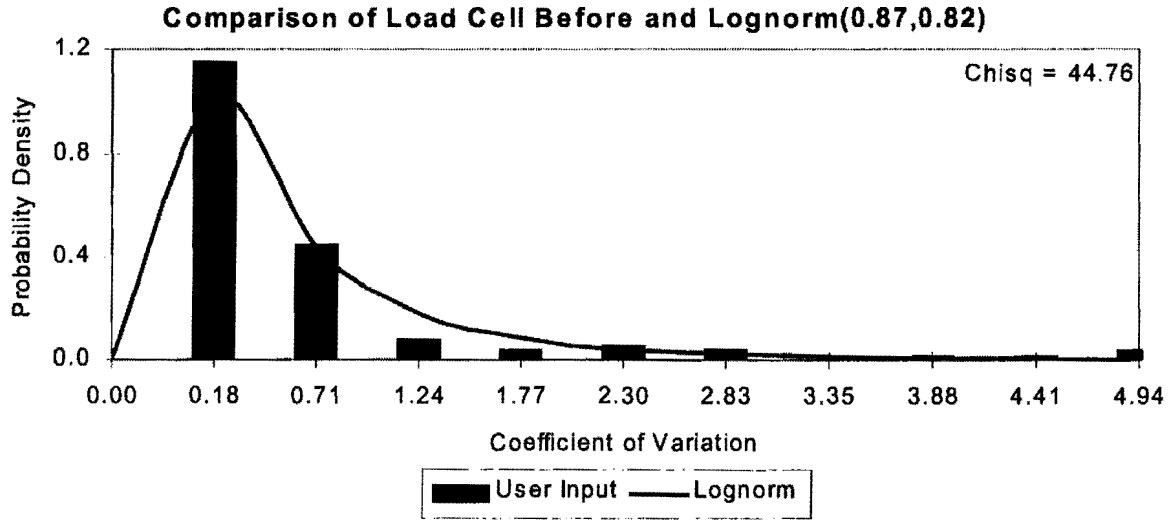

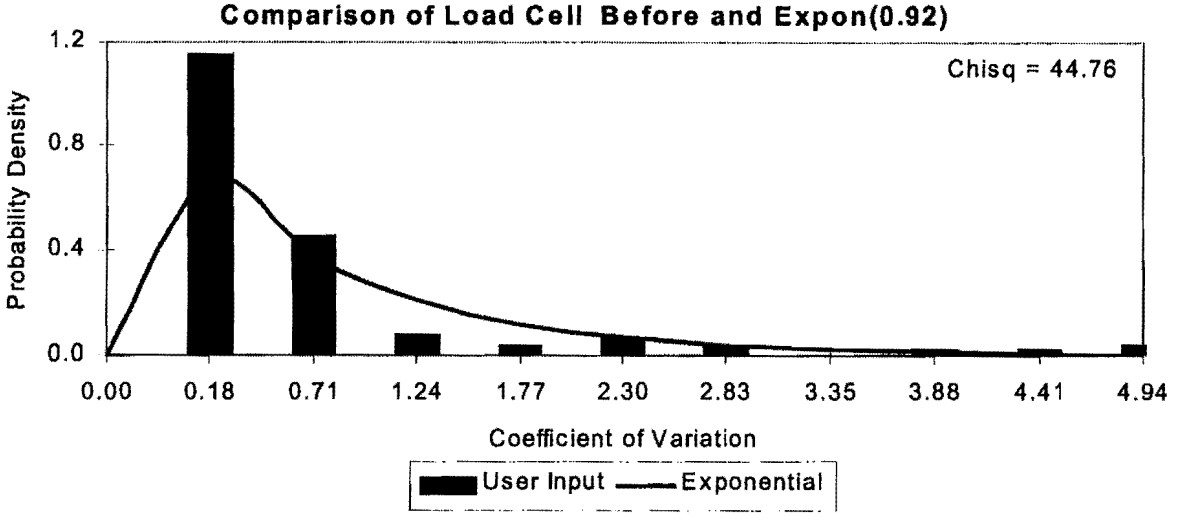

Statistical Distribution By Sensor Before SHRP Calibration

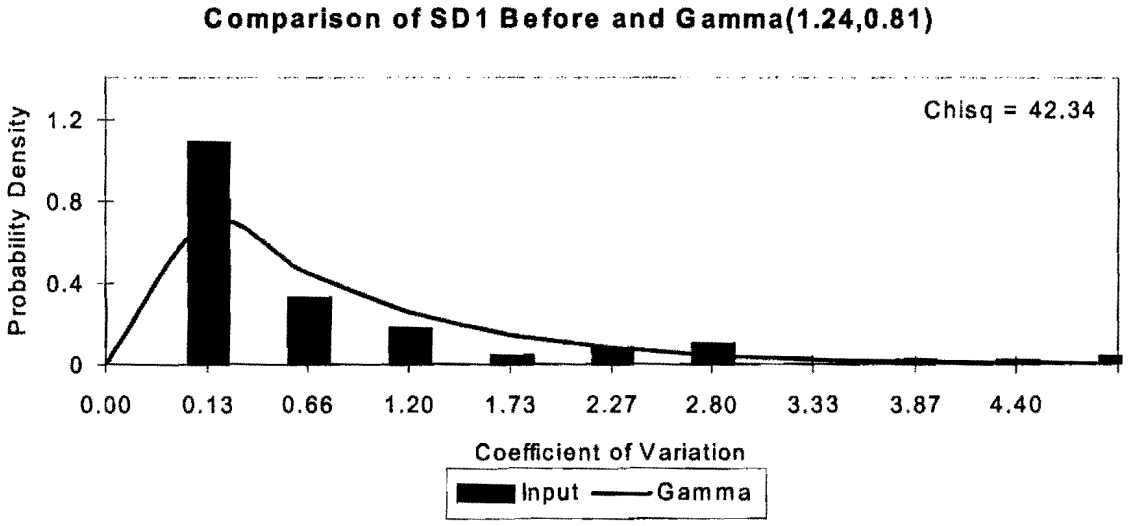

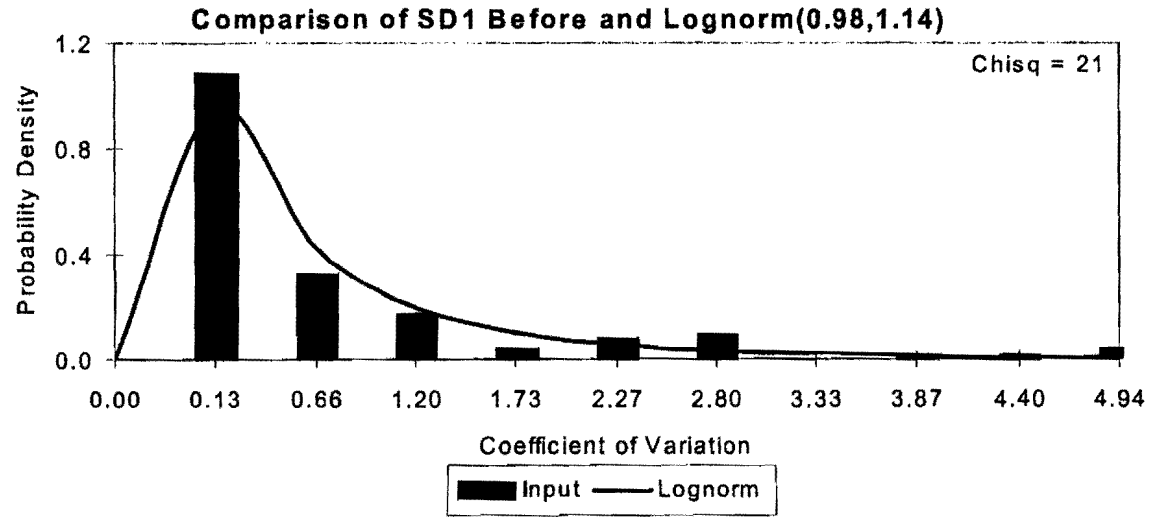

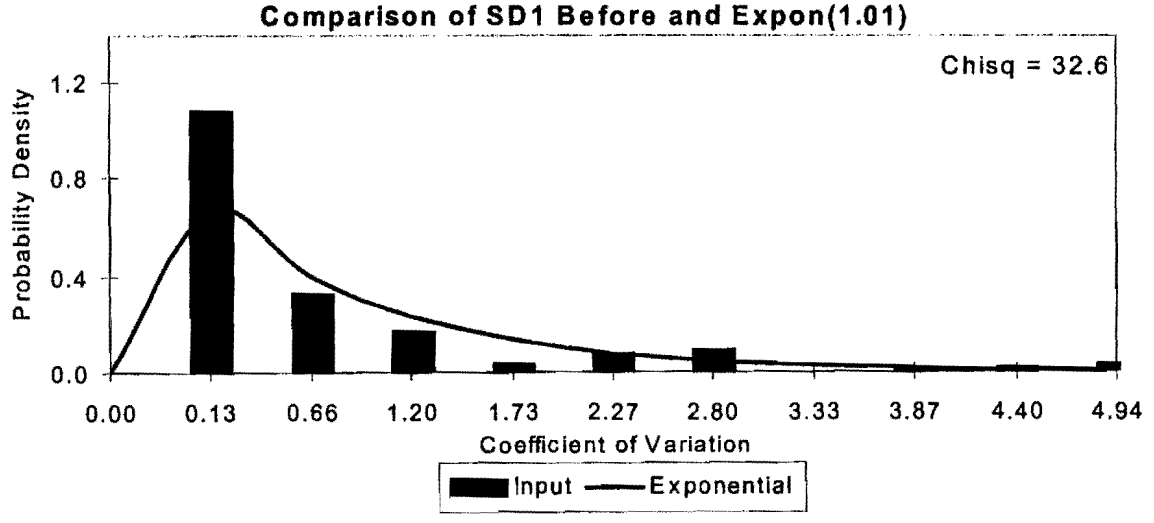

Statistical Distribution By Sensor Before SHRP Calibration

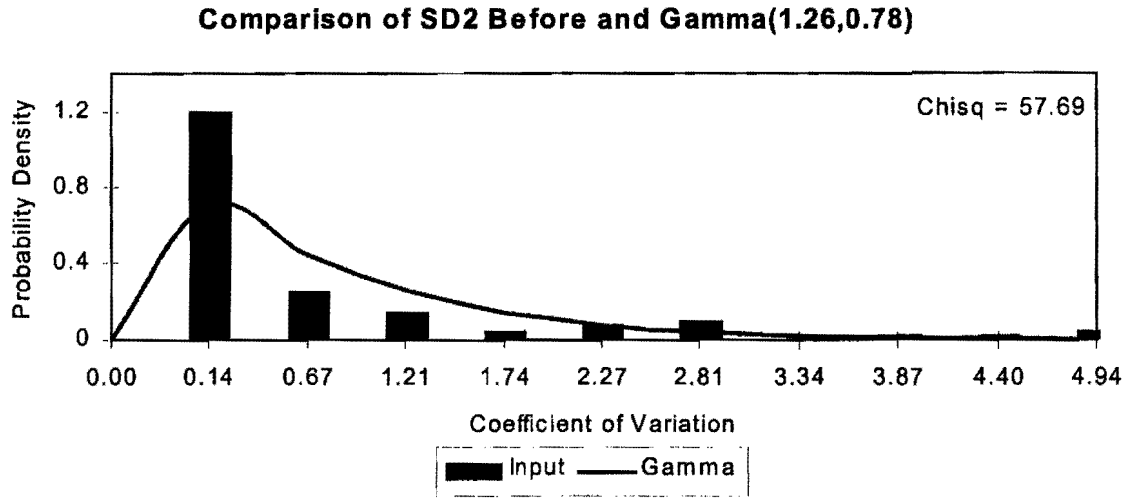

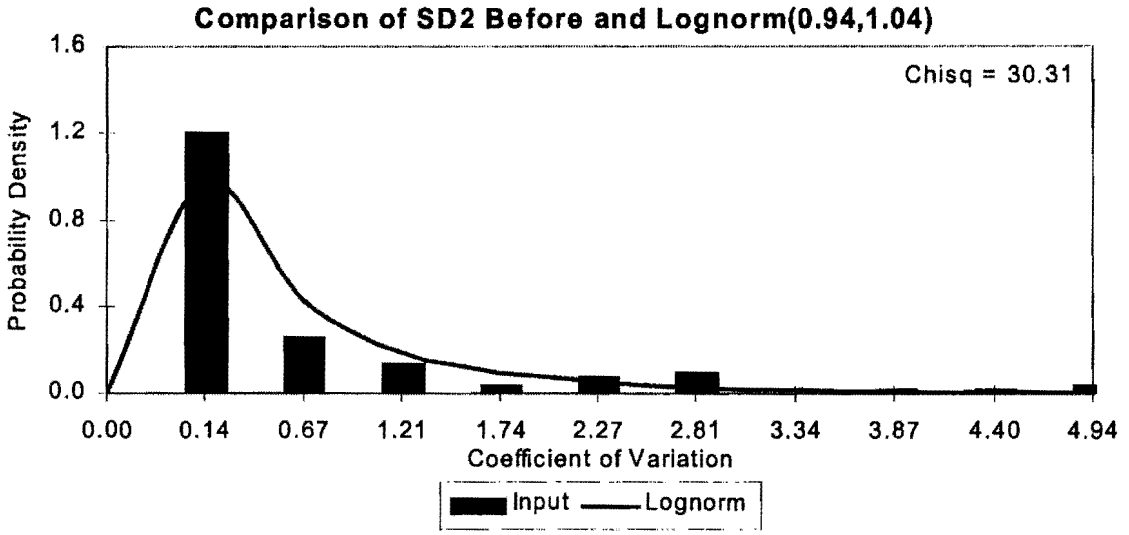

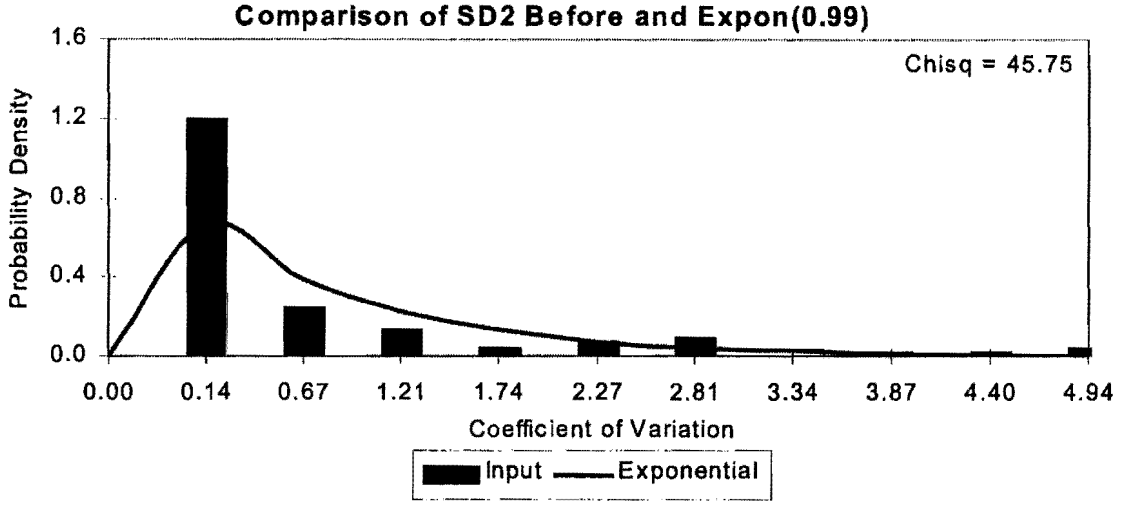

Statistical Distribution By Sensor Before SHRP Calibration

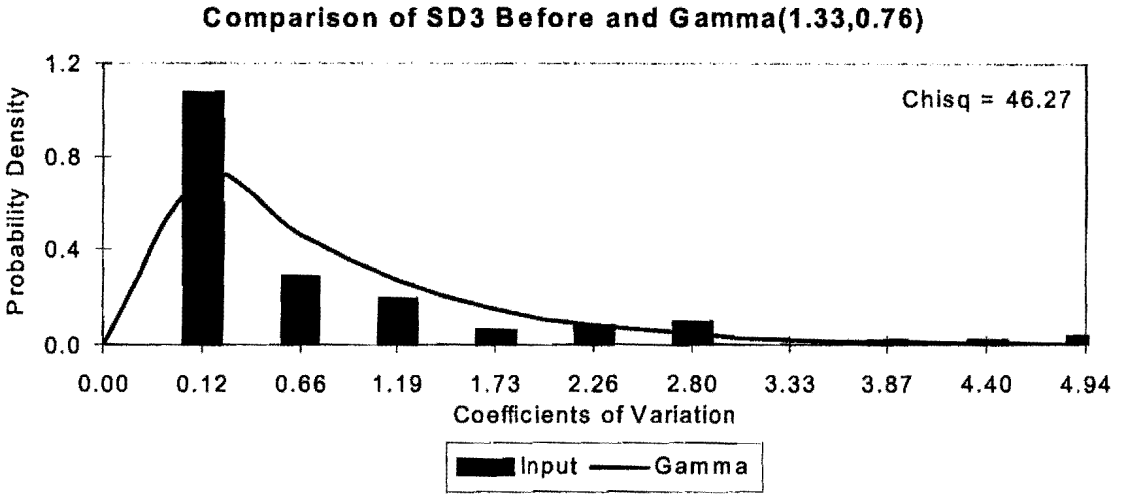

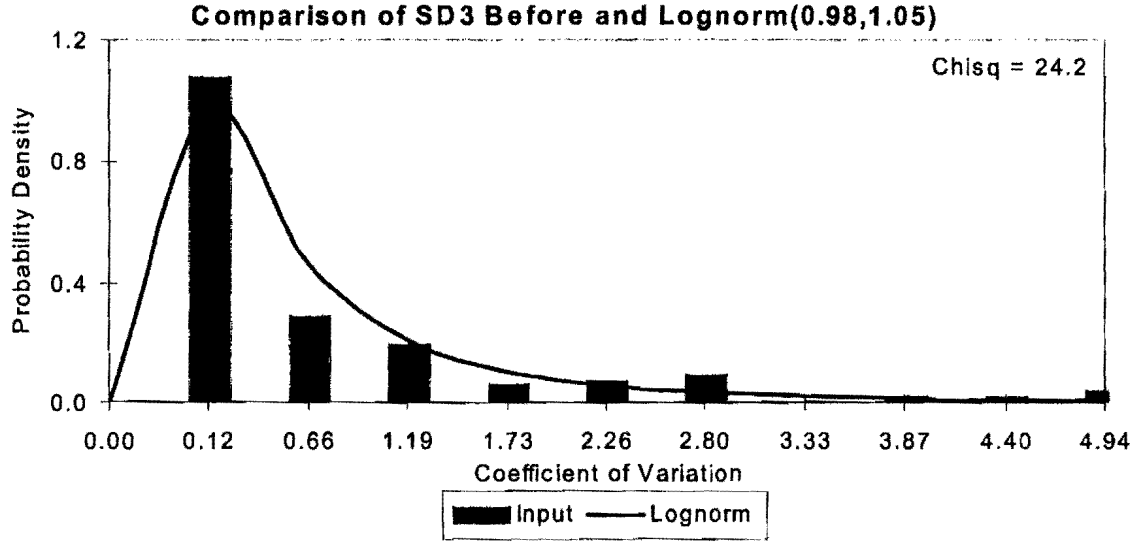

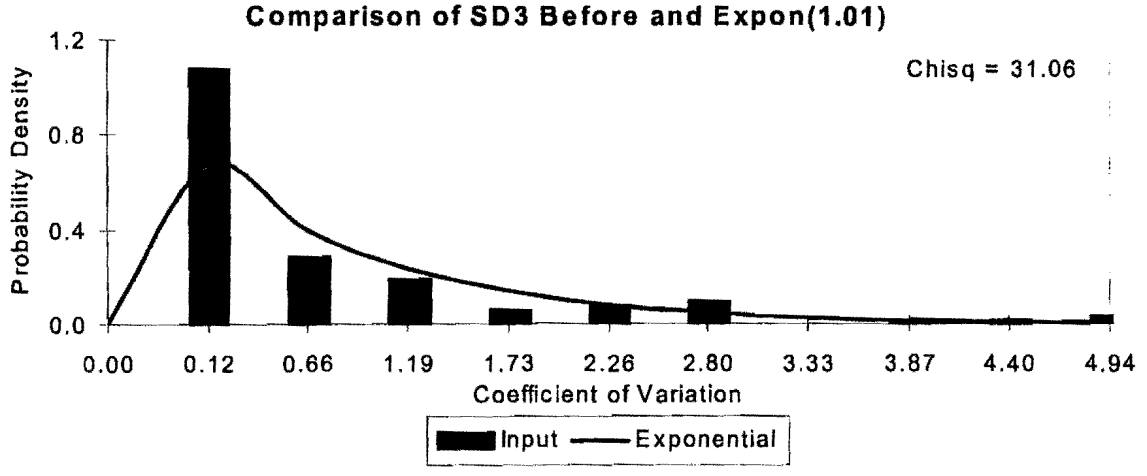

Statistical Distribution By Sensor Before SHRP Calibration

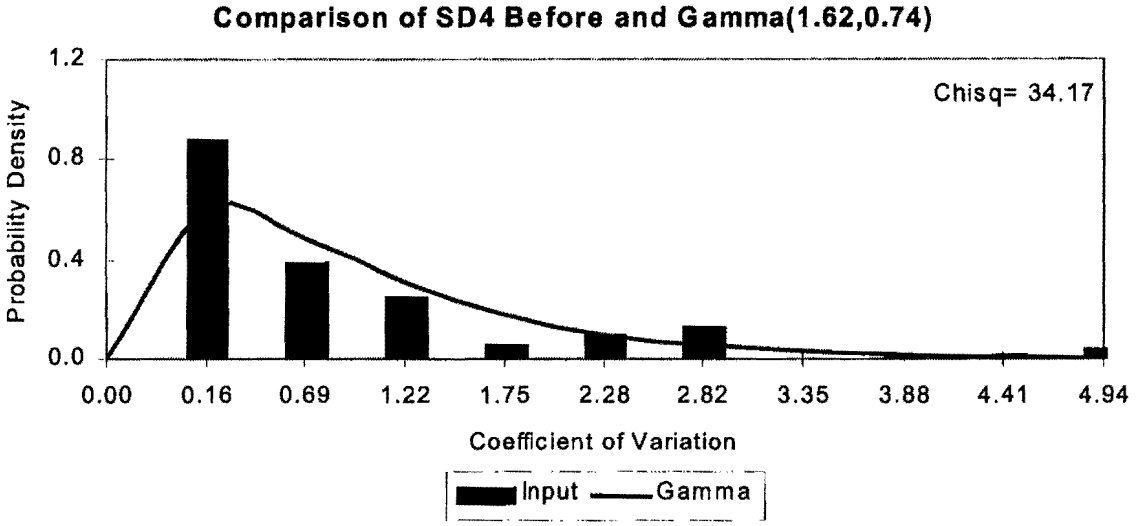

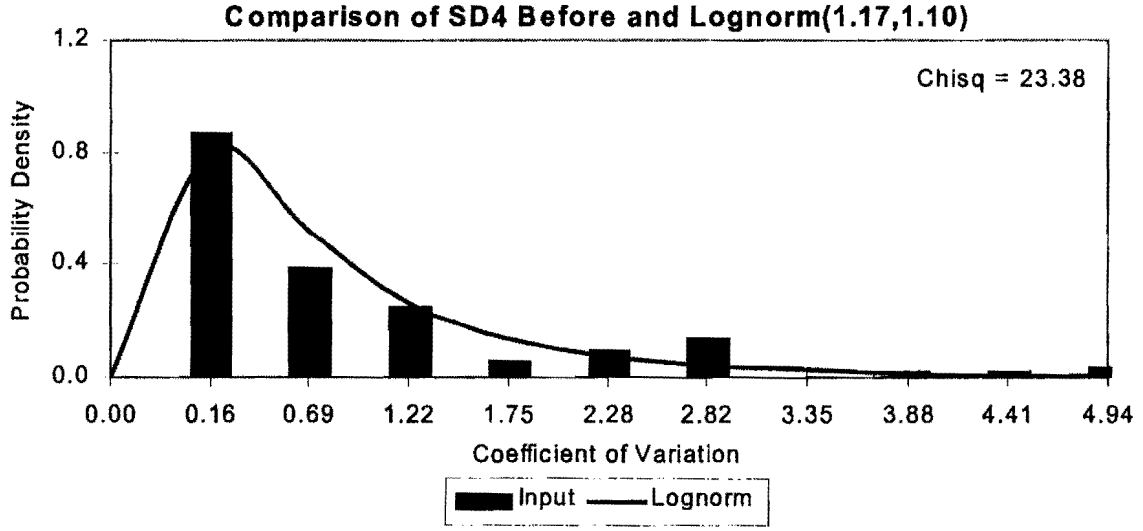

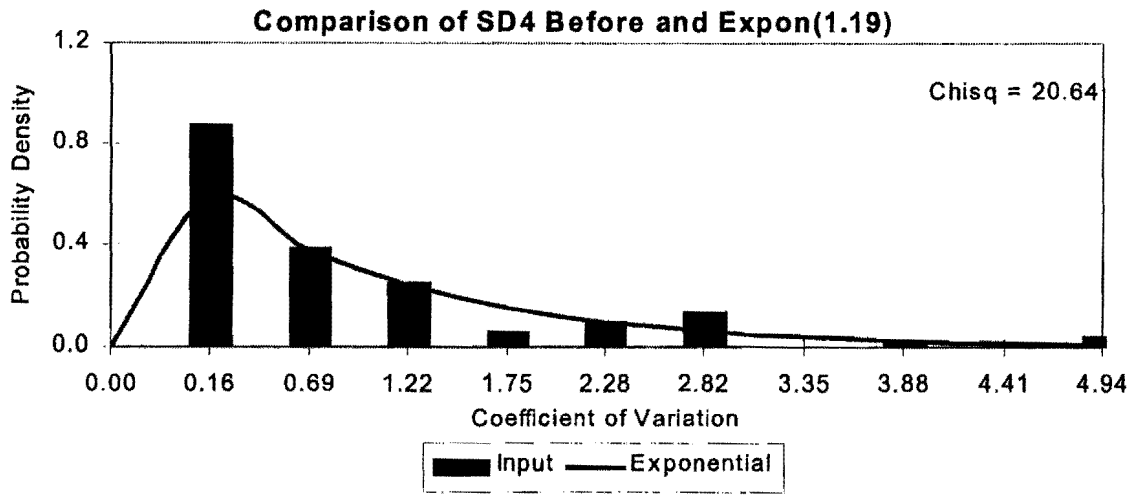

Statistical Distribution By Sensor Before SHRP Calibration

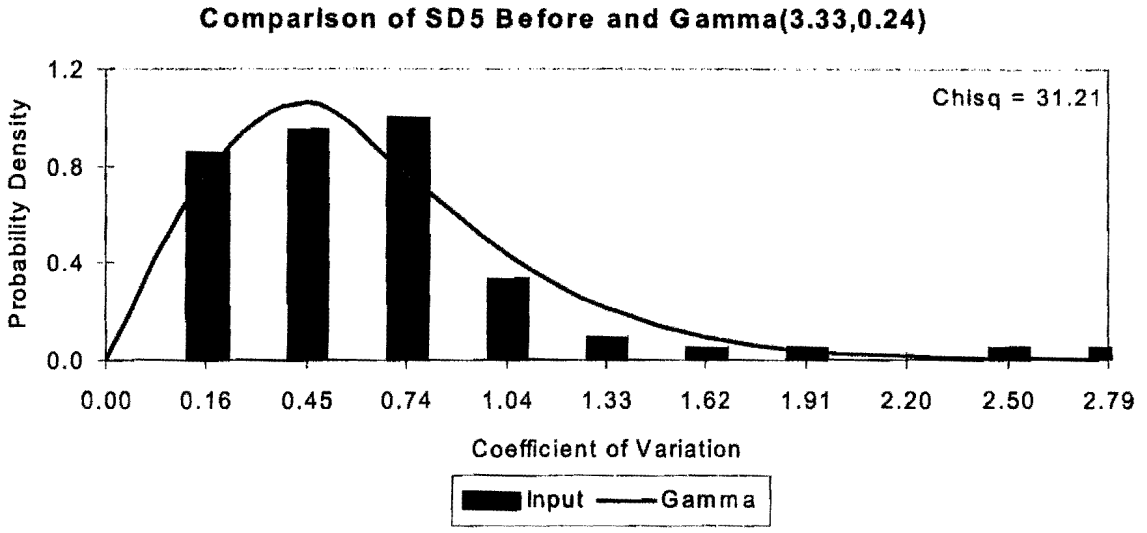

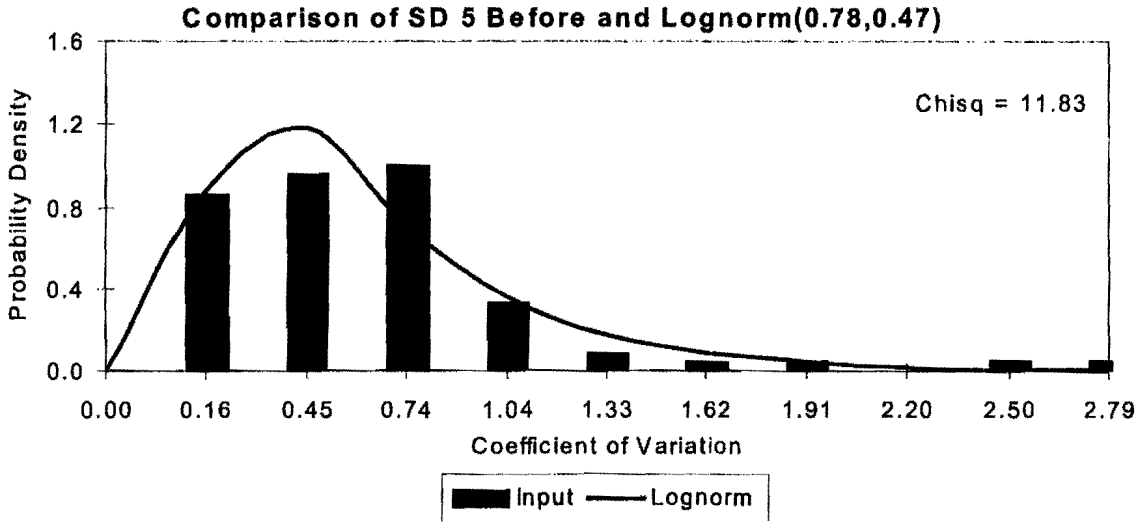

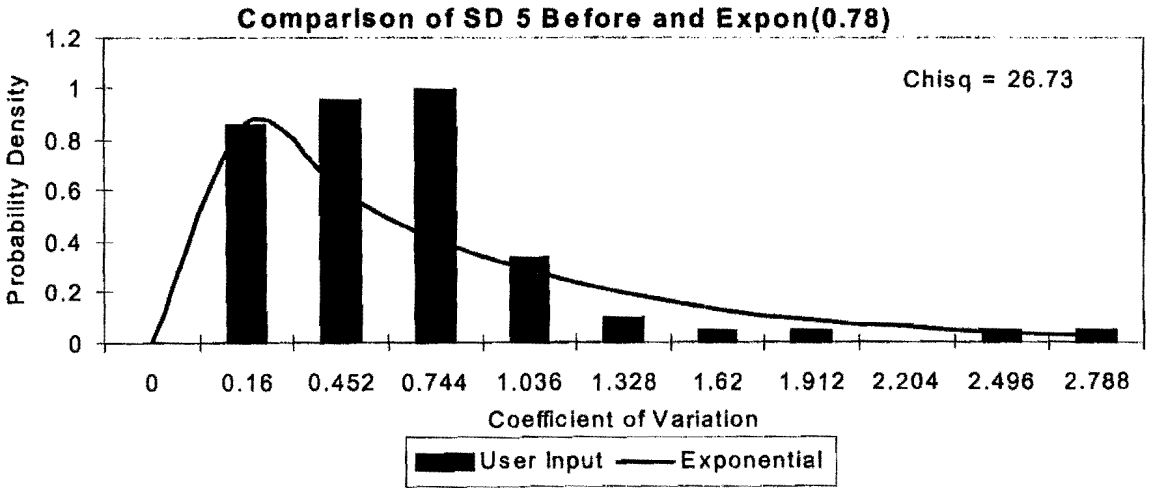

Statistical Distribution By Sensor Before SHRP Calibration

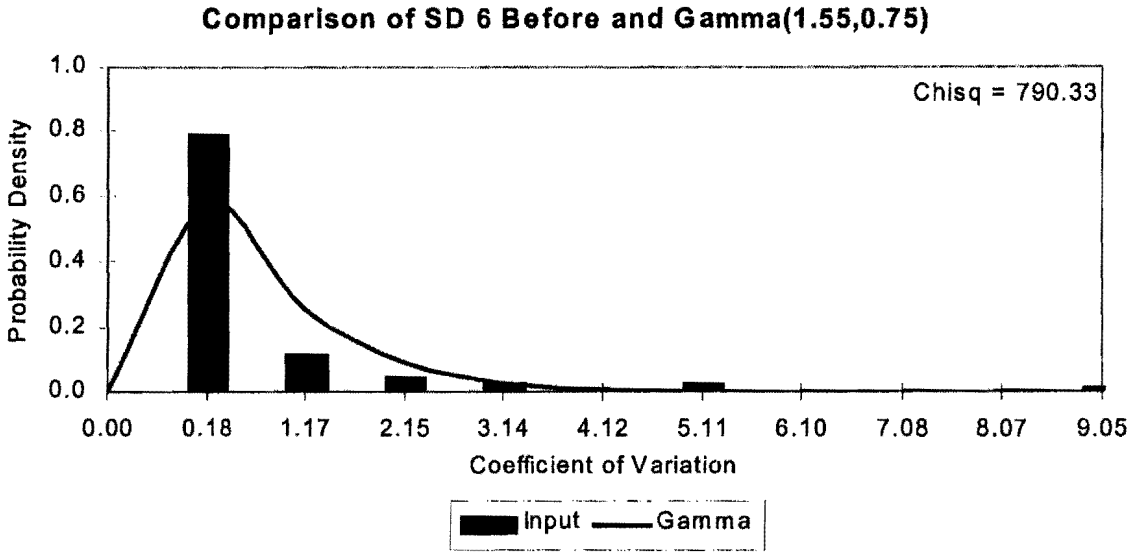

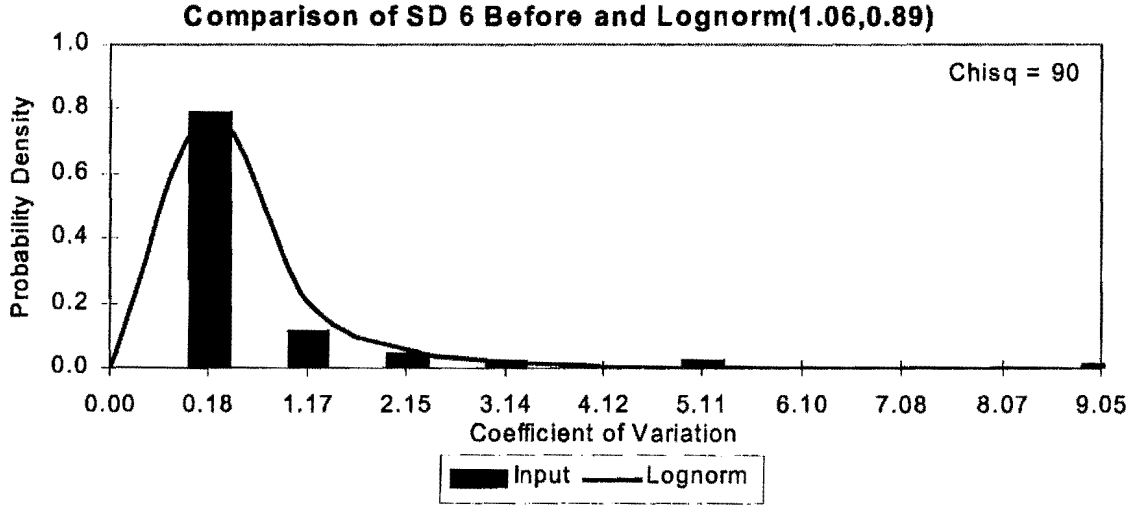

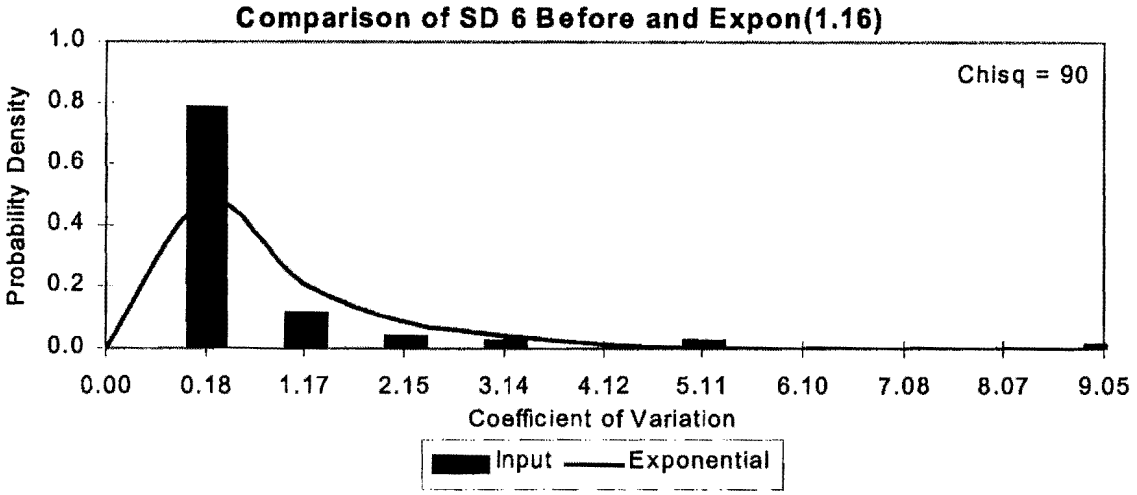

Statistical Distribution By Sensor Before SHRP Calibration

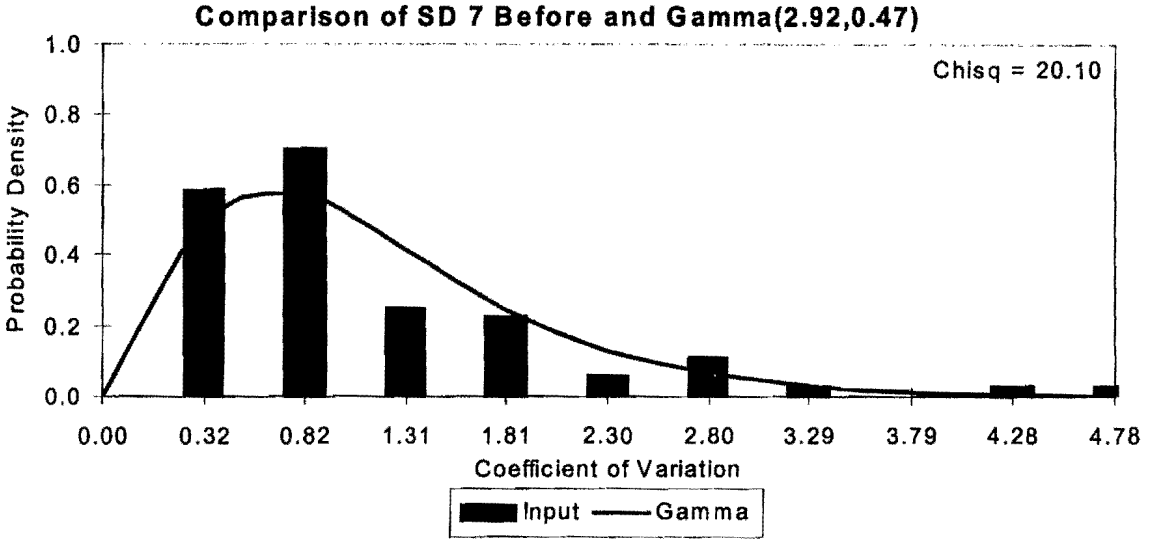

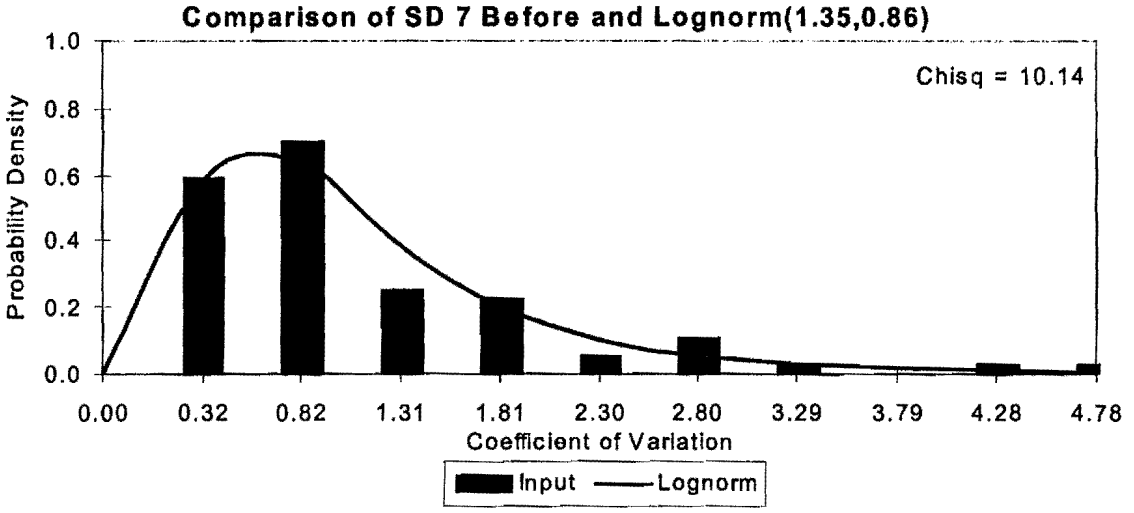

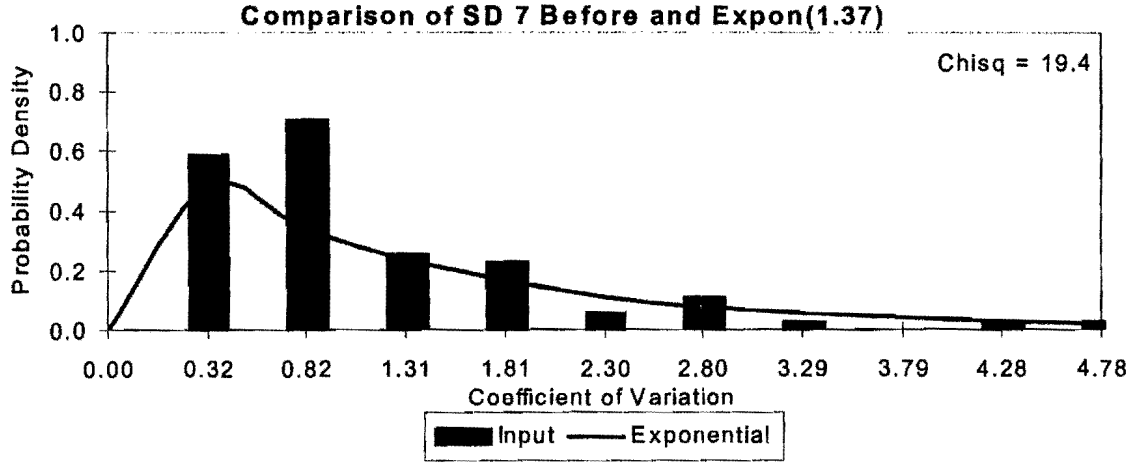

Statistical Distribution By Site After SHRP Calibration

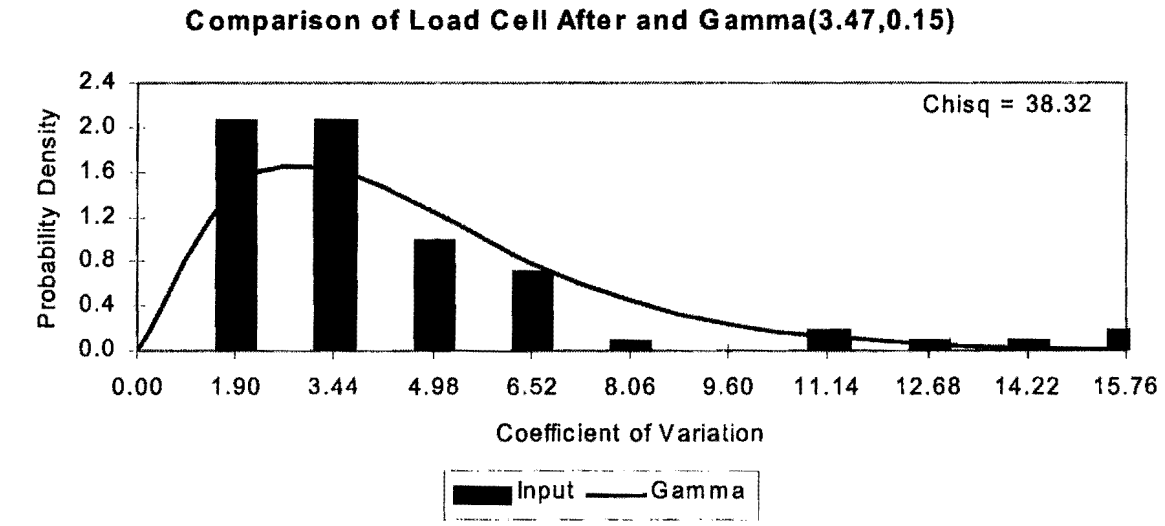

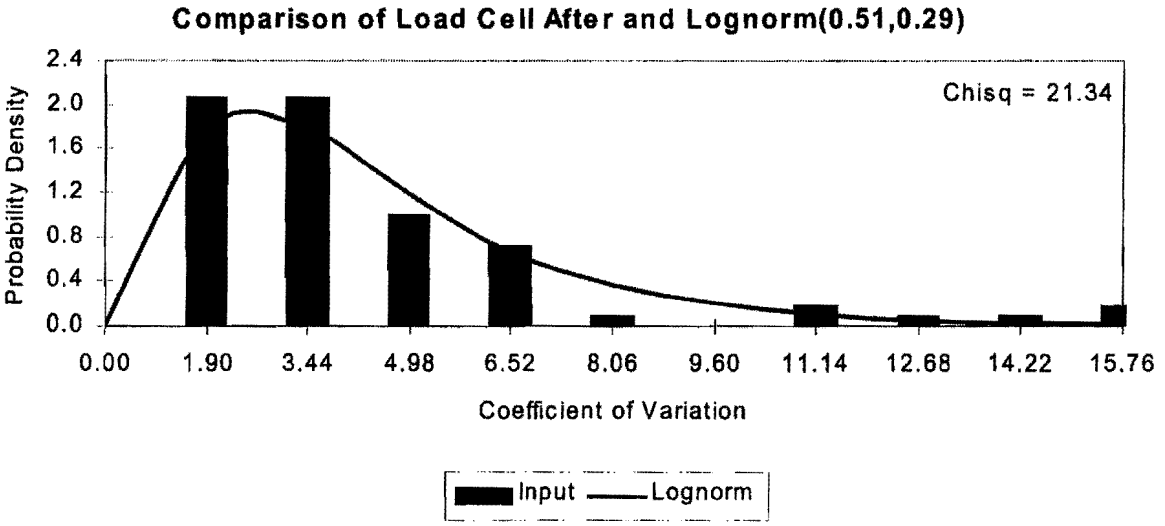

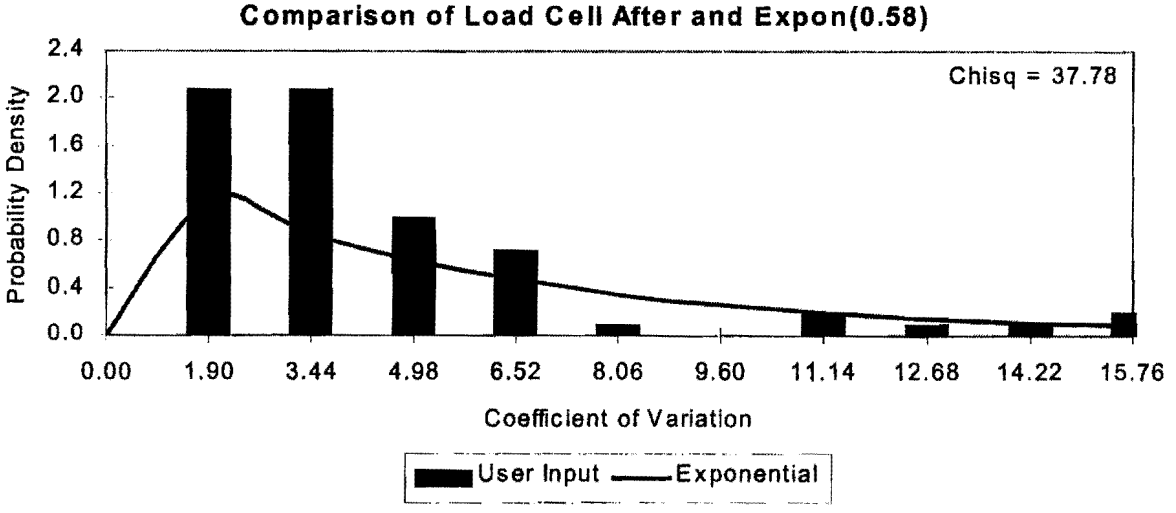

Statistical Distribution By Site After SHRP Calibration

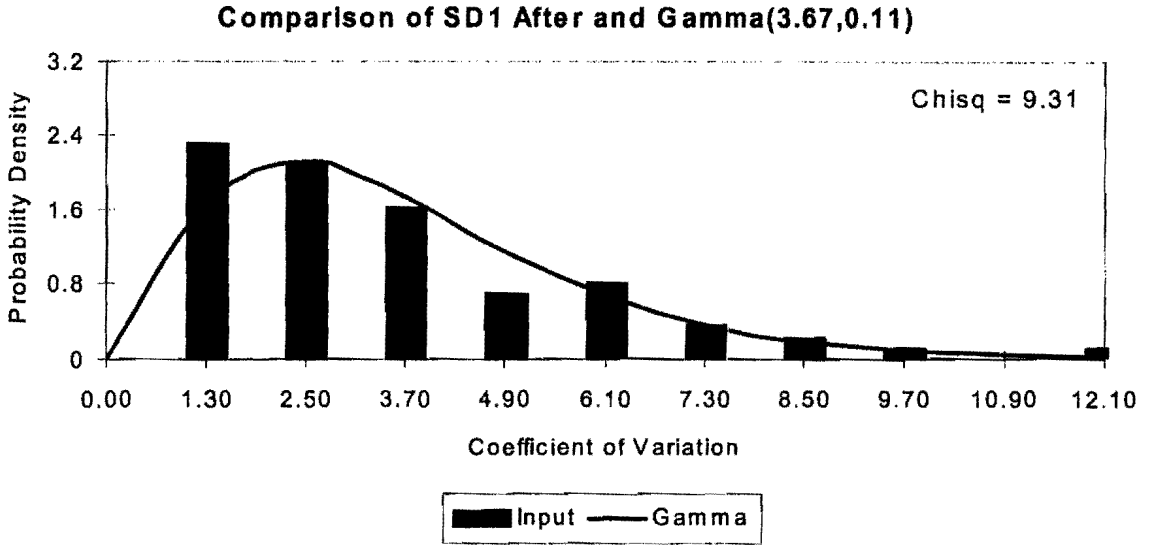

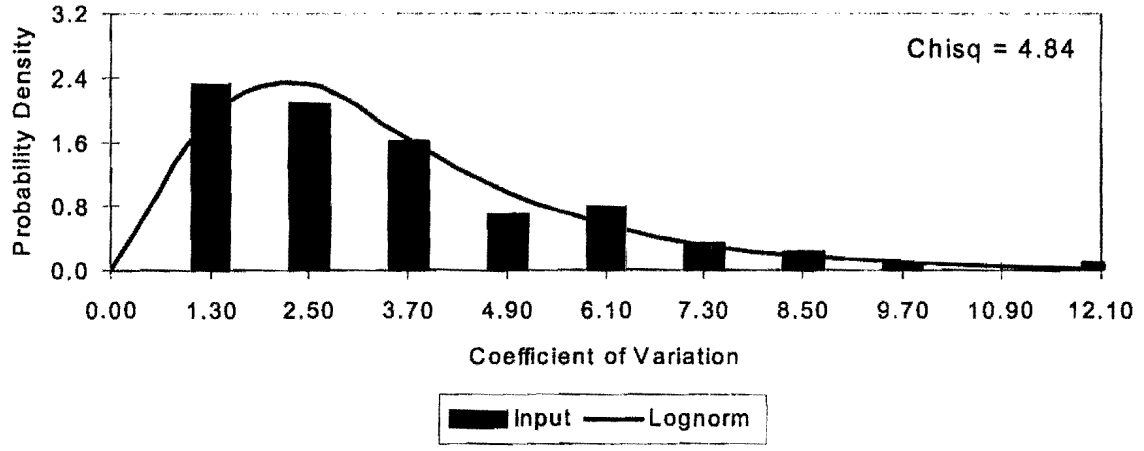

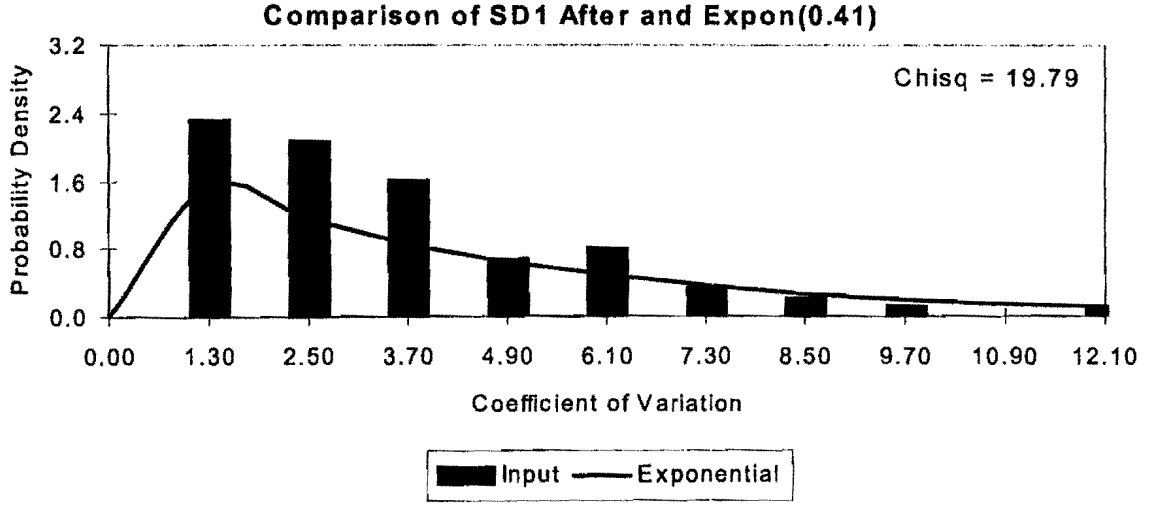

Statistical Distribution By Site After SHRP Calibration

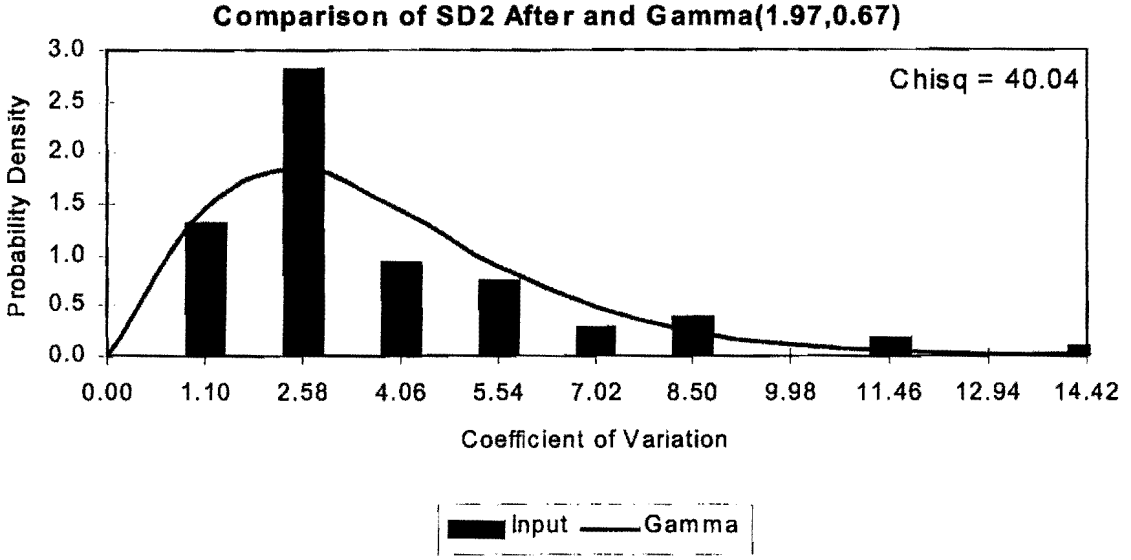

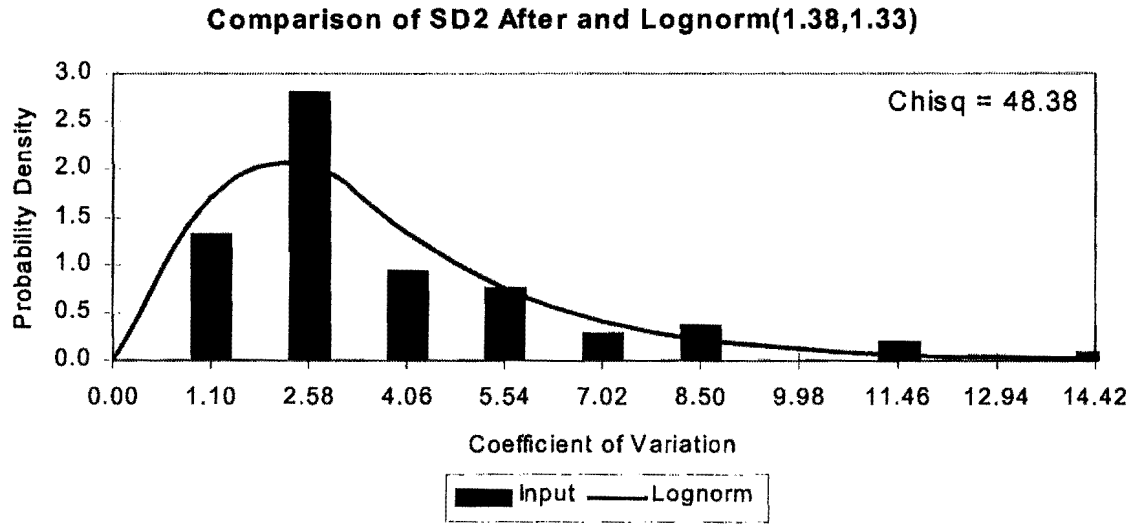

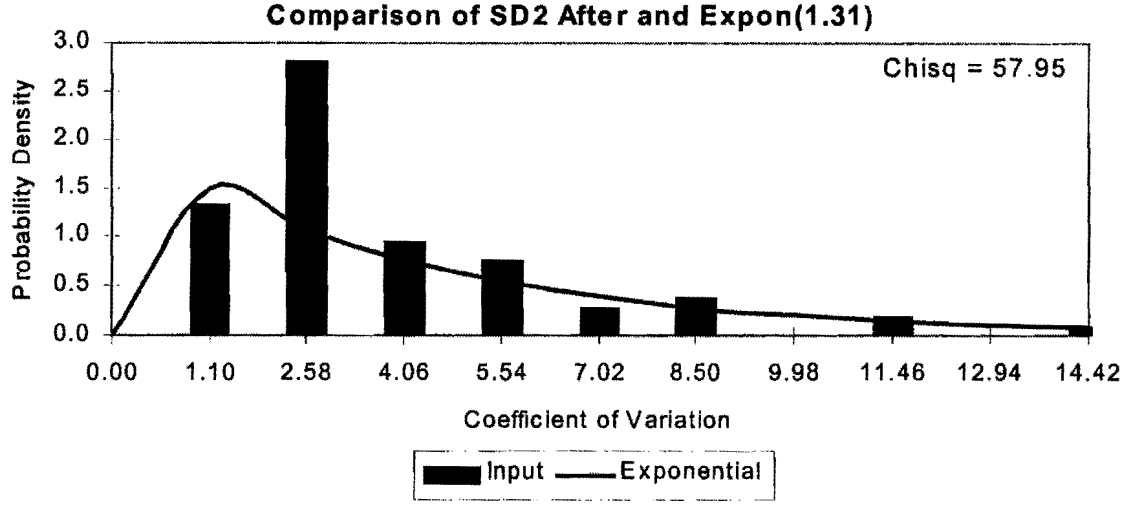

Statistical Distribution By Site After SHRP Calibration

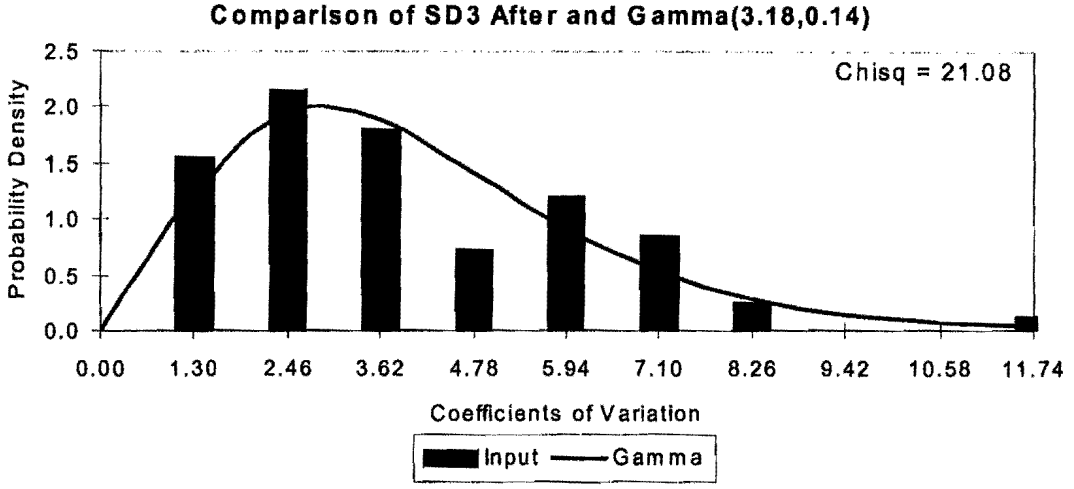

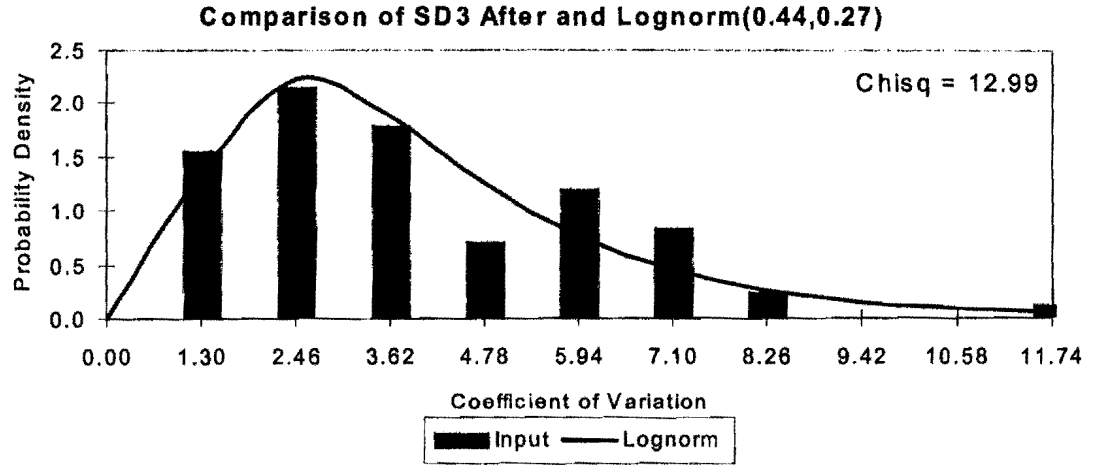

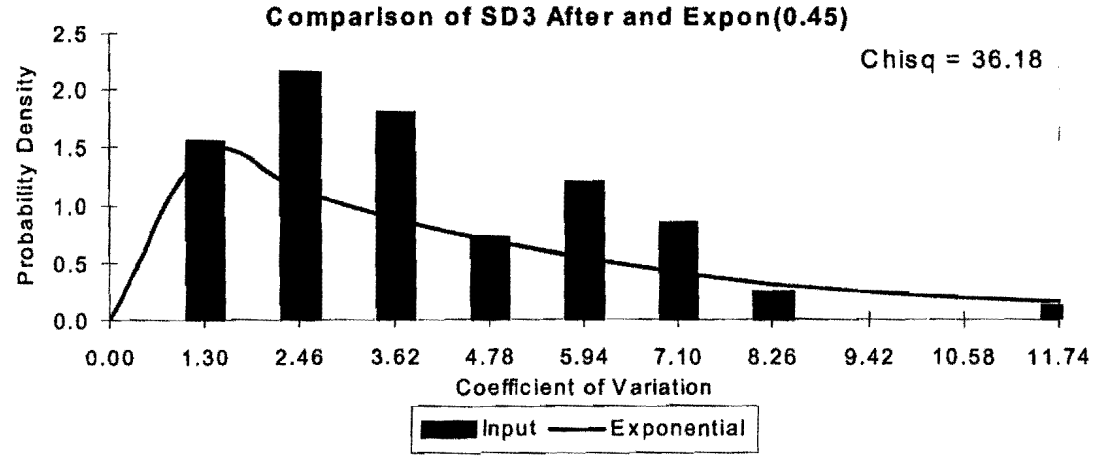

Statistical Distribution By Site After SHRP Calibration

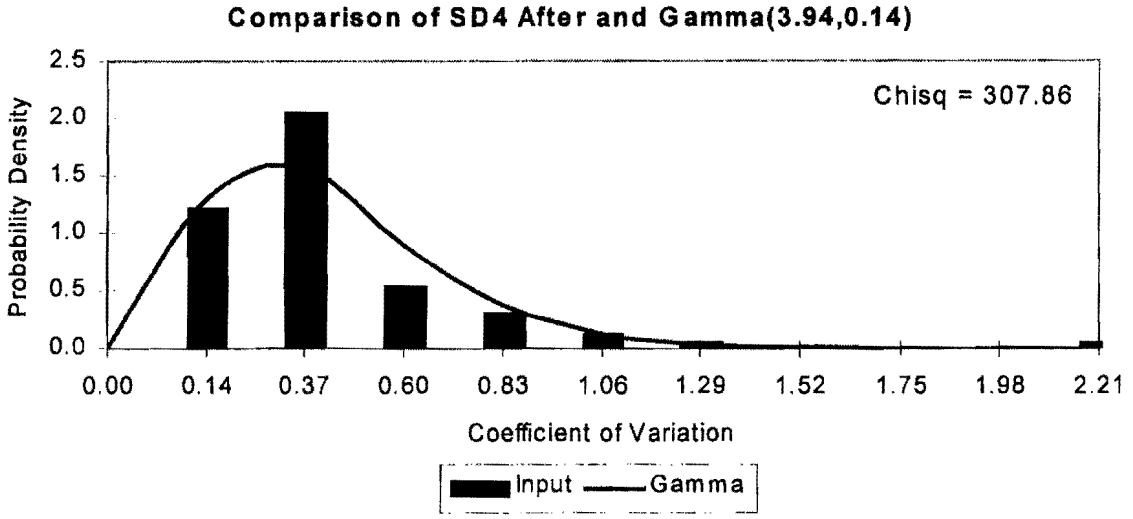

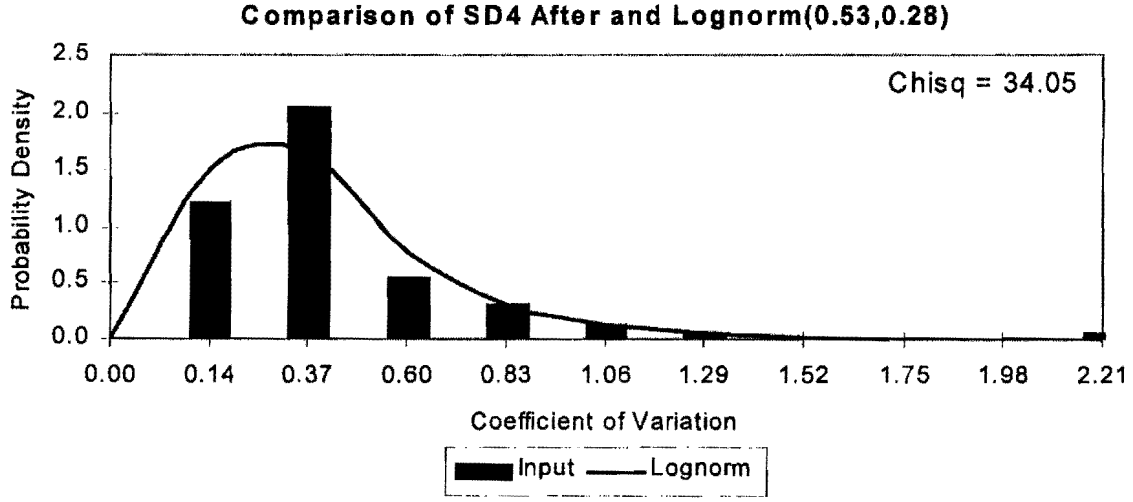

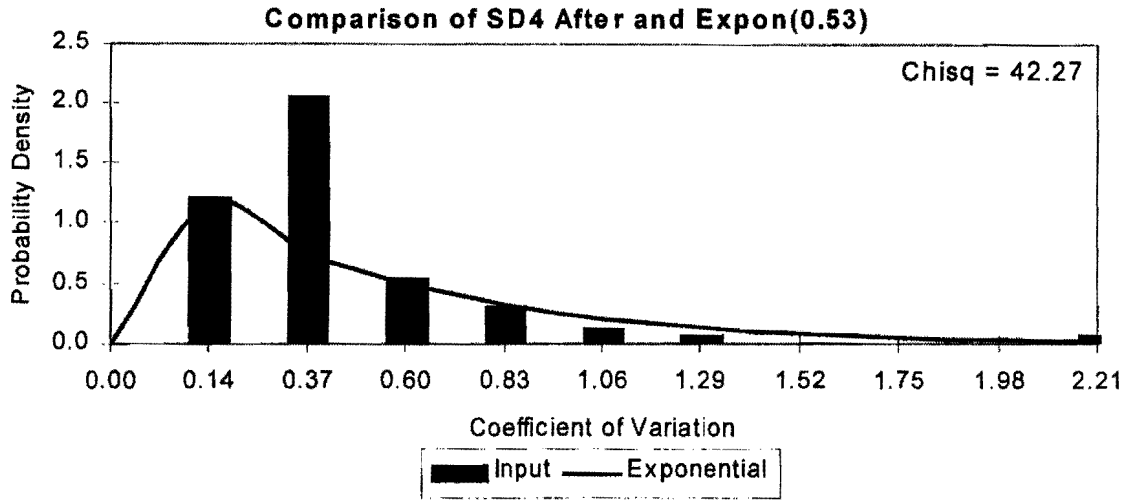

Statistical Distribution By Site After SHRP Calibration

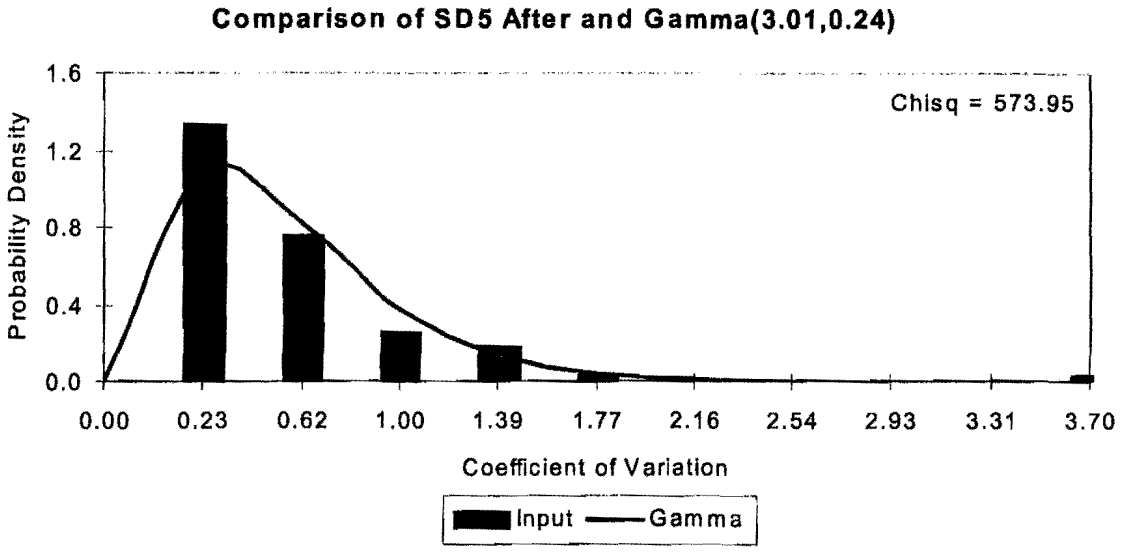

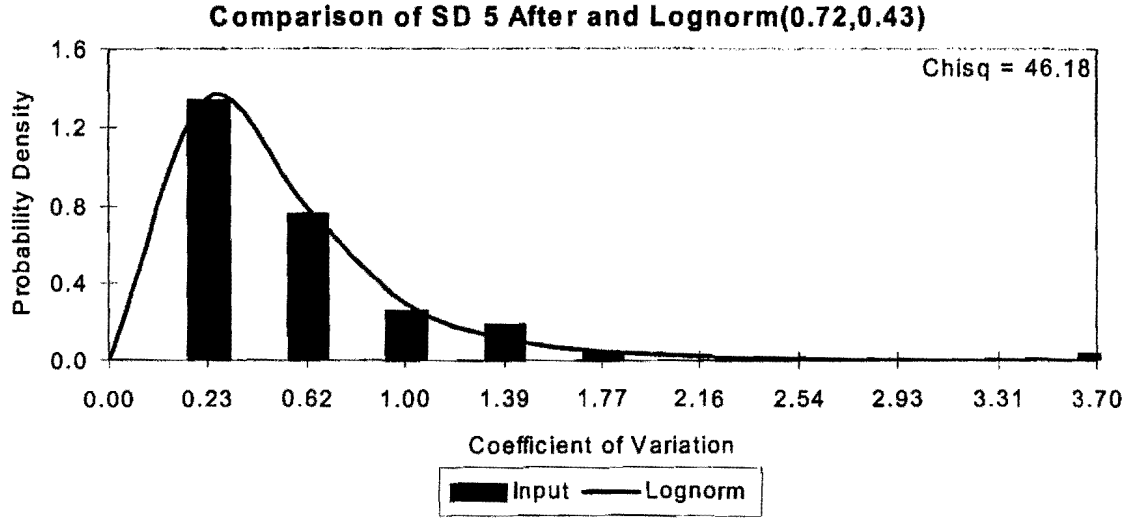

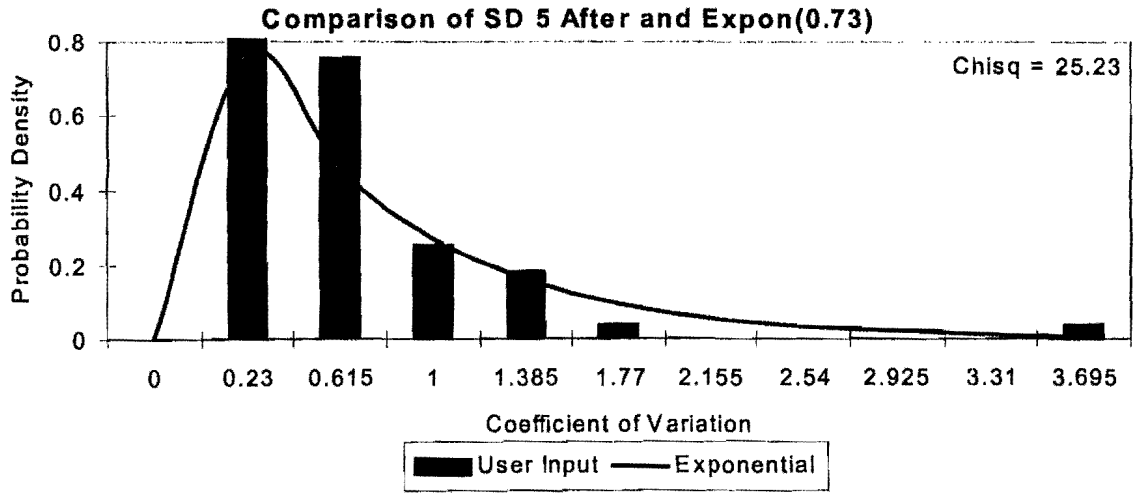

Statistical Distribution By Site After SHRP Calibration

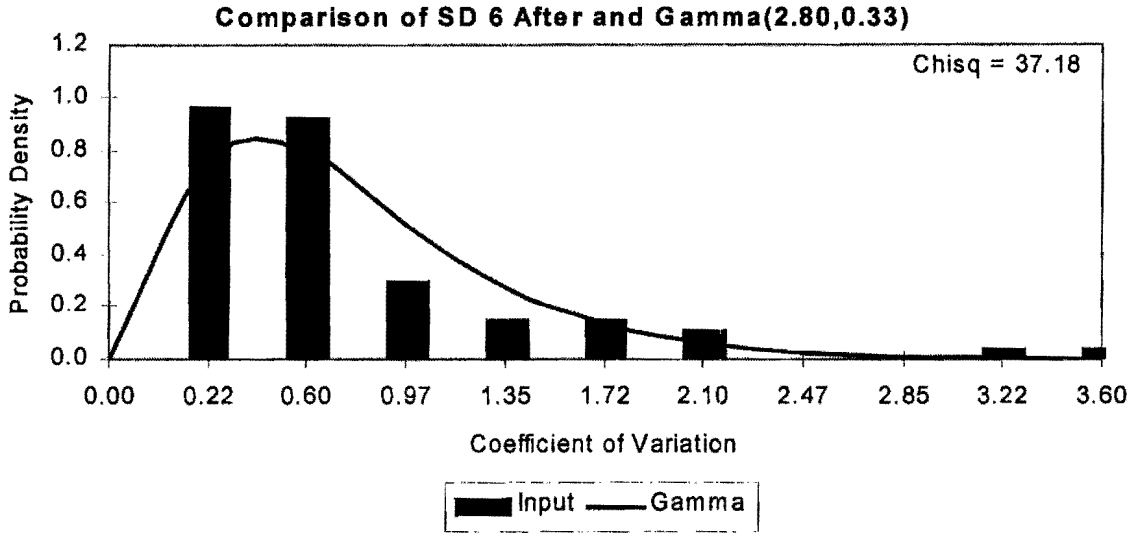

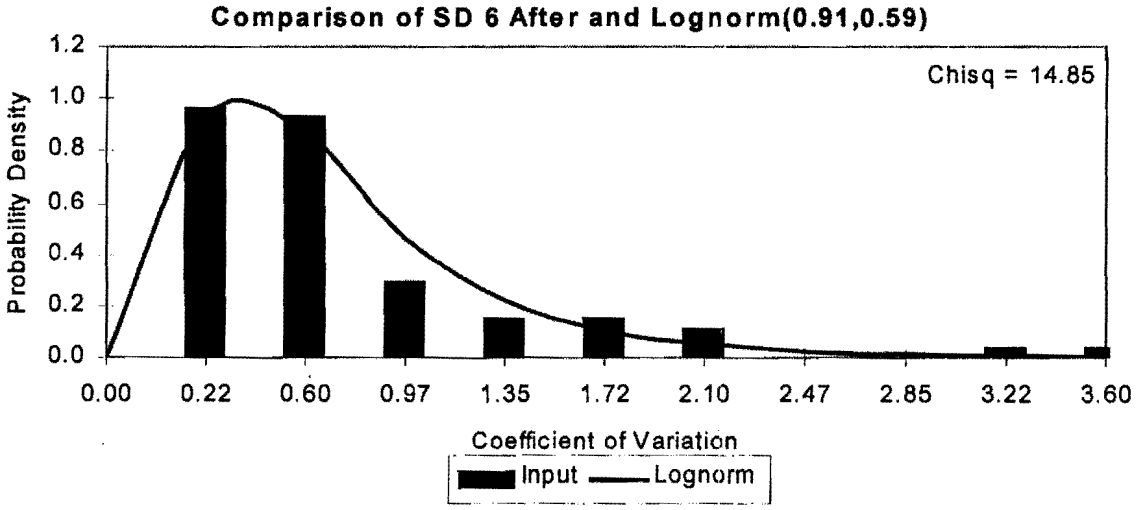

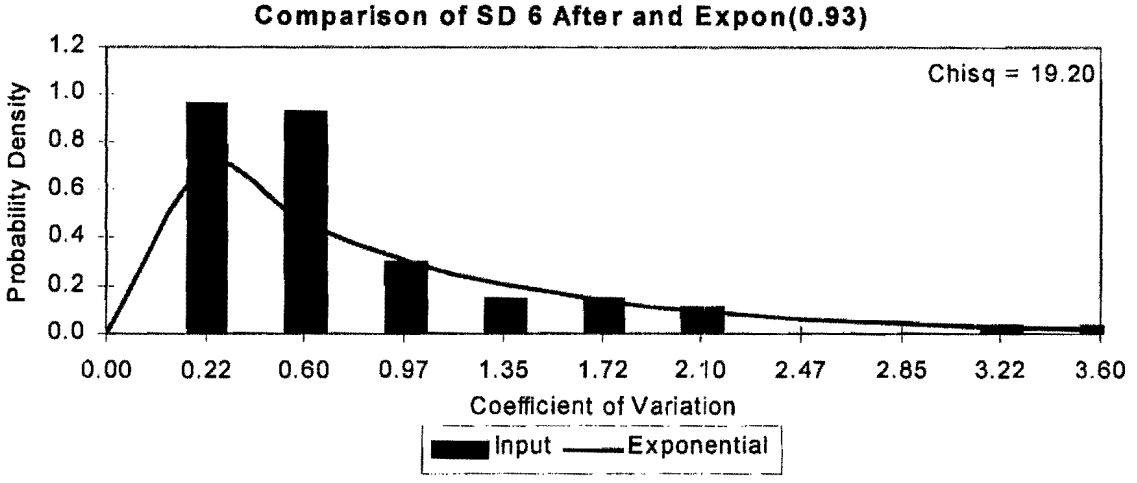

Statistical Distribution By Site After SHRP Calibration

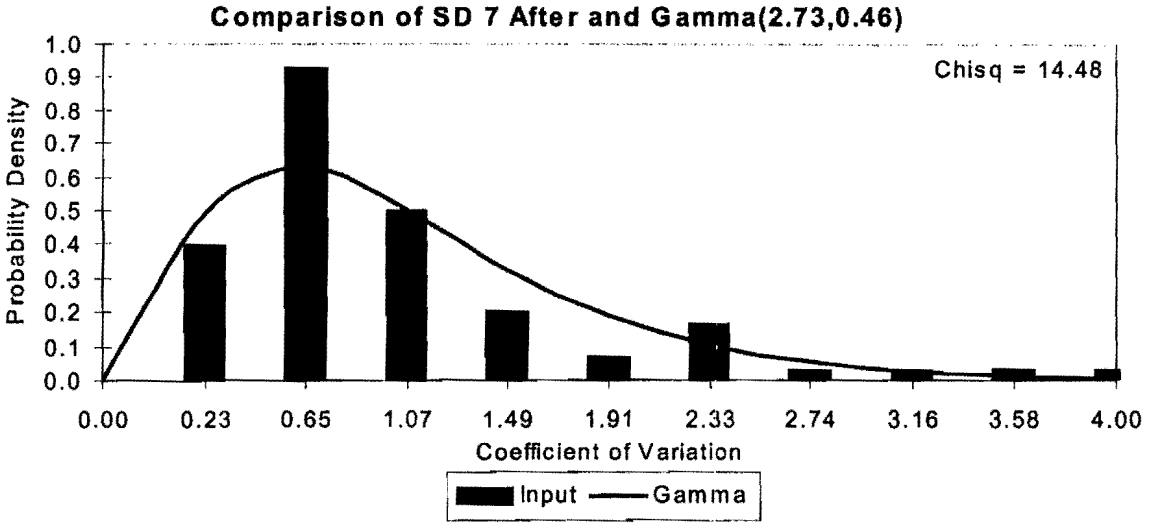

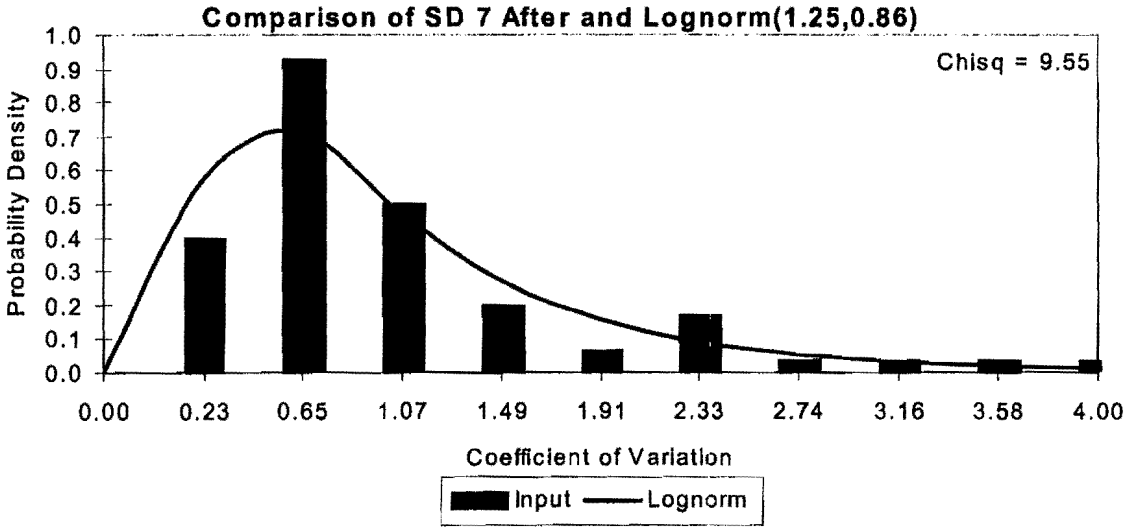

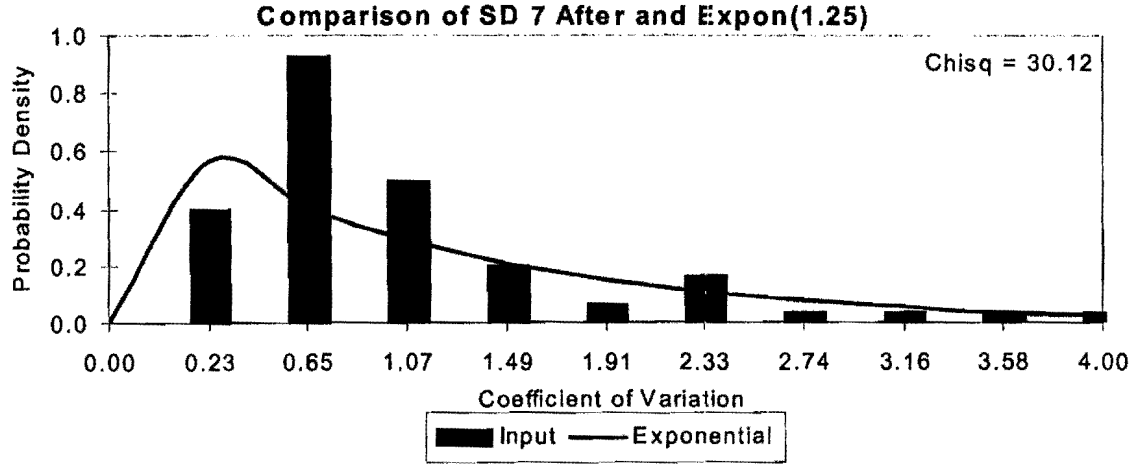

Appendix B

Reproducibility Distribution Charts

Statistical Distribution By Height Before SHRP Calibration

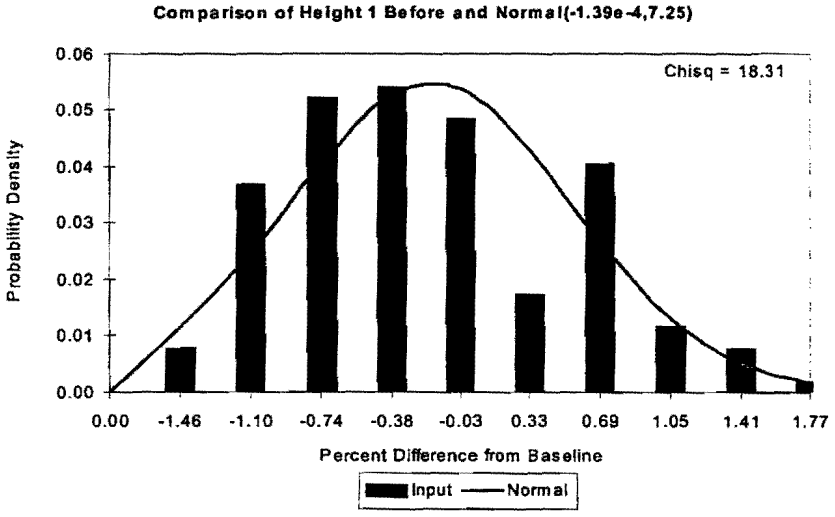

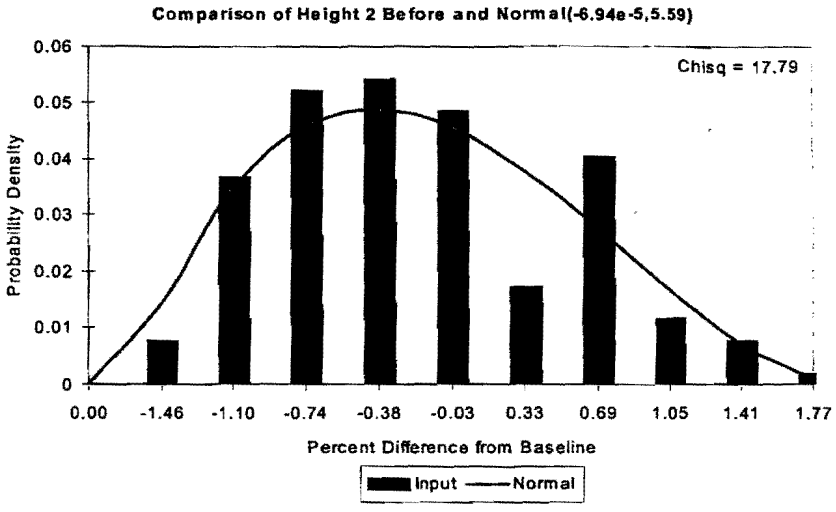

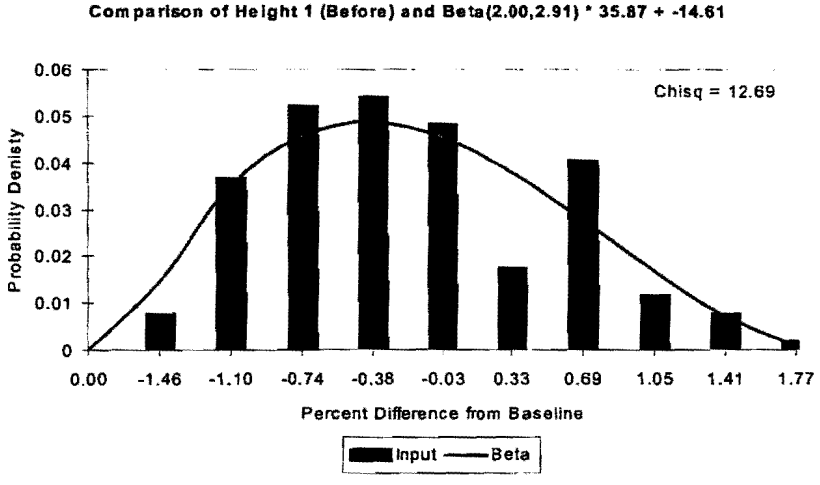

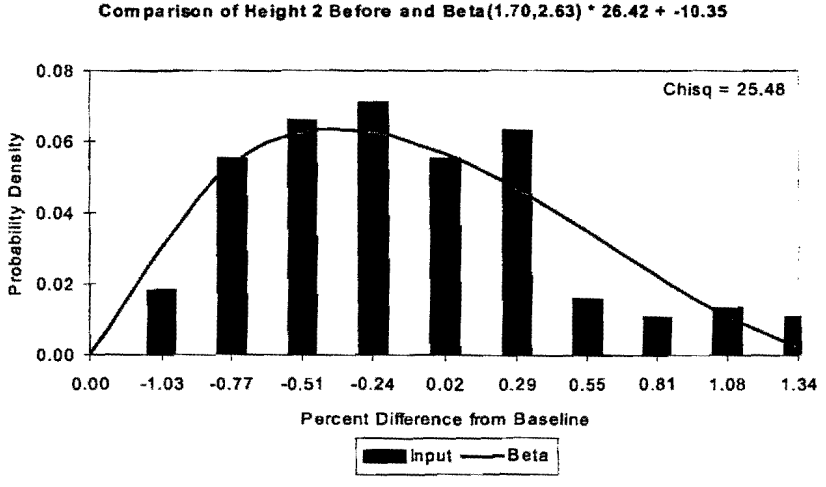

Statistical Distribution By Height Before SHRP Calibration

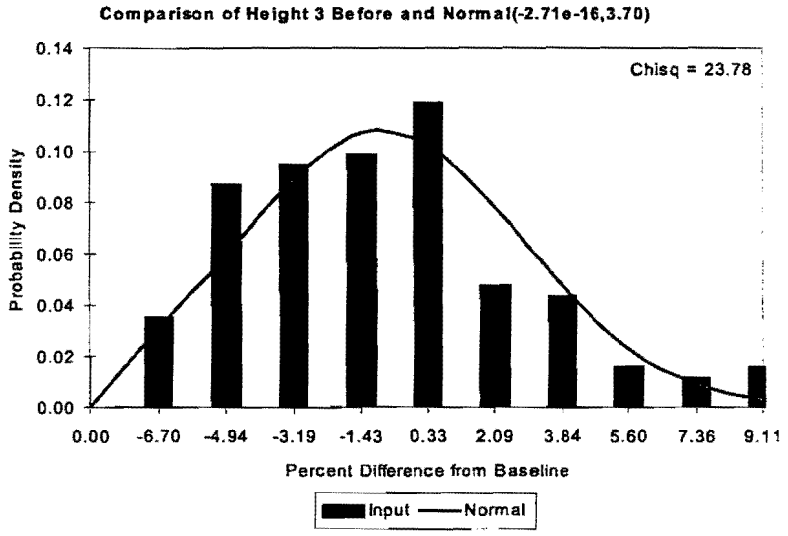

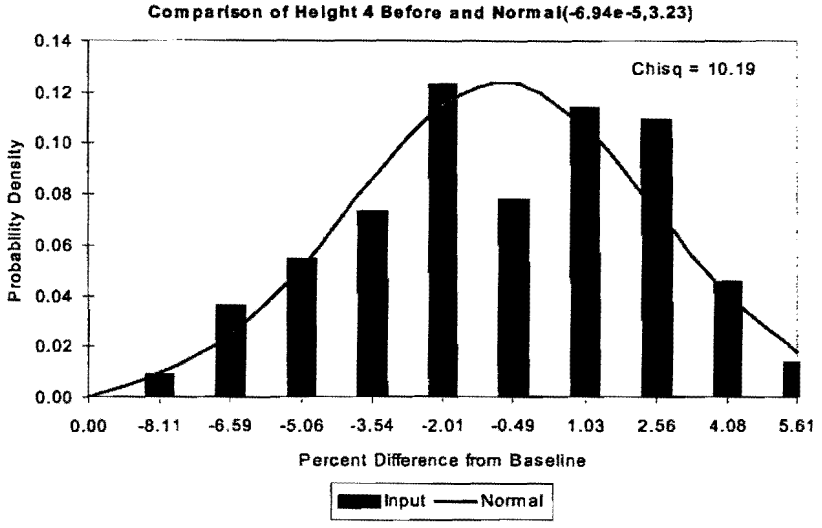

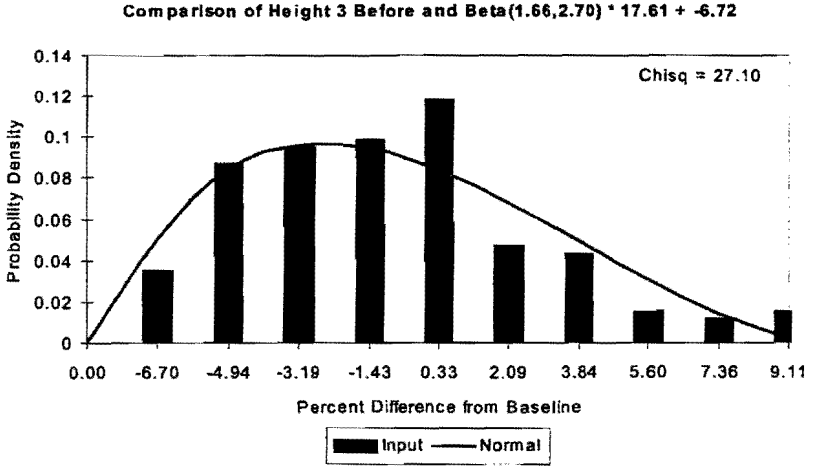

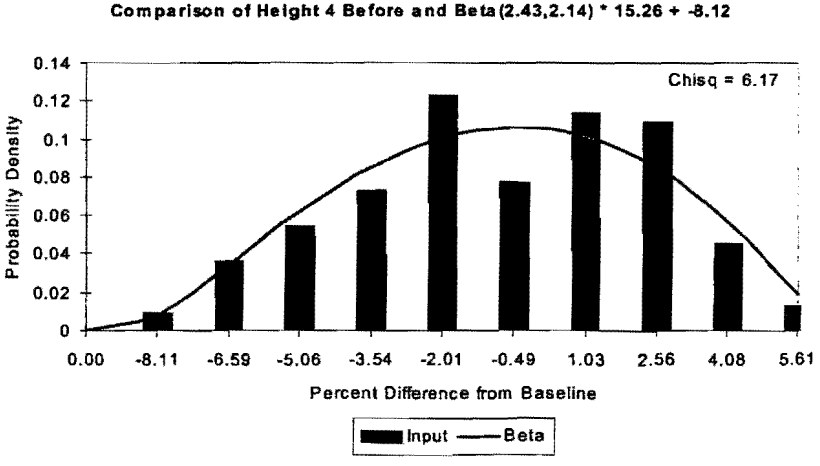

Statistical Distribution By Height After SHRP Calibration

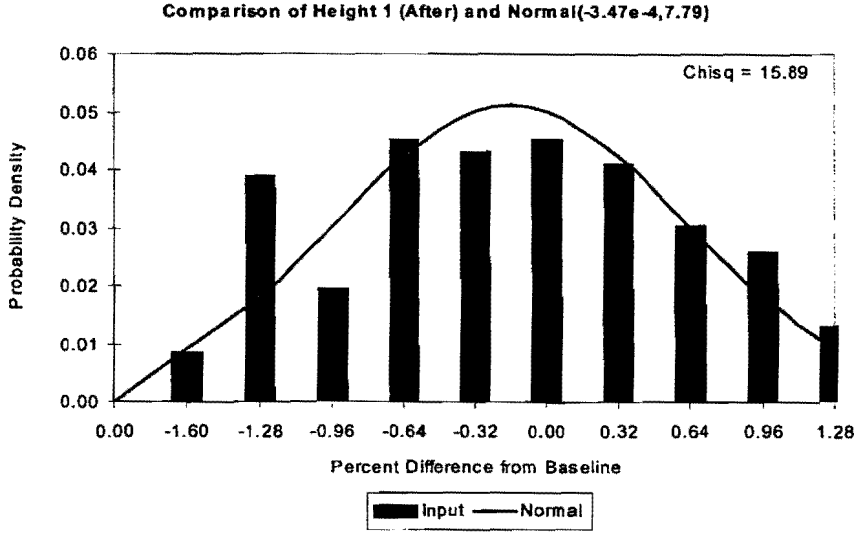

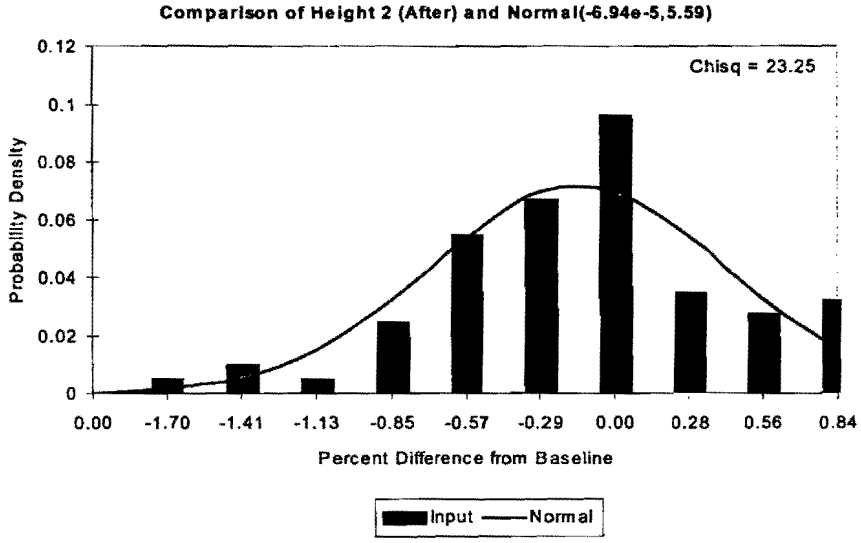

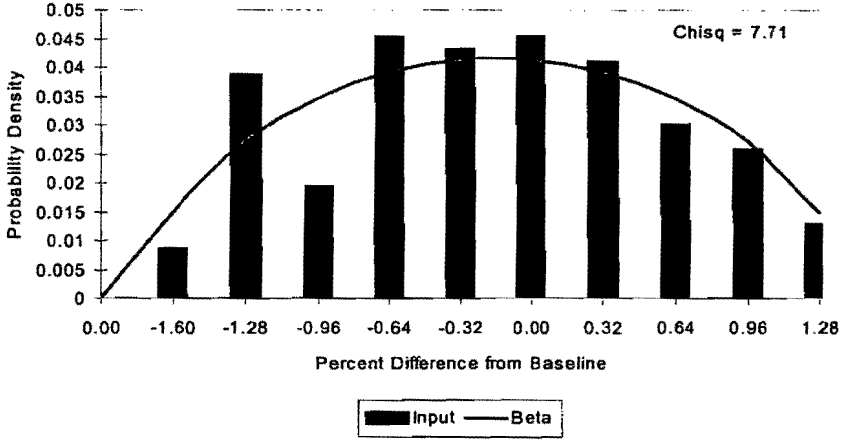

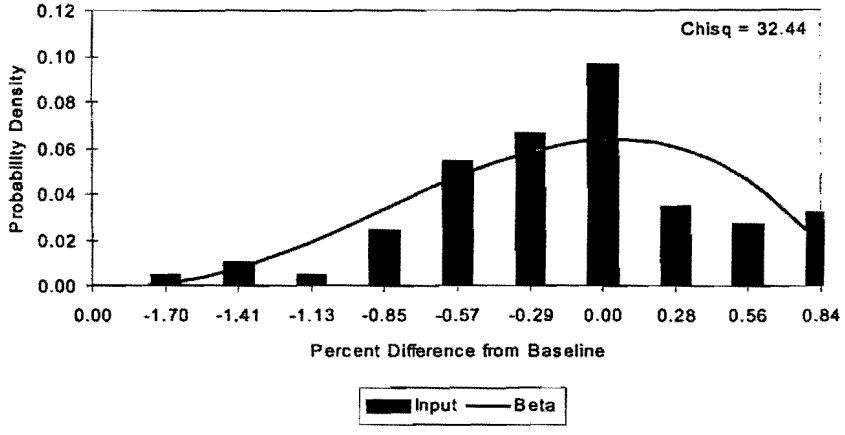

Statistical Distribution By Height After SHRP Calibration

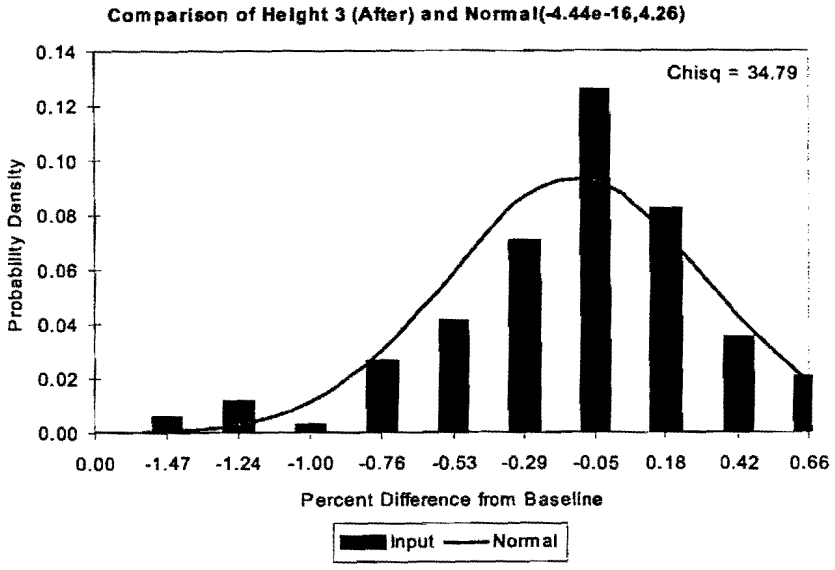

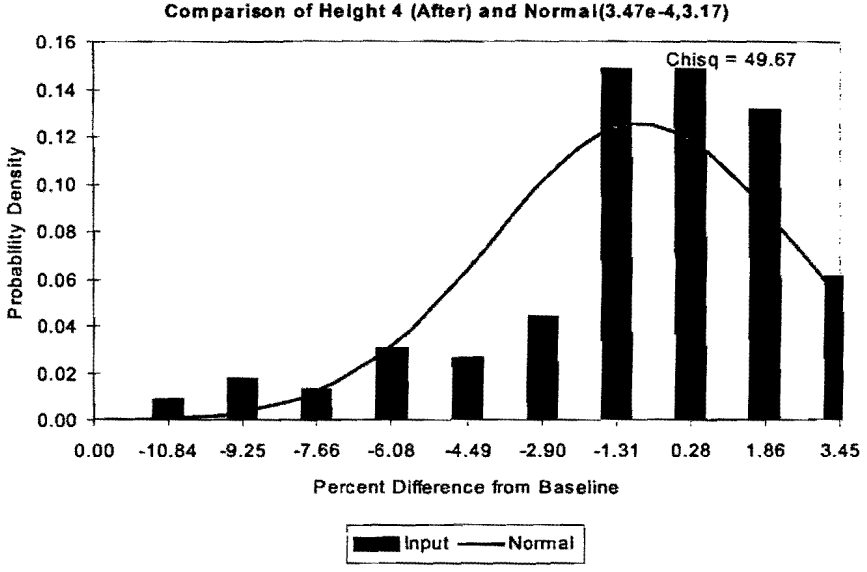

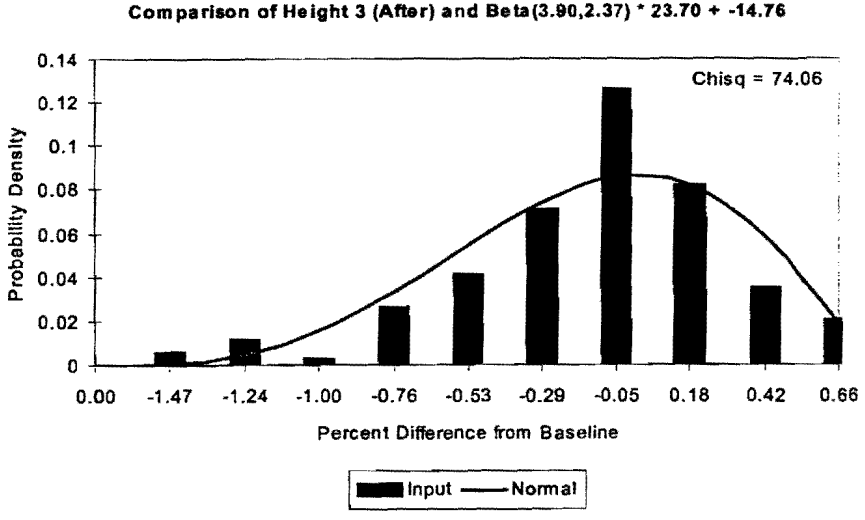

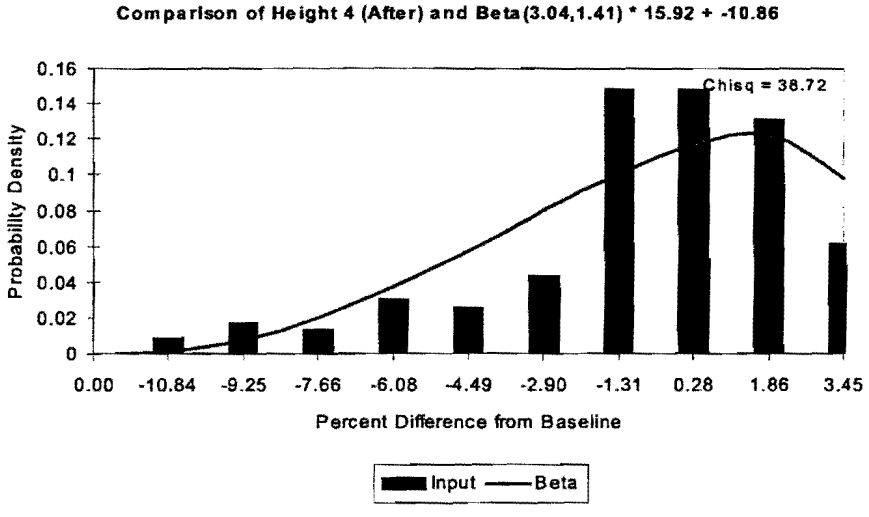

Statistical Distribution By Sensor Before SHRP Calibration

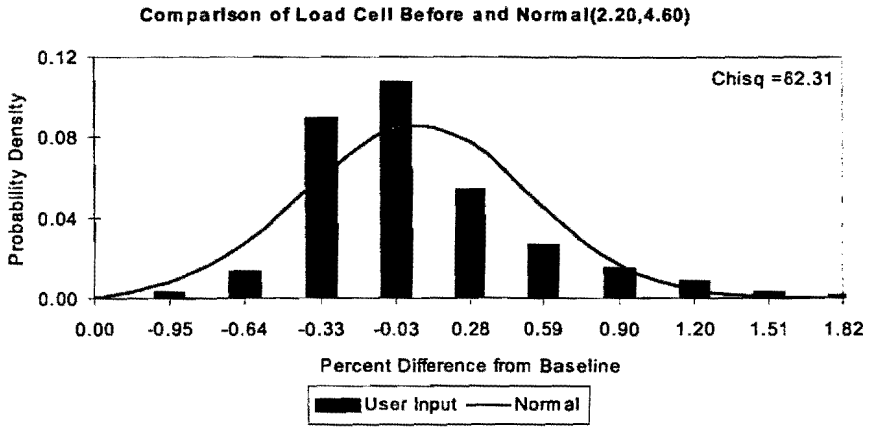

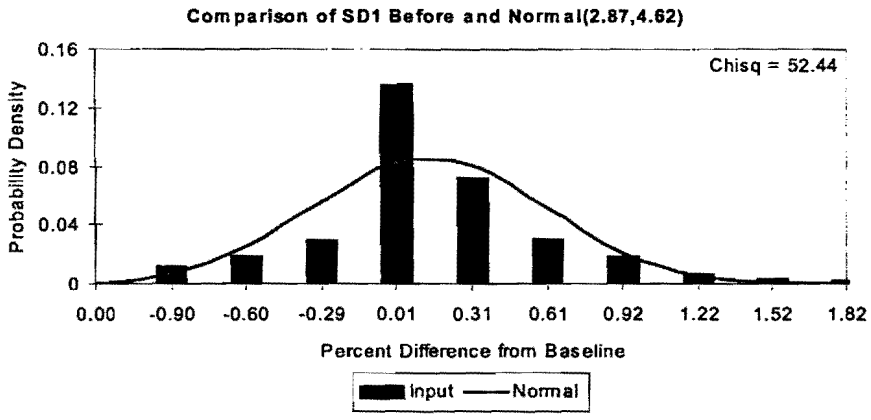

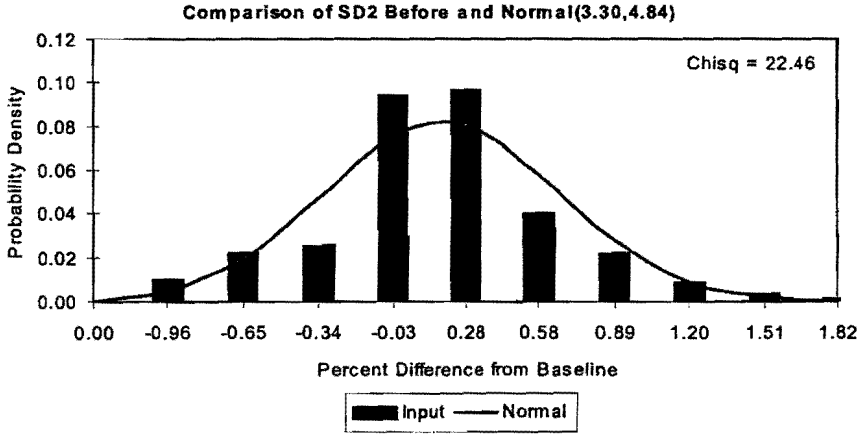

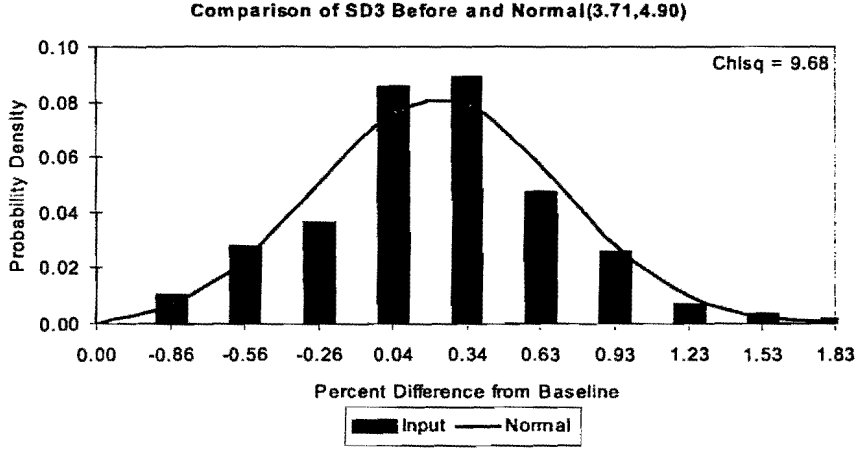

Statistical Distribution By Sensor Before SHRP Calibration

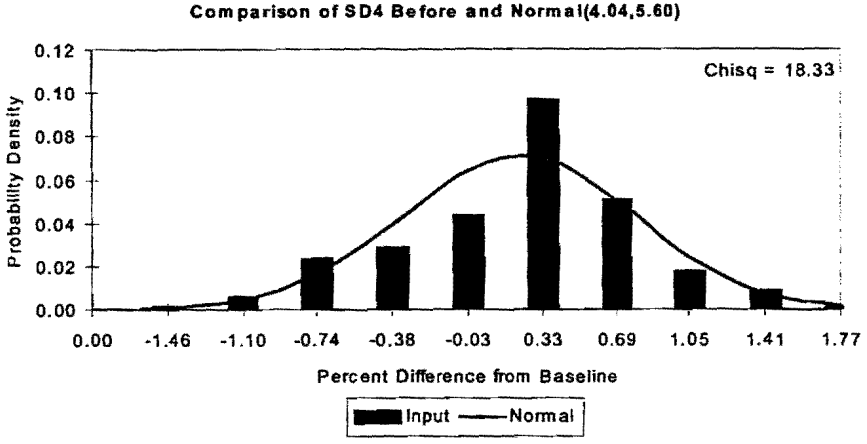

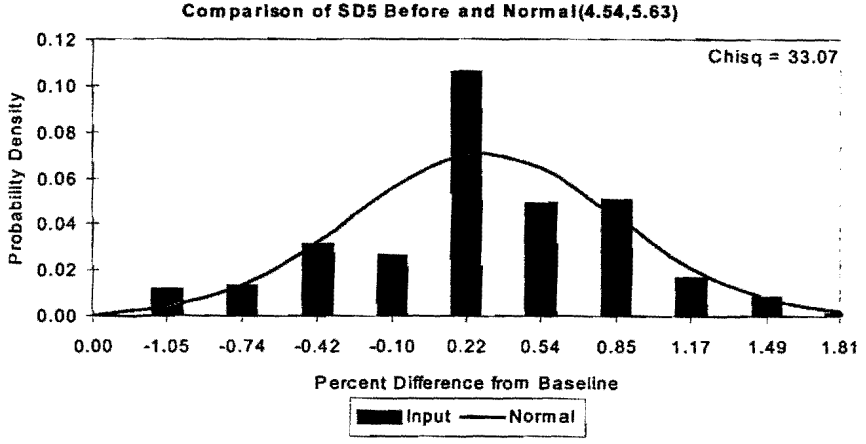

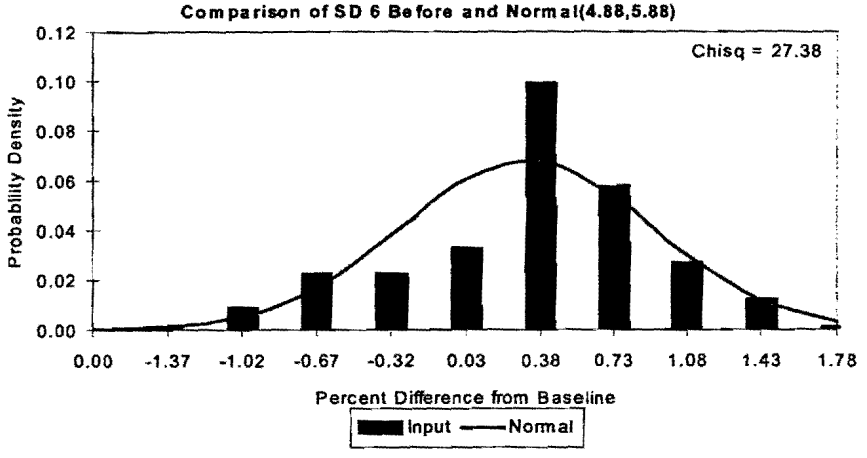

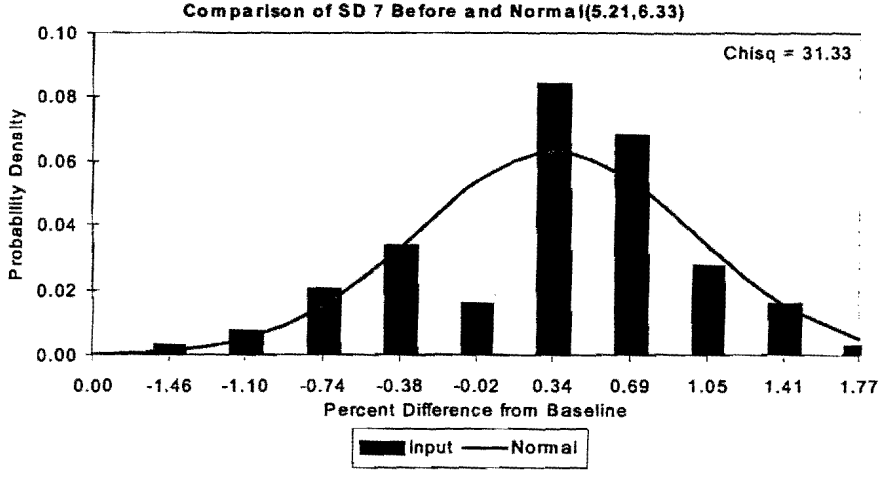

Statistical Distribution By Sensor After SHRP Calibration

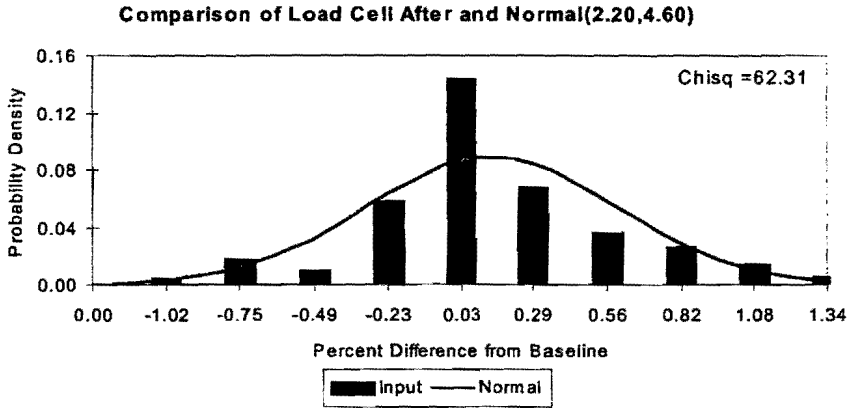

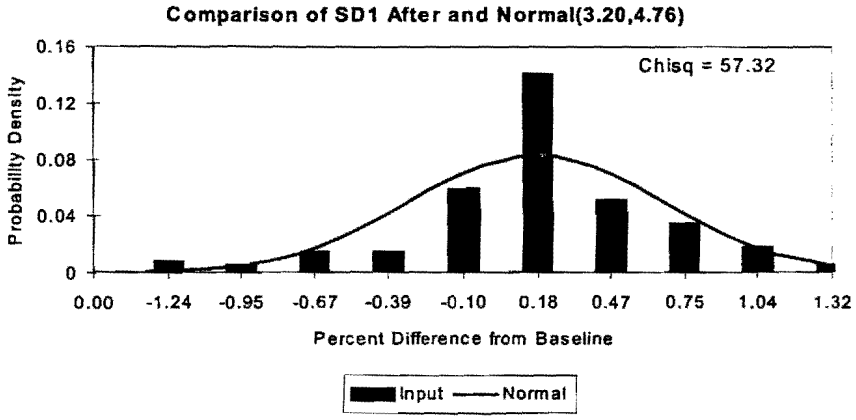

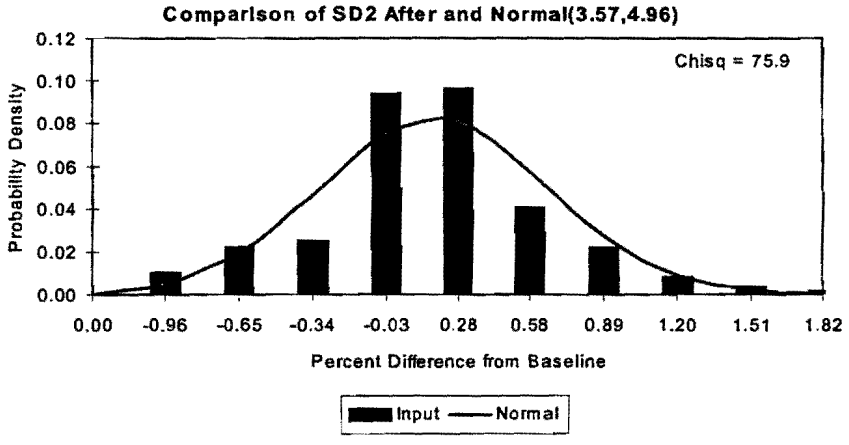

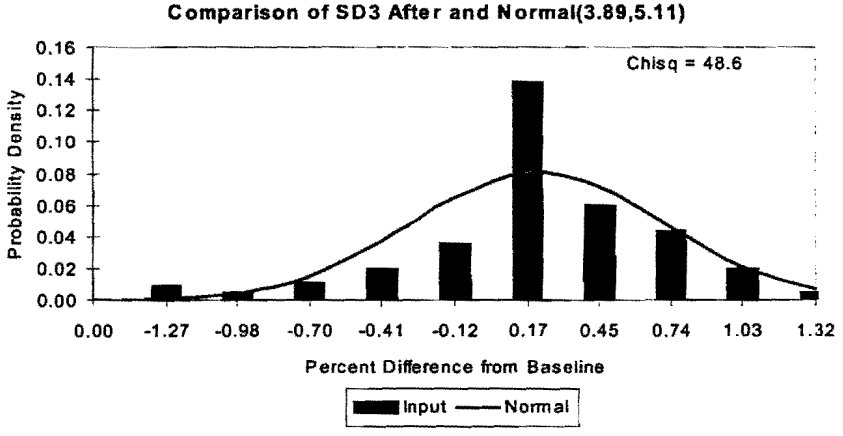

Statistical Distribution By Sensor After SHRP Calibration

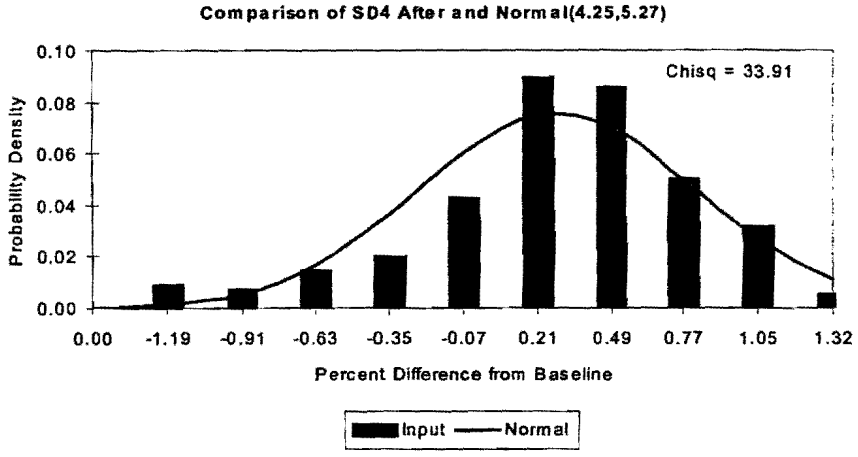

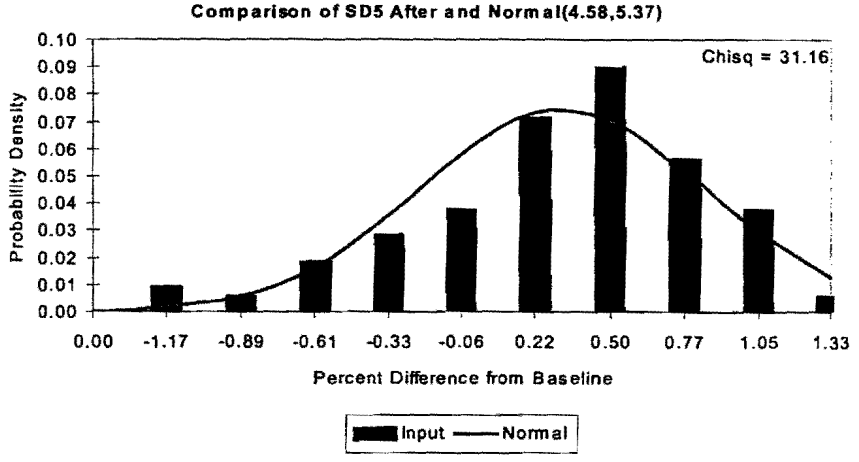

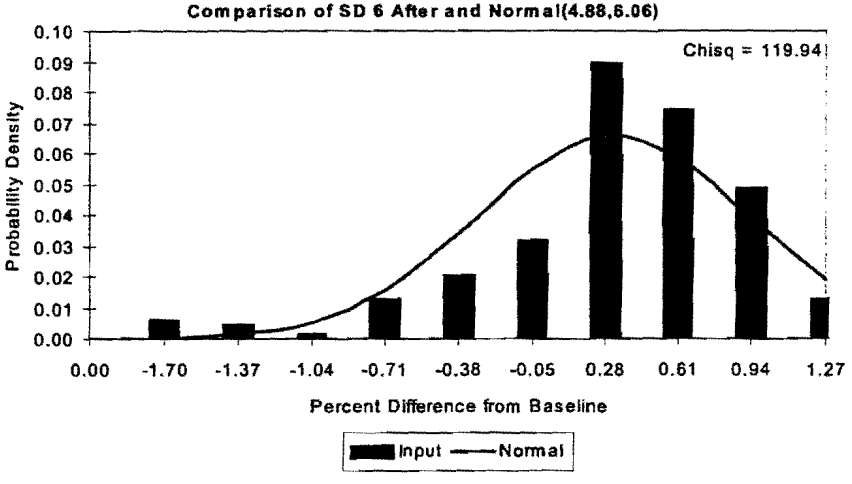

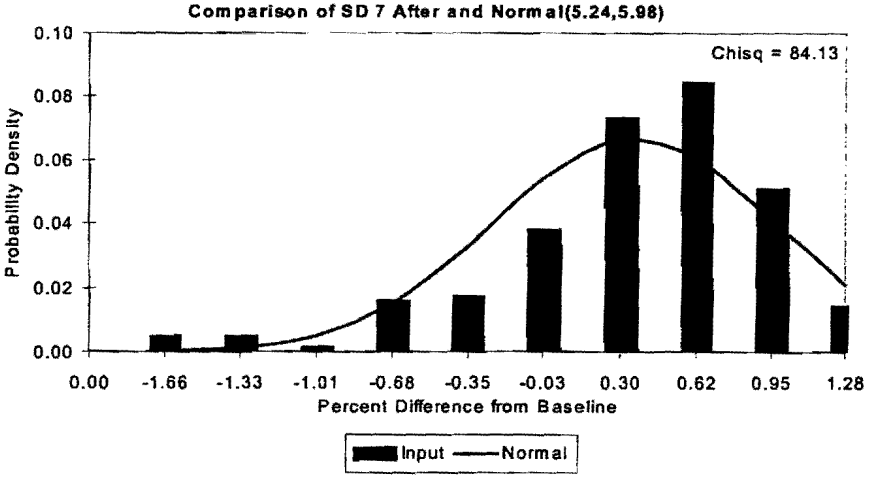

Statistical Distribution By Site Before SHRP Calibration

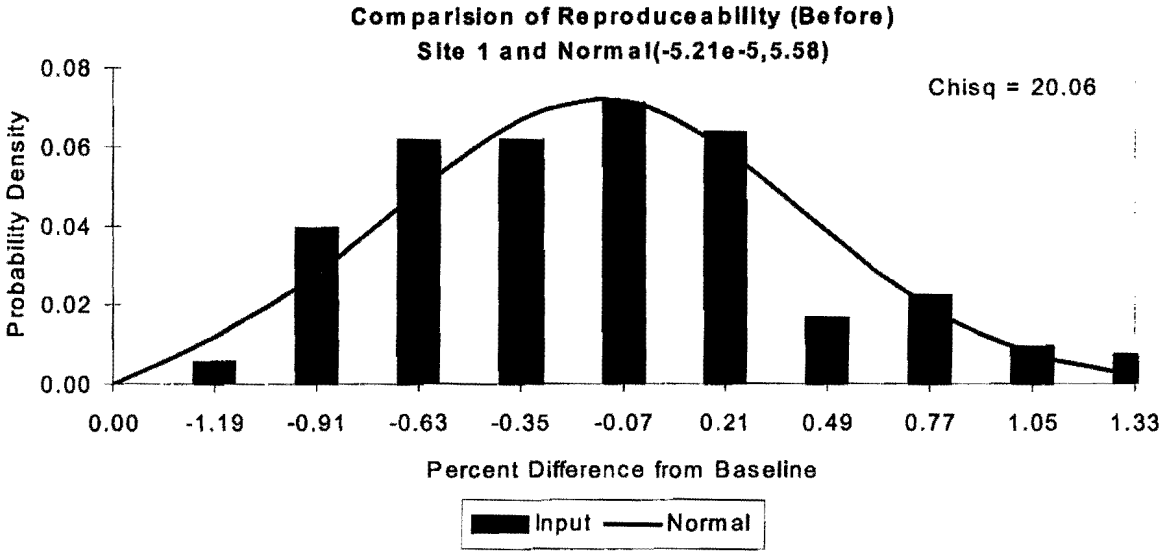

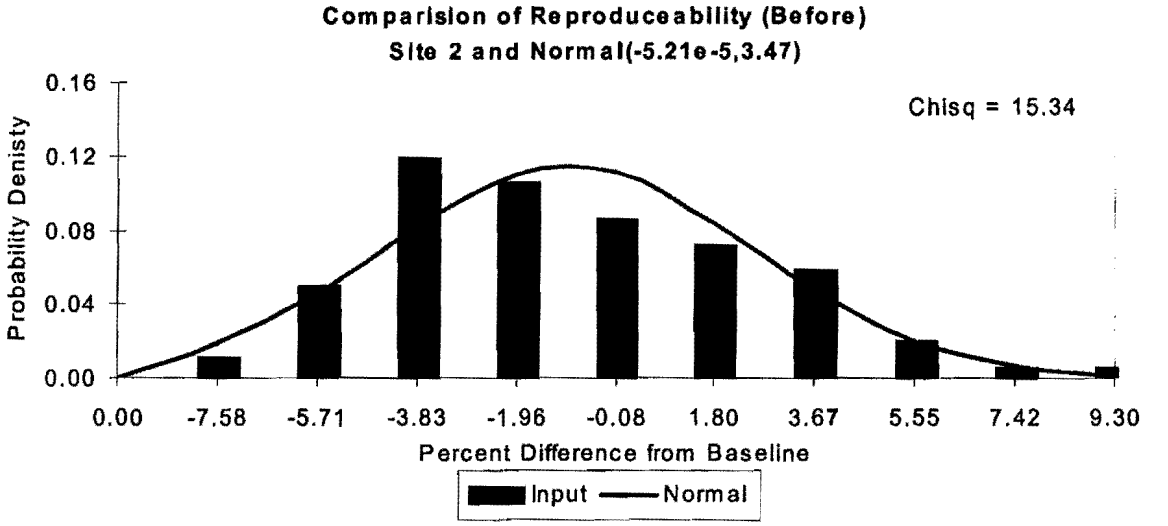

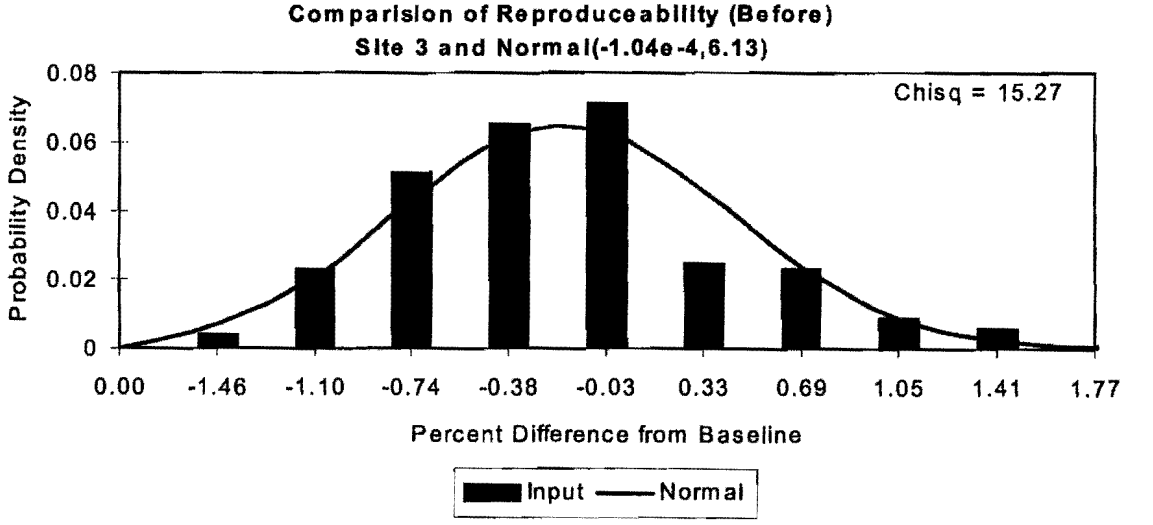

Statistical Distribution By Site After SHRP Calibration